Aus der Abteilung Genvektoren

Des Helmholtz Zentrum München

Vorstand: Prof. Dr. Wolfgang Hammerschmidt

Notch2 signaling in the primary T-cell-dependent immune response in mice

Dissertation
zum Erwerb des Doktorgrades der Naturwissenschaften
an der Medizinischen Fakultät der
Ludwig-Maximilians-Universität zu München

vorgelegt von

Tea Babushku

aus

Skopje, Nordmazedonien

Jahr

2022

Mit Genehmigung der Medizinischen Fakultät

der Universität München

Betreuerin:	PD Dr. Ursula Zimber-Strobl
Zweitgutachter:	Prof. Dr. Vigo Heissmeyer
Dekan:	Prof. Dr. med. Thomas Gudermann
Tag der mündlichen Prüfung:	23. März 2023

Contents

Abstract

Canonical Notch2 signaling, induced upon Dll-1-ligand binding on follicular fibroblasts, has a pivotal role in the differentiation of MZB cells. Over the years, it has been assumed that mainly transitional B cells are the precursors of MZB cells. Recently, our lab revealed a remarkable plasticity between the mature B cell subsets in mice, in which FoB cells can also act as precursors for MZB cells. However, the underlying mechanisms controlling this transdifferentiation process remain rather elusive. Moreover, it is still poorly understood whether Notch2 signaling synergizes with other signaling pathways or whether it predisposes certain FoB cell qualities, in order to facilitate their differentiation into MZB cells.

This current study hypothesized that the Notch2 signal strength regulates MZB cell generation and that there may be a tight cooperation between antigen-induced B cell activation and Notch2 signal induction during this FoB-to-MZB differentiation process. By using a specialized CBF:H2B-Venus Notch reporter mouse strain, B cell populations receiving a Notch signal were examined at steady-state and during an ongoing TD immune response. It was discovered that Venus expression – the proxy for active Notch signaling – progressively increased during B cell development, culminating with the highest Venus expression in splenic MZB cells. These findings implied that Notch signaling is activated in most peripheral B cells, and FoB and transitional cells with the highest Notch signaling activity preferentially mature into MZB cells. The pool of MZB cells exhibited heterogeneous Venus expression, suggesting that Notch signaling is dynamically regulated in the MZ and that some MZB cells lose their Notch signal with time. Upon TD immunization, Venus expression was strongly decreased in most GC B cells, but was still sustained in a portion of LZ-GC cells, where Notch signaling likely supports the switching to IgG1, as well as the positive selection or survival of $IgG1^+$ memory cells. During PC differentiation, Venus expression persisted up until the plasmablast stage, but was turned off in the terminally differentiated PCs. Here, downregulation of Notch signaling may be necessary to enable long-lived PC formation. By analyzing transgenic mice with inducible constitutive activation or conditional ablation of Notch2 in a GC-B-cell-specific manner upon TD immunization, we were able to concomitantly prove the existence of an interplay between B cell activation and upregulation of Notch2 receptor signaling in regulating subsequent cell differentiation decisions. Combined immunization data from three mouse models provided evidence that FoB cells which down modulate Notch2 signaling differentiate into GC B cells, whereas activated FoB cells with high Notch2 receptor expression and enhanced Notch2IC signaling are deviated away from the GC, and initiate MZB and plasmablasts differentiation instead. The newly-generated MZB cells fully resembled

wildtype MZB cells with regards to their cell surface phenotype and their splenic localization in the MZ. They were generated as a systematic response to the TD-antigen immunization and seemed to persist as terminally-differentiated MZB cells over a 4-week time period in the spleen. Among them, we found MZB cells with phenotypic signs of prior GC experience, indicating that the murine MZB cell compartment may be qualitatively heterogeneous and may partially be derived from GC B cells. Given that the human marginal zone mostly comprises memory B cells emerging from GC reactions, we now propose that the murine MZB cell compartment resembles the human MZ pool to a greater extent, than previously believed.

Zusammenfassung

Der kanonische Notch2-Signalweg spielt bei der Differenzierung von MZB-Zellen eine entscheidende Rolle. Die Aktivierung des Notch2-Rezeptors wird durch die Interaktion von B-Zellen mit Dll-1-Liganden exprimierenden follikulären Fibroblasten induziert. Über die Jahre wurde vermutet, dass hauptsächlich unreife transitionelle B-Zellen die Vorläuferzellen von MZB-Zellen sind. Wir konnten jedoch vor kurzem nachweisen, dass eine gewisse Plastizität zwischen reifen FoB-Zellen und MZB-Zellen besteht. Die zugrundeliegenden Mechanismen, die diesen Transdifferenzierungsprozess regeln, sind jedoch noch weitgehend unbekannt. Darüber hinaus ist es noch unklar, inwieweit Notch2-Signale mit anderen Signalwegen kooperieren, um die MZB-Zell-Differenzierung auszulösen, bzw. ob FoB-Zellen bestimmte Voraussetzung mitbringen müssen, damit sie zu MZB-Zellen differenzieren können.

In dieser Studie wurde die Hypothese aufgestellt, dass die Stärke des Notch2-Signals die Bildung von MZB-Zellen reguliert und dass es bei dem Differenzierungsprozess von FoB- zu MZB-Zellen einen engen Zusammenhang zwischen der Antigen-induzierten B-Zell-Aktivierung und der Induktion von Notch2-Signalen gibt. Um diese Hypothese zu beweisen, wurde mit Hilfe von CBF:H2B-Venus-Notch-Reporter-Mäusen untersucht, welche B-Zellpopulationen Notch-Signale erhalten. Es wurde festgestellt, dass die Venus-Expression - die ein aktives Notch-Signal wiederspiegelt - während der B-Zell-Entwicklung stetig ansteigt und dass diese in MZB-Zellen am höchsten ist. Diese Ergebnisse deuten darauf hin, dass nahezu alle B-Zellen von Zeit zu Zeit ein Notch-Signal erhalten und dass B-Zellen, die das stärkste Notch-Signal erhalten, zu MZB-Zellen differenzieren. Allerdings wies der Pool von MZB-Zellen eine heterogene Venus-Expression auf, was darauf hindeutet, dass der Notch-Signalweg in der MZ dynamisch reguliert wird und einige MZB-Zellen ihr Notch-Signal mit der Zeit verlieren. Außerdem konnte ich zeigen, dass die Venus-Expression in den meisten Keimzentrums-B-Zellen stark verringert ist. Jedoch konnte in einem Teil der „Light-zone“-Keimzentrums-B-Zellen eine hohe Venus-Expression nachgewiesen werden. Vermutlich sind dies Zellen, die positiv selektioniert werden und in diesem Zuge ein Notch-Signal erhalten. Unsere Ergebnisse deuten darauf hin, dass Notch-Signale während der positiven Selektion das „Switching“ zu IgG1 bzw. das Überleben von $IgG1^+$-Gedächtnis-B-zellen unterstützten. Während der PC-Differenzierung blieb die Venus-Expression bis zum Plasmablasten-Stadium erhalten, wurde aber in den terminal differenzierten PC ausgeschaltet. Unsere Ergebnisse deuten darauf hin, dass Notch-Signale zwar die Plasmablasten-Differenzierung treiben, aber während der terminalen PC-Differenzierung abgeschaltet werden müssen. Durch die Analyse von transgenen Mäusen mit induzierbarer

konstitutiver Aktivierung oder Inaktivierung von Notch2 im Zuge von TD-Immunreaktionen konnten wir das Zusammenspiel zwischen B-Zell-Aktivierung, Hochregulierung des Notch2-Rezeptors und damit verbundene Zell-Differenzierungsprozessen nachweisen. Die Immunisierungsdaten, die wir in diesen Mäusen erhoben haben, deuteten stark darauf hin, dass FoB-Zellen, in denen die Notch2-Signale abgeschaltet werden, sich zu Keimzentrums-B-Zellen entwickeln, während aktivierte FoB-Zellen, die ein starkes Notch2-Signal erhalten, entweder zu MZB-Zellen oder Plasmablasten heranreifen. Die während der Immunreaktion neu gebildeten MZB-Zellen ähnelten sowohl hinsichtlich ihrer Zelloberflächenmarker-Expression als auch ihrer Lokalisation normalen MZB-Zellen. Die neu gebildeten MZB-Zellen blieben über einen Zeitraum von mindestens 4 Wochen in der MZ der Milz erhalten. Einige der während der Immunreaktion gebildeten MZB-Zellen hatten noch einen Keimzentrums-ähnlichen Phänotyp, was darauf hindeutet, dass sie von Keimzentrums-B-Zellen abstammen. Diese Daten könnten darauf hinweisen, das sowohl das humane als auch murine MZB-Zellkompartment aus einer heterogenen Population aus naiven und Gedächtnis-B-Zellen besteht. Das humane und murine MZB-Zellkompartment wären somit ähnlicher als ursprünglich angenommen.

List of Figures

List of Tables

List of Abbreviations

ADAM = A Disintegrin and metalloproteinase domain-containing protein

AID / Aicda = activation-induced cytidine deaminase

ANK = Ankyrin repeats

ANOVA = analysis of variance tests

APCs = antigen-presenting cells

app. = approximately

ASCs = antibody-secreting cells

BAFF = B cell activating factor

BC = bridging channel

Bcl6 = B-cell lymphoma 6

BCM = B-cell medium

BCR = B cell receptor

BCZ = B-cell zone

Blimp1 = B-lymphocyte-induced maturation protein 1

BLNK = B-cell linker protein

BM = bone marrow

BSA = bovine serum albumin

Btk = Burtons tyrosine kinase

C = constant region of immunoglobulin chains

C- = carboxy

CAR = coxsackie/adenovirus receptor

Cat# = Catalogue number

CBF1 = C promoter-binding factor 1

CCL = Chemokine (C-C motif) ligand

CCR7 = C-C chemokine receptor type 7

CD = cluster of differentiation

CD40L = CD40 ligand

CD40R = CD40 receptor

CSR = class switch recombination

CXCR = C-X-C chemokine receptor

d. = day

DAB = 3,3'-diaminobenzidine

DAPI = 4',6-diamidin-2-phenylindol

DCs = dendritic cells

Dll = delta-like ligand

DMSO = Dimethyl sulfoxide

DNA = Diribonucleotide acid

DZ = dark zone

EDTA = ethylene diamine tetra acetate

EF = extrafollicular foci

EGF = epidermal growth factor

ELISA = enzyme-linked immunosorbent assay

ELISpot = enzyme-linked immunospot assay

et. al. = et alia, Latin for "and others"

FACS = Fluorescence-activated cell sorting, here an acronym for a type of Flow Cytometry

Fbw = F-box-containing protein

FCS = fetal calf serum

FDCs = follicular dendritic cells

Fig. = Figure

fl = floxed or flanked by lox-P sites

FoB(s) = follicular B cell(s)

FSC = forward scatter

GC(s) = germinal center(s)

h = hour

H2B = human histone 2B

hCD2 = human CD2 receptor

Hes = hairy enhancer of split

Hey = hairy related

hi = high

HRP = horse radish peroxidase

HSCs = hematopoietic stem cells

IC = intracellular

ICAM = Intercellular Adhesion Molecule

ICOS-L = ICOS ligand

IF = immunofluorescence

Ig = immunoglobulin

IgH = immunoglobulin heavy chain

IgL = immunoglobulin light chain

IHC = immunohistochemistry

IL = interleukin

i.p. = intraperitoneal

IRES = internal ribosome entry site

Irf4 = Interferon Regulatory Factor 4

KI = knock-in

KO = knock-out

LN = lymph nodes

LNR = LIN12-Notch repeats

lo = low

lox-P = locus of X-over P1

LPS = lipopolysaccharide

LZ = light zone

mA = milliampere

MACS = magnetic cell separation

MAML = Mastermind Like Transcriptional Coactivator

MBCs = memory B cells

MFI = mean fluorescence intensities

MHC = major histocompatibility complex

mid / int = intermediate

min = minutes

MINT = Msx2-interacting nuclear target protein

ml = milliliter

mM / M = millimolar / molar

MMM = marginal metallophillic macrophage

mRNA = messenger Ribonucleic acid

mTECs = medullary thymic epithelial cells

MZ = marginal zone

MZB(s) = marginal zone B cell(s)

MZM = marginal zone macrophage

MZP(s) = marginal zone precursor(s)

µl = microliter

N- = amino

N/A = not applicable

N2KO = Notch2 knock-out

neg = negative

NfκB = Nuclear factor κ-light-chain-enhancer of activated B-cells

NK = natural killer cells

NLS = nuclear localization signal

Notch2IC / N2IC = intracellular Notch2

Notch-ECD = extra cellular domain of Notch

Notch-ICD = intracellular domain of Notch

Notch-TM = transmembrane domain of Notch

NP-CGG = 4-hydroxy-3-nitrophenylacetyl-chicken-gamma-globulin

NRR = negative regulatory region

OD = optical density

p.i. = post immunization / post injection

Pax5 = Paired Box 5

PB = plasmablast

PBS = phosphate-buffered saline solution

PC(s) = plasma cell(s)

PCR = polymerase chain reaction

PEST = proline-glutamine-serine-threonine-rich region

PFA = paraformaldehyde

pos = positive

PPs = Peyer's Patches

RAG = recombination-activated gene(s)

RAM = RBPJ-association molecule

RBC(s) = red blood cell(s)

RBPJ = Recombining binding protein suppressor of hairless

Rep = reporter

RP = red pulp

rpm = rounds per minute

RT = room temperature

S1PR = Sphingosine-1-phosphate receptor

SA-AP = streptavidin-coupled alkaline phosphatase

SCF = Skp1, Cullins, F-box proteins, a multisubunit E3 ubiquitin ligase family

SD = standard deviation

SHM = somatic hypermutation

SLOs = secondary lymphoid organs

SP = spleen

S-S = disulfide bridges

SSC = side scatter

SV40 = simian vacuolating virus 40

T1/T2/T3 = transitional B cells

TACI = Transmembrane activator and CAML interactor

TAD = transactivation domain

TCR(s) = T-cell-receptor(s)

TCZ = T-cell zone

TD = T-cell-dependent

TE = Tris EDTA

TF = transcription factor

T_h = T helper cells

TI = T-cell-independent

TLRs = Toll-like-receptors

UI = unimmunized / uninjected

UV = ultraviolet

v/v = volume per volume

VCAM = Vascular cell adhesion protein

V_H, V_L = variable heavy chain and light chain region

WP = white pulp

wt = wildtype

Xpb1 = X-box-binding protein 1

α = anti

˚C = degree Celsius

‘ = minute

‘’ = second

% = percentage

1 Introduction

1.1 The immune system and its two branches: innate and adaptive immunity

The immune system is a biological defense mechanism, which comprises a complex collection of organs and cells. Their main purpose is to protect the organism from invaders, such as viruses, parasites, tumor cells or bacteria. During their lifespan, mammals are constantly threatened by pathogens, which have different entry routes into the body and can cause a wide range of diseases (Cooper and Alder, 2006). Therefore, a highly-specialized and well-coordinated immune response is a necessity to combat hazardous infections and prevent cellular damage. Unlike plants and invertebrates, the mammalian immune system has evolved into two specialized branches: innate and adaptive immune response. The innate immune system is the first line of defense against foreign agents, which enter the body through the skin or mucosal membranes. It acts within the first 0 to 96 hours of infection and provides the same protection against all pathogens, which is why it is considered a non-specific immune response. The second line of defense is provided by the adaptive immune system. It is highly-specific for each infectious agent and becomes activated in cases when the innate immune system fails to clear the pathogen. Thus, it is more accurate, but also much slower than the innate immune response, as it acts with a delay of 4 to 7 days. Moreover, the adaptive immune response has the remarkable power to “remember” a pathogen, so that when the body encounters it again after some time, it can respond quicker. This phenomenon is described as long-lasting immunological memory (Bonilla and Oettgen, 2010; Kenneth M. Murphy, 2016; Nicholson, 2016).

Just like the cellular components in the blood, the cells of the innate and adaptive immune system develop from pluripotent hematopoietic stem cells (HSCs) in the bone marrow. The HSCs are formed right after birth and give rise to the myeloid and the common lymphoid progenitor (*Fig. 1*). The myeloid progenitor produces macrophages and dendritic cells, which are major components of the innate immunity. The lymphoid progenitor generates B and T lymphocytes and natural killer (NK) cells (Hardy and Hayakawa, 2001; Kearney et al., 1997). While NK cells are also part of the innate immune system, B and T cells are key players in the adaptive immune response. The adaptive immune system is subdivided into cellular and humoral immune response. The cellular immune response is executed by T cells and NK cells, whereas the humoral immune response is mediated by B cells (Hoffman et al., 2016; Paust et al., 2010).

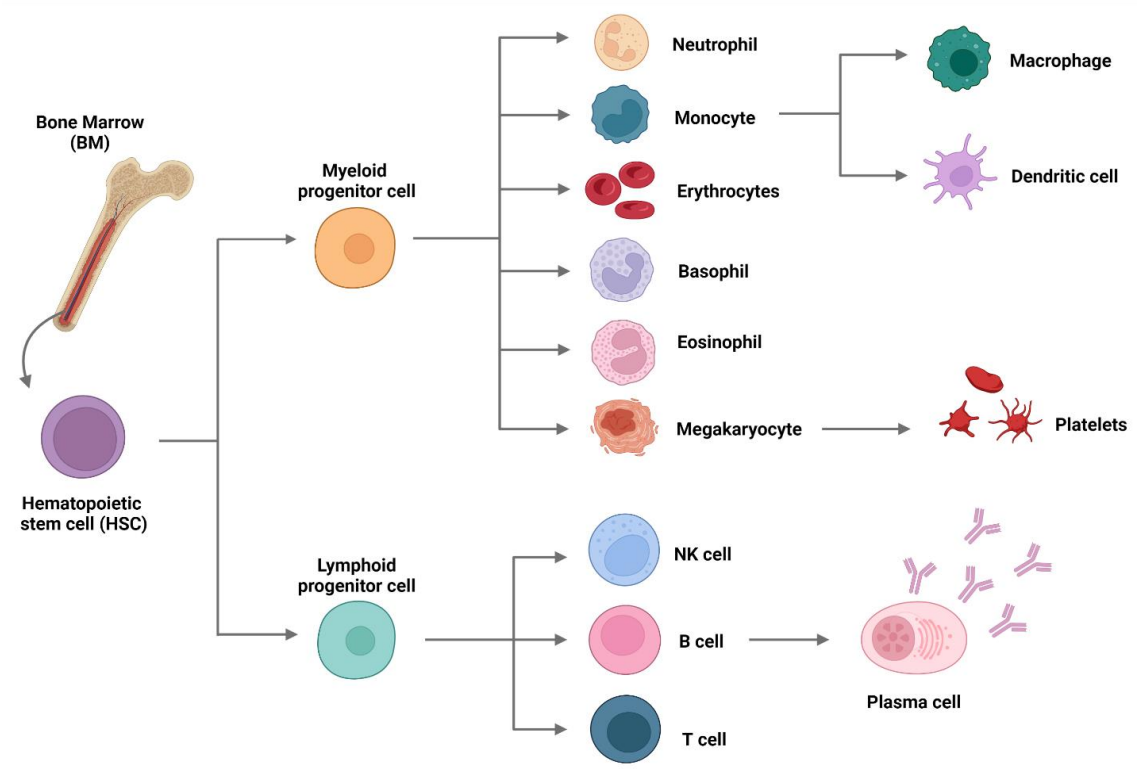

Fig. 1: A simplified scheme of hematopoiesis of blood cells and immune cells. Hematopoietic stem cells in the bone marrow give rise to multipotent myeloid and lymphoid progenitor cells. These progenitors generate a profile of terminally differentiated lymphoid cells (B, T and NK cells) or myeloid cells (megakaryocytes, eosinophils, neutrophils, basophils, erythrocytes and monocytes). B cells produce effector plasma cells upon activation. Monocytes in the myeloid lineage give rise to macrophages and dendritic cells. (Figure created in BioRender Premium, biorender.com)

Because expansion of immune cell subsets remains permanently even after the immune response is shut down again, strict regulatory mechanisms between the two arms of the immune system are a prerequisite to avoid dangerous disorders in the body (Kenneth M. Murphy, 2016).

1.2 B Lymphocytes – development, activation, functions

Although B and T cells share a common cellular progenitor, they mature at different sites in the body. If the lymphoid progenitor in the bone marrow receives a signal through the Notch1 receptor, it becomes committed to the T cell linage and migrates via the blood to the thymus, where fully mature T cells are developed (Maillard et al., 2005; Radtke et al., 2004, 1999; Yang et al., 2010). On the other hand, B cells arise in the bone marrow and continue their early maturation at this site (Bhattacharya, 2019; Shahaf et al., 2016). The true characterization of B cells started in the mid-1960s and early 1970s with help from experimental animal models, clinical evaluation of immunodeficient patients and the

growing technology of cell surface molecule phenotyping (LeBien and Tedder, 2008). From there on, B lymphocytes have continuously triggered intellectual curiosity and have challenged the experimental skills of researchers and clinicians (LeBien and Tedder, 2008).

In mice, the mature B cell subsets in the spleen are divided into B1 and B2 cells, distinguished by their phenotype, developmental differences, tissue distribution and function. B1 cells are mainly found in the peritoneum, but a minor population is also located in the spleen (Allman and Pillai, 2008; Baumgarth, 2017, 2016). Contrary to B2 cells, B1 cells are generated in the fetal liver and have the capacity of self-renewal and antibody production in the periphery (Baumgarth, 2017; Hayakawa et al., 1986). Given that the mature B2 cell subsets are the main focus of this thesis, their development, maturation, activation and function will be discussed in more detail in the upcoming chapters.

1.2.1 B cell development and maturation

1.2.1.1 Early B cell development in the bone marrow

The early B cell development in the bone marrow aims to produce a repertoire of immature B cells with non-self-reactive B-cell-receptors (BCRs) and high diversity of antigen specificities (Hardy and Hayakawa, 2001; Melchers, 2015; Vale et al., 2015). The BCR is a complex of several components: an immunoglobulin heavy chain (IgH), light chain (IgL) and a pair of accessory signaling proteins, Igα and Igβ. The IgH and IgL chains are made of constant (C) and variable (V_h and V_L) regions, the latter ensuring antigen binding and specificity. On the other hand, Igα and Igβ mediate downstream intracellular signaling upon BCR ligation (Hardy and Hayakawa, 2001; Maity et al., 2018; Melchers, 2015; Vale et al., 2015). The commitment to the B cell lineage is initiated by a tightly regulated cooperation between the IL7 cytokine receptor and transcription factors, such as EBF, E2A and Pax5 (Busslinger, 2004; Medvedovic et al., 2011; Northrup and Allman, 2008; Ramírez et al., 2010). The lymphoid progenitor first gives rise to early pro-B cells (*Fig. 2A*). In the early pro-B cell stage, V(D)J rearrangements are mediated by expression of the recombination-activated genes RAG-1 and RAG-2, resulting with the combining of a D_h to J_h segment. V(D)J recombination then continues to completion in the late pro-B cell stage, where V_h to D_h-J_h joining is performed (Tonegawa, 1993). Upon successful rearrangement of the IgH locus, the cells are positively selected to express the surface pre-BCR, which contains the rearranged Igμ heavy chain and a surrogate light chain. Pre-BCR signaling marks the entry into the large pre-B cell stage, where it promotes cellular expansion through proliferation and cell division (reviewed in (Winkler and Mårtensson, 2018)). Following this, large pre-B cells enter the resting, small pre-B cell stage (*Fig. 2A*).

Here, the rearrangement of the IgL chain happens by combining a V_L to J_L segment. At this stage, pre-B cells have two opportunities for proper V-J recombination, one on each of the two IgL alleles (Clark et al., 2014; Herzog et al., 2009; Mårtensson et al., 2007). If the recombination fails, the cells undergo cell death. If a light chain is successfully rearranged, it replaces the surrogate IgL chain and dimerizes with the *Igμ* heavy chain, producing a full IgM surface molecule. These cells then join the pool of immature B cells, which are defined by their intact, antigen-specific BCRs (Bossy et al., 1991; Jones et al., 2020) (*Fig. 2A*). Lastly, the immature B cells are tested for their BCR specificity. If the cell possesses a strongly auto-reactive BCR or does not have any BCR specificity, it is either eliminated by clonal deletion or it is selected for receptor-editing. This process allows the cell to change its BCR specificity for one final time by further V(D)J rearrangements (Clark et al., 2014; Edry and Melamed, 2004; Kenneth M. Murphy, 2016). Immature B cells that pass the selection test carry unique, non-self-reactive BCRs with only one antigen specificity (Jones et al., 2020). Thus, they can leave the bone marrow via the blood stream and migrate to the spleen, where they continue the maturation (Kenneth M. Murphy, 2016; Minges Wols et al., 2010; Shahaf et al., 2016).

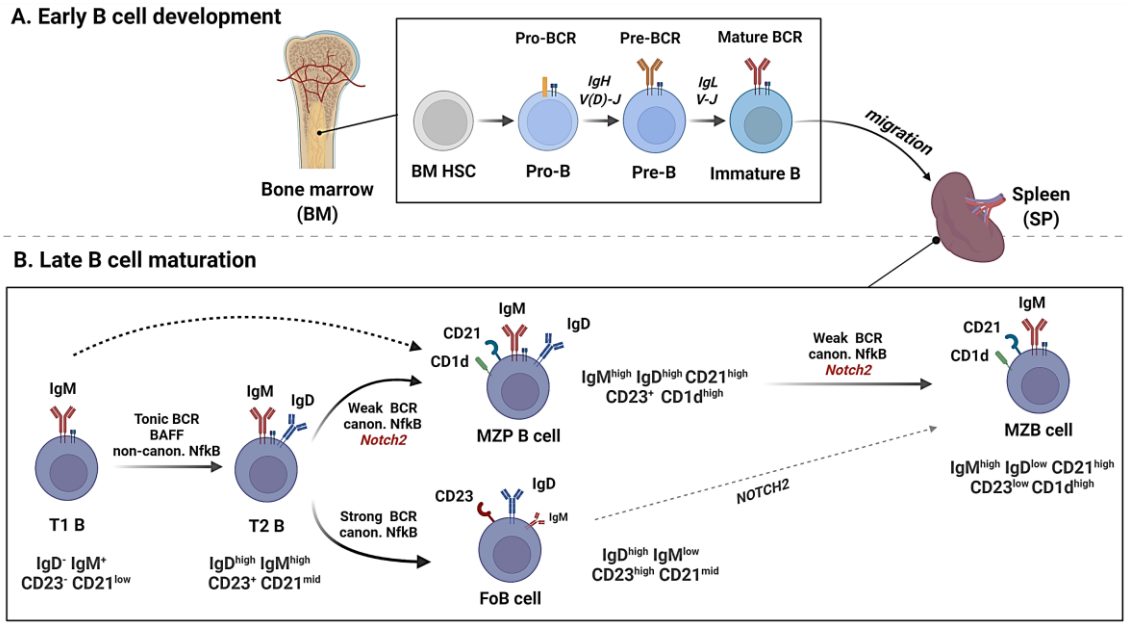

Fig. 2: Current model of early (BM) and late (SP) B cell development in mice. (A) In the BM, the hematopoietic stem cell (HSC) gives rise to pro-B cells. Here, rearrangement of the heavy chain IgH locus takes place, leading to the large pre-B cell stage. Following proliferation and cell expansion in the large pre-B cell stage, cells enter the small pre-B phase, where the pre-BCR is internalized and recombination of the IgL light chain locus happens. Cells with successfully rearranged heavy and light chains build an intact, functional BCR and are defined as immature B cells. **(B)** BM-derived immature B cells migrate to the SP where they develop into T1 and T2 cells. T2 cells further mature into follicular (FoB) cells, and - over a MZ precursor (MZP) stage - to marginal zone (MZB) cells. This binary cell fate decision is defined by the collaboration of

different signaling pathways, Notch2 signaling being the most important one among them. Each SP B cell type can be distinguished in flow cytometry by expression of cell surface IgD, IgM, CD23, CD21 and CD1d (Figure created in BioRender Premium, biorender.com).

1.2.1.2 Late B cell maturation and B2 cell subsets in the spleen

The immature B cells arrive in the spleen as most recent emigrants from the BM. They are called transitional (T) cells because they represent a short developmental transition from immature to fully mature B cells (*Fig. 2B*). They go through several stages during development, known as T1, T2 and T3 cells (Allman et al., 2001; Chung et al., 2002). It has been established that tonic BCR signaling and BAFF receptor signals positively regulate the survival of transitional cells (Batten et al., 2000; Cancro, 2009; Chung et al., 2003; Gross et al., 2001; Kraus et al., 2004; Lam et al., 1997; Loder et al., 1999; Moore et al., 1999; Sasaki et al., 2004; Schiemann et al., 2001; Tze et al., 2005). All transitional cells express the surface marker of immaturity AA4.1, however, its levels are diminished upon terminal differentiation into mature follicular B (FoB) and marginal zone B (MZB) cells (Allman et al., 2001; Chung et al., 2003; Pillai and Cariappa, 2009; Yeramilli and Knight, 2011). As they go over from the T1 to T2 stage, transitional cells upregulate IgM, IgD, CD23 and CD21 expression, thus slowly priming their phenotype for the subsequent cell fate decision between FoB and MZB cells (Allman et al., 2001; Chung et al., 2003; Pillai and Cariappa, 2009) (*Fig. 2B*).

Among the mature B cells in the spleen, FoB cells are the more abundant population with around 90%, whereas MZB cells add up to only 5-10% (Srivastava et al., 2005b). Moreover, FoB and MZB cells differ in their cell surface phenotype, immunological function and anatomical localization. FoB cells recirculate between lymphoid organs, whereas MZB cells are mostly sessile in the name-giving marginal zone (MZ) and can occasionally migrate between the B cell follicle and the MZ (Arnon et al., 2013; Cinamon et al., 2008; Martin and Kearney, 2002; Pillai et al., 2005). The distinction of FoB and MZB cells is possible due to their polar-opposite surface marker phenotype: FoB cells express high CD23 and IgD levels, but low IgM, CD1d and CD21. On the contrary, MZB cells are $CD23^{low}IgD^{low}$, but $IgM^{high}CD21^{high}CD1d^{high}$ (Pillai et al., 2005). However, neither FoB nor MZB cells are completely negative for the opposing surface proteins, which led to the identification of intermediate cellular phenotypes in between transitional, FoB and MZB cells. One such population is the so-called marginal zone precursor (MZP) cell subset. The MZPs have a surface marker phenotype between immature T2 and mature MZB cells (i.e. $IgM^{high}IgD^{high}CD21^{high}CD23^{mid}$), and have been described to arise as an earlier stage before the terminal MZB cell differentiation (*Fig. 2B*). Another intermediate mature B cell population being discussed are the follicular type 2 cells (FoB-II). They differ from conventional FoB and MZB cells due to a higher IgM expression and intermediate levels

of CD21, thus making FoB-II cells $IgM^{high}IgD^{high}CD21^{mid}CD23^{+}$ (Allman et al., 2004; Allman and Pillai, 2008; Loder et al., 1999; Pillai and Cariappa, 2009; Srivastava et al., 2005a, 2005b).

Between the late 1990s and 2010, a lot of studies were dedicated on unraveling the mechanisms behind peripheral B cell maturation. Today's widely-accepted model was introduced by Pillai and Cariappa in 2009, under consideration of the many previous findings. Their model indicates that a complex cell fate decision starts in T2 cells, regulated by the interplay and strength of several signaling pathways, such as BCR, NfκB and Notch2 signaling (Pillai and Cariappa, 2009). It is proposed that a strong BCR signal through the Btk kinase drives T2 cells towards FoB cell differentiation, combined with avoidance of Notch2 signaling activation (Cariappa et al., 2001; Hardy et al., 1983; Hikida et al., 2003; Pillai and Cariappa, 2009; Wen et al., 2003). On the other hand, a weaker BCR signal in T2 cells was crucial to drive the development of MZB cells over the MZP stage (Cariappa et al., 2001; Pillai et al., 2005; Samardzic et al., 2002; Wen et al., 2005). Also, functional signaling through the BCR co-receptor CD19 was implied as important for MZB cell differentiation, since knock-out of CD19 in mice fully obstructed MZB cell development (Lechner et al., 2021; Martin and Kearney, 2000; Sato et al., 1995). Furthermore, the BAFF receptor has been shown to positively regulate FoB cell development from T2 cells, through synergism with BCR signaling and induction of the non-canonical NfκB pathway (Cancro, 2009; Pillai and Cariappa, 2009). In contrast, mice deficient for components of the canonical NfκB pathway, such as p50, c-Rel or IκBα, showed attenuated MZB cell differentiation (Cariappa et al., 2000; Ferguson and Corley, 2005; Pillai and Cariappa, 2009; Sasaki et al., 2006), suggesting that specification of the MZB cell fate is regulated by canonical NfκB signaling. Lastly, abundant research over the last two decades established the activation of the Notch2 signaling pathway as an indispensable event for proper MZB cell development (Cariappa et al., 2001; Cinamon et al., 2008, 2004; Gibb et al., 2010; Hampel et al., 2011; Hozumi et al., 2004; Kanayama et al., 2005; Lechner et al., 2021; Martin and Kearney, 2000; Oyama et al., 2007; Pillai and Cariappa, 2009; Saito et al., 2003; Simonetti et al., 2013; Tan et al., 2009; Tanigaki et al., 2002; Tanigaki and Honjo, 2007). These studies and the role of Notch2 in MZB cell differentiation are reviewed in more detail in *chapter 1.3.4*.

Pillai and Cariappa's model of splenic B cell maturation has been challenged by many follow-up studies, in an attempt to broaden the view of a binary cell fate decision in T2 cells. In this sense, it has been suggested that MZB cell development could potentially happen at later stages of B cell development i.e. from fully mature FoB cells as their precursors (Agenès and Freitas, 1999; Dammers et al., 1999; Gómez Atria et al., 2022;

Srivastava et al., 2005a, 2005b; Vinuesa et al., 2003). Other research groups have postulated a plasticity between one common precursor cell population and the mature FoB and MZB cells (Allman et al., 2004). In this regard, the possibility has been discussed that a fraction of mature recirculating FoB-II cells can act as precursors for MZB cells (Cariappa et al., 2007). FoB-II cells are thought to directly feed into the pool of MZPs, where they potentially act as reservoir for the mature MZB lineage (Pillai and Cariappa, 2009). Moreover, there was evidence that strong Notch2-signaling starts in these FoB-II cells rather than in T2 cells (Liu et al., 2015), suggesting that FoB cells are the precursors for MZP and terminally developed MZB cells. Most recently, our lab could definitively prove this hypothesis by showing that transplantation of highly-purified mature FoB cells ($CD23^{high}CD21^{low}$) into immunocompetent mice led to generation of donor-derived MZB cells via an intermediate MZP stage (Lechner et al., 2021).

1.2.2 Splenic architecture and B cell localization sites

FoB and MZB cells have distinct spatial localization sites in the spleen, which provide them their unique immunological features. According to structure and function, the spleen is divided into two major regions (*Fig. 3*): the red pulp (RP), responsible for filtering out aged or dead red blood cells (RBCs) and the white pulp (WP), which is the region inside and around lymphoid follicles and executes the surveillance of pathogens (Cyster, 2000; Lewis et al., 2019). The WP is compartmentalized into a T cell zone (TCZ) and B cell-rich zone (BCZ). The bridging channel (BC) is a connecting extension between the RP and WP and contains mostly T cells and antibody-secreting cells, but also some dendritic cells (DCs). The purpose of the BC is for activated B and T lymphocytes to enter or exit the WP and migrate via the marginal zone (MZ) to the RP (Bajénoff et al., 2008; Lewis et al., 2019; Mebius and Kraal, 2005) (*Fig. 3*). The BCZ comprises B cell follicles, which apart from FoB cells also contain other cells important for the survival and activation of B cells (e.g. follicular dendritic cells (FDCs) crucial for antigen presentation to FoB cells) (Lewis et al., 2019). During an active immune response, the BCZ is also the host for specialized structures called germinal centers (GCs). Blood entry from the circulation happens through the splenic artery inside the follicle and is subsequently administered via arterioles throughout the spleen. The terminal arterioles end up in the MZ sinus, from where part of the blood is drained into the MZ, before being recollected into the venous sinusoidal system and returned into the circulatory system (Cyster, 2000; Lewis et al., 2019). The MZ is a specialized, blood-perfused area, which spatially separates the RP from the WP, and is missing in lymph node follicles. It hosts the innate-like MZB cells (Lewis et al., 2019), which together with DCs bind and transport blood-borne pathogens to resident FoB and T cells in the WP (Arnon et al., 2013; Calabro et al., 2016;

Lewis et al., 2019). Apart from MZB cells, the MZ contains two types of macrophages: marginal metallophilic macrophages (MMM) and MZ macrophages (MZM) (*Fig. 3*). MMMs delineate the borders of the MZ, whereas MZMs are scattered throughout the MZ, but both actively contribute to the filtering of blood (Davies et al., 2013; Lewis et al., 2019; Mebius and Kraal, 2005).

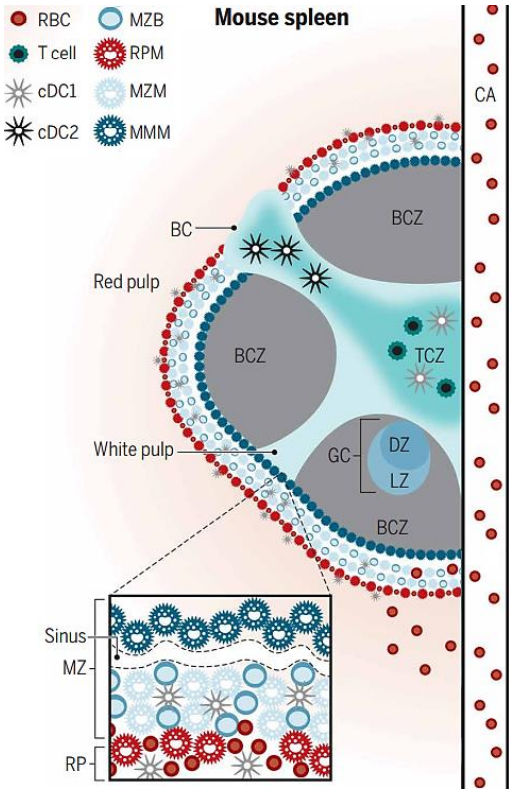

Fig. 3: Murine splenic architecture depicting lymphocytes and their localization. Modified scheme of the splenic architecture, based on Fig. 1 from the Review "Structure and function of the immune system in the spleen" published in *Science Immunology* by Lewis, Williams and Eisenbarth, 2019 (Lewis et al., *Sci. Immunol.* 4, 2019). Exclusive Copyright license is given by the American Association for the Advancement of Science.

A MZ structure containing MZB cells has also been proposed to exist in human spleens. However, the human splenic architecture is more complex because the lymphocyte follicles contain a substructure, called perifollicular area (Cerutti, Cols and Puga, 2013; Lewis, Williams and Eisenbarth, 2019). Due to limited implementation of advanced imaging techniques on the human spleen, the extent to which the mouse and human MZ functionally and structurally resemble each other remains unclear to date (Lewis et al., 2019).

1.2.3 B cell activation

The naïve B cell subsets usually remain in a resting state, until they encounter their cognate antigen. B cell activation is initiated by the binding of antigen to the BCR, ultimately leading to production of plasma cells and release of soluble antibodies (Doherty et al., 2018; Zhang et al., 2018). Depending on the nature of the antigen, the place where antigen encounter happens and the accompanying co-stimulatory signals by other immune cells, two mechanisms of B cell activation may occur, each one specific to the targeted B cell population (FoB or MZB cells) (Kenneth M. Murphy, 2016; MacLennan et al., 1997). If upon antigen recognition by the BCR, B cell activation and plasma cell production happens in the absence of T-cell-mediated support, a T-cell-independent (TI) immune response will be activated. If accessory signals come from the T-cell-receptors (TCRs) on $CD4^+$ T helper cells and from professional antibody-presenting cells (APCs),

a T-cell-dependent (TD) immune reaction will take place (Doherty et al., 2018). These two different routes, which determine the outcome of B cell activation, are reviewed in more detail in *chapters 1.2.3.1* and *1.2.3.2* below.

1.2.3.1 T-cell-independent (TI) immune response

The TI immune response is mediated by innate-like B1 and MZB cells (Alugupalli et al., 2004; Haas et al., 2005; Martin et al., 2001). Its main purpose is to overpass the time gap until the high-affinity, GC-derived antibody response driven by FoB cells is initiated (Hsu et al., 2006; MacLennan et al., 2003; Martin et al., 2001). Unlike the TD immune response, the TI immune reaction does not call for affinity maturation of BCRs and has a dispensable role in the production of long-lived plasma cells (PCs) and memory B cells (MBCs). Thus, it provides an early, rapid and rather unspecific reaction to the pathogen. The TI immune response can be triggered by diverse pathogens, which are classified into TI type 1 and type 2 antigens. TI-1 antigens, such as the lipopolysaccharide (LPS) cell wall component from gram-negative bacteria, can be directly bound to both BCRs and Toll-like-receptors (TLRs), regardless of antigen specificity (Bekeredjian-Ding and Jego, 2009; Minguet et al., 2008; Peng, 2005; Rawlings et al., 2012). TI-type 2 antigens include viral capsids and polysaccharides from cell walls of encapsulated bacteria. They exhibit highly repetitive structures and bind to several antigen-specific BCRs at the same time, causing extensive cross-linking and activation of the BCR/Btk signaling cascade (Liao et al., 2017; Mond et al., 1995; Vos et al., 2000). B cell activation by TI antigens also modifies the expression of receptors for chemoattractants: it induces the upregulation of CXCR4, the downregulation of CXCR5, S1PR1 and CCR7, and alters the expression of several cell-to-cell adhesion molecules (e.g. ICAMs, VCAMs), in a way that will provide unhinged mobility to the activated B cells (Cinamon et al., 2004; Hargreaves et al., 2001; Lo et al., 2003; Zaretsky et al., 2017) (*Fig. 4A*). Thus, they can move towards the outer T-cell zone, where they proliferate and expand their size, becoming B cell blasts. After two cell cycles, the B cell blasts that have been induced to become plasmablasts will migrate from the T-cell zone towards the RP, where they group into structures called extrafollicular foci (EF) and further develop into short-lived, low-affinity PCs (Hsu et al., 2006; MacLennan et al., 2003). Most of these plasmablasts and plasma cells are capable of IgM and IgG3 antibody secretion (Cerutti et al., 2013; Gray et al., 1996; MacLennan et al., 2003; Zhang et al., 2018) (*Fig. 4A*).

1.2.3.2 T-cell-dependent (TD) immune response

FoB cells are the main executers of the TD immune response, even though MZB cells have also been suggested to respond to TD antigens and to join germinal centers (GCs) inside splenic follicles (Song and Cerny, 2003). TD immune reactions can be triggered

by viruses, parasites, whole cells, soluble proteins or haptens conjugated to proteins, such as NP-CGG (Liao et al., 2017; Stein, 1992). To encounter a TD antigen, FoB cells are constantly patrolling through the blood and secondary lymphoid organs (SLOs), where they look for APCs with a full, unprocessed antigen exposed on their surface (Cyster, 2010, 2005; Cyster and Schwab, 2012; Zhang et al., 2018). Upon ligation by the BCR, the antigen becomes ingested, internally processed and presented on surface major histocompatibility complex (MHC) class II proteins (Carrasco and Batista, 2007; Lanzavecchia, 1990) (*Fig. 4B*). This process triggers BCR signaling, accompanied by upregulation of the CCR7 chemokine receptor, which navigates FoB cells towards the B-/T- cell zone border in the follicle, where its ligands, chemokines CCL19 and CCL21, are highly enriched (Förster et al., 2008, 1999; Reif et al., 2002). In parallel with FoB cell activation, $CD4^+$ T cells within the T-cell zone are also activated because they possess TCRs specific for processed parts of the same antigen. They recognize the antigen presented via MHC-II on B cells and become armed T helper (T_h) cells (*Fig. 4B*). At the same time, the CXCR5 chemokine receptor is upregulated, which triggers the migration of T_h cells towards the B-cell zone along the gradient of its ligand CXCL13 (Haynes et al., 2007). This coordinated migration of B and T cells, specific for the same antigen, positions both cell types at the interface between the T- and B- cell zone and enhances the chances for interaction (Oracki et al., 2010). The MHCII-peptide complex on FoB cells is bound by the TCR on activated T_h cells, resulting with the formation of an "immunological synapse" (Basso et al., 2004; Duchez et al., 2011; van Kooten and Banchereau, 2000). Here, an interplay of several co-stimulatory receptor-ligand molecules induces an adequate immune response by activating intracellular signaling pathways in both B and T cells (reviewed in (Dustin, 2014)). One crucial interaction is between the CD40 receptor on B cells and CD40 ligand (CD40L) on T_h cells (Basso et al., 2004; van Kooten and Banchereau, 2000). In addition, secretion of stimulatory cytokines by T_h cells, such as interleukins (IL) 2, 4, 12 and 21, provide further lymphocyte co-activation (Dustin, 2014; Kenneth M. Murphy, 2016; Nelms et al., 1999; Peng et al., 1996) (*Fig. 4B*). Following these signaling events, B and T cells proliferate at the B-/T- cell boundary for several days, until the FoB cells choose to either enter the GC reaction or to migrate outside and form extrafollicular foci (EF) (Fairfax et al., 2008; MacLennan et al., 2003; Oracki et al., 2010; Paus et al., 2006; Victora and Nussenzweig, 2012; Zhang et al., 2018) (*Fig. 4B*). The decision between the two paths is dependent on the BCR affinity for the antigen: FoB cells carrying high-affinity BCRs move towards the RP and produce low-affinity, short-lived antibody-secreting cells; FoB cells with a lower antigen-affinity reenter the follicle and seed into GCs (MacLennan et al., 2003; Oracki et al., 2010).

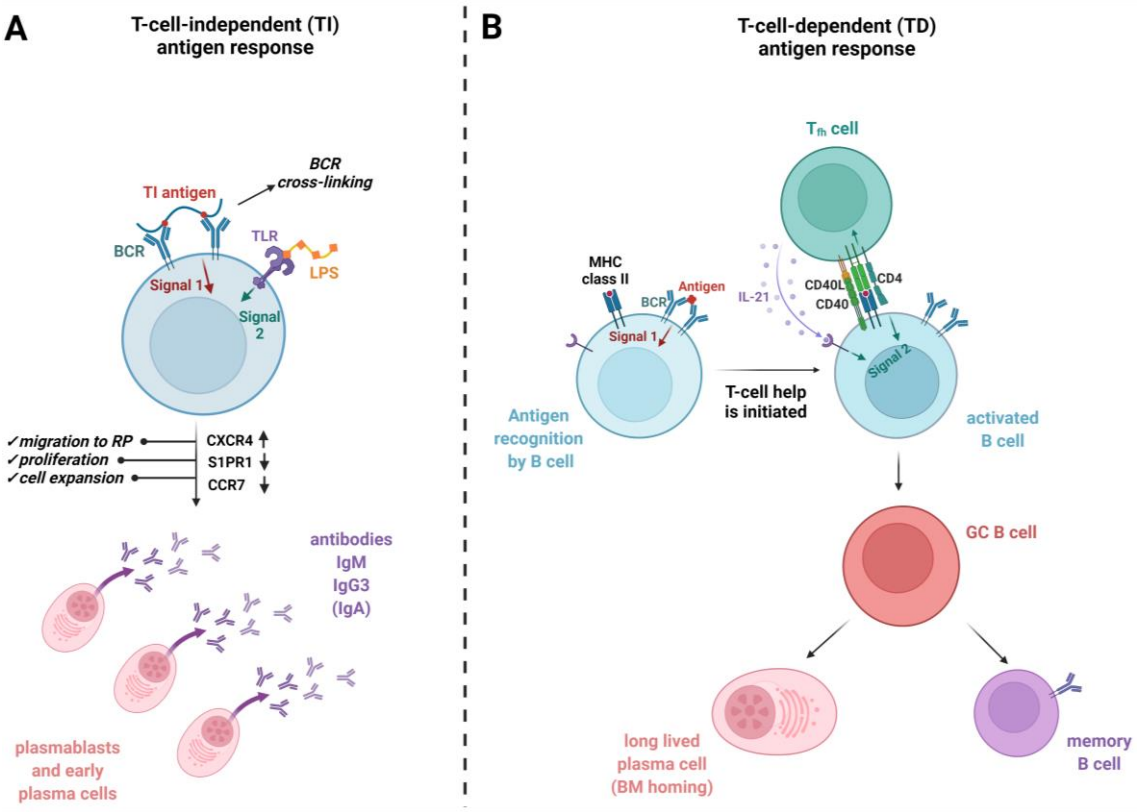

Fig. 4: T-cell-independent (TI) and T-cell-dependent (TD) pathways of B cell activation and plasma cell production. (A) TI immune responses do not require T cell help. B cells are independently activated by TI antigens, like TI-1 LPS which binds to TLR4 (signal 2) or TI-2 repetitive antigens (e.g. polysaccharides) which bind to several BCRs and cause crosslinking (signal 1), resulting with B cell migration, proliferation and expansion. TI reactions produce bursts of plasmablasts and short-lived IgM- or IgG3-secreting plasma cells. **(B)** TD immune response is initiated upon BCR ligation by antigen, which upon processing is presented on the cell surface as a MHC-II:peptide complex. Co-stimulation is provided by T cells, which recognize the MHC-II:peptide complex via the TCR. Additional activation signals come from the CD4 co-receptor on T cells, the CD40:CD40L interaction between B and T cells, as well as secretory cytokines (e.g. IL21) produced by T cells, forming a so-called immunological synapse. These events lead to GC formation and subsequent high-affinity long-lived plasma cell and memory B cell production (Figure created in BioRender Premium, biorender.com)

GCs are the hallmark of the TD immune response and their purpose is to generate high-affinity effector cells against the pathogen (Mesin et al., 2016; Victora and Nussenzweig, 2012). They localize at the B-/T- cell zone border in the spleen, lymph nodes and Peyer's Patches. The early GC is fully formed between day 5 and 7 of antigen encounter and reaches a mature peak between day 11 and 14. While most GCs persist over several weeks, in some cases they can be sustained for a few months (Victora, 2014). Two important processes take place in the GC: (1) affinity maturation via somatic hypermutation (SHM) and (2) class switch recombination (CSR). Both require the action of the activation-induced cytidine deaminase (AID) and DNA repair mechanisms (Honjo et al., 2002;

Revy et al., 2000; Shlomchik and Weisel, 2012). SHM introduces changes in the variable Ig gene regions, resulting with modifications in the antigen-binding BCR domain. Through repeated rounds of SHM with a mutation rate of 10^{-3}/nt, the repertoire of BCR antigen specificity is strongly diversified (Larson and Maizels, 2004; Liu et al., 1997; Teng and Papavasiliou, 2007). On the other hand, CSR was proposed to happen rather infrequently inside the GC. Instead, most CSR events are induced in activated pre-GC cells, prior to the differentiation into GC B cells and the onset of SHM (Roco et al., 2019). The CSR targets the IgH constant gene regions, leading to replacement of μ and δ constant regions with either γ, ε or α. This process is known as isotype switching and results with the generation of different PCs and antibody isotypes, such as IgG1, IgG3, IgA and IgE, each with diverse effector functions (Kenneth M. Murphy, 2016; Muramatsu et al., 2000; Yu and Lieber, 2019). Another special quality of the GC is its compartmentalization into a dark (DZ) and light zone (LZ). Entry into the GC happens through the DZ, where centroblasts proliferate and expand very rapidly, while undergoing affinity maturation via SHM to improve their antigen specificity (Mesin et al., 2016). The emerging hypermutated B cell clones then move into the LZ, where they are called centrocytes. Here, the BCR affinity is tested, so that cells that bind most tightly and specifically to the antigen are positively selected (Heesters et al., 2014). Only B cells with high affinity BCRs can recognize the antigen presented on FDCs and can outcompete the remaining cells for the limited T_{fh} cell help in the LZ. These cells become instructed towards one of three known cell fates: (1) high-affinity PCs, (2) memory B cells (MBCs) and (3) persistent $cMyc^{+}CD30^{+}$ LZ-GC cells, which re-enter the DZ for further affinity maturation (Calado et al., 2012; Dominguez-Sola et al., 2012; Mesin et al., 2016; Weniger et al., 2018). The GC-derived PC production predisposes higher BCR affinity, Blimp1 upregulation and high amounts of CXCR4, which guides the PCs along the CXCL12 gradient towards GC exit through the DZ (Suan et al., 2017). The remaining cells with a lower-affinity BCR exit the GC through the LZ as MBCs. The PCs are long-lived effector cells that migrate through the blood and home to the bone marrow. They secrete affinity-matured antibodies of different Ig subclasses, which neutralize pathogens. MBCs, as their name suggests, are capable of long-term protective immunological memory. They remain in a resting state in peripheral lymphatic tissue for long periods of time, but can be rapidly reactivated upon antigen challenge, leading to a highly-specific secondary immune response (MacLennan et al., 2003; Mesin et al., 2016).

1.2.3.3 Plasma cell (PC) differentiation: stages and molecular mechanisms

Over 7 decades of fruitful studies have made it clear that PCs are the result of B cell differentiation. The widely accepted model of PC differentiation relies on two groups of

transcription factors (TF), which are mutually exclusive and repress each other's function (Oracki et al., 2010). On one side are TF that mediate sustained B-cell gene expression and suppress PC production, such as Pax5 and Bcl6. On the other side, Blimp1, Irf4 and Xbp1 govern the PC gene program and induce PC differentiation (Oracki et al., 2010; Shapiro-Shelef and Calame, 2005). Ex vivo MZB cells were shown to possess signs of early gene expression changes, typical for PC differentiation. In comparison to FoB cells, MZB cells expressed higher levels of Blimp1 and lower amounts of Bcl6, which is likely the predisposition for them to respond very rapidly to pathogens and produce bursts of early PCs in the first 3-4 days of antigen encounter (Fairfax et al., 2008, 2007; Oracki et al., 2010).

The B cell identity is founded and maintained by Pax5, which is expressed during early B cell development and in all splenic mature B cells (Boller and Grosschedl, 2014; Medvedovic et al., 2011; Nutt et al., 2001; Oracki et al., 2010). Pax5 establishes its restricted role to B cells through activation of target genes involved in Ig gene rearrangement and BCR signaling (via CD19, B-cell linker BLNK and CD79a), as well as induction of AID activity in the GC during SHM and CSR (Gonda et al., 2003; Oracki et al., 2010; Schebesta et al., 2007). Simultaneously, Pax5 inhibits signature gene transcription for PC differentiation, by repressing Ig heavy and light chain genes and Xbp1 (Delogu et al., 2006; Horcher et al., 2001; Linderson et al., 2004; Nera et al., 2006; Oracki et al., 2010; Revilla-I-Domingo et al., 2012; Rinkenberger et al., 1996; Roque et al., 1996; Singh and Birshtein, 1993). Bcl6 is required for the formation of germinal centers and maintains the expression of GC-specific genes by suppressing cell cycle- and PC-specific genes (Alinikula et al., 2011; Alinikula and Lassila, 2011; Ci et al., 2009; Dent et al., 1997; Robinson et al., 2020; Tunyaplin et al., 2004). The main function of Bcl6 is to interfere with Blimp1 expression, in order to prevent premature differentiation into antibody-secreting cells (Garis and Garrett-Sinha, 2021; Reljic et al., 2000; Shaffer et al., 2000). Blimp1 is a crucial switch between B cell identity and PC development, as it suppresses mature B cell genes (Pax5, Ciita, Id3) and GC-specific genes (Bcl6 and Aicda), while simultaneously inducing the PC-specific gene Xbp1 (Lin et al., 2002, 1997; Martins and Calame, 2008; Sciammas and Davis, 2004; Shaffer et al., 2002). Additionally, Blimp1 upregulates chemokine receptor CXCR4, which drives plasmablast migration and subsequent PC homing to the bone marrow (Sciammas and Davis, 2004). Moreover, Blimp1 has been shown to be critical in the mature PC development and the long-term maintenance of PCs, but it is not necessary to initiate PC differentiation from activated B cells (Kallies et al., 2007; Oracki et al., 2010; Shapiro-Shelef and Calame, 2005). This is the job of Irf4, which has an implied role in initiation of both GC and PC differentiation, however, its expression levels in activated B cells determine their subsequent cell fate. A moderate, transient

expression of Irf4 induces Bcl6 expression and promotes GC initiation, but not subsequent GC formation and maintenance (Klein et al., 2006; Ochiai et al., 2013). If there is a persistently high, above-threshold Irf4 expression in B cells, then this will be sufficient to directly repress Bcl6 and induce Xbp1, thus initiating PC differentiation at the expense of GC formation (Saito et al., 2007; Shapiro-Shelef et al., 2003; Shapiro-Shelef and Calame, 2005). Work with Irf4-deficient mice revealed barely any detectable PC responses in these mice, suggesting they are devoid of the whole Blimp1-dependent PC program (Klein et al., 2006; Mittrücker et al., 1997; Oracki et al., 2010; Sciammas et al., 2006). Thus, Irf4 precedes Blimp1 in the mechanism that regulates PC development over several cell stages: Irf4 starts the PC gene program in activated B cells and maintains it in proliferating B cell blasts, up until the plasmablast stage. Then, Irf4 is lost and Blimp1 gradually takes over in the final stages of mature, short- and long-lived PC development. Each of these PC stages are further characterized by different cell surface marker expression. For instance, typical B cell markers MHCII, CD19 and B220 are highly expressed on activated B cells and pre-plasmablasts, but start to be downregulated on plasmablasts, so that mature PCs are completely negative for all of them. In parallel, typical PC markers CD138, CXCR4 and TACI are missing in activated B cells and pre-plasmablasts, but their levels progressively increase from the plasmablast stage onwards (Fairfax et al., 2008; Lalor et al., 1992; Oracki et al., 2010; Pracht et al., 2017; Smith et al., 1996). By staining for these surface markers in flow cytometry, the different stages of PC development in mice can be identified, separated and followed over time.

1.3 Notch receptor signaling

The family of Notch receptors and their core signaling pathway are highly conserved throughout evolution (Radtke et al., 2010). The Notch signaling pathway got its name from an early study by Thomas Hunt Morgan, who described the existence of fruit flies with notches at the edges of their wing blades (Morgan, 1917). Several decades later, it was proven that this phenotype was caused by partial loss of function of the *Drosophila Notch* gene (Kidd et al., 1986; Wharton et al., 1985). Notch signaling is involved in a wide range of biological processes, such as cell survival, proliferation, differentiation and regulation of cell fate decisions (Alberi et al., 2013; Fortini et al., 2014; Fouillade et al., 2012; Koch et al., 2013; Noah and Shroyer, 2013; Perrimon et al., 2012; Zanotti and Canalis, 2013). However, the impact of Notch can differ in different biological systems, organs and tissues, at times leading to opposed cellular responses (Bray, 2006).

1.3.1 Notch receptors: structure and activation

The family of Notch receptors in mammals consists of four members (Notch1, 2, 3 and 4), which share structural and sequence homologies and can interact with five ligands of the Delta-like (Dll) or Jagged family (Dll1, 3, 4 and Jagged1, 2) (Radtke et al., 2013, 2010; Saito et al., 2003). The interaction between a Notch receptor and its ligand results with activation of the Notch signaling cascade (Bray, 2006), suggesting that signaling activity only happens upon cell-to-cell contact. Structurally speaking, all Notch receptors are heterodimers, composed of an extracellular ligand-binding part (Notch-ECD) and a transmembrane/intracellular domain (Notch-TM/ICD), anchoring the receptor in the plasma membrane (Notch-TM) and mediating target gene transcription (Notch-ICD) (Chillakuri et al., 2012) (*Fig. 5*). Prior to being presented on the cell surface as single-pass type 1 transmembrane glycoproteins, the Notch receptors go through an important maturation step. This is introduced by a Furin-like convertase, which mediates S1 proteolytic cleavage of Notch precursors in the *trans*-Golgi network (Blaumueller et al., 1997; Lake et al., 2009; Logeat et al., 1998). The S1 cleavage is believed to be crucial for the production of the mature receptors and their cell surface expression (Garis and Garrett-Sinha, 2021). However, the precise function and significance for signaling remains to be determined, as this is still controversial and differs among Notch family members. Following S1 cleavage, the N-terminal (Notch-ECD) and C-terminal part (Notch-TM/ICD) of the Notch protein remain non-covalently associated via disulfide (S-S) bridges, forming a heterodimer receptor (Blaumueller et al., 1997; Logeat et al., 1998; Schroeter et al., 1998; van Tetering and Vooijs, 2011). The extracellular domain (ECD) contains 29 to 36 epidermal growth factor (EGF)-like repeats responsible for ligand recognition and binding (*Fig.5*). This part of the ECD exhibits differences in size among different Notch family members. Next, there are three cysteine-rich LIN12-Notch repeats (LNR) that are recipients of intracellular signals during development in various species. Following it, there is a hydrophobic stretch of amino acids, which together with the LNR forms a negative regulatory region (NRR) adjacent to the cell membrane. The NRR has an essential function in preventing ligand-independent activation of Notch receptors, by protecting the S2 cleavage site from metalloproteases (Kopan and Ilagan, 2009). The Notch-ICD contains several functional elements important for signal transduction: a RAM domain (RBPJ-association molecule), six Ankyrin repeats (ANK) for interaction with the RBPJ transcription factor (termed CBF in humans), a pair of nuclear localization signals (NLS) important for guidance and localization of Notch-ICD in the nucleus upon release, a transactivation domain (TAD) and a conserved proline-glutamine-serine-threonine-rich (PEST) region, which regulates protein stability (Gordon et al., 2008; Radtke et al., 2010) (*Fig. 5*).

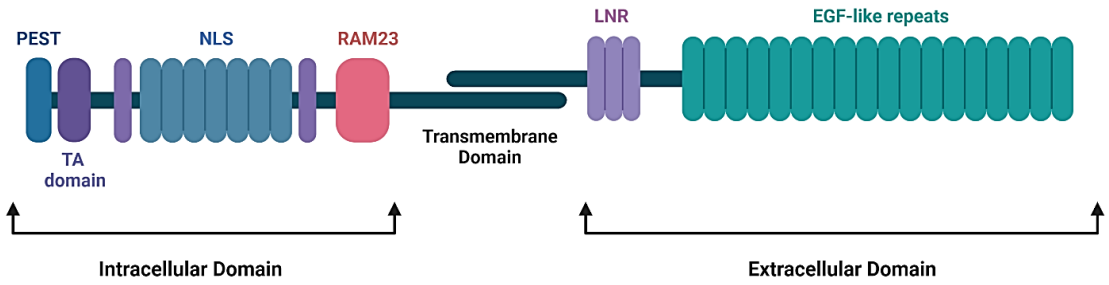

Fig. 5: Structure of the Notch receptor (on the example of the Notch2 receptor). All mammalian Notch receptors (1-4) contain an extracellular (ECD) domain composed of up to 36 EGF-like repeats for proper ligand-binding, followed by three LNR domains, which make sure to prevent ligand-independent receptor activation. The heterodimerisation domain (HD) is found in the transmembrane domain (TM) and links the ECD with the intracellular domain (ICD). The ICD starts with a RAM23 domain, followed by Ankyrin repeats for RBPJ binding and a pair of nuclear localization signals (NLS) for translocation into the nucleus upon cleavage. The C-terminal end contains a transactivation domain (TAD) typical for Notch1 and 2 only, and a PEST domain for protein stabilization (Illustration created BioRender Premium, biorender.com).

Notch signaling stands out, compared to other conserved signaling cascades, due to its unique mechanism of proteolysis. The interaction between the Notch-ECD and its appropriate ligand expressed on a neighboring cell results with a regulated set of proteolytic cleavages that transform the transmembrane form of Notch into a nuclear transcriptional co-activator (*Fig. 6*). Thus, crosslinking of the ECD leads to the S2 cleavage, executed by metalloproteinase domain-containing ADAM enzymes (ADAM10 and 17) at an extracellular site, which becomes exposed through conformational changes induced by ligand-binding (Logeat et al., 1998; Mumm et al., 2000; Mumm and Kopan, 2000; van Tetering et al., 2009). This S2 cleavage causes membrane shedding of Notch-ECD, which is endocytosed by the ligand-providing cell. This is followed by S3 cleavage mediated by a γ-secretase multicomplex, which cuts within the membrane-spanning domain (TM) and releases the Notch-ICD from the plasma membrane (Schweisguth, 2004; van Tetering and Vooijs, 2011). Notch-ICD then translocates into the nucleus, where it promotes transcriptional activation through direct interaction with the DNA-binding protein RBPJ (Nowell and Radtke, 2017; Radtke et al., 2013, 2010). Without Notch-ICD, RBPJ acts as a transcriptional repressor of Notch target genes. It is still DNA-bound, but is clustered together with histone deacetylases and repressor proteins (Kopan and Ilagan, 2009; Kovall et al., 2017; Radtke et al., 2010). Thus, by direct binding to RBPJ, Notch-ICD promotes the displacement of co-repressors and the recruitment of co-activators, such as MAML1-3 and p300, thereby inducing Notch target gene transcription (Nowell and Radtke, 2017) (*Fig. 6*). Among the most prominent target genes of Notch-ICD are those of the hairy enhancer of split (*Hes*) and the hairy related (*Hey*) gene families (reviewed in (Borggrefe and Oswald, 2009)).

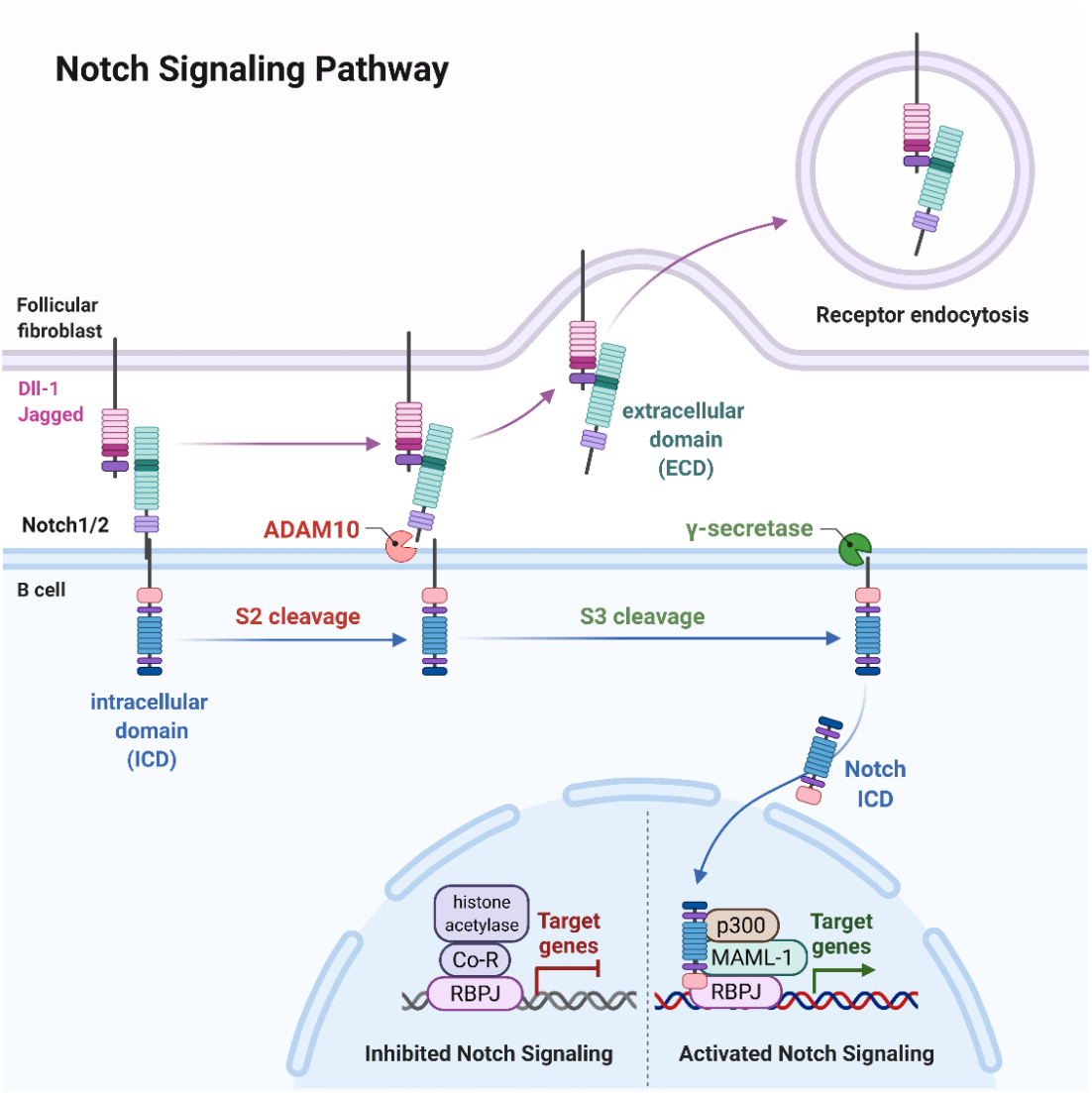

Fig. 6: Scheme of the Notch signaling pathway upon ligand-induced receptor activation. Upon interaction with the Dll-1-ligand expressed on a neighboring cell (cell-to-cell contact), Notch receptor activation leads to two consecutive proteolytic cleavages: S2 mediated by ADAM10 metalloproteases in the extracellular domain, followed by S3 executed by γ-secretase within the TM domain. Both cleavage events together lead to a release of Notch-ICD from the plasma membrane and translocation to the nucleus, where it binds to the DNA-binding transcription factor RBPJ and recruits further co-activators MAML-1 and p300, ultimately activating Notch target gene transcription (Illustration created with BioRender Premium, biorender.com).

1.3.2 Regulatory mechanisms of Notch signaling activity

The Notch signaling pathway is sensitive to receptor/ligand dosage and requires fine-tuning of its activity (Bray, 2006). The *Notch* gene in mammals exhibits haploinsufficiency, indicating that two copies of the gene are necessary to preserve sufficient and normal receptor function. Consequently, inactivation of one copy of *Notch2* or *Notch1* is associated with Alagille's syndrome and a type of aortic disease, respectively (Garg et al., 2005; McDaniell et al., 2006; Oda et al., 1997). On the other hand, overexpression

of Notch through constitutive activation of Notch-ICD can lead to cancerous transformations and B- and T-cell malignancies, such as lymphomas (Ellisen et al., 1991; Jundt et al., 2002; Kiel et al., 2012; Koch and Radtke, 2007; Lee et al., 2009; Rosati et al., 2009; Rossi et al., 2012; Trøen et al., 2008). Thus, to avoid diseases, it is important to keep Notch signaling activity under tight spatiotemporal control. For this purpose, multiple regulatory mechanisms at different levels have evolved in mammals (Bray, 2006; Brou, 2009; Kopan and Ilagan, 2009; Schweisguth, 2004).

One mechanism is to restrict the expression of Dll/Jagged ligands on neighboring cells or the expression of Notch receptors on the cell surface through endocytosis and lysosomal degradation. When ligand is absent, surface Notch becomes continuously endocytosed and either trafficked to late endosomes for degradation or recycled to the plasma membrane (Brou, 2009; Chastagner et al., 2008; Jehn et al., 2002; McGill et al., 2009). Similarly, Notch ligands can also be cleared from cells by endocytosis and degradation, through the activity of E3 ubiquitin ligases *Neur* and *Mib* (reviewed in (Dutta et al., 2022)). The internalization of active Notch receptors to the lysosome, where they are degraded, is an especially important mechanism of desensitization. In mammalian cells, the E3 ubiquitin ligases *Itch* and *Deltex* have been shown to target Notch for endocytosis. *Itch* in particular contains special phospholipid-binding motifs which targets it to the plasma membrane, several motifs involved in its interaction with Notch-ICD, and one domain with ubiquitin ligase activity. In this way, *Itch* promotes Notch ubiquitination and subsequent degradation, thus regulating Notch-ICD signaling activity (Brou, 2009; Qiu et al., 2000; Schweisguth, 2004).

Another elegant way of regulating Notch activity is through post-translational modifications, such as the O-glycosylation of the Notch-ECD (Takeuchi and Haltiwanger, 2014, 2010). Fringe glycosyl-transferases prevent Notch receptor signaling induced by Jagged through addition of N-acetyl glucosamine to several EGF-like repeats in the Notch-ECD. Jagged can still undisturbedly bind to Notch-ECD, but their interaction is non-productive (Benedito et al., 2009; Yang et al., 2005). At the same time, Fringe glycosylation increases Dll-Notch binding, thereby potentiating Dll-mediated Notch signaling (Besseyrias et al., 2007; Chen et al., 2001; Haines and Irvine, 2003; Hicks et al., 2000; Moloney et al., 2000; Yang et al., 2005). Even after significant research efforts, the exact mechanisms which Fringe uses to modulate Notch signaling are still not completely clear.

An additional mechanism of negative regulation may act on the transcriptional level i.e. on the level of Notch-ICD/RBPJ binding, thus modulating the nuclear transcriptional activator complex. It is possible that the Notch-ICD alone may compete with repressor proteins for the interaction with RBPJ. Alternatively, the Notch-ICD/RBPJ/MAML1 co-activator complex as a whole may directly compete with RBPJ co-repressor complexes for

DNA binding (Schweisguth, 2004). Kuroda *et al.* suggested that the repressor protein MINT is one candidate, which directly outcompetes Notch-ICD for the binding to RBPJ, thus obstructing the formation of the Notch transcriptional activation complex and silencing Notch signaling activity (Kuroda et al., 2003). It is still not understood whether the density of the chromatin, around the DNA segment where Notch-ICD/RBPJ/MAML1 binds, also contributes to the regulation of these events. Lastly, activated Notch signaling can be efficiently switched off through proteasomal degradation of Notch-ICD. This mechanism controls the half-life of Notch protein activity. Upon nuclear translocation, Notch-ICD typically becomes targeted for degradation via ubiquitination of its PEST stability domain, leading to termination of further target gene transcription (Deimling et al., 2007; O'Neil and Look, 2007). Proteasomal degradation of Notch is mediated by members of the SCF-type ubiquitin ligase family. One prominent example is *Fbw7* (F-box containing protein), also known as Sel-10, which binds Notch-ICD together with three other components of the SCF complex and mediates its ubiquitination and degradation (Sancho et al., 2013; Schweisguth, 2004; Wu et al., 2001). Collectively, Notch signaling seems to be regulated through a complex mechanistic network, targeting both ligand/receptor interactions and Notch-ICD signaling strength, in order to achieve a Notch-high or Notch-low state in cell-specific, spatial and temporal manner.

1.3.3 CBF:H2B-Venus mouse model: a reporter of Notch signaling activity

The transcription factor CBF1 (=RBPJ) is an evolutionary conserved component of the Notch signaling pathway and a direct mediator of Notch target genes activation by binding to cis-regulatory regions (CBF1 binding sites) in their promoters (Kovall et al., 2017). In this sense, CBF1 binding sites were deemed a suitable target for the production of reporter animals of Notch signaling at a single-cell resolution level. Nowotschin *et al.* designed the first mouse reporter strain, in which individual cells transducing a Notch signal through Notch-ICD could be visualized and tracked (Nowotschin et al., 2013). The CBF:H2B-Venus mouse strain was generated by a random insertion of a construct, in which four CBF1-binding sites are linked to the SV40 minimal promoter and are placed in front of a protein fusion, consisting of human histone H2B and the yellow fluorescent protein (YFP) isoform Venus. After endogenous activation of the Notch receptors, Notch-ICD translocates to the nucleus and binds through CBF1 (=RBPJ) to the CBF-binding sites, thus activating transgene expression (*Fig. 7*). The cells which express this transgene can be visualized in FACS as bright Venus-positive due to the expression of the nuclear-localized fluorescent protein (Nowotschin et al., 2013).

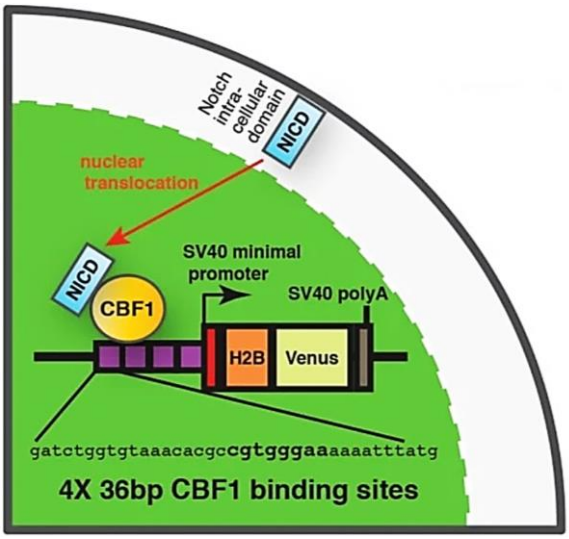

Fig. 7: Scheme of the CBF:H2B-Venus construct design, used to generate the transgenic Notch-reporter mouse model. The picture was extracted and adapted from Figure 1 of the original methodology article published by Sonja Nowotschin et al. in *BMC Developmental Biology* 2013, 13:15 (Nowotschin et al., 2013). The ectopic expression of Notch-ICD in cells activates the canonical Notch signaling pathway and leads to transgene expression by binding of Notch-ICD to the CBF-binding sites, directing the SV40 promoter to start the transcription of the H2B:Venus fusion gene. Cells expressing the transgene upon activation of the Notch pathway can be assessed using flow cytometry.

Roo and Staal reviewed the CBF:H2B-Venus mouse model and compared it to other existing reporter strains with regards to its eligibility for the examination of Notch signaling in adult hematopoietic stem cells (HSCs). They discussed that a disadvantage of this reporter model is the delayed expression of the histone-Venus fusion protein after the onset of Notch2 signaling and the endurance of the Venus protein (reviewed in (Roo and Staal, 2020)). Between 2017 and 2020, several research labs already made use of this Notch-reporter mouse model, in order to examine the effects of Notch signaling in various tissue and cell types during different cellular processes (Demitrack et al., 2017; Finn et al., 2019; Li et al., 2020; Salguero-Jiménez et al., 2018; Shawber et al., 2019). Even though the CBF:H2B-Venus Notch-reporter strain is increasingly being used in different fields of biology to study Notch signaling in different cell types (heart, lung, stomach, HSCs, placenta), it has yet to be employed in studies in immunology or B cell biology.

1.3.4 Notch signaling in MZB cell development

Even though both Notch1 and Notch2 are found on early B lymphocytes in the BM, mainly Notch2 is further expressed on mature B cells. In contrast, Notch1 is highly present in the T-cell lineage and drives T cell maturation, but Notch2 is dispensable (Saito et al., 2003; Tan et al., 2009; Walker et al., 2001; Witt et al., 2003a). An abundance of studies using different transgenic mouse models confirmed the absolute necessity of the

Notch2 signaling pathway in the differentiation of MZB cells. Accordingly, B-cell-specific knock-out of RBPJk (Tanigaki et al., 2002) or the Notch2 receptor itself (Saito et al., 2003), as well as loss-of-function of essential Notch2 signaling pathway components like the Notch receptor-cleaving enzyme ADAM10 (Gibb et al., 2010; Hammad et al., 2017) or the co-activator MAML1 (Oyama et al., 2007) all resulted with a severe loss of MZB cells, but no change in the amounts of FoB cells. The interaction of Notch2 with the Dll1-ligand was identified as the trigger for canonical Notch2/RBPJ/MAML1 pathway activation, which then drives MZB development (Hozumi et al., 2004). Consequently, knock-out or downmodulation of Dll1 also inhibited MZB cell differentiation, without affecting any other lymphocyte subsets (Hozumi et al., 2004; Moriyama et al., 2008). Interestingly, MZB development was shown to not only depend on the presence of functional Notch2 signaling and the Dll1-ligand. Also, changes in Notch2 surface receptor levels or in the Notch2-ICD signaling activity grossly influenced the efficiency of MZB cell generation. Indeed, B-cell-specific Notch2 haploinsufficiency ($Notch2^{fl/wt}$) was enough to cause a significant attenuation of MZB differentiation (Saito et al., 2003), whereas constitutively active Notch2IC signaling in B cells strongly shifted them towards the MZB cell fate at the expense of FoB cells, even when CD19 signaling was absent (Hampel et al., 2011). Lastly, murine splenic B cells deficient for MINT, a co-repressor of Notch2/RBPJ signaling, differentiated three times more efficiently into MZB cells with a concomitant decrease of FoB cells (Kuroda et al., 2003).

Since Dll-1 is the crucial ligand regulating Notch2 activation and the abundance of MZB cells, its expression on different splenic cell types was thoroughly examined over the years. At last, the Dll-1 ligand was conclusively proven to be expressed on fibroblastic stromal cells in the B cell follicle (Fasnacht et al., 2014) (*Fig. 6*), disproving previous indications of Dll-1 presence on splenic DCs, macrophages and endothelial cells of MZ and RP blood vessels (Hozumi et al., 2004; Moriyama et al., 2008; Tan et al., 2009). Thus, the splenic WP is the site where Notch2 activation and initiation of MZB cell differentiation takes place. It is believed that emerging transitional cells get a strong Notch2 signal through Dll-1 for the first time in the WP, after which they are selected for MZB cell differentiation. The Dll-1-Notch2 interaction starts with weaker binding, but is further strengthened by lunatic and manic fringe glycosyl-transferases, thus solidifying the MZB cell fate of transitional cells (Allman and Calamito, 2009; Pillai and Cariappa, 2009; Tan et al., 2009). In case transitional cells get a weaker Notch2 signal through Dll-1 interaction, which is not enhanced and dissipates quickly, then they are believed to be driven towards the FoB cell fate. Most recently, it was conclusively shown that MZB cell differentiation also happens beyond the transitional cell stages i.e. in the mature B cell population. In particular, mature FoB cells can fully convert their phenotype and change their

splenic localization to become typical MZB cells, if and when they receive the necessary above-threshold Notch2 signal in the B cell follicles (Gómez Atria et al., 2022; Lechner et al., 2021) (*Fig. 2B*). Our lab showed that the FoB to MZB conversion process was Notch2-signal-dependent, since induction of Notch2IC in mature FoB cells of CD19-KO mice led to new MZB cell differentiation and re-population of the otherwise empty MZ compartment (Lechner et al., 2021). Additionally, Gomez Atria *et al.* revealed that in lymphopenic spleens, the initiation of FoB to MZB cell transdifferentiation was dependent on the expression of Notch2 receptors on B cells and of Dll-1 Notch ligands by splenic Ccl19-Cre^{+} fibroblastic stromal cells (Gómez Atria et al., 2022). Even though these prior data provided strong evidence that FoB cells are precursors for MZB cells and there is undeniable plasticity between the mature B cell subsets, it still remains unclear how this trans-differentiation process is controlled, apart from its reliance on Notch2-Dll-1 signaling. Whether Notch2 synergizes with other signaling pathways and whether it predisposes the presence of certain B cell qualities and functions, in order to establish the correctly located mature MZB cell population, is still not completely understood and should be further researched.

2 Aims of the study

As already previously reviewed, earlier findings established that constitutive activation of Notch2 signaling in B cells has a strong differentiation-inducing potency towards the MZB cell lineage (Hampel et al., 2011), whereas conditional inactivation of Notch2 in B cells or the Dll-1-ligand in non-hematopoietic cells causes loss of MZB cells (Hozumi et al., 2004; Saito et al., 2003). This suggests that the Notch2 signal strength may regulate the MZB cell development. Recently published work by our group (Lechner et al., 2021) revealed that transplantation of purified FoB cells into immunocompetent recipients led to the appearance and generation of donor-derived MZB cells. Despite these strong evidence that FoB cells serve as precursors for MZB cells under physiological conditions, it is still elusive how this differentiation process is regulated in mice.

In order to clarify whether the Notch signal strength, possibly regulated by the level of Notch2 receptor expression on the cell surface or by the availability of Dll-1-expressing fibroblasts in the B cell follicle, plays a role in specifying the MZB cell fate, it should first be examined which B cell types receive a Notch signal during B cell development and maturation. In this sense, CBF:H2B-Venus Notch-reporter mice should be analyzed, which express the Venus fluorescent protein upon active Notch signaling. The Venus expression should be examined in different resting B lymphocytes from spleen and bone marrow.

Furthermore, the interplay between Notch2 and BCR-signaling has been shown to positively control MZB cell development (Lopes-Carvalho and Kearney, 2004; Martin and Kearney, 2000; Oliver et al., 1999; Pillai and Cariappa, 2009; Wen et al., 2005). Some existing data indicate that BCR signaling acts upstream of Notch2, thus priming transitional (T) cells to become receptive to Notch2 ligands (Hammad et al., 2017), as well as inducing the expression of Notch2 surface receptor on FoB cells (Lechner et al., 2021). Therefore, we now asked whether B cell activation through BCR and CD40 engagement leads to activation of Notch2 signaling and whether it drives FoB cells towards MZB cell development. To answer this question, it should be first determined which cell populations receive a Notch signal upon TD immunization. In a second step, it should be analyzed whether MZB cells are newly-generated in the course of TD immune responses in a Notch2-dependent manner. To this end, conditional Notch2IC-KI and Notch2-KO mice in combination with the GC-B-cell-specific strain Cγ1-Cre, as well as the respective control mice with unaltered Notch2 signaling, should be analyzed at different time points after TD immunization. The fate of the transgenic antigen-responding B cells should be closely followed, particularly in terms of their MZB cell surface marker expression and localization in the MZ.

3 Materials

Table 1 summarizes all recourses used in this study, including antibodies, commercially available kits, transgenic mouse models, analytical research instruments and software for scientific data analysis.

Table 1: List of critical reagents used in the study.

ANTIBODIES			
Name and conjugate, clone, dilution factor	**Company**	**Identifier (Cat#)**	**Application**
AA4.1-PE, AA4.1, 1:200	eBioscience	12-5892-82	FACS
Bcl6-AlexaFluor647, K112-91, 1:50	BD Biosciences	561525	FACS
Blimp1-PE, sc47732PE, 1:50	Santa Cruz	sc-13206 PE	FACS
BP-1 (Ly-51)-PE, BP-1, 1:50	BD Biosciences	553735	FACS
CAR (E1-1)-FITC, sc-56892, 1:25	Santa Cruz	sc-56892 FITC	FACS
CD1d-AlexaFluor647, 1B1, 1:200	BioLegend	123511	FACS
CD138-BV421, 281-2, 1:200	BD Biosciences	562610	FACS
CD138-PE, 281-2, 1:600	BD Biosciences	553714	FACS
CD19-BV510, 1D3, 1:200	BD Biosciences	562956	FACS
CD19-PeVio770, REA749, 1:200	miltenyi	130-112-037	FACS
CD21/CD35-BV421, 7G6, 1:200	BD Biosciences	562756	FACS
CD23-PE, B3B4, 1:200	BD Biosciences	553139	FACS
CD23-AlexaFluor647, B3B4, 1:100	BD Biosciences	562826	FACS
CD23-PeVio770, B3B4, 1:200	BD Biosciences	562825	FACS
CD38-PeVio770, / , 1:100	miltenyi	130-102-374	FACS
CD43-Biotin, S7, 1:350	BD Biosciences	553269	FACS
CD43-BV421, S7, 1:200	BD Biosciences	562958	FACS
CD5-Horizon V450, 53-7.3, 1:200	BD Biosciences	561244	FACS
CD45R/B220-PerCP, RA3-6B2, 1:100	BD Biosciences	553093	FACS
CD45R/B220-APC, RA3-6B2, 1:250	BD Biosciences	553092	FACS
CD45R/B220-PE, RA3-6B2, 1:350	BD Biosciences	553090	FACS
CD45R/B220-FITC, RA3-6B2, 1:200	BD Biosciences	553088	FACS
CD80-PE, 16-10A1, 1:400	eBioscience	12-0801-82	FACS
CD86-PeCy5, GL1, 1:200	eBioscience	15-0862-82	FACS

CD86-APC, / , 1:100	BD Biosciences	558703	FACS
CD95-BV421, JO2, 1:200	BD Biosciences	562633	FACS
CD95-PE, /, 1:350	BD Biosciences	554258	FACS
CXCR4 (CD184)-PE, 2B11, 1:400	eBioscience	12-9991-81	FACS
human CD2 (hCD2)-FITC, REA972, 1:50	miltenyi	130-116-251	FACS
human CD2 (hCD2)-PeVio770, / , 1:100	miltenyi	130-099-933	FACS
human CD2 (hCD2)-APC, RPA-2.10, 1:100	eBioscience	12-0029-42	FACS
human CD2 (hCD2)-PE, RPA-2.10, 1:100	eBioscience	12-0029-42	FACS
ICAM (CD54)-Biotin, 3E2, 1:200	BD Biosciences	553252	FACS
ICOS-L (CD275)-PE, HK5.3, 1:100	eBioscience	12-5985-82	FACS
IgD-APC, 11-26c.2a, 1:300	BD Biosciences	560868	FACS
IgD-Biotin, 11-26c, 1:350	eBioscience	13-5993-82	FACS
IgG1-PE, A85-1, 1:800 (1:3000 IC-FACS)	BD Biosciences	553443	FACS
IgG1-BV450, A85-1, 1:200	BD Biosciences	562107	FACS
IgM-APC, II/41, 1:100	BD Biosciences	553409	FACS
IgM-Horizon V450, R6-60.2, 1:100	BD Biosciences	559502	FACS
IgM-PeCy7, R6-60.2, 1:300	BD Biosciences	552867	FACS
Irf4-eFluor660, 3E4, 1:100	eBioscience	50-9858	FACS
Irf4-PE, 3E4, 1:500	eBioscience	12-9858-82	FACS
Ki67-PE, SolA15, 1:500	Invitrogen	12-5698-82	FACS
Notch2-PE, HMN2-35, 1:80	BioLegend	130707	FACS
Streptavidin (SA)-PerCP, / , 1:100	BD Biosciences	554067	FACS
Streptavidin (SA)-APC, / , 1:400	BD Biosciences	554061	FACS
TACI-APC, ebio8G10-3, 1:100	Invitrogen	17-5924-82	FACS
rat-anti-mouse IgG3-Biotin, R40-82, 1:500	BD Biosciences	553401	ELISpot
rat-anti-mouse IgE-Biotin, R35-118, 1:500	BD Biosciences	553419	ELISpot
rat-anti-mouse IgM-Biotin, R6-60.2, 1:500	BD Biosciences	553406	ELISpot

rat-anti-mouse IgG1-Biotin, A85-1, 1:500	BD Biosciences	553441	ELISpot, ELISA
Avidin D-HRP, / , 1:2000	Vector	ZA0623	ELISpot, ELISA
rat-anti-mouse IgM-HRP, YF97, 1:5000	Southern Biotech	1021-05	ELISA
rat-anti-mouse IgEa-Biotin, UH297, 1:500	BioLegend	408804	ELISA
Rat-anti-mouse-hCD2-Biotin, RPA-2.10, 1:50	BD Biosciences	555325	Histology (IHC)
Rabbit-anti-mouse Laminin, L9393, 1:100	Sigma-Aldrich	L9393	Histology (IHC)
Streptavidin-AlexaFluor594, / , 1:500	Life Technologies	S11227	Histology (IF)
Streptavidin-AP (Alkaline Phospha-tase), / , 1:200	Sigma-Aldrich	S2890	Histology (IHC)
anti-Rabbit IgG-Peroxidase, / , 1:200	Sigma-Aldrich	A0545	Histology (IHC)
Goat-anti-rabbit IgG-Cy3 (Cya-nine3), / , 1:500	Jackson Immu-noResearch	111-165-003	Histology (IF)
Goat-anti-rat IgG-AlexaFluor488, / , 1:500	Jackson Immu-noResearch	112-545-003	Histology (IF)
Rat-anti-mouse CD90.2 (Thy1.2)-Biotin, 53-2.1, 1:100	BD Biosciences	553011	Histology (IF)
Rat-anti-mouse B220-APC, RA3-6B2, 1:500	BD Biosciences	553092	Histology (IF)
Rat-anti-mouse Irf4 purified, 3E4, 1:100	eBioscience	14-9858-80	Histology (IF)
Rat-anti-mouse GL-7-FITC, GL7, 1:100	BD Biosciences	870937	Histology (IF)
Rat-anti-mouse GL-7-APC, GL7, 1:100	BD Biosciences	144606	Histology (IF)
Rat-anti-MOMA1-Biotin, ab51814, 1:100	abcam	ab51814	Histology (IF)
Rat-anti-mouse-IgD-Biotin, 11-26c, 1:100	eBioscience	13-5993-82	Histology (IF)
Rat-anti-Mouse IgM, 1020-01, 1:100	Southern Biotech	1020-01	Histology (IF)
CHEMICALS AND RECOMBINANT PROTEINS			

Name	Company	Identifier (Cat#)	Application
Taq DNA Polymerase, recombinant	Invitrogen	10342053	PCR
NP-CGG	Biosearch Technologies	N-5055C-5	Immunizations
RBC Lysis Buffer	eBioscience	00-4333	Single cell suspension prep.
MACS Buffer	Miltenyi	130-091-221	Cell washing
Roti-Histofix 4%	Carl Roth	P087	Fixation of cells
Tissue-Tek O.C.T. Compound	Sakura	SA62550	Histology (IHC)
ProLong Glass Antifade Mountant	Invitrogen	P36984	Histology (IHC)
Kaisers Gelatin	Carl Roth	6474.1	Histology (IHC)
F(ab)2 Fragment Anti-Mouse IgM (1,3 mg/ml)	Jackson ImmunoResearch	JIM-115-006-020-1MG	In vitro cell culture
IL4, Mouse (5 µg)	Sigma-Aldrich	I1020	In vitro cell culture
IL21, Mouse (10 µg)	Miltenyi	130-108-949	In vitro cell culture
CD40 Monoclonal Antibody (HM40-3) (500 µg)	eBioscience	16-0402-85	In vitro cell culture
LPS (Lipopolysaccharide) (5 mg)	Sigma-Aldrich	L1887-5MG	In vitro cell culture
D-PBS	Gibco	14190-169	Cell washing
ELISA Assay Diluent (5X)	Biozol Diagnostica (BioLegend)	BLD-421203	IgE ELISA
COMMERCIAL ASSAYS AND KITS			
LIVE/DEAD Fixable Blue Dead Cell Stain Kit	Invitrogen	L23105	Dead cells staining
CD43-microbeads B Cell Isolation Kit, mouse	Miltenyi	130-090-862	B cell purification
Avidin/Biotin Blocking Kit	Vector	SP-2001	Histology
AEC Peroxidase Substrate Kit	Vector	SK-4200	Histology
Blue Alkaline Phosphatase Substrate Kit	Vector	SK-5300	Histology
SureBeads Protein G Magnetic beads	Bio-Rad	161-4023	Serum depletion IgE ELISA
TRANSGENIC MOUSE STRAINS			

Notch2IC^{STOPfl}	U. Zimber-Strobl (Hampel et al., 2011)	N/A	Matings
R26/CAG-CAR∆1^{STOPfl}	M. Schmidt-Supprian (Heger et al., 2015)	N/A	Matings
Notch2$^{fl/fl}$	U. Zimber-Strobl (Besseyrias et al., 2007)	N/A	Matings
γ1-cre	U. Zimber-Strobl (Casola et al., 2006)	N/A	Ex vivo Experiments, Matings
CBF:H2B-Venus (Notch-reporter)	Jackson Laboratories (Nowotschin et al., 2013)	JAX Stock No 020942	Ex vivo Experiments, Matings
BALB/c	Charles River Germany	JAX Stock No 000651	Ex vivo Experiments, Matings
ANALYTICAL RESEARCH DEVICES			
LSRFortessa Flow Cytometer	BD Biosciences	N/A	Flow Cytometry
Confocal Microscope TCS-SP5 II	Leica	N/A	IF Imaging
ImmunoSpot Series 5 UV Analyzer (CTL Europe)	ImmunoSpot	N/A	ELISpot Spot Counting
ELISA Microplate reader (Photometer Sunrise RC), Infinite 200 pro	Life Sciences, Tecan	N/A	ELISA Titer Measurements
Axioscope (Zeiss) microscope with AxioCam MRc5 digital camera and NEOFLUAR objective	Carl Zeiss GmbH	N/A	IHC Imaging
Quantum ST-4 UV chamber	Vilber Lourmat	101141731	Visualization of PCR products
SOFTWARE			
FlowJo V10	FlowJo LLC	https://www.flowjo.com	Analysis of FACS data
ImageJ 1.50e	NIH, USA	https://imagej.nih.gov/ij/index.html	Microscopy Image processing
GraphPad Prism V8-V10	GraphPad Software	https://www:graphpad.com	Graph production and Statistics

3.1 Mouse models

CBF:H2B-Venus BALB/c

CBF:H2B-Venus Notch-reporter mice (described in (Nowotschin et al., 2013)) were purchased from The Jackson Laboratory, backcrossed into the Balb/c background and further maintained in house. Extensive information on this mouse model is given in the *Introduction chapter 1.3.3* and in *Figure 7.*

Cγ1-cre

In this mouse model, the Cre-coding sequence, preceded by an IRES cassette, is inserted behind the last membrane-coding exon of the Igγ constant region (*Cγ1*) gene locus (Casola et al., 2006). Thereby, expression of genes of interest with loxP-site-flanked regions is achieved in a GC B cell-specific manner.

R26/CAG-CARΔ1^{STOPfl}/Cγ1-Cre

R26/CAG-CARΔ1^{STOPfl} mice (Heger et al., 2015) were crossed to the Cγ1-cre strain to generate R26/CAG-CARΔ1^{STOPfl}/Cγ1-Cre mice (from here on referred as control/CAR). They served as age-matched controls for the Notch2$^{fl/fl}$//CAR/Cγ1-Cre and Notch2IC-^{STOPfl}/Cγ1-Cre animals. They contain the human coxsackie/adenovirus receptor CAR under the control of the CAGGS promoter, preceded by a lox-P-flanked STOP cassette. Cre recombinase activity driven by the *Cγ1* promoter leads to deletion of the STOP cassette, resulting in an expression of a truncated version of the CAR receptor on the cell surface. The cells can be tracked by staining with an anti-CAR antibody.

Notch2$^{fl/fl}$//CAR/Cγ1-Cre

To achieve the Notch2$^{fl/fl}$//CAR/Cγ1-Cre strain (referred as N2KO//CAR), we crossed mice carrying the Notch2$^{fl/fl}$ targeted gene (Besseyrias et al., 2007) into the control/CAR strain. In this mouse strain, the exons 28 and 29, which code for the C-terminal part of RAM23 and the nuclear localization signal (NLS) are flanked with lox-P sites. Upon Cre-mediated recombination, exons 28 and 29 of the *notch2* gene and the STOP cassette upstream of the *car* gene in the *rosa26* locus are excised. Because the downstream exons 30 to 32 in the *notch2* gene are out of frame, the complete functional ICD-coding part of the *notch2* locus is not translated. Thereby, the Cre-recombined B cells express a truncated non-functional Notch2, but also CAR on the cell surface, and can be tracked via anti-CAR antibody staining.

Notch2IC^{STOPfl}/Cγ1-Cre

Notch2IC^{STOPfl} animals (Hampel et al., 2011) were mated with Cγ1-cre mice, to produce Notch2IC^{STOPfl}/Cγ1-Cre mice (hereafter termed N2IC/hCD2). In this mouse model, the

conditional *notch2IC* allele is directly coupled to the coding sequence for the human CD2 (hCD2) receptor through an IRES site. These transgenes are preceded by a lox-P-site-flanked STOP cassette and inserted in the *rosa26* locus, under the activity of the CAGGS promoter. Cre recombinase-mediated excision will ensure expression of both Notch2IC inside the cell and hCD2 on the cell surface. Thus, cells with ligand-independent, constitutively active N2IC expression can be tracked by staining for hCD2 in flow cytometry.

BALB/c

The BALB/c mice are members of a widely-used inbred albino mouse strain and were initially purchased from Charles River. They were used to breed all aforementioned mouse strains and to backcross F1 CBF:H2B-Venus mice, to avoid any strain-specific differences between mouse models.

4 Methods

4.1 Molecular Biology

4.1.1 Mouse genotyping

In order to ensure that the correct animals were used in each experiment, all transgenic mice were routinely genotyped. The genotyping proceeded in three steps. First, genomic DNA was isolated and purified from murine ear clippings. The ear tissue was incubated with 510 µl lysis buffer (100 mM Tris/HCl pH=8, 0,2% SDS, 5 mM EDTA, 200 mM NaCl and 100 µg/ml Proteinase K) over night at 56 ˚C under constant shaking in a Thermo Mixer. The following day, 170 µl saturated 5 M NaCl was added in order to precipitate the proteins. Following centrifugation for 10 min at 20.000xg and 4 ˚C, the supernatant was collected and transferred into a fresh tube, pre-filled with 500 µl of 100% (v/v) iso-propanol. The tubes were inverted several times and centrifuged again under the same conditions, after which the supernatant was discarded. Then, the DNA pellets were left to dry at room temperature for a few minutes, were subsequently washed with 70% (v/v) ethanol and centrifuged another time. Afterwards, the pelleted DNA was dried at 37 ˚C and dissolved in 100 µl TE buffer (10 mM Tris pH=7.9, 1 mM EDTA) while shaking at 37 ˚C for 2-3 h. Second, one or several polymerase chain reactions (PCR) were performed in order to amplify modified genes of interest, depending on the specific genotype of the transgenic mice. The used primers (*Table 2*), PCR reaction programs (*Table 3*) and the recipes for each PCR mixture (*Table 4*) are given in the respective tables below. All primers were obtained from Metabion, the DMSO from Carl Roth and the remaining components from Thermo Fischer. PCR reactions were performed in thermal cyclers from Biometra. In the final step, the amplified PCR products were detected using agarose gel electrophoresis. The gels were made by Krisztina Zeller and were subsequently loaded with 15 µl from a mixture containing the PCR product (25 µl) and ready-to-use 6x loading dye (5 µl). Electrophoresis was done in gel chambers (PEQLAB Biotechnologie GmbH) pre-filled with 1x TAE buffer at 90-120 V for up to 1 h 30 min. Due to the intercalation of the ethidium bromide with the nucleic acids, the resulting PCR products were visualized under a UV luminescence screen (Quantum ST-4, Vilber).

Table 2: Primers and their sequences used for genotyping.

PCR	Oligonucleotide	Sequence (5' to 3' direction)
CAR	CAR for CAR rev	cag cca ctc gat gat gta cag cgg cag gag cga gag ccg cct ac
Notch2IC	Notch2 se Notch2 as	gag aag cag aga tga gca gat a gtg aga tgt gac act tct gag c
ROSA26	Rosa for Rosa rev	ctc tcc caa agt cgc tct g tact cc gag gcg gat cac aag c
γ1-Cre	IgG1 KPN1 Cre13 IgG1 rev3	tgt tgg gac aaa cga gca ggt ggc tgg acc aat gta aat a gtc atg gca atg cca agg tcg cta g
Notch2$^{fl/fl}$	Notch2 se2 (left) Notch2 as2 (right)	cca ttt caa gtg ttc gtg tcc cac att cat cga tgt tct ctt ca
Notch2-Δ	del Notch 2 sense del Notch 2 antisense	gtc gct gtt gtc atc atc gtg caca ta tgc ctt agc
Venus (Notch-Reporter)	Venus fw Venus rev	atc tgc acc acc ggc aag tca tgt ggt cgg ggt agc

Table 3: Master Mix recipe for each PCR reaction. Ingredients are given in µl.

Ingredient	CAR	Notch2IC	ROSA26	γ1-Cre	Notch2$^{fl/fl}$	Notch2-Δ	Venus
dH_2O	18.85	19.1	18.4	19	18.85	18.9	20
Taq buffer (10x)	2.5	2.5	2.5	2.5	2.5	2.5	2.5
$MgCl_2$ (50 mM)	0.5	1.5	1	1	1	1	1
dNTP (10 mM)	0.5	0.5	0.5	0.5	0.5	0.5	0.5

Primer (100 µM)	0.25	0.1	0.1	0.1	0.25	0.1	0.1
Taq Poly-merase (5U/µl)	0.15	0.15	0.15	0.15	0.15	0.15	0.15
DMSO (100%)	-	-	0.25	-	-	0.25	-
DNA (5-10 ng)	2	1	1.5	1	1.5	1	1

Table 4: Time (‘/’’) and temperature (˚C) for each phase of each PCR program.

Phase	CAR	Notch2IC	ROSA26	γ1-Cre	Notch2$^{fl/fl}$	Notch2-Δ	Venus
Pre-heating	∞ , 95˚C, lid 104˚C						
1. Initializa-tion	3’ 95˚C	5’ 95˚C	5’ 95˚C	2.3’ 95˚C	2.3’ 95˚C	2.3’ 95˚C	2’ 95˚C
2. Denatura-tion	15’’ 95˚C	45’’ 94˚C	45’’ 95˚C	40’’ 94˚C	45’’ 94˚C	45’’ 94˚C	15’’ 95˚C
3. Hybridiza-tion	30’’ 62˚C	45’’ 59˚C	45’’ 58˚C	40’’ 58˚C	45’’ 58˚C	45’’ 55˚C	15’’ 64˚C
4. Elongation	1’ 72˚C	1’ 72˚C	1’ 72˚C	40’’ 72˚C	1’ 72˚C	2’ 72˚C	45’’ 68˚C
5. Final Elongation	10’ 72˚C	10’ 72˚C	10’ 72˚C	10’ 72˚C	10’ 72˚C	10’ 72˚C	10’ 68˚C
Cooling	∞ , 4˚C						
No. of cycles (Step 2 to 4)	32	32	33	30	29	29	40

4.2 Mouse-related assays

Immunized and unimmunized (UI) control and mutant mice were sacrificed between 10 to 18 weeks of age. For each experiment, control animals were assigned in an age-matched manner. All mouse strains were bred and maintained in-house under specific pathogen-free conditions. Experiments were carried out in compliance with the German Animal Welfare Law and were approved by the government of Upper Bavaria.

4.2.1 Mouse Immunization (in vivo work)

To trigger TD immune responses, 10- to 18- week-old animals were routinely injected intraperitoneally (i.p) with 100 µg of alum-precipitated 4-hydroxy-3-nitrophenylacetyl (NP)-chicken-gamma-globulin (CCG) (Biosearch Technologies, Novato, CA) diluted in 200 µl sterile PBS (Gibco). Mice were subsequently analyzed 4, 7, 9, 14, 17, 22, 26 or 30 days after antigen injection. Respective unimmunized (UI) animals were taken down on the day of the experiment and were used as a day 0 time point.

4.2.2 Preparation of murine lymphocytes

Euthanization of the mice was performed in a CO_2 chamber with gradual application of 5% CO_2. In cases where blood was not extracted from the heart, death was ensured by cervical dislocation. Following organ extraction, the spleens (SP) were preserved in 1% B cell medium on ice (BCM; 1x RPMI 1640 supplemented with 1% (v/v) heat-inactivated fetal calf serum (FCS) (PAA Cell culture Company), 100 U/ml penicillin, 100 g/ml streptomycin, 1 mM sodium pyruvate, 2 mM L-glutamine, 1x non-essential amino acids, and 50 µM β-mercaptoethanol (all purchased from Gibco)). Bone marrow (BM) cells were collected by flushing the femur and tibia bones with 1% BCM and a cannula. Blood was extracted directly from the heart by punctuation with a syringe and needle or with a Pasteur pipette. Afterwards, it was either placed in a fresh tube on ice for later serum preparation or it was mixed with 1 mL PBS with 0.5 M EDTA, if FACS analysis should be performed. For the preparation of single cell suspension, the spleen was mashed through a 70 µM strainer. Following centrifugation at 1200 rpm for 10 min at 4 ˚C (Rotanta 460-R, Hettich centrifuge), SP and BM cell suspensions were lysed for 3 min at room temperature by resuspending the pellets in 1 mL of RBC buffer (1x, eBioscience) to remove erythrocytes from the remaining cells. The reaction was terminated by addition of 12 mL 1% BCM and centrifugation under the same conditions. For blood samples, the cell suspensions were lysed in the same manner at least 2 to 3 times with 2 mL RBC lysis buffer. Finally, cells from the SP and BM were resuspended in 1 mL 1% BCM and were counted to establish the cell number for further experiments. This was done by preparing 1:100 (SP) and 1:50 (BM) dilutions and by using Neubauer counting chambers and a light microscope with phase contrast (Zeiss Axio).

4.2.3 Isolation of B cells

For the purification of total naïve B cells, the CD43 depletion B cell Isolation Kit (Miltenyi) was used. Cells were MACS-purified following the instructions of the manufacturer. The

isolated B cells were checked for their purity levels in FACS, and if ≥95% B cell yield was achieved, the cells were used in in vitro stimulation assays.

4.2.4 Serum preparation from blood

To measure immunoglobulin antibody titers in the serum of mice, the extracted blood was kept at 4 ˚C for at least 4 h. Then, the blood was centrifuged for 20 min at 15000 rpm, 4 ˚C. The resulting supernatant (= serum) was collected into a fresh tube and centrifuged one more time for 15 min at 15000 rpm, 4 ˚C. Lastly, the ready-to-use serum was frozen at -80 ˚C for its later use in ELISA assays.

4.3 ELISA (enzyme-linked immunosorbent assay)

In part, the protocol for ELISA was followed and adapted as described in (Babushku et al., 2022; Scheffler et al., 2021; Sperling et al., 2019). NP-specific antibody titers of different isotypes were measured in ELISA. NUNC plates (Nunc) were coated with NP3-BSA or NP14-BSA (10 mg/ml, Biosearch Technologies) in a 1:2000 dilution in carbonate buffer (0.1 M $NaHCO_3$, pH=9.5). Plates were incubated over night at 4 ˚C. The numbers after the coated NP conjugate refer to the conjugation ratio of NP to the carrier protein (BSA). Low-affinity antibodies only bind to NP at a high conjugation ratio (i.e. NP14), whereas high affinity antibodies bind to both conjugation ratios (i.e. NP3 and NP14). Thus, NP3 helps measure only the high-affinity NP-specific antibodies, whereas NP14 is a measure for total NP-specific antibodies, both low- and high-affinity. The following morning, plates were washed three times with 200 µl/well PBS, followed by blocking for 2 h with 50-100 µl/well blocking buffer (1% milk powder in PBS for IgG1/IgG3 ELISA, 5% milk powder in PBS for IgM ELISA, 10% FCS in PBS for IgE ELISA). Then, serum from immunized and unimmunized (UI) mice was prepared in a 1:10 (IgM ELISA) or 1:100 dilution (IgG1/IgG3 ELISA) in the respective blocking buffer. For NP-specific IgE ELISA, serum samples were diluted 1:5 in a special ELISA diluent (BioLegend). All IgG-switched antibodies were first removed from the serum samples using the SureBeads™ Magnetic Beads system (BIO-RAD). The serum depletion and all subsequent steps, up until the measurement of NP-IgE titers, were performed according to the protocol described in (Arámburo-Galvez et al., 2018). The sera were pipetted in a 1:2 serial dilution distributed downwards over 8 wells, starting with 100 µl/well of diluted serum in the first row of the plate. The sera were then incubated for 1 h at room temperature, followed by washing of the plate three times with 200 µl/well PBS. For IgG1/IgG3/IgE ELISA, the respective biotinylated antibody specific for the isotype was added in a 1:500 dilution in blocking buffer, and incubated for 30 min at room temperature. For IgM ELISA, a directly coupled

anti-IgM-HRP antibody was used in a 1:5000 dilution in blocking buffer and was incubated for 1 h at room temperature. All details about the specific antibodies are given in *Table 1*. For the IgG1/IgG3/IgE ELISA, the plates were washed again with 200 µl/well PBS and incubated with 1:2000-diluted streptavidin horseradish peroxidase (HRP) Avidin D (Vector) in the respective blocking buffer. After another washing step with PBS, the HRP was detected with 100 µl/well developing buffer (1 tablet o-Phenylenediamine (Sigma, P-7288) + 35 mL substrate buffer (0.1 M citric acid, 0.1 M Tris (Sigma)) + 21 µl H_2O_2 (Sigma)). Upon addition of the buffer, plates were gently tapped and the absorbance was determined with a microplate ELISA reader (Photometer Sunrise RC, Tecan) at an optical density (OD) at 405 nm and reference wavelength of 620 nm. To correctly quantify the measured titers and compare different independent assays, internal standards consisting of pooled serums from six to eight NP-CGG immunized mice were used. All NP-specific titers in the *Results* section are given as log10 relative units.

4.4 ELISpot (enzyme-linked immunospot assay)

In part, the protocol for ELISpot was followed and adapted as described in (Babushku et al., 2022; Scheffler et al., 2021; Sperling et al., 2019). For the detection of NP-specific antibody secreting cells (ASCs) within the splenic or bone marrow cells, an ELISpot assay was used. 96-well membrane plates (Millipore) were coated overnight at 4 °C with 50 µl/well of NP3– (high-affinity antibody binding) or NP14–BSA (binding of high and low-affinity antibodies) (25 µg/ml; Biosearch Technologies), diluted 1:400 in carbonate buffer. On the following day, plates were washed three times with 200 µl/well PBS and were blocked for 3 h at 37 ˚C with 10% B-cell medium (BCM supplemented with 10% FCS and the other supplements as described in chapter *4.2.2*). $5x10^5$ splenocytes or BM cells in 10% BCM/FCS were seeded per well (except for IgE ELISpot, where $1x10^6$ cells/well were plated), and the plates were incubated for 24 h at 37 ˚C. The next day, plates were washed six times with 200 µl/well PBS-T (PBS with 0.025% Tween20). Then, biotinylated antibodies against the detecting isotype (anti-IgM/IgG1/IgG3/IgE, details given in *Table 1*) were diluted 1:500 in PBS/1%BSA, added in a volume of 100 µl/well and incubated for 2 h at 37 ˚C. Another wash sequence with PBS-T was performed (three times 200 µl/well), followed by the addition of 50 µl/well streptavidin horseradish peroxidase Avidin D (Vector) diluted 1:2000 in PBS/1% BSA. Plates were incubated for 45 min at room temperature. Afterwards, plates were washed three times with PBS-T and three times with PBS. For the development of spots, a special buffer was prepared as follows: one tablet of each 3,3'- Diaminobenzidin peroxidase-substrate (0.7 mg/ml, Sigma-Aldrich, gold and silver tablets) was dissolved in 5 ml distilled water, the solution was poured together (total volume 10 ml) and filtered through a sterile filter in a fresh falcon. 50 µl/well

of this buffer was added and incubated for 8 min (splenocytes) or 12 min (BM cells), after which individual spots were visible. The reaction was stopped by addition of 150 µl/well water, plates were thoroughly washed several times with water and left to dry in the dark for two days. Spots were visualized and counted with the ImmunoSpot Series 5 UV Analyzer (CTL Europe).

4.5 Flow Cytometry (FACS)

Antibodies used for flow cytometry are listed in *Table 1*. All analyses were performed on the LSRII FACS Fortessa (BD Biosciences). Results were evaluated using FlowJo V10. Depending on the experimental set-up, either surface or intracellular (IC) staining (in particular for Irf4, Blimp1, Bcl6 and Ki67) was performed. In both cases, after preparation of single cell suspensions from spleen and BM, $1x10^6$ - $2x10^6$ cells per staining were distributed into round-bottom 96-well FACS plates (Greiner Bio One).

4.5.1 Surface staining

For surface staining of lymphocytes, cells were washed with 200 µl/well PBS (Gibco), followed by centrifugation for 5 min at 1200 rpm, 4 ˚C. To exclude dead cells from the analysis, LIVE/DEAD fixable BLUE Dead Cell Stain kit (Invitrogen) was used (diluted 1:1000 in PBS). 50 µl of the dye was added per sample and the plate was incubated for 20 min on ice in the dark. Afterwards, cells were washed once with 150 µl/well PBS and then again with 200 µl/well MACS buffer (Miltenyi). Following centrifugation, cell pellets were resuspended with 25 µl of antibody mixtures, appropriately diluted in MACS buffer, and were incubated for 25 min on ice in the dark. The used antibodies were coupled to one of the following fluorochromes: FITC, PE, PerCP, APC, eFluor660, Alexa Fluor647, Horizon V450, Brilliant Violet 421, Brilliant Violet 510, PeCy7, PeCy5 or Pe-Vio770. After the staining step, cells were washed one time with 180 µl/well MACS buffer, centrifuged under the same conditions, resuspended in 100 µl/well MACS and transferred into FACS tubes for acquisition.

4.5.2 Intracellular (IC) staining

For intracellular FACS, cells were fixed with 2% paraformaldehyde (1:2 PBS-diluted Histofix) for 10 min at room temperature and permeabilized in ice-cold 100% methanol for at least 10 min on ice. To include only living cells into the analysis, cells were stained for 5 min on ice with LIVE/DEAD Fixable Blue Dead Cell Stain Kit (Invitrogen) before fixation (Babushku et al., 2022). Following a washing step with 100 µl/well PBS and then with 200 µl/well MACS buffer, the cells were incubated for 1 h at room temperature with the

corresponding antibodies (diluted appropriately in MACS buffer). Lastly, samples were washed with 180 µl/well MACS buffer, centrifuged, resuspended into 100 µl/well MACS buffer and transferred into FACS tubes for measurement.

4.5.3 Gating strategies (FlowJo)

Identification of B cell populations

To exclude doublets, the forward scatter area (FSC-A) and height (FSC-H) of lymphocytes were plotted against each other. By mapping DAPI (UV) against the FSC-A, only living cells were included in the analysis (DAPI-negative). Lymphocytes were correctly identified by using their size and granularity (FSC-A vs. SSC-A). Finally, to only look at B lymphocytes in the spleen, B220$^+$ or CD19$^+$ cells were gated in a histogram (*Fig. 8A*). This gating strategy was employed for the analyses of B cell subsets in all mouse strains. In case of the Cγ1-Cre mouse models, which expressed either the CAR or hCD2 reporter genes, antigen-responding reporter-positive B cells were subsequently gated in histograms (CAR$^+$ or hCD2$^+$) (*Fig. 8B)*.

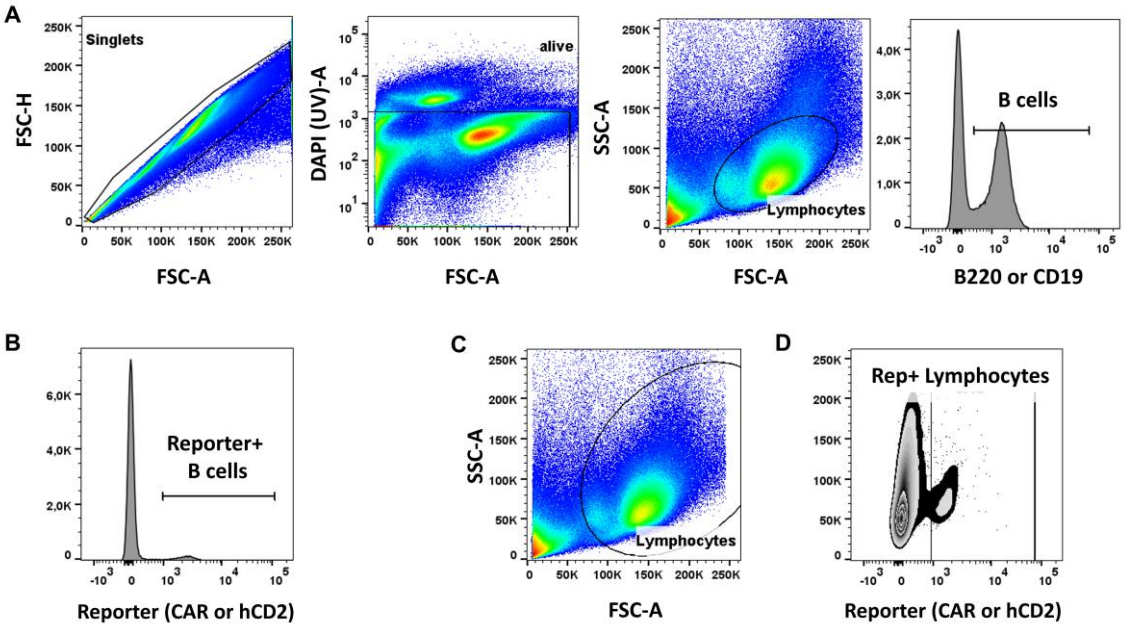

Fig. 8: Gating strategies to identify lymphocytes, B cells, PCs and reporter-expressing cells in the spleen. (A) Exemplary FACS plots for the sequential gating of singlets, living cells, lymphocytes and B220$^+$ / CD19$^+$ B cells among splenocytes. **(B)** Representative histogram depicting the gating of reporter-positive B cells in all Cγ1-Cre-based mouse models. **(C)** Gating strategy used to include plasma cells among the lymphocytes. Singlets and living cells were pre-gated as in (A). A larger lymphocyte gate was used for correct PC identification. **(D)** For all Cγ1-Cre strains, reporter-expressing lymphocytes were subsequently gated from the large lymphocyte gate (C) in a CAR or hCD2 vs. SSC-A plot.

Identification of plasma cells (PCs)

To examine plasma cells in all analyzed mice, singlets and $DAPI^-$ living cells were gated as described above. But, in the case of PCs, a large lymphocyte gate was used in the FSC-A vs. SSC-A plots because plasma cells are bigger in size and are more granular than the remaining lymphocytes (*Fig. 8C*). For PC analysis in the Cγ1-Cre transgenic animals, the reporter-expressing lymphocytes were subsequently gated as CAR^+ or $hCD2^+$ in reporter vs. SSC-A plots (*Fig. 8D)*.

4.6 Cell culture

All cell culture experiments were carried out under sterile conditions by using a work-bench (Bio Flow technique), sterile pipettes (Gilson/Eppendorf) and expendable tools. The cultivation of cells was performed in an incubator (Binder) at 37 °C, 6% CO2 and 95% humidity. The isolation of B cells from murine spleens was done using the CD43-depletion naïve B cell Isolation Kit (Miltenyi) according to the manufacturer's instructions. The purified total B cells were seeded at a density of $5x10^5$ cells per well in flat-bottom 96-well plates (Nunc). Cells were kept in 10% B-cell medium (RPMI-1640 medium (Gibco), supplemented with 10% FCS (PAA Cell culture Company) and the other supplements as described in chapter *4.2.2*). Depending on the in vitro assay, cells were stimulated with either only one or a combination of several of the following stimuli: (1) AffiniPure F(ab′)2 goat anti-mouse IgM (15 µg/ml; IgM µ-chain, Dianova), (2) anti-CD40 antibody (2.5 µg/ml; eBioscience HM40-3), (3) IL4 (Interleukin-4, 10 ng/ml; Sigma-Aldrich), (4) IL21 (Interleukin-21, 10 ng/ml; Miltenyi), (5) LPS (Lipopolysaccharide, 50 µg/ml; Sigma-Aldrich). Cells were harvested at 24 h, 48 h and 72 h and analyzed by flow cytometry (FACS) after staining with an anti-Notch2-PE antibody (BioLegend). To measure the ex vivo Notch2 surface expression at 0 h, an unstimulated (US) cell sample was taken prior to in vitro culture with the stimuli. Dead cells were excluded from the analysis by staining them on ice with the fixable BLUE live/dead cell staining kit (Invitrogen) prior to the Notch2 surface antibody staining. To obtain enough cells for FACS compensations, some splenic cells were additionally stimulated with anti-CD40 (2.5 µg/ml; eBioscience HM40-3).

4.7 Histology

To visualize the localization of different cell populations in the spleens of analyzed mice, histology and subsequent microscopy of splenic tissue sections were performed. Details about the antibodies and other materials used for this purpose are given in *Table 1*. Murine splenic pieces were embedded in O.C.T. compound (VWR Chemicals, USA), snap frozen on dry ice and stored at −20 °C. Splenic tissue sections were sliced with a

cryostat into 7 µm thick slices, mounted on glass slides, air dried for 30 min and stored at −80 °C for later use in immunofluorescence (IF) or chromogenic immunohistochemistry (IHC). IF and IHC protocols were mostly followed as previously described in (Sperling et al., 2019), (Lechner et al., 2021) and (Babushku et al., 2022).

4.7.1 Immunofluorescence (IF)

Splenic tissue slides were air-dried for 20 min, fixed with PBS-diluted 3% PFA (Histofix, Carl Roth) for 10 min, rinsed shortly in PBS and then rehydrated for 8 min in PBS + 50 mM NH_4Cl. For the visualization of the MZ, T- and B- cell zone, sections were first blocked with 1% BSA, 5% rat serum, 5% chicken serum in PBS for 30 min, followed by Avidin/Biotin blocking (Vector) according to the manufacturer's instructions. After washing three times with PBS, primary antibodies (goat-anti-mouse IgM, anti-Thy1.2-Biotin, and anti-MOMA1-Biotin), secondary antibodies (chicken anti-goat IgG AF647) and finally Streptavidin-AF594, were each incubated for 1 h at room temperature in 0.5% BSA/PBS. To detect plasmablasts and plasma cells, sections were permeabilized and blocked for 20 min with 0.3% Triton X, 1% BSA and 5% goat serum in PBS. Primary (rat-anti-mouse Irf4, rabbit-anti-mouse Laminin) and secondary antibodies (goat-anti-rat AlexaFluor488 or goat-anti-rat AlexaFluor647, goat-anti-rabbit Cy3) were incubated for 1 h at room temperature in 1% BSA/PBS. In the last step, fluorophore-coupled antibodies (anti-mouse B220-APC) were incubated for 2 h at room temperature, if appropriate. For the detection of germinal center (GC) structures, sections were blocked for 30 min with 1% BSA and 5% rat serum in PBS. Then, sections were blocked again using the Avidin/Biotin blocking kit (Vector). Rat-anti-mouse GL-7-FITC or GL7-APC antibody was incubated overnight at 4 ˚C. The following day, directly-coupled antibodies (Thy1.2-Biotin, MOMA1-Biotin, and B220-APC) and Streptavidin-AlexaFluor594 were incubated for 1 h at room temperature in 1% BSA/PBS (Babushku et al., 2022). The Venus nuclear reporter for Notch signaling activity was directly visualized in splenic sections of CBF:H2B-Venus mice, without the need of additional antibody staining. Slides were embedded in ProLong Glass Antifade (Invitrogen). Images were acquired on a TCS SP5 II confocal microscope (Leica) and composition of picture stacks was done in ImageJ.

4.7.2 Chromogenic Immunohistochemistry (IHC)

To visualize and track the localization of reporter-expressing cells in N2IC/hCD2 mice, immunohistochemical staining for hCD2 in combination with Laminin was done. Frozen splenic sections were air-dried for 20 min, fixed with ice-cold acetone for 10 min, washed with PBS three times for 5 min and then blocked with 1% BSA and 5% goat serum in PBS. To mask and block endogenous biotins within the samples, they were blocked

again using the Avidin/Biotin blocking kit (Vector). Detection of the expression of the surface marker hCD2 was done by staining with a biotinylated mouse-anti-hCD2 antibody (1:100 diluted in 1%BSA/PBS), combined with rabbit-anti-Laminin antibody staining (1:500 in 1%BSA/PBS) to delineate the basement membranes of endothelial cells lining the MZ sinus. Sections were incubated overnight at 4 ˚C. Samples were washed three times for 5 min with PBS, followed by secondary antibody staining with streptavidin-coupled alkaline phosphatase (1:200) and peroxidase-coupled anti-rabbit IgG (1:200) for 1 h at room temperature. Afterwards, enzymatic chromogenic development of the sections was done with the AEC substrate kit and Blue AP substrate kit (Vector) following the manufacturer manual. Lastly, slides were air-dried for 45 min and were embedded in Kaiser's Gelatin (Carl Roth). Evaluation of the stained sections was done using an Axioscope (Zeiss) microscope with a Zeiss Plan NEOFLUAR objective 10x or 20x/0.3. Images were acquired with an AxioCam MRc5 digital camera (Carl Zeiss GmbH) combined with an AxioVision rel.4.6.3.0 software.

4.8 Statistics

The GraphPad Prism Software (v8-v10) was used to generate all graphs and bar charts, as well as perform all statistical analyses, including tests for normal distribution and equal variance and determination of p-values. If the data set did not follow a Gaussian distribution, the Mann-Whitney test was used for statistical analysis. For the comparison of two groups, two-tailed t-tests were applied. In cases where at least three groups were compared, one-way or two-way ANOVA test with multiple comparisons was used, following the recommendations by the GraphPad software. The chosen statistical test is always indicated in the figure legends. Error bars in all figures define the mean ± SD. The following p values are indicated in the graphs: $p>0.05$ (ns), $p\leq0.05$ (*), $p\leq0.01$ (**), $p\leq0.001$ (***) and $p<0.0001$ (****).

5 Results

5.1 Notch signaling in B lymphocytes of CBF:H2B-Venus mice

5.1.1 Notch signaling begins in the earliest stages of B cell maturation in the bone marrow

The Notch2 signaling pathway has been known to have a potent role in specifying the MZB cell lineage upon B cell maturation in the spleen (Pillai and Cariappa, 2009). However, little is known about Notch signaling in the developing B cell subsets of the bone marrow. Therefore, bone marrow B cells from CBF:H2B-Venus reporter mice were analyzed for their Venus expression (Nowotschin et al., 2013). The nuclear expression of the Venus fluorescent protein in B cell populations serves as a direct read-out of Notch-signaling activity inside the cells and can be easily monitored in FACS.

To look whether Notch signaling begins in the early stages of B cell development, bone marrow B lymphocytes were stained for the surface markers CD43 and B220. As B cells develop from pro-B to pre-B cells, their CD43 expression decreases. $CD43^{+}B220^{low}$ pro-B and early pre-B cells can be further separated in Hardy's fractions A to C′ by staining for the surface markers BP-1 and CD24 (Hardy and Hayakawa, 2001; Scheffler et al., 2021). Pro-B cells increase both their BP-1 and CD24 abundance, as they gradually develop from fraction A to C'.

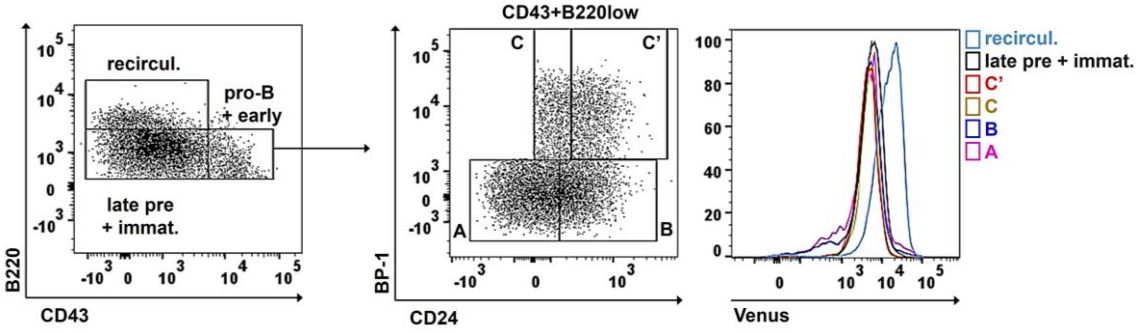

Fig. 9: All B lymphocytes in the bone marrow receive a Notch signal. Representative FACS analysis of lymphocytes in the bone marrow from CBF:H2B-Venus mice. The plot on the far left is pre-gated on living $B220^{+/mid}$ lymphocytes and further subdivided into B cell subsets according to the CD43/B220 expression: pro- and early pre- ($CD43^{+}B220^{low}$), late pre- and immature ($CD43^{low}B220^{low}$) and recirculating ($CD43^{-}B220^{high}$) B cells. The plot in the middle shows the separation of $CD43^{+}B220^{low}$ cells into Hardy's fractions A-C' according to the abundance of CD24 and BP-1: A: $BP\text{-}1^{-}CD24^{-}$; B: $BP\text{-}1^{-}CD24^{+}$; C: $BP\text{-}1^{+}CD24^{mid}$; C′: $BP\text{-}1^{+}CD24^{high}$. The histogram on the right shows the overlay of Venus expression in all gated cell populations. n=5 mice. Similar figure in (Babushku et al., 2022).

Successful separation of these fractions revealed that some cells in fractions A and B had lower Venus levels than most CD43^{+}B220^{low} cells, implying that the first Notch signaling activity appears in the earliest developmental cell stages of pro-B cells (*Fig. 9)*. A portion of B cells can migrate back to the BM from the periphery and are thus referred as recirculating B cells. Unlike developing B cells, they have increased expression of B220. The FACS analysis showed that CD43^{-}B220^{high} recirculating B cells had markedly higher Venus expression, in comparison to the developing CD43^{+}B220^{low} cells and the CD43^{-}B220^{low} late pre-B and immature B cells (*Fig. 9)*.

5.1.2 Notch signaling progressively increases during terminal B cell development in the spleen

The well-established model implies that after rearranging their BCRs, immature B cells exit the BM and migrate to the spleen as transitional (T1) B cells (AA4.1^{+}B220^{+}IgM^{+}CD23^{-}) (Loder et al., 1999). Upon arrival in the spleen, T1 cells mature into T2 (AA4.1^{+}B220^{+}IgM^{+}CD23^{+}) and T3 (AA4.1^{+}B220^{+}IgM^{-}CD23^{+}) cells. The transitional T2 cells can make a binary cell fate decision to differentiate into follicular B (FoB) (AA4.1^{-}B220^{+}CD23^{+}CD21^{low}) or marginal zone B (MZB) cells (AA4.1^{-}B220^{+}CD23^{low}CD21^{+}) (Allman et al., 2001; Loder et al., 1999; Martin and Kearney, 2000; Pillai et al., 2005; Pillai and Cariappa, 2009).

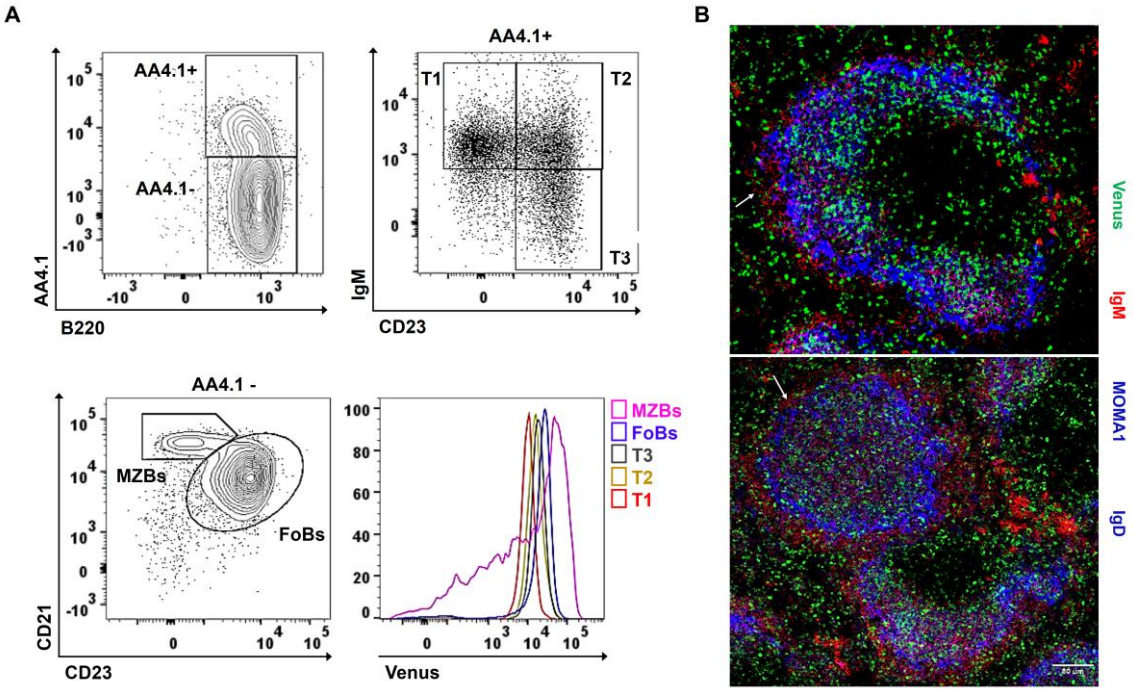

Fig. 10: All splenic transitional and mature B cells receive a Notch signal, but some MZB cells lose their Venus expression. (A) Exemplary FACS analysis of splenocytes from CBF:H2B-Venus mice. Cells are pre-gated on living B220^{+} lymphocytes and further separated into transitional AA4.1^{+}B220^{+} B cells and mature AA4.1^{-}B220^{+} B cells, according to their differing AA4.1 expression. By co-staining for CD23 and IgM,

the transitional B cells are subdivided into T1 (IgM^+CD23^-), T2 (IgM^+CD23^+) and T3 (IgM^-CD23^+) cells. Using the abundance of cell surface markers CD23 and CD21, mature B cells are divided into FoB ($CD23^+CD21^{low}$) and MZB ($CD23^-CD21^{high}$) cells. The histogram on the far right represents an overlay of Venus expression in all gated cell populations. n=5 mice. **(B)** Representative splenic sections from CBF:H2B-Venus mice. Cryosections were stained for MZB cells (IgM^+, red), FoB cells (IgD^+, blue) and metallophilic macrophages lining the MZ sinus ($MOMA1^+$, blue). MZB cells are located in a ring around the follicle, whereas FoB cells are filling the inside of follicles. Venus-expressing nuclei (green) are directly visualized without antibody staining. The scale bar represents 50 µm. White arrows mark individual IgM^+ MZB cells without Venus expression. n=3 mice. Similar figure in (Babushku et al., 2022).

To examine which B cells get a Notch signal in the spleen, the Venus expression was analyzed in transitional and mature B cell subsets from CBF:H2B-Venus mice. Separation of these B cell subsets by staining for the respective cell surface markers in FACS revealed that all of them are Venus-positive (*Fig. 10A*). Of note, the Venus expression in splenic B cell populations was higher than the one in most bone marrow B cells. Moreover, Venus was gradually upregulated from T1 over T2 to T3 cells, continued to increase in FoB cells and culminated with the highest Venus expression in MZB cells. Even though MZB cells had the strongest Venus signal out of all splenic B cells, a portion of them were $Venus^{low}$, indicating that there are MZB cells which downregulate or lose Notch signaling under homeostatic conditions (*Fig. 10A*). This finding was further supported and confirmed by immunohistochemical staining of splenic tissue with a different panel of MZB/FoB markers (IgM/IgD), showing that some IgM^+IgD^- MZB cells are indeed $Venus^-$ (*Fig. 10B*).

5.1.3 Most splenic B1 cells downregulate or completely lose Notch signaling

Even though B1 cells are mainly located in the peritoneum, the spleen is also a niche for this cell type (Baumgarth, 2017, 2016; Hayakawa et al., 1986). Accordingly, the functions of B1 cells differ depending on the organ in which they reside. In the spleen, they mostly have effector functions through IgM and cytokine secretion, whereas in the peritoneal cavity they possess memory cell qualities and can be driven to migrate towards the spleen, where they differentiate into antibody-secreting cells (Baumgarth, 2017, 2016). Previous research has shown that Notch signaling has a role in promoting the development and maintenance of B1 cells in the peritoneum (Witt et al., 2003b). Unlike B2 cells, B1 cells are only a minor population in the spleen. Therefore, no studies have been performed to examine the potential influence of Notch1 or Notch2 signaling in B1 cells inhabiting the spleen, likely because B2 cells are the dominant splenic B cell subset.

To inspect whether B1 cell subsets are also recipients of a Notch signal in the spleen, FACS-stained B1 cells were gated as $CD43^+CD23^-CD19^+$ and were examined for their Venus expression. The analysis showed that, contrary to $CD23^+$ FoB cells, a big fraction of splenic B1 cells had low Venus expression (*Fig. 11*), suggesting they may not continuously be exposed to Dll1-ligand expressing cells. By staining for CD5, a prominent marker distinguishing B1a from B1b cells, it was revealed that while most B1a ($CD5^+B220^{low}$) and B1b ($CD5^-B220^{low}$) cells are Venus-negative, they both contain a fraction with high Venus expression, similar to $CD23^+$ FoB cells. Moreover, the proportion of $Venus^{high}$ cells was much bigger in the B1a than in the B1b fraction (*Fig. 11*).

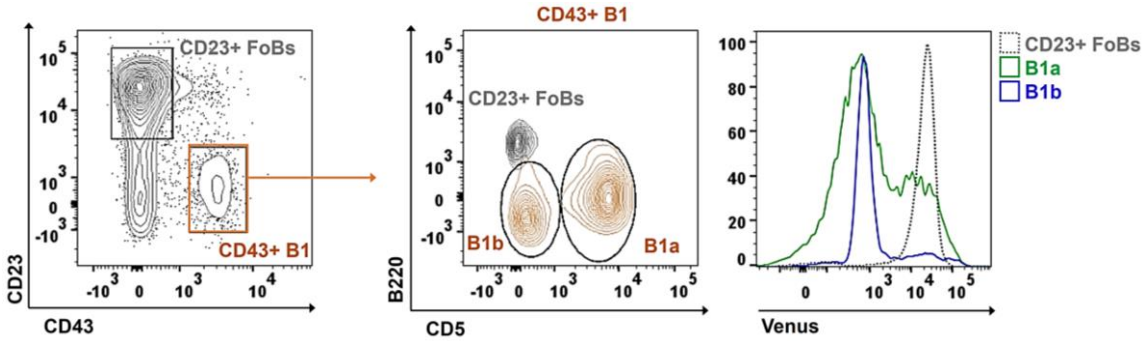

Fig. 11: A major fraction of B1 cells downregulate Venus, suggesting they do not get a Notch signal. Exemplary FACS plots from one unimmunized (UI) CBF:H2B-Venus mouse. Splenocytes are pre-gated on living $CD19^+$ B cells and further subdivided into B2 and B1 cell subsets according to the CD43/CD23 expression: B1 cells are $CD43^+CD23^-$, whereas follicular (FoB) cells are $CD23^+CD43^-$. MZB cells are excluded from the gates and should be located in the ungated $CD43^-CD23^-$ population. The plot in the middle shows the subsequent separation of $CD43^+$ B1 cells into B1a and B1b cells, according to the abundance of CD5: B1a are $CD5^+$, whereas B1b do not express any CD5. Fitting with their known phenotype, both B1 subsets (orange) are $B220^{low}$, compared to $CD23^+$ FoBs (grey) which are only $B220^{high}$. The histograms on the right show an overlay of Venus levels in all three cell populations. n=5 mice. Similar figure in (Babushku et al., 2022).

Of note, the Venus signal in majority of B1 cells was rather low, which is similar to the portion of MZB cells that lost the Venus signal (*Fig. 10A*). This revelation is interesting because it can possibly be attributed to the functional similarities between B1 and MZB cells, despite their different developmental origin. For instance, both cell types have the capacity of self-renewal in the periphery, can differentiate into antibody-producing cells even in the absence of external antigen and can take part in the primary response towards bacterial and viral pathogens (Kreslavsky et al., 2018). Thus, the discovery that many B1 cells downregulate or do not get a Notch signal in the spleen, just as some MZB cells do not, may be related to the similar functional qualities of these two B cell subsets.

5.1.4 B cell subsets in the peritoneum and lymph nodes are recipients of a Notch signal

Next, we examined the Venus expression in B lymphocytes of other lymphoid organs, such as the peritoneum and the lymph nodes. The FACS data revealed that both B1 and B2 cells in the peritoneum exhibited high Notch signaling activity (*Fig. 12*). Unlike splenic B1 cells, which were mostly Venus-low, most peritoneal B1 cells were Venus-high and thus recipients of a Notch signal. Previous research found Notch2 mRNA to be more highly-enriched in peritoneal B1 cells, compared to the Notch1 mRNA levels, which were almost undetectable (Saito et al., 2003). However, mice lacking the RBPJ mediator of Notch signaling, as well as mice with a conditional B-cell-specific Notch2 deletion did not show any defects in the B1 cell subset of the peritoneum (Saito et al., 2003; Tanigaki et al., 2002). Thus, the observed Notch signaling in peritoneal B1 cells may be only transient and necessary to support survival and maintenance of B1 cells in the peritoneum at given times.

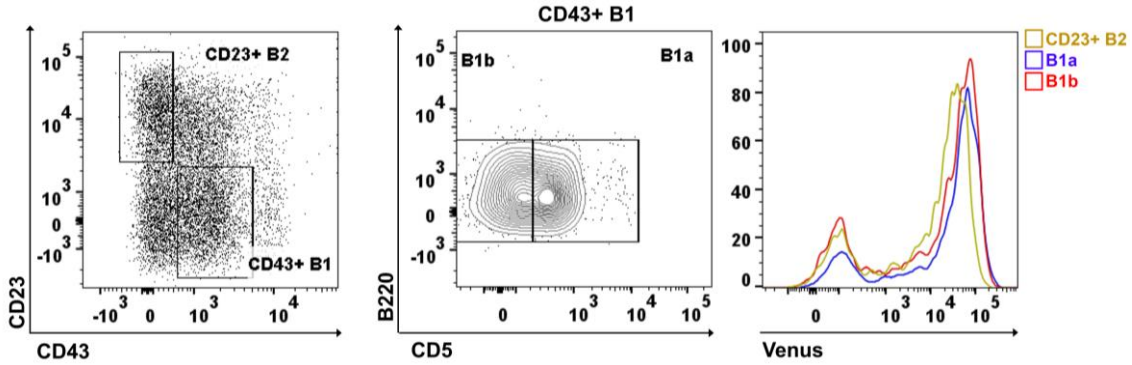

Fig. 12: Peritoneal B2, B1a and B1b cells exhibit similar Venus expression and receive a Notch signal. Exemplary FACS plots from one CBF:H2B-Venus mouse. Splenocytes are pre-gated on living $CD19^+$ B cells and further subdivided into B2 ($CD23^+CD43^-$) and B1 ($CD43^+CD23^-$) cells. The plot in the middle shows the separation of $CD43^+$ B1 cells into B1a ($CD5^+$) and B1b ($CD5^-$) cells. The histograms show an overlay of Venus in the three cell populations. n=5 mice.

In the lymph nodes, we discovered that all $CD19^+B220^+$ B cells were Venus-positive and exhibited high Notch signaling, compared to the $CD19^-B220^-$ non-B cells which were mostly Venus-low or negative (*Fig. 13*). The subdivision of B cells into FoB and MZB cells confirmed the lack of MZB cells in other SLOs. MZBs are sessile in the MZ of the spleen and do not recirculate to the lymph nodes, in contrast to FoB cells (Cinamon et al., 2008; Martin and Kearney, 2002; Pillai et al., 2005). Thus, all $CD19^+$ B cells in the lymph nodes were $CD23^+CD21^{low}$ FoB cells that retained high Venus expression, very similar to the previously described $CD23^+$ FoB cells of the spleen.

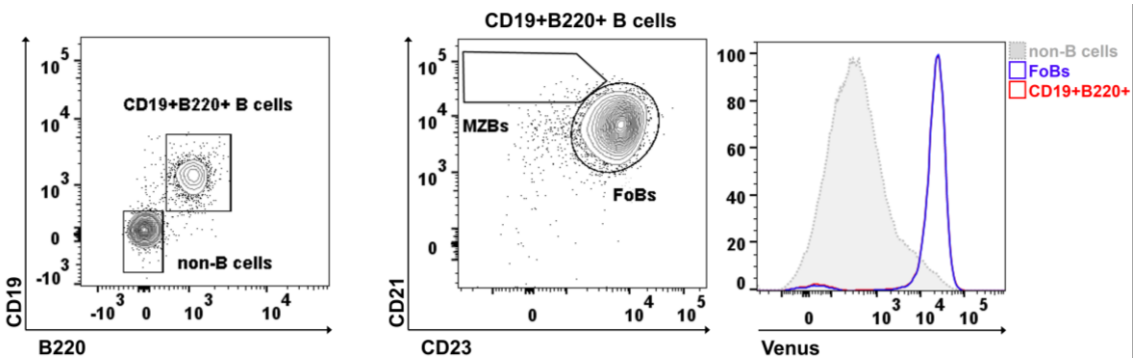

Fig. 13: CD19⁺ FoB cells in the lymph node exhibit high Notch signaling activity. Representative FACS analysis from one CBF:H2B-Venus mouse. Splenocytes are pre-gated on living cells and further subdivided into $CD19^+B220^+$ B cells and $CD19^-B220^-$ non-B cells. The plot in the middle shows the separation of $CD19^+B220^+$ B cells into FoB ($CD23^+CD21^{low}$) and MZB ($CD23^{low}CD21^{high}$) cells. The histograms show an overlay of Venus in $CD19^+B220^+$ and $CD23^+CD21^{low}$ B cells, compared to non-B cells. n=5 mice.

5.2 Notch2 surface expression is strongly induced upon in vitro activation of B cells

Notch2 has already been identified as an important player in peripheral B cell maturation towards the MZB cell lineage from transitional and FoB cells (Lechner et al., 2021; Pillai and Cariappa, 2009). However, not much has been known about the role of Notch2 in B cell activation, or whether it is important during the differentiation of activated B cells into other B cell subsets in primary immune responses. To learn more about Notch2 in B cell activation, it was first examined whether in vitro activation of purified B cells by different stimulating agents leads to changes in the expression of Notch2 on the cell surface. FACS analysis revealed that Notch2 surface expression was strongly induced on B cells as early as 24 h post stimulation (*Fig. 14*). Interestingly, the kinetics of Notch2 expression over time differed with different stimulating agents, which may correlate with the signaling receptors that they trigger (e.g. CD40R, BCR, TLR etc.). B cells treated with anti-IgM or anti-CD40 alone, as well as with LPS showed a similar progression of Notch2 surface expression over time. There was an immediate upregulation at 24 h, which was stably sustained at later time points (*Fig. 14A*), suggesting that Notch2 signaling may synergize with the BCR, CD40 or TLR pathways to promote and sustain the activated state of B cells. Surprisingly, the combined stimulation of B cells with the interleukins IL4 and/or IL21 and anti-CD40 resulted with a counter-regulation of Notch2 at later time points. While Notch2 surface expression was strongly induced at 24 h, it became rapidly down-regulated at 48 h and 72 h (*Fig. 14B*). Recent work by a master student (E. Telumyan, 2022) under my supervision demonstrated that CD95 expression was continuously up-regulated, whereas CD38 was strongly downregulated from 0 h to 72 h on B cells stimulated with these cytokines (CD40+IL4 and CD40+IL4+IL21).

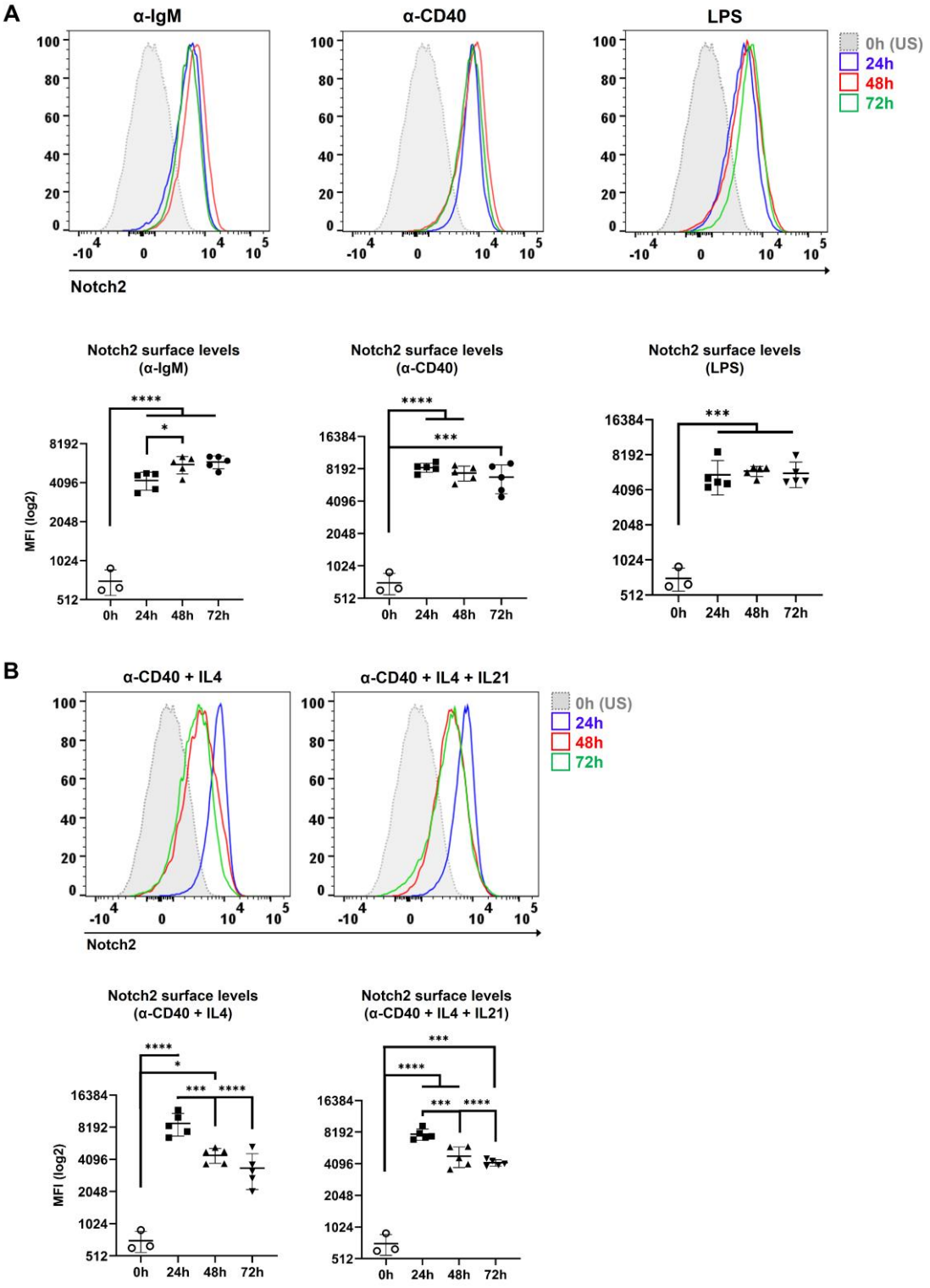

Fig. 14: Kinetics of the Notch2 surface receptor expression on activated B cells over time. (A) Notch2 surface levels following anti-IgM (for BCR), anti-CD40 (for CD40R) and LPS (for TLRs) stimulus. **(B)** Notch2 receptor expression on the surface of B cells activated through anti-CD40 + IL4 or anti-CD40 + IL4 + IL21 stimulation. **(A-B)** The upper rows show exemplary FACS overlays from one mouse. Each colored histogram depicts the Notch2 surface expression on purified B cells at a given time point after stimulation. The filled grey histograms show ex vivo Notch2 expression on unstimulated B cells prior to culture (0 h). In the lower row, a graphical summary of logarithmized (log2) median fluorescent intensities (MFI) of Notch2 is given for all analyzed mice. n=5, except for 0 h n=3. Ordinary one-way-ANOVA, Tukey's multiple comparisons test.

Thus, most cells analyzed at 72 h were $CD95^{high}CD38^{-}$ and adopted a so-called GC-like phenotype in vitro (E. Telumyan, 2022).This observation was in accordance with the role of CD40, IL4 and IL21 receptor signaling in the differentiation and maintenance of germinal center (GC) cells after TD antigen encounter in-vivo. The data presented in *Fig. 14* revealed that the previously observed transition of CD40 + IL4 (+ IL21) -activated B cells into GC-like B cells (E. Telumyan, 2022) was also accompanied by a progressive downregulation of Notch2 surface expression over 72 h (*Fig. 14B*). These findings were of particular significance for the next steps in this study because they hinted towards the possibility of a distinct dynamic regulation of Notch2 during TD immune responses in-vivo as well, which we proceeded to examine more closely. The most interesting findings of the analyses are presented in the next chapters.

5.3 Notch signaling in the TD immune response of CBF:H2B-Venus mice

Considering the findings from the in vitro B cell stimulation assays with cytokines that mimicked T-cell-dependent activating agents, the next part of this study focused on analyzing the expression of Venus, as proxy for active Notch signaling, in B cell subsets that arise specifically after primary immunization with a TD antigen. For this purpose, previously described CBF:H2B-Venus mice were injected intraperitoneally with 100 µg NP-CGG, and the splenic immune response was analyzed after 7 and 14 days post injection (p.i.).

5.3.1 Notch signaling is downregulated in most splenic germinal center (GC) cells

FACS analysis of the germinal center (GC) response in the spleen revealed that the Venus expression was strongly downregulated in most GC B cells at day 7 and 14, compared to the non-GC B cells. Notably, there was a progressive downregulation of the Venus expression in GC B cells over time, from day 7 to day 14 post immunization (*Fig. 15A*). These findings were re-confirmed by immunofluorescence staining for GC B cells in histology. Indeed, most of the cells inside the GC structures were Venus-negative, and only a few Venus-bright $GL7^{+}$ cells were detected in the spleen (*Fig. 15B*). Interestingly, the Venus-positive GC B cells seemed to be clustered on the inside of the B cell follicle at the border with the T-cell zone, where GC structures were seeded. This may indicate that Notch signaling is strongly active at the initial B-/T- cell contact when B cells become activated, which is in accord with the first observations from the in vitro stimulation experiments.

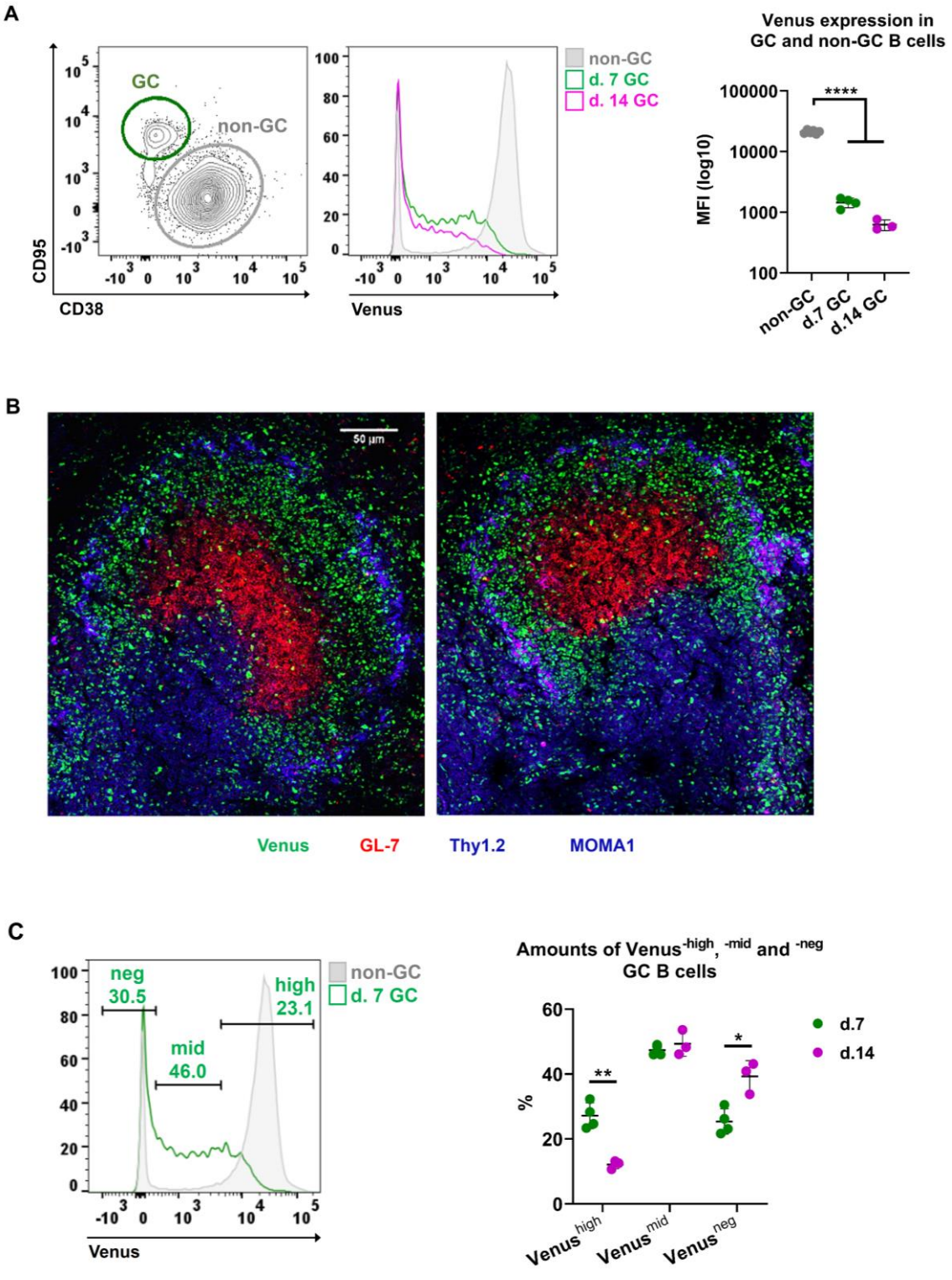

Fig. 15: Venus expression is downregulated in most splenic GC B cells over time. FACS plots are representative for day 7 p.i. Cells were pre-gated on living B220$^+$ lymphocytes. **(A)** GC B cells were gated as CD95$^+$CD38^{low}, non-GC B cells as CD38$^+$CD95$^{mid\text{-}low}$. The histogram shows the overlay of Venus at indicated time points. The graph on the right summarizes median fluorescent intensities (MFI) of Venus in the analyzed populations. n=4 at day 7, n=3 at day 14. Tukey's one-way ANOVA of logarithmized MFI values. **(B)** Histology of splenic cryosections at day 7 p.i. Tissues were stained for GC cells (GL7$^+$, red), T cells (Thy1.2$^+$, blue) and metallophilic macrophages (MOMA1$^+$, blue). The Venus signal (green) is directly visualized without antibody staining. The scale bar represents 50 µm. n=2 mice. **(C)** Representative histogram

overlay of Venus expression in GC and non-GC B cells at day 7 p.i. The GC and non-GC subsets were gated as in (A). GC B cells were sub-divided into 3 populations according to the Venus expression: Venus^{high}, Venus^{mid} and Venus^{neg}. The graph on the right depicts the frequencies of the 3 Venus-subpopulations in the GC at indicated time points in percentage (%). n=4 at day 7, n=3 at day 14. Sidak's 2-way-ANOVA. Similar figure in (Babushku et al., 2022).

Upon further examination of the histograms of Venus expression in GC B cells, it was discovered that a small fraction of GC B cells remained Venus^{high} at both day 7 and 14 post immunization. The frequencies of these Venus^{high} GC B cells were higher at day 7 than at day 14 (*Fig. 15C*). While the percentages of Venus^{high} cells significantly decreased, those of Venus^{neg} cells concomitantly increased, confirming once again that Notch signaling is continuously downregulated with the progression and maturation of the GC.

5.3.2 Venus-expressing GC B cells that receive a Notch signal are enriched in the light zone

The discovery that a portion of GC B cells still retained high Venus expression prompted us to investigate the light zone (LZ) and dark zone (DZ) distribution of these cells.

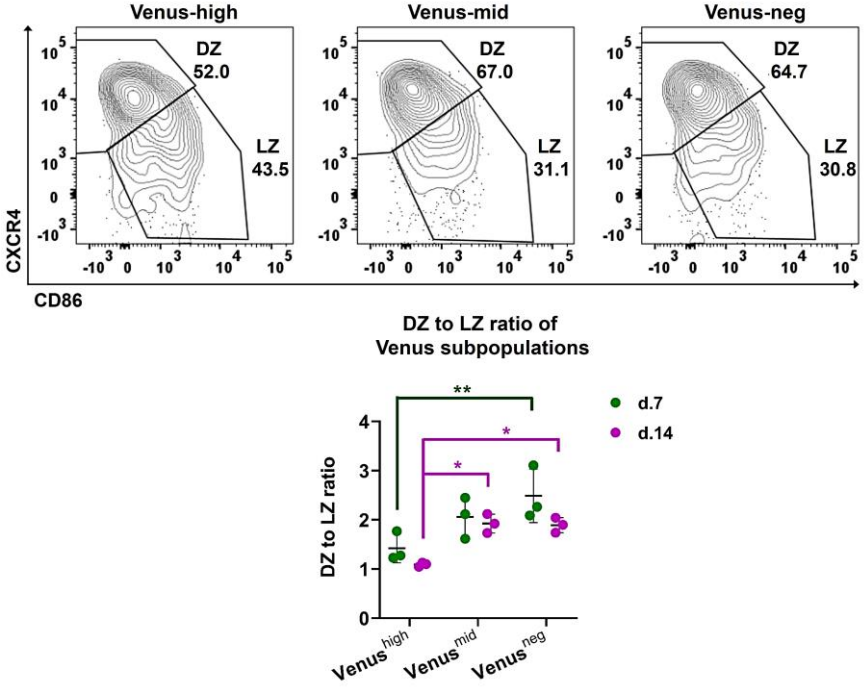

Fig. 16: Venus-positive cells predominantly have a LZ phenotype in the GC. Representative FACS analysis from day 7 p.i. Plots were pre-gated on living B220^{+}CD95^{+}CD38^{low} GC B cells. Subsequently, the GC B cells were subdivided into 3 Venus populations: Venus^{high}, Venus^{mid} and Venus^{low} (as shown in *Fig. 15C*), and were examined for their dark zone (DZ; CXCR4^{high}CD86^{low}) and light zone (LZ; CXCR4^{low}CD86^{high})

distribution. The graph summarizes the ratios of the percentages of DZ to LZ cells in the 3 Venus subpopulations. A lower DZ to LZ ratio implies that there is an enrichment of the indicated Venus subpopulation in the LZ. n=3. Sidak's 2-way-ANOVA. Similar figure in (Babushku et al., 2022).

The CXCR4 and CD86 surface staining revealed that around half of the Venus^{high} GC B cells had a LZ phenotype, compared to only a third of the Venus^{mid} and Venus^{neg} cells. The significantly lower DZ/LZ ratio in Venus^{high} cells, especially in comparison to that of Venus^{neg} cells, indicated that Venus^{high} GC cells were enriched in the LZ, whereas Venus^{mid} and Venus^{neg} cells were predominantly found in the DZ *(Fig. 16)*.

5.3.3 Notch signaling is downregulated in GC B cells of the lymph nodes and Peyer's Patches

Germinal centers form not only in the spleen, but also other SLOs, such as the Peyer's Patches (PPs, *Fig. 17A*) and lymph nodes (LN, *Fig. 17B*) (Klein and Dalla-Favera, 2008; Stebegg et al., 2018). Therefore, we examined the Venus signal in GC B cells in these organs and compared them to the remaining B cell population after 7 and 14 days post immunization. The analyses revealed similar findings as in GCs of the spleen.

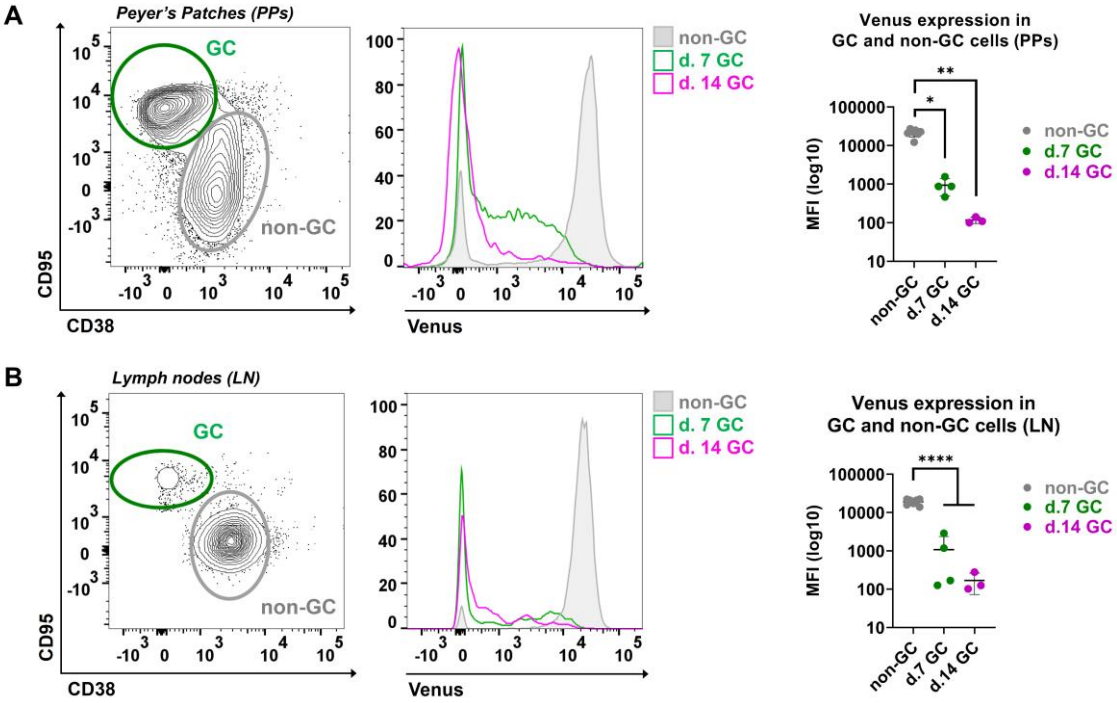

Fig. 17: Venus expression is strongly downregulated in GC B cells in PPs and LN over time. FACS plots are representative for day 7 p.i. Cells were pre-gated on living B220^{+} lymphocytes. GC B cells were gated as CD38^{low}CD95^{+}, non-GC cells as CD38^{+}CD95$^{mid\text{-}low}$. The histogram shows the overlay of Venus in the gated populations at d.7 and d.14. The graphs depict median fluorescent intensities (MFIs) of Venus in GC vs. non-GC B cells. n=4 at day 7, n=3 at day 14. Tukey's one-way ANOVA of logarithmized MFIs. **(A)** Venus in GC vs. non-GC cells of Peyer's Patches (PPs). **(B)** Venus in GC vs. non-GC in lymph nodes (LN).

The Venus expression was strongly downregulated in most CD38^{low}CD95^{+} GC B cells and this downregulation was progressively increasing with time, compared to the non-GC B cells in both LN and PPs (*Fig. 17A-B*). Thus, Notch signaling becomes continuously down modulated or turned off in all GCs formed across different SLOs in mice during the primary TD immune response, confirming that Notch signaling activity and GC B cell differentiation are inversely correlated and incompatible with one another.

5.3.4 Notch signaling is lost in most plasma cells

Next, the Venus signal was examined in the plasma cell population (PCs) of the spleen, as well as of the blood and bone marrow. PCs are initially generated in the spleen, but later on they migrate through the blood towards their homing niche in the bone marrow, thus this population can be detected at all three sites in mice (Pracht et al., 2017; Roth et al., 2014).

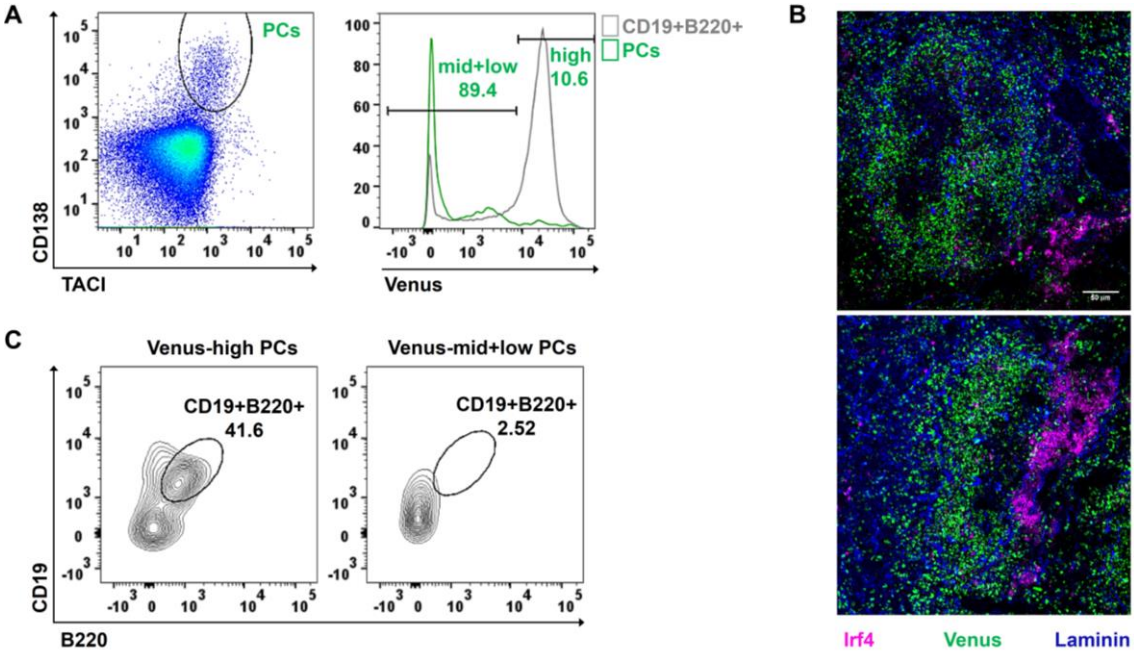

Fig. 18: Venus expression is strongly downregulated in most splenic plasma cells. Representative FACS analysis from day 7 p.i. Splenocytes were pre-gated on living lymphocytes with a large FSC/SSC gate and analyzed for plasma cells (PCs). **(A)** Exemplary FACS plot showing the TACI/CD138 staining for PCs (TACI^{+}CD138^{+}). The histogram depicts an overlay of Venus in PCs (green) and B220^{+}CD19^{+} B cells (grey). The Venus expression in PCs was subdivided into Venus^{high} and Venus$^{mid+low}$ cells. The gates and percentages refer to the green histogram for PCs. **(B)** Immunofluorescence staining from day 7 p.i. Splenic sections were stained for PB/PCs (Irf4^{+}, pink) and for basement membranes of endothelial cells (Laminin, blue). The scale bar represents 50 µm. n=2 mice. **(C)** The Venus^{high} and Venus$^{mid+low}$ PCs gated as in (A) were further stained for the distribution of surface markers CD19 and B220, to distinguish the CD19^{+}B220^{+} (pre-) plasmablasts from the mature PCs (CD19^{-}B220^{-}). Similar figure in (Babushku et al., 2022).

We found that the Venus expression was almost completely lost in around 90% of splenic plasma cells, compared to CD19^{+} B cells. Even though most PCs had strongly downregulated the Venus and thus had turned off Notch signaling, a fraction among them (app. 10%) still retained high Venus expression in the spleen (*Fig. 18A*). Histology of splenic tissue further confirmed that plasma cells are mostly Venus^{neg}, with only a few Irf4^{+}Venus^{+} cells being detected (*Fig. 18B*). Further examination of the Venus^{high} TACI^{+}CD138^{+} PCs revealed that a major portion of them expressed high levels of surface CD19 and B220, compared to the Venus$^{mid+low}$ PCs, which were almost uniformly CD19^{-}B220^{-} (*Fig. 18C*). During the stages of PC differentiation in mice, the developmental precursors of plasma cells are dependent on CD19-signaling and also express B220 on the cell surface, but these markers are then gradually lost in later stages of PC maturation (Oracki et al., 2010; Pracht et al., 2017). Thus, these results implied that the Venus-expressing PCs with active Notch signaling in the spleen are (pre-) plasmablasts (PB), rather than fully matured plasma cells.

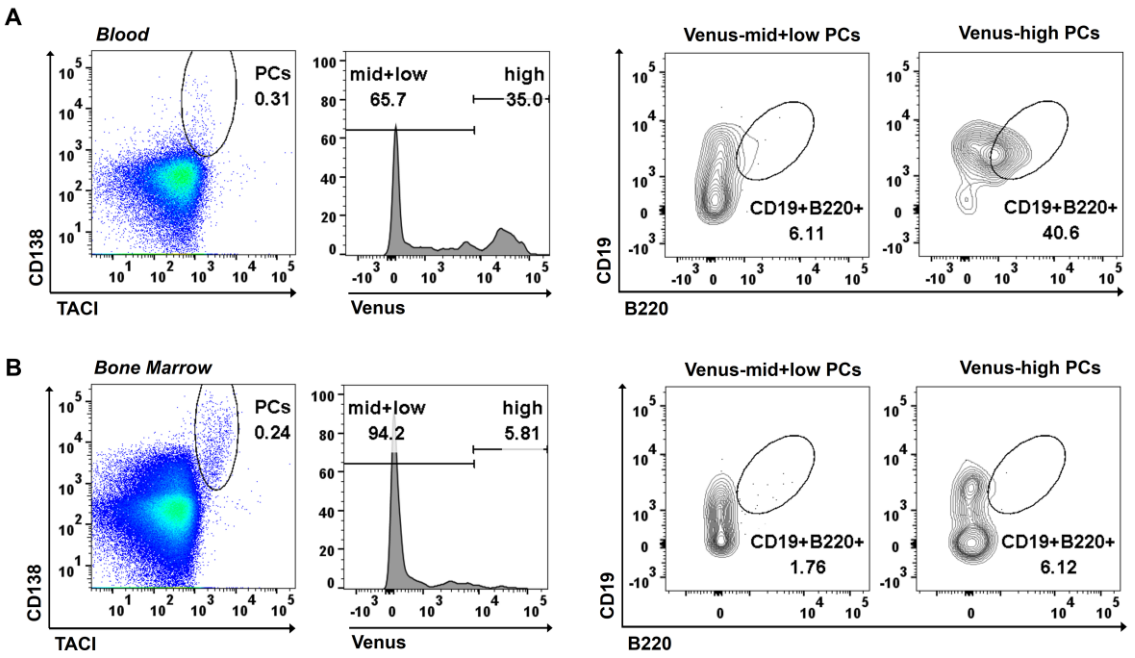

Fig. 19: Venus expression is downregulated in almost all bone marrow PCs, whereas many PCs in the blood are still Venus-high. (A) Exemplary analysis from day 7 p.i. in the blood. FACS plots show the TACI/CD138 staining for PCs. The histogram depicts the Venus expression in PCs, subdivided into Venus^{high} and Venus$^{mid+low}$ cells. The Venus^{high} and Venus$^{mid+low}$ PCs were further stained for CD19 and B220, to distinguish CD19^{+}B220^{+} plasmablasts from mature PCs (CD19^{-}B220^{-}). **(B)** Representative FACS analysis for PCs in the bone marrow at day 14 p.i. Detection of PCs and subdivision of Venus expression into mid+low and high is done as in (A).

Examination of the PCs in the blood and the bone marrow revealed that Venus expression was indeed downregulated or lost in a bigger fraction of TACI^{+}CD138^{+} PCs, similar

to the splenic PCs (*Fig. 19*). However, compared to the spleen, we found increased amounts of Venus^{high} PCs in the blood at day 7 p.i. All of them were uniformly positive for CD19 and around half of them also co-expressed B220 (*Fig. 19A*). On the other hand, there were barely any Venus^{high} PCs detected in the bone marrow at day 14 p.i. (*Fig. 19B*). These findings imply that Notch signaling is retained in plasmablasts and possibly short-lived PCs in the spleen and blood, whereas it is completely downregulated in fully-matured long-lived PCs of the bone marrow.

5.3.5 Notch signaling is downregulated in splenic IgG1-switched B cells

Early germinal centers contain mostly IgM$^+$ cells, but between day 7 and 14 of the immune response, GC B cells switch at a high rate to IgG1$^+$ cells (Sundling et al., 2021). Therefore, the Venus expression was analyzed in IgG1-switched B cells at days 7 and 14 after immunization. It was discovered that the Venus signal was downregulated in IgG1$^+$ B cells, both with a GC (CD38$^-$) and non-GC (CD38$^+$) phenotype (*Fig. 20*).

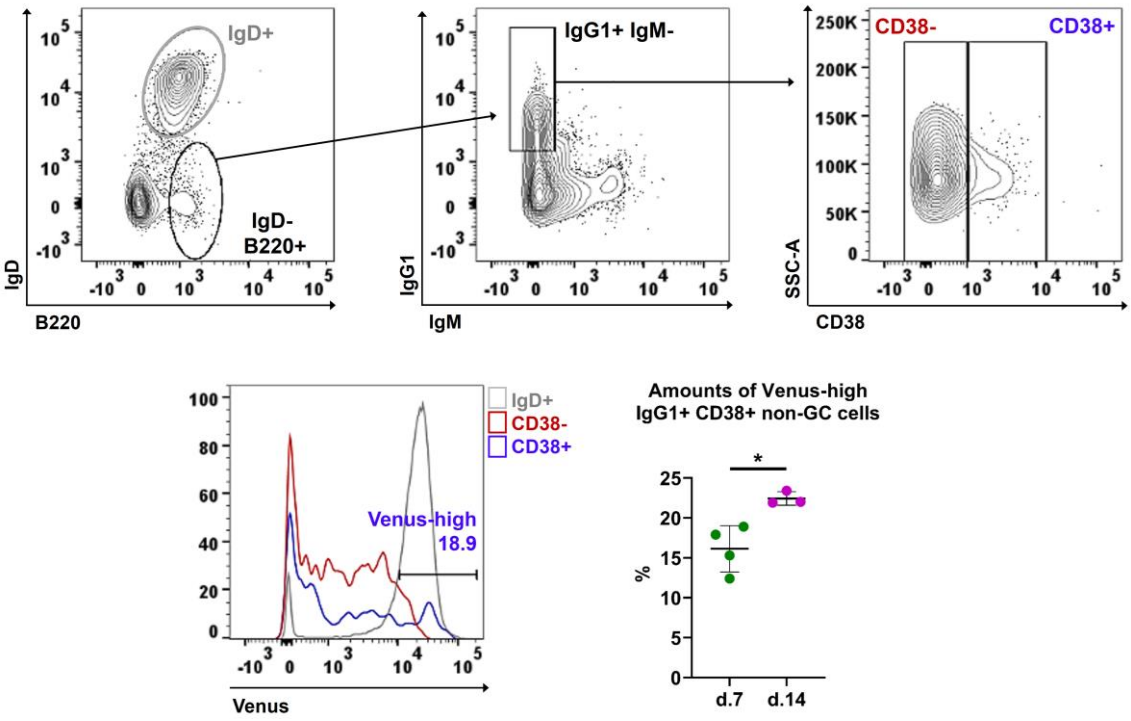

Fig. 20: Venus expression is downregulated in most IgG1$^+$ B cells. Representative FACS analysis from day 7 p.i. Splenocytes were pre-gated on living lymphocytes. Splenic IgG1-switched B cells were identified through sequential gating as B220$^+$IgD$^-$IgM$^-$IgG1$^+$ cells. Using the CD38 expression levels, the IgG1$^+$ cell population was further subdivided into GC (CD38$^-$) and non-GC (CD38$^+$). The histograms in the lower row depict the overlay of Venus expression in IgG1$^+$ GC (red) and non-GC (blue) B cells, compared to the one in IgD$^+$ B cells (grey). The gate and percentage refer to the blue histogram of Venus^{high} cells among IgG1$^+$CD38$^+$ non-GC cells. The graph compiles the frequencies (%) of Venus^{high} IgG1$^+$CD38$^+$ non-GC cells at indicated time points. n=4 at day 7, n=3 at day 14. Welch's unpaired t-test. Similar figure in (Babushku et al., 2022).

A big fraction of the IgG1$^+$ non-GC cells had decreased Venus expression, which may suggest that most positively-selected IgG1$^+$ B cells do not immediately regain Notch signaling activity upon their immergence from the GC. Interestingly, some IgG1$^+$ non-GC cells retained high Venus expression and their frequencies significantly increased from day 7 to day 14, in accordance with the GC progression (*Fig. 20*). This finding implied that either (1) early IgG1 memory cells arising from activated cells in a GC-independent manner exhibit a still ongoing Notch signaling activity, or (2) some high-affinity, GC-derived IgG1 memory cells receive a *de novo* Notch signal in the periphery.

5.4 Effects of GC B cell-specific inactivation or constitutive activation of Notch2 on the TD immune response

The progressive loss of Venus in most, but not all, GC cells, IgG1$^+$ B cells and PCs indicated that Notch signaling needs to be down-modulated during different stages of the GC reaction. Its regulation in B cells upon TD immunization appears to be dynamic and should therefore be examined in more detail. The CBF:H2B-Venus mouse model is not a specific reporter for just the Notch2 signaling activity through the Notch2-ICD. The Venus expression is indicative of the presence of Notch-ICD signaling, activated through both the Notch1 and Notch2 receptors in B cells.

To investigate the role of particularly Notch2 signaling during the primary immune response, we generated and analyzed conditional Notch2 transgenic mice in combination with the Cγ1-Cre strain, thus ensuring a GC B cell-specific inactivation (N2KO//CAR) or constitutive activation of Notch2 signaling (N2IC/hCD2) upon NP-CGG immunization (*Fig. 21*). As control, a reporter mouse strain was used, which expressed the human coxsackie/adenovirus receptor (CAR) upon Cre-mediated recombination (termed control/CAR) in the *rosa26* locus (*Fig. 21A*). To trace the B cells that successfully underwent Cre-mediated recombination of the loxP-flanked regions, we made use of the reporter gene CAR in the N2KO//CAR and control/CAR mice (*Fig. 21A-B*), and hCD2 (truncated version of the human CD2 receptor) in N2IC/hCD2 mice (*Fig. 21C*). The genetic targeting strategy is designed so that CAR-expressing cells in N2KO//CAR mice express a truncated, non-functional Notch2 receptor with only an extracellular portion, but no intracellular signaling domain (*Fig. 21B*), whereas hCD2-expressing cells from N2IC/hCD2 animals exhibit ligand-independent constitutively active Notch2-ICD inside the cell (*Fig. 21C)*. Antibody staining against CAR or hCD2 in flow cytometry enables the reliable tracking of antigen-responding cells, which have deleted the lox-P-flanked regions of interest. A detailed description of the gene targeting strategies used to produce these mouse strains is given in chapter *3.1 Mouse models.*

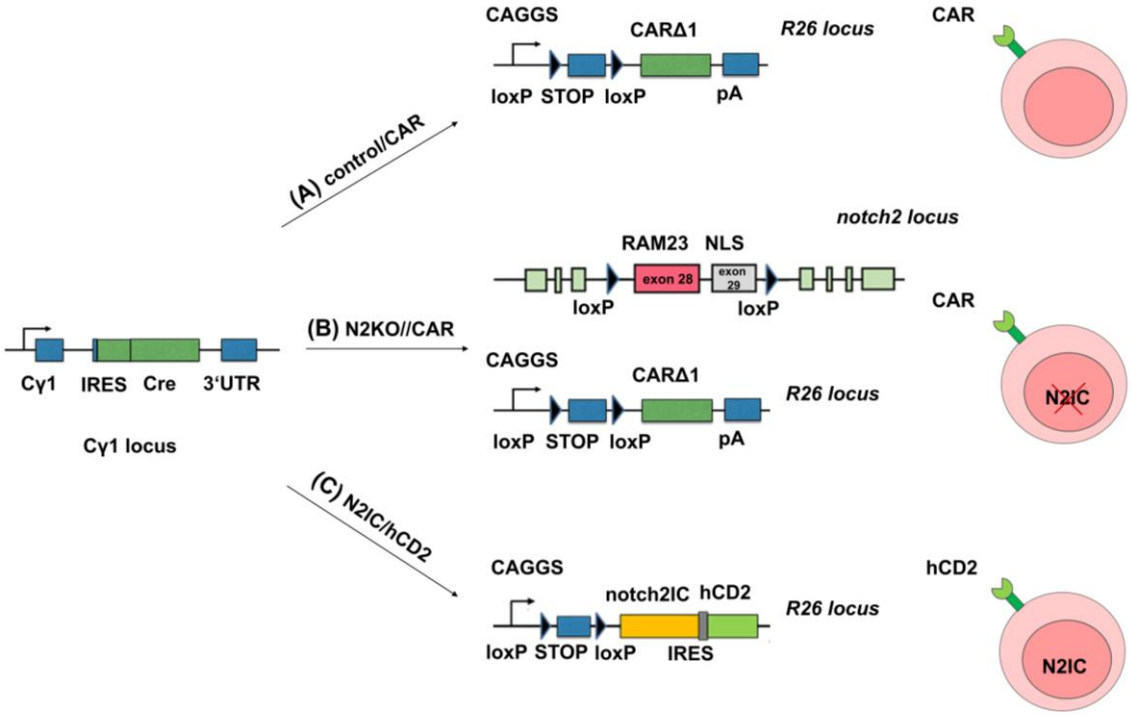

Fig. 21: Generation of Cγ1-Cre transgenic mice with a conditional GC-B-cell-specific inactivation or constitutive activation of Notch2. In the Cγ1-Cre strain, the Cre-coding sequence is preceded by an IRES sequence and inserted after the last membrane-coding exon of the Igγ constant region, under the *Cγ1* promoter activity. **(A)** R26-CARΔ1^{stopfl} mice were crossed with Cγ1-Cre animals to produce the control/CAR strain. Here, a lox-P-flanked stop cassette is placed in front of the *carΔ1* transgene, which codes for the coxsackie/adenovirus receptor (CAR), under the control of the *rosa26* CAGGS promoter. Cre-mediated excision results in CAR expression on the cell surface. **(B)** In N2KO//CAR animals, the lox-P-flanked *carΔ1* transgene is placed in the *rosa26* locus. In the murine *notch2* locus, exon 28 coding for the C-terminal tail of RAM23 and exon 29 coding for the NLS are flanked with lox-P sites. Upon Cre-mediated recombination, the intracellular and transmembrane parts of Notch2 are excised, together with the lox-P-flanked stop cassette upstream of the *carΔ1* transgene. Thereby, a truncated non-functional Notch2 with only the extracellular part and the CAR surface receptor are simultaneously expressed. **(C)** In N2IC/hCD2 mice, the coding sequence for *notch2IC,* preceded by a lox-P-flanked STOP cassette is inserted in the *rosa26* locus. An IRES element is fused to the *hcd2* gene*,* coding for a truncated version of the human CD2 receptor. Cre-mediated excision results in expression of Notch2IC inside the cell and hCD2 on the cell surface. Similar figure in (Babushku et al., 2022).

5.4.1 Efficiency of the induction of reporter gene expression upon NP-CGG immunization

Upon immunization, the expression of CAR or hCD2 on the cell surface is irreversible and stable, allowing to reliably track cells with recombined lox-P regions among the B cell population over a 4-week time period. The specificity of the anti-CAR and anti-hCD2 antibodies was confirmed, as little to no background signal was detected in the absence of NP-CGG (unimmunized (UI) mice) (*Fig. 22A*). All mouse strains had comparable frequencies of reporter^{+} B cells in the spleen. The reporter-expressing B cells showed a

similar kinetics over time: the first CAR$^+$ and hCD2$^+$ B cells appeared at day 4 post immunization, accounting for around 2% of total B cells. Their amounts significantly increased with time and reached a peak at day 14, which was in accordance with the progression of the GC. This was followed by a sharp decline back to around 2% reporter$^+$ B cells at day 30 *(Fig. 22B).*

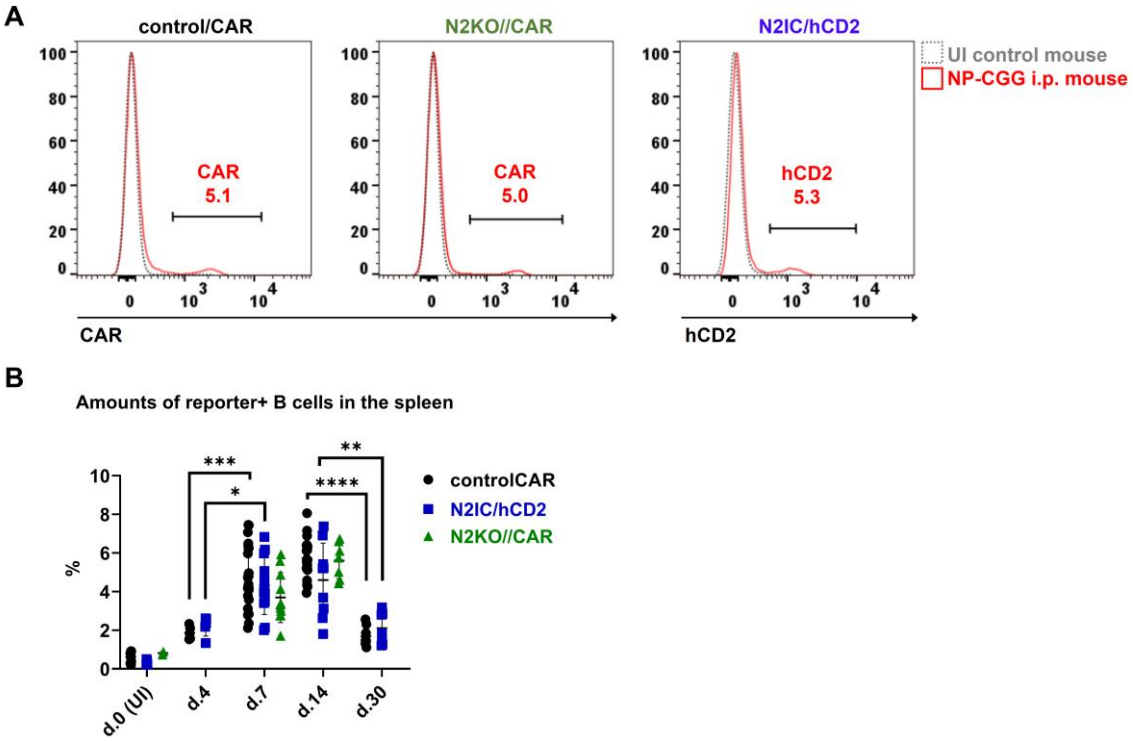

Fig. 22: Deletion efficiency of lox-P-flanked regions in the spleen. (A) Exemplary FACS analyses of splenic reporter$^+$ B cells in the indicated genotypes after immunization with 100 µg NP-CGG. Cells were pregated on living B220$^+$ lymphocytes. Histograms depict the overlays of CAR or hCD2 expression between immunized (red) and uninjected (UI) mice (grey). **(B)** Graphical summary of the frequencies of detected reporter$^+$ B220$^+$ cells at indicated time points in percentages (%). n≥2 at day 0, n=4 at day 4, n≥11 at day 7, n≥7 at days 14 and 30. Tukey's 2-way-ANOVA multiple comparisons test. Similar figure in (Babushku et al., 2022).

5.4.2 GC formation is diminished by induction of N2IC, but not by Notch2 inactivation

FACS analyses for germinal center (GC) cells revealed that N2IC/hCD2 mice were incapable to generate normal GC B cell frequencies, compared to control/CAR animals (*Fig. 23A-B*). Despite similar percentages of reporter$^+$ B cells in both genotypes, N2IC-expressing cells did not differentiate into GC B cells, resulting with the significantly decreased amounts of N2IC/hCD2$^+$ GC B cells over the total observation period (*Fig. 23C*). On the other hand, the frequencies of GC B cells in N2KO//CAR animals were comparable to those in control/CAR mice (*Fig. 22A-B*), indicating that inactivation of Notch2 does not interfere with proper GC B cell differentiation. (*Fig. 23C)*. These findings were

in accord with the Venus expression in GCs of CBF:H2B-Venus mice, which revealed that Notch signaling was strongly downregulated in cells with a GC phenotype.

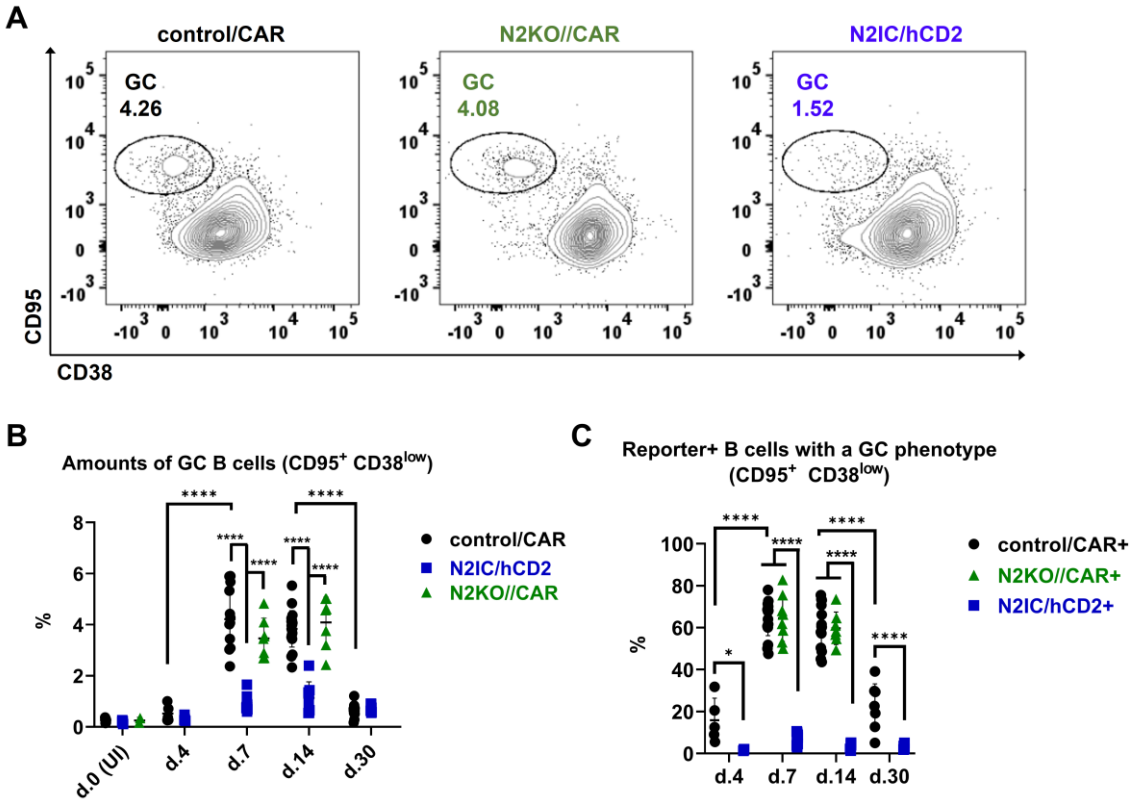

Fig. 23: Induction of N2IC interferes with proper GC B cell differentiation. (A) FACS analysis are representative for day 7 p.i. Splenic cells were pre-gated on living B220^{+} lymphocytes and stained for GC B cells (CD95^{+}CD38^{low}). **(B)** The graph depicts the frequencies (%) of GC B cells in the spleen of mice from all 3 genotypes at indicated time points. **(C)** Summary of the percentages of reporter^{+} B cells with a GC phenotype at indicated time points **(B-C)** 2-way-ANOVA multiple comparisons test. n≥2 at day 0, n=4 at day 4, n≥11 at day 7, n≥7 at days 14 and 30. Similar figure in (Babushku et al., 2022).

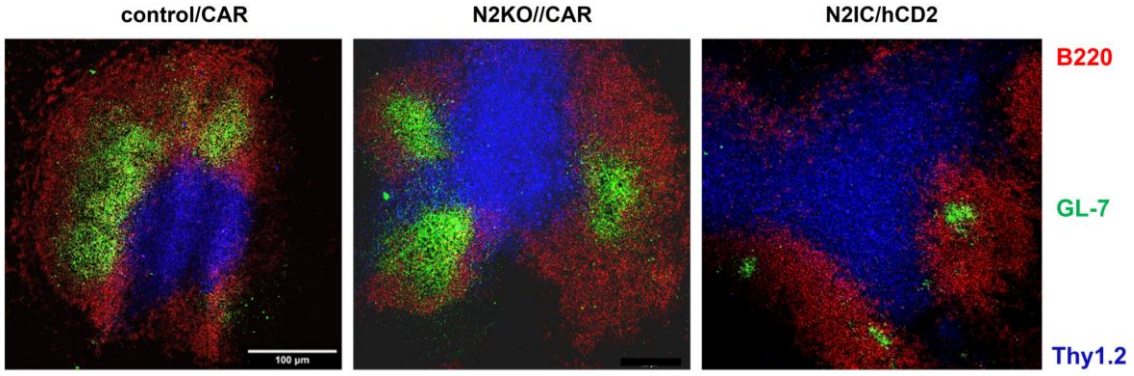

Fig. 24: N2IC/hCD2 mice form fewer and smaller GC structures with improper localization in the B cell follicle. Immunofluorescence staining of splenic tissue from mice of the indicated genotypes. Images are representative for day 7 after NP-CGG immunization. The following cell populations were visualized: GC B cells (GL7^{+}, green), total B cells (B220^{+}, red) and T cells (Thy1.2^{+}, blue). Images were obtained with the

Leica TCS SP5 II confocal microscope and composites were produced in ImageJ. The scale bar shows 50 µm. n=4 mice per genotype. Similar figure in (Babushku et al., 2022).

Immunohistochemical staining for GC structures confirmed that N2IC/hCD2 mice formed significantly fewer and smaller germinal centers, which were not properly localized at the B-/T-cell border, whereas GC B cells in N2KO//CAR and control animals clustered into larger structures located at the B-/T-cell boundary on the inside of the follicle (*Fig. 24*).

5.4.3 Notch2-deficient cells upregulate Bcl6 and correctly enrich in the dark and light zone of the GC

The finding that inactivation of Notch2 does not obstruct GC formation was quite interesting and led to further analyses of Notch2-deficient cells. It was discovered that most N2KO//CAR$^+$ and control/CAR$^+$ cells upregulated the GC initiation factor Bcl6, which facilitated their predominant GC B cell phenotype (*Fig. 25A-B*).

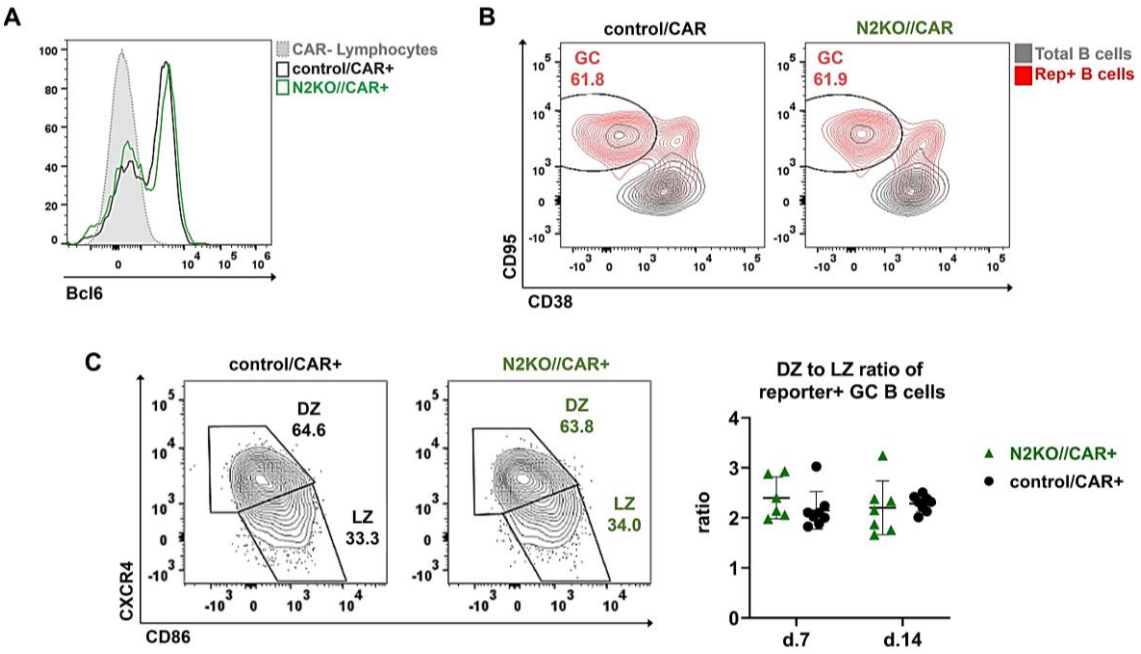

Fig. 25: Notch2-deficient cells induce Bcl6 and adopt the expected DZ/LZ phenotype. Representative FACS plots from day 7 p.i. **(A)** Cells were stained after fixation and permeabilization. Plots were pre-gated on living reporter$^+$ lymphocytes. Histograms show the overlay of Bcl6 in reporter$^+$ and reporter$^-$ cells. **(B)** Reporter$^+$B220$^+$ cells were stained for GC markers. Contour plots show the overlay of CD38 vs. CD95 expression in reporter$^+$ cells (red) and total B cells (black). Gates and percentages refer to the red plots. **(C)** Plots were pre-gated on reporter$^+$ GC B Cells and further analyzed for their dark zone (CXCR4^{high}CD86^{low}) and light zone (CXCR4^{low}CD86^{high}) phenotype. The graph shows the DZ/LZ ratio of reporter$^+$ GC B cells at d7 and 14 p.i. n=6 N2KO//CAR mice, n=8 control/CAR mice. Parts of the figure similar in (Babushku et al., 2022).

However, some reporter$^+$ cells had a CD38^{high} and CD95^{high}CD38^{high} non-GC phenotype, indicating that not all antigen-responding cells enter the germinal center, but some reporter$^+$ cells remain in an activated cell stage (*Fig. 25B*). Additionally, we found that in the GC, the N2KO//CAR$^+$ GC B cells were correctly distributed between the light (LZ) and dark zone (DZ) compartments. Around two thirds of them were DZ centroblasts, and one third had the LZ centrocytes phenotype, just like control/CAR$^+$ cells (*Fig. 25C*).

Taken together, these findings imply that inactivation of Notch2 does not influence the differentiation of Notch2-deficient cells into GC B cells and their correct compartmentalization inside the germinal center.

5.4.4 Inactivation of Notch2 in GC B cells impairs their isotype switching to IgG1

Since N2KO//CAR mice did not have an abolishment of GC differentiation, it was next inspected whether lack of Notch2 may influence other aspects of the germinal center, such as the production of IgG1-switched cells. While similar amounts of reporter$^+$IgG1$^+$ B cells were detected in both genotypes at day 7, there were significantly less IgG1$^+$ B cells in N2KO//CAR mice by day 14 in comparison to controls (*Fig. 26A*).

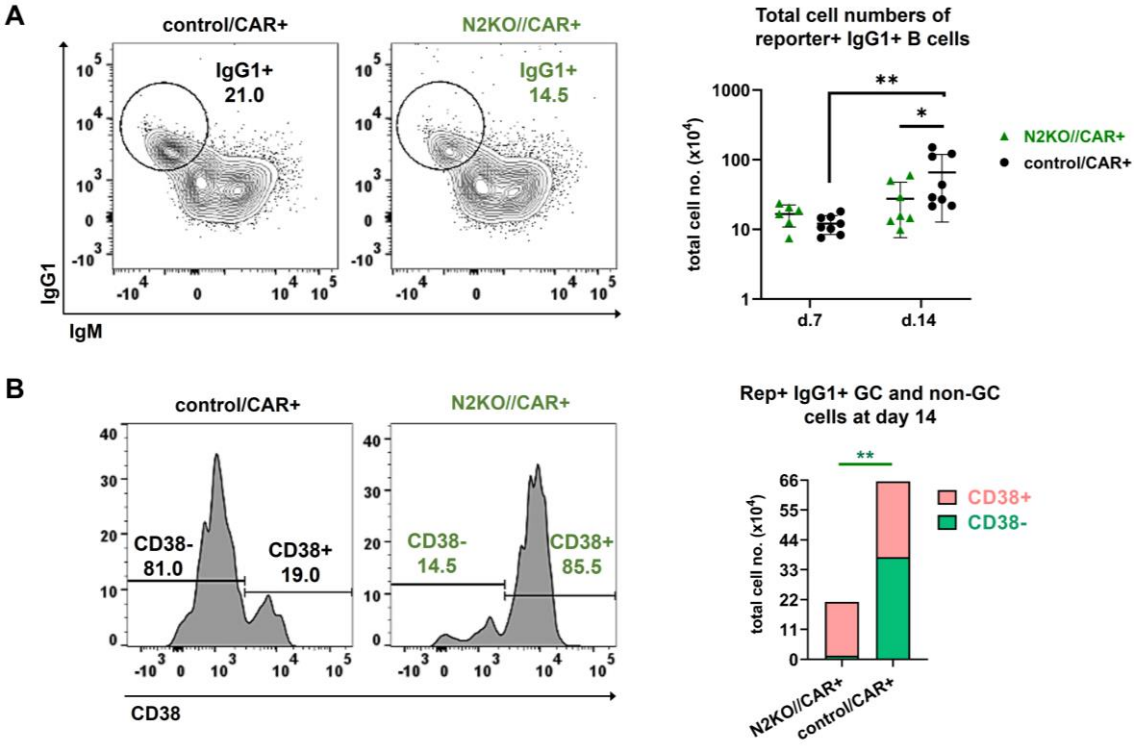

Fig. 26: Inactivation of Notch2 leads to reduced total cell numbers of IgG1$^+$ GC B cells by day 14 of the immune response. Representative FACS plots from day 14 p.i. FACS plots are pre-gated on living reporter$^+$B220$^+$ cells. **(A)** CAR$^+$ B cells were stained with IgM and IgG1, and gated for the percentages of IgG1$^+$IgM$^-$ cells. The graph depicts the total cell numbers of reporter$^+$IgG1$^+$ cells (x 10.000) at indicated time

points. 2-way-ANOVA Sidak's multiple comparisons test. **(B)** Previously gated CAR$^+$IgG1$^+$IgM$^-$ B cells were further subdivided in GC and non-GC cells using the CD38 expression levels in histograms. The stacked bar chart summarizes the total cell numbers of CD38$^-$ (GC) and CD38$^+$ (non-GC) B cells as fractions from the total reporter$^+$IgG1$^+$ B cells at day 14 p.i. 2-way-ANOVA Sidak's multiple comparisons test. **(A-B)** n=6 N2KO//CAR mice, n=8 control/CAR mice. Similar figure in (Babushku et al., 2022).

Indeed, the numbers of IgG1$^+$ B cells in control/CAR mice increased with the natural GC progression, whereas they did not further expand in N2KO//CAR animals during the second week of the immune reaction. Separation of IgG1$^+$ cells into GC (CD38$^-$) and non-GC (CD38$^+$) revealed that the striking difference at day 14 appeared because the IgG1$^+$ GC B cells in N2KO//CAR mice did not increase at all with progressing time (*Fig. 26B*). Most of the generated N2KO//CAR$^+$IgG1$^+$ cells had a non-GC phenotype, suggesting that lack of functional Notch2 leads to an impaired IgG1 class-switch recombination in GC B cells.

5.4.5 Notch2 deficiency leads to less plasma cells in the spleen at day 7 p.i.

Apart from IgG-switched memory cells, another B cell subset that is produced during the primary immune response are plasma cells (PCs). They can be derived from germinal centers, but also from pre-GC cells (extrafollicular PC differentiation) (MacLennan et al., 2003; Vinuesa et al., 2003; Zhang et al., 2018). Examination of the frequencies of splenic plasma cells in the early wave of PC production at day 7 showed that Notch2-deficient cells generated slightly less CD138^{high}B220$^-$ cells in comparison to control/CAR$^+$ cells (*Fig .27*).

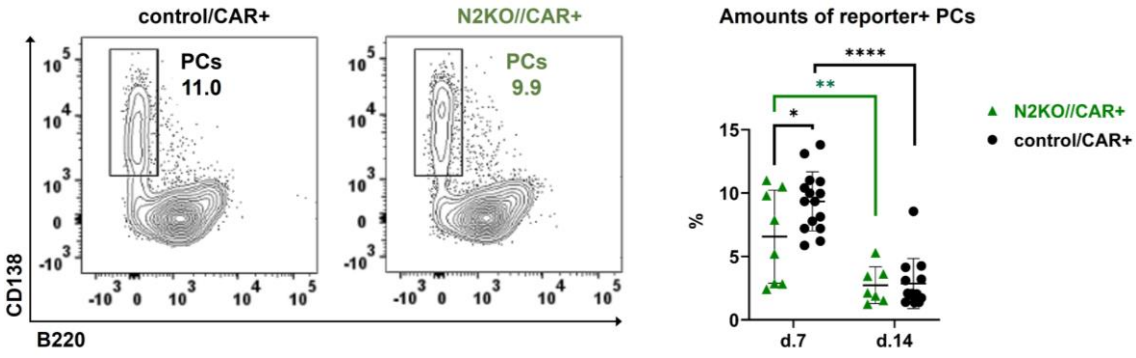

Fig. 27: Notch2-deficient cells produce slightly less plasma cells at day 7 p.i. Representative FACS analyses from day 7 p.i. Splenocytes were pre-gated on living reporter$^+$ cells using a large lymphocyte gate and were stained for B220 and CD138. PCs are defined as CD138^{high}B220$^-$. The graph summarizes the frequencies of reporter$^+$ PCs in percentages (%) at indicated time points. Sidak's 2-way-ANOVA. n≥7 N2KO//CAR mice, n≥11 control/CAR mice. Similar figure in (Babushku et al., 2022).

However, no difference was observed at day 14 in the spleen, likely because the PCs have already migrated to other organs, such as the bone marrow as a homing niche.

To detect the numbers of unswitched and switched antibody-secreting cells (ASCs) in the spleen, ELISpot analysis were performed. The data did not reveal differences in any isotype of NP-specific PCs between N2KO//CAR and control/CAR mice. However, there was a strong tendency for diminished total and high-affinity IgG1 PCs in N2KO//CAR mice (*Fig. 28A*). Moreover, ELISA analysis of secreted NP-specific antibody titers at day 7 showed an increase in the NP-IgM titers in the serum of N2KO//CAR animals, but no differences in the secreted IgG1 and IgE titers (*Fig. 28B*). Together, these data suggested a positive influence of Notch2 signaling on the production of IgG1$^+$ PCs in the spleen. In addition, inactivation of Notch2 may stimulate the early migration of IgM-secreting cells from the spleen into the blood, which may explain why we detected higher IgM antibody titers in the serum, but we did not detect increased amounts of IgM ASCs in the spleen of N2KO//CAR mice at day 7 p.i. (*Fig. 28*).

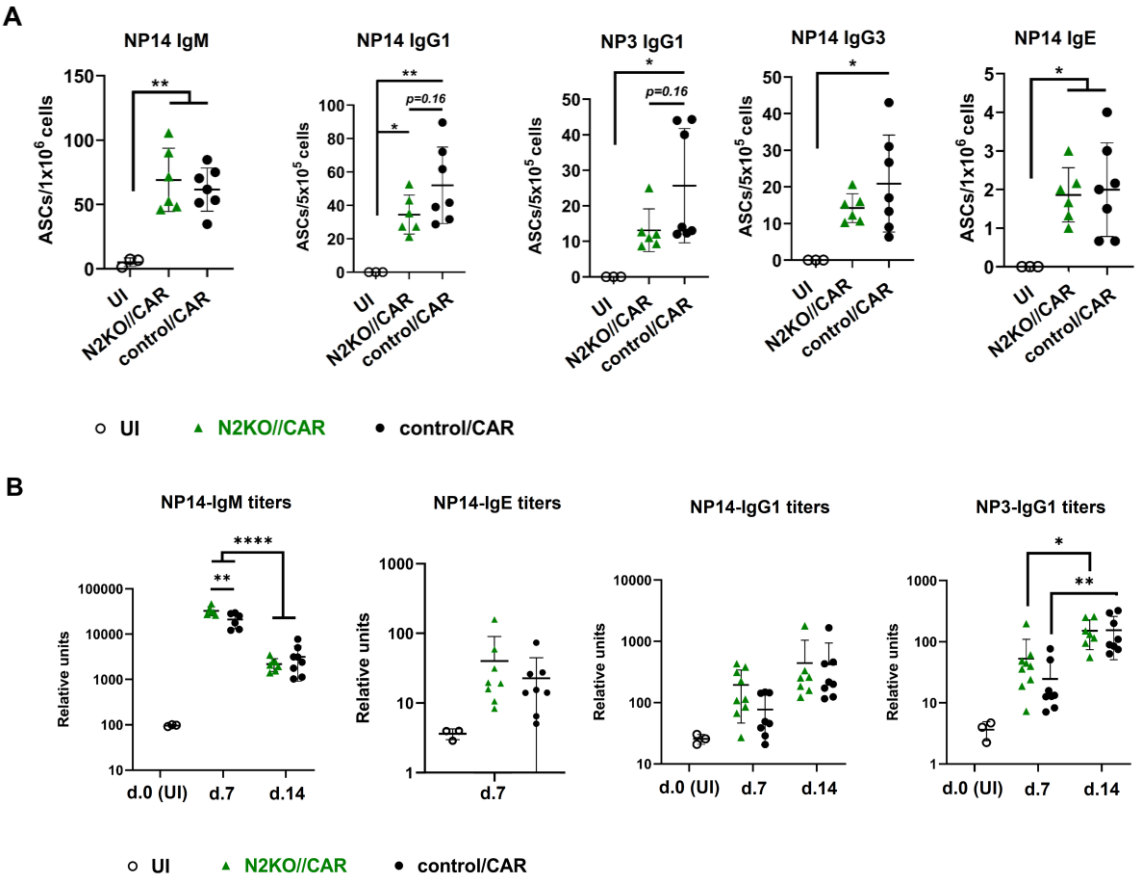

Fig. 28: Analysis of NP-specific PCs in spleen and NP-specific secreted antibodies in the serum of N2KO//CAR mice. Plates were coated with NP14- or NP3-BSA to detect total (high and low affinity) and only high affinity-binding ASCs (or titers), respectively. **(A)** Numbers of NP-specific antibody-secreting cells (ASCs) within a defined number of splenic B cells with the indicated isotype were determined by ELISpot at day 7 p.i. High affinity NP-specific ASCs are detected by NP3-BSA, whereas NP14-BSA captures all NP-

specific ASCs. 1-way-ANOVA, Tukey's multiple comparisons test. n≥6 immunized mice, n=3 UI mice. **(B)** Total NP-specific IgM, IgG1 and IgE antibody titers (captured by NP14-BSA), and high-affinity NP-IgG1 titers (binding to NP3-BSA) were measured in the serum of N2KO//CAR and control/CAR mice using ELISA. 2-way-ANOVA, Sidak's multiple comparisons test. n≥7 immunized mice, n=3 UI mice.

5.4.6 Induction of N2IC traps the cells in an CD38^{high} non-GC phenotype

The results so far showed that N2IC/hCD2 mice did not form germinal centers, even though they still had comparable amounts of reporter$^+$ B cells as control/CAR animals. In order to clarify the phenotype of these N2IC-expressing cells, the distribution of the CD38 and CD95 expression was analyzed in more detail. Contrary to control/CAR$^+$ cells and N2KO//CAR$^+$ cells (*Fig. 25B*), over 90% of N2IC-expressing B cells had a non-GC phenotype with high CD38 and intermediate or low CD95 expression (*Fig. 29A*).

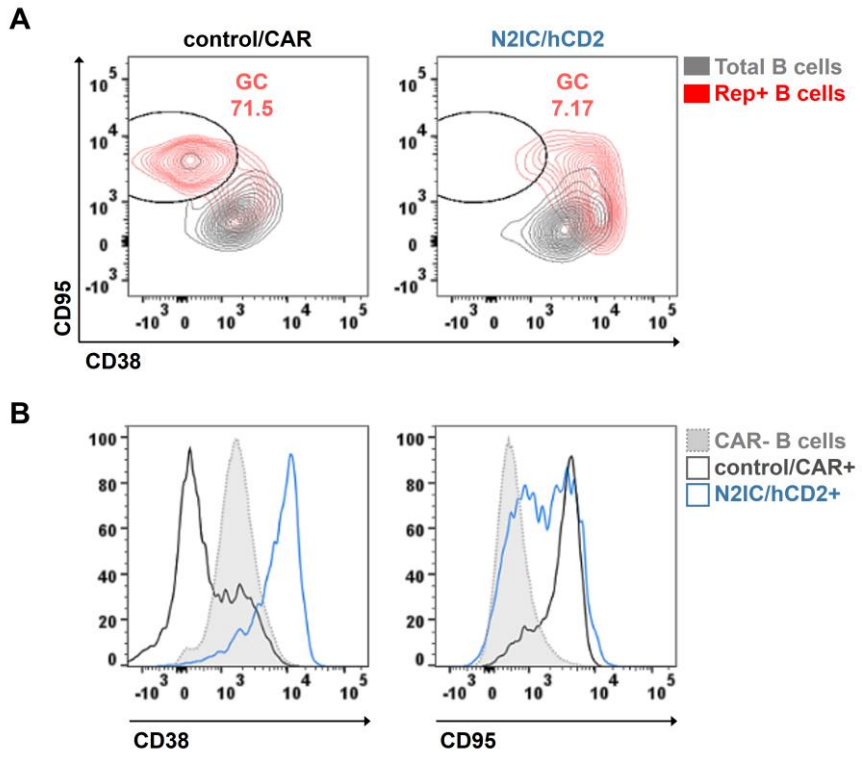

Fig. 29: N2IC/hCD2$^+$ cells strongly induce CD38 expression and adopt a non-GC B cell phenotype. Representative FACS plots from day 7 p.i. Plots were pre-gated on living reporter$^+$B220$^+$ B lymphocytes. **(A)** Cells were stained for GC markers CD38 and CD95. GC cells were gated as CD95^{high}CD38^{low}. Contour plots show the overlay of CD38/CD95 expression in reporter$^+$ (red) and total B cells (black). Gates and percentages refer to the red plots. **(B)** Histograms depict the overlays of CD38 and CD95 expression in the reporter$^+$ B cells from N2IC/hCD2 (blue) and control/CAR mice (black), compared to those of reporter$^-$ control/CAR B cells (grey). Similar figure in (Babushku et al., 2022).

Indeed, constitutive active N2IC led to a strong upregulation of CD38 in all B cells and to an induction of CD95 expression in a portion of these cells (*Fig. 29B*). Due to this marker

shift, particularly in CD38, N2IC/hCD2$^+$ cells had a non-GC B cell phenotype and many of them were even trapped in an activated B cell state. This implied that the small GC B cell frequencies (1-2%) detected in N2IC/hCD2 animals were predominantly generated by the hCD2$^-$ B cells. In broader sense, the N2IC-knockin model corroborated the findings with CBF:H2B-Venus and N2KO//CAR mice that Notch2 signaling and GC formation are inversely correlated, and Notch2 signaling needs to be downregulated to allow for GC B cell differentiation.

5.4.7 N2IC expression in B cells suppresses Bcl6 and induces Irf4, leading to enhanced plasma cell differentiation

Bcl6 is a transcription factor required for the formation of germinal centers (Dent et al., 1997). In resting B cells, the GC fate is introduced by Bcl6 and Bach2 (Muto et al., 2010; Shaffer et al., 2000), whereas initiation of plasma cell differentiation requires decreased expression of both, together with increased expression of the transcription factors Irf4 and Xbp1 (Scharer et al., 2020; Sciammas et al., 2006). Considering the lack of GC B cells in N2IC/hCD2 mice, I examined the expression of Bcl6 and Irf4 in N2IC/hCD2$^+$ cells by intracellular antibody staining and subsequent FACS acquisition. As expected for control/CAR mice, most reporter$^+$ cells strongly induced Bcl6, but kept Irf4 levels very low (*Fig. 30*), which was in accord with their dominant GC B cell phenotype.

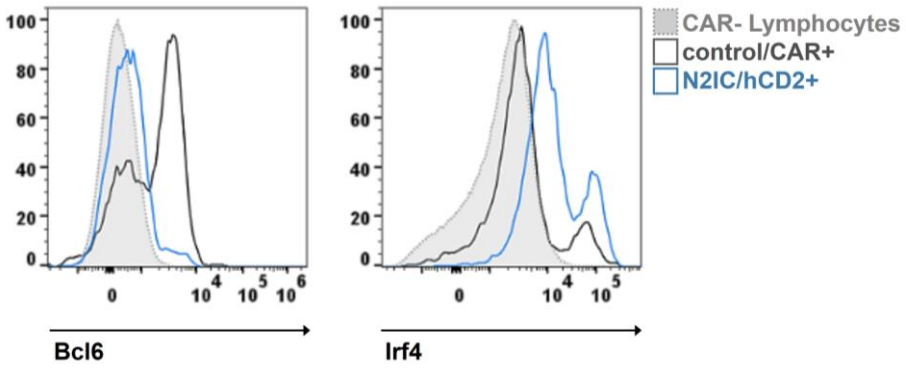

Fig. 30: N2IC expression suppresses Bcl6, but induces Irf4 expression in B cells. Representative FACS histograms from day 7 p.i. Cells were stained for intracellular proteins following permeabilization and fixation and analyzed by FACS. Plots were pre-gated on living reporter$^+$ lymphocytes. The histograms depict overlays of Bcl6 (left) and Irf4 (right) expression in reporter$^+$ cells from N2IC/hCD2 (blue) and control/CAR mice (black), compared to those of reporter$^-$ control cells (grey). n≥6 mice per genotype. Similar figure in (Babushku et al., 2022).

On the other hand, N2IC-expressing cells exhibited impaired Bcl6 upregulation, consistent with their inability to differentiate into GC B cells. Instead, the N2IC expression

led to a strong Irf4 induction and a complete shift of its expression levels in all N2IC/hCD2$^+$ cells compared to control/CAR$^+$ cells (*Fig. 30*).

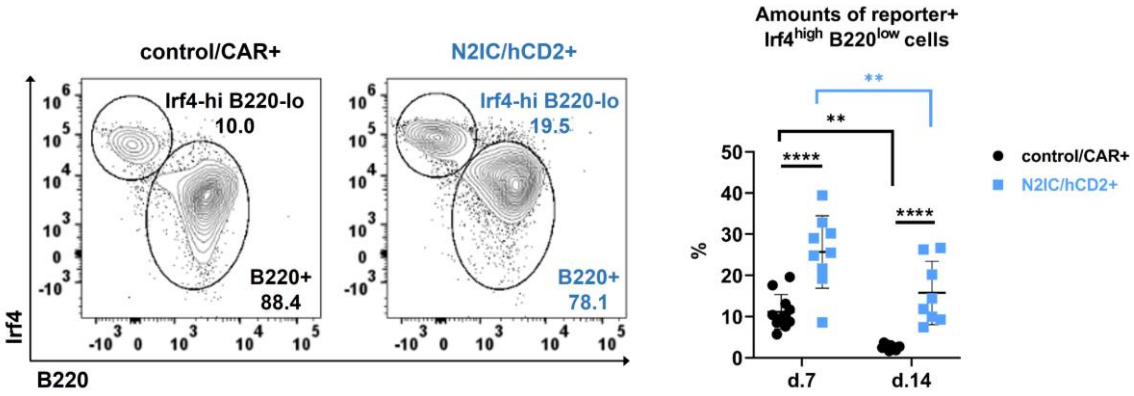

Fig. 31: N2IC/hCD2$^+$ cells undergo enhanced plasma cell differentiation. Representative FACS analysis from day 7 p.i. Cells were stained for intracellular markers following permeabilization and fixation and later analyzed by FACS. Plots were pre-gated on living reporter$^+$ lymphocytes and subsequently stained for Irf4 and B220. Two subpopulations were identified: Irf4^{high}B220^{low} (PCs) and Irf4^{mid}B220$^+$ (B cells). The graph on the right depicts the frequencies of reporter$^+$ Irf4^{high}B220^{low} cells at days 7 and 14 p.i. 2-way-ANOVA, Sidak's multiple comparisons test. n≥9 mice. Similar figure in (Babushku et al., 2022).

Even though most N2IC-expressing cells were Irf4^{mid}, there was a second subpopulation which was Irf4^{high} and was also detected in reporter$^+$ cells from control/CAR mice. A co-staining with B220 revealed that these Irf4^{high} cells were uniformly B220$^-$ in both genotypes, consistent with a plasmablast and plasma cell phenotype (*Fig. 31*). Interestingly, the percentages of Irf4^{high}B220$^-$ cells at day 7 and 14 were significantly higher in N2IC/hCD2 compared to control mice, indicative of an enhanced PC differentiation. Histology re-confirmed the increased amounts of Irf4$^+$ cells in N2IC/hCD2 mice, which were predominantly located in the extra follicular regions between neighboring B cell follicles (*Fig. 32*). This suggested that there is a substantial increase in the total PCs frequencies in N2IC/hCD2 animals, and the phenotype is entirely caused by the enhanced PC differentiation capacity of the transgenic hCD2$^+$ cells.

In sum, it can be concluded that N2IC-expessing cells are navigated away from the GC fate, which is normally introduced by Bcl6, because they strongly upregulate its opposing factor Irf4 instead and are thereby triggered to differentiate into bursts of plasmablasts and plasma cells.

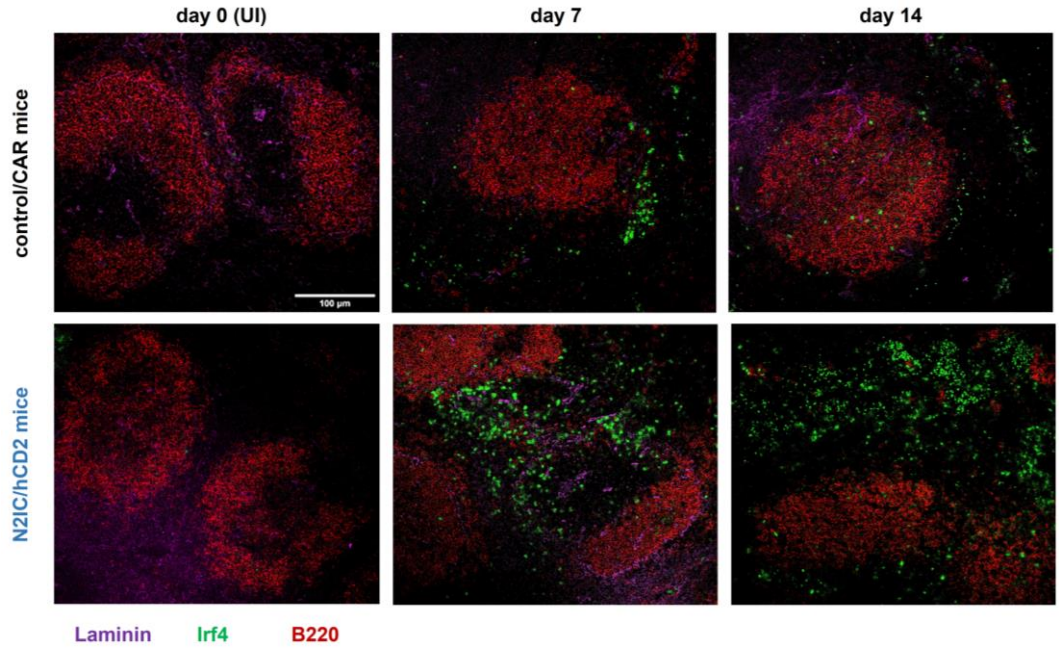

Fig. 32: Immunohistological staining revealed raised amounts of total Irf4⁺ plasma cells in N2IC/hCD2 mice. Immunofluorescence histology staining of splenic tissue from uninjected mice (UI, day 0), and NP-CGG injected N2IC/hCD2 and control/CAR animals. Sections were stained for the detection of plasmablasts and PCs (Irf4$^+$, green), B cells (B220$^+$, red) and basement membranes of endothelial cells lining the MZ (Laminin, purple). The image scale bar depicts 100 µm. n=4 mice per genotype. Similar figure in (Babushku et al., 2022).

5.4.8 The N2IC/hCD2⁺ plasma cells do not upregulate Blimp1 and persist as highly-proliferating, IgM-secreting plasmablasts

Next, it was examined whether the Irf4^{high}B220$^-$ cells in N2IC/hCD2 mice further matured into terminally differentiated plasma cells. In an attempt to specify the differentiation stage of N2IC-expressing PCs, the expression of the long-lived plasma cell transcription factor Blimp1 was analyzed.

As depicted in *Fig. 33*, the majority of N2IC/hCD2$^+$ cells did not upregulate Blimp1. On the contrary, over half of the control/CAR$^+$Irf4^{high} cells were also Blimp1^{high} at day 7 post immunization. In the course of PC development, Irf4 is upstream of Blimp1 and of the terminal differentiation to plasma cells (Sciammas et al., 2006). This indicates that most N2IC-expressing Irf4^{high}Blimp1^{low} cells are stuck at an earlier PC maturation stage i.e. the plasmablast stage, whereas most control/CAR$^+$Irf4^{high}Blimp1^{high} cells are fully matured and terminally differentiated plasma cells. Fitting with this statement, there was a sharp decrease in the amounts of Irf4^{high}Blimp1^{high} PCs from day 7 to day 14 in the spleen of control/CAR mice, but no change in this minor PC fraction in N2IC/hCD2 mice (*Fig. 33, green bars*). Thus, these cells are indeed long-lived PCs in control/CAR animals, which

had left the periphery and likely migrated towards their homing niche in the BM by day 14.

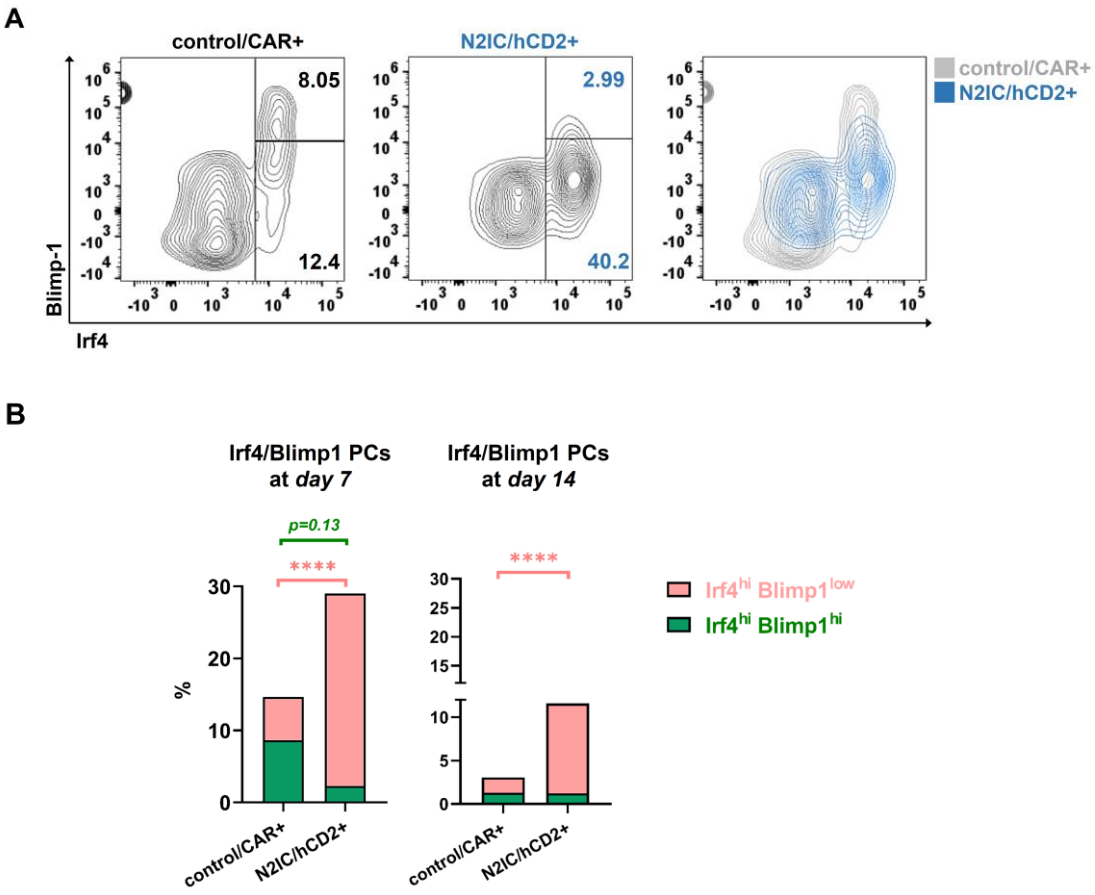

Fig. 33: N2IC/hCD2^{+}Irf4^{high} plasma cells are Blimp1^{-} and are stuck in a plasmablast stage. (A) Representative FACS plots from day 7 p.i. Cells were intracellularly stained after fixation and permeabilization. Splenocytes were pre-gated on living reporter^{+} lymphocytes and further stained for Irf4 and Blimp1. Two cell subsets were gated: Irf4^{high}Blimp1^{low} (PB) and Irf4^{high}Blimp1^{high} (mature PCs). The overlay shows the distribution of Irf4 and Blimp1 expression in control/CAR^{+} (grey) and N2IC/hCD2^{+} cells (blue). **(B)** The stacked bar charts summarize the frequencies of the gated Irf4^{high}Blimp1^{high} and Irf4^{high}Blimp1^{low} cells in both genotypes at day 7 and 14 p.i. Sidak's 2-way-ANOVA. n=5 mice per genotype. Similar figure in (Babushku et al., 2022).

In summary, the data so far suggested that induction of N2IC drives cells with high Irf4 expression towards the PC fate, but the differentiation is terminated at the stage of plasmablasts. The statement fits well with the data from immunized CBF:H2B-Venus mice. Here, the Notch signal (Venus expression) was still retained in plasmablasts (CD19^{+}B220^{mid}), but was completely lost in terminally differentiated PCs (CD19^{-}B220^{-}), indicating that Notch2 signaling has to be turned off during the final stages of PC development.

To strengthen the point that N2IC-expressing Irf4^{high}Blimp1^{low} cells are plasmablasts, the expression of the nuclear protein Ki67 was analyzed in these cells, compared to control/CAR^{+} PCs. Ki67 is a marker of proliferation. Previous research has identified a CD19^{+} PC subpopulation with high Ki67 levels in the spleen of TD-immunized mice. These cells were described as proliferating plasmablasts (Pracht et al., 2017). In contrast, the remaining CD19^{-} PC subset had lower Ki67 expression and was described as mature resting plasma cells. The Ki67 staining revealed that N2IC-expressing Irf4^{high}B220^{low} cells had increased Ki67 expression, compared to control/CAR^{+} PCs at both day 7 and 14 post immunization (*Fig. 34*). This was indicative of a stronger proliferation of N2IC/hCD2^{+}Irf4^{high}B220^{low} cells, consistent with their plasmablast phenotype.

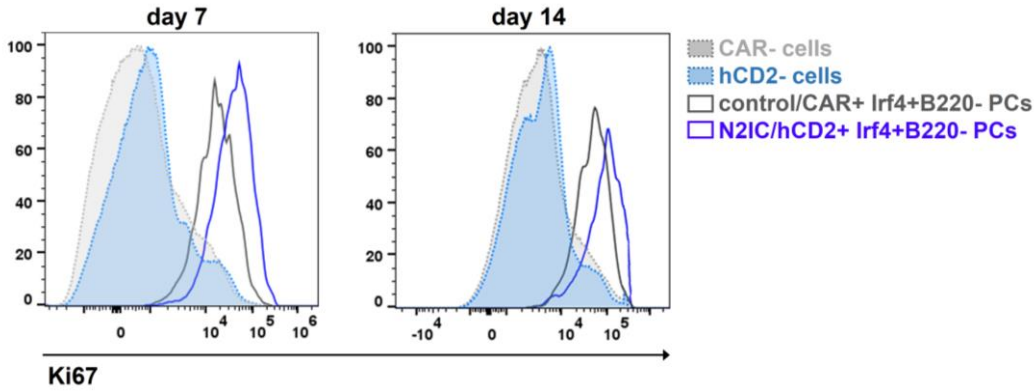

Fig. 34: N2IC-expressing Irf4^{high} plasmablasts exhibit increased expression of proliferation marker Ki67. Cells were stained for intracellular markers after fixation and permeabilization and subsequently analyzed by FACS. Splenocytes were pre-gated on living reporter^{+}Irf4^{high}B220^{-} cells (PCs) and analyzed for Ki67 expression. Histogram overlays from day 7 and 14 show the Ki67 levels in PCs of control/CAR^{+} (grey) and N2IC/hCD2^{+} cells (blue), compared to total non-transgenic CAR^{-} (grey dotted) and hCD2^{-} cells (blue dotted). FACS analyses are representative for n≥5 mice at day 7 and n≥3 mice at day 14.

To finalize the characterization of the plasma cell response in N2IC/hCD2 mice, we examined the amounts of NP-specific antibody-producing cells (ASCs) from different isotypes in the spleen and BM via ELISpot, as well as the NP-specific antibody titers in the serum via ELISA. The ELISpot analyses with splenic cells disclosed significantly increased numbers of unswitched IgM-producing cells and strongly diminished numbers of switched IgG1- and IgG3-secreting cells in N2IC/hCD2 mice, compared to controls (*Fig. 35A*). While NP-specific IgM^{+} ASCs were still abundant at later time points, almost no IgG-switched NP-specific ASCs remained in the spleens of N2IC/hCD2 mice by day 14 (*Fig. 35A*). The ELISpots of the BM reflected the findings in the spleen. Increased amounts of NP-specific IgM^{+} ASCs, but decreased frequencies of IgG1^{+} NP-ASCs were detected in the BM two weeks after immunization (*Fig. 35B*). Consistent with these data,

the measurement of NP-specific IgG1 titers in the serum of N2IC/hCD2 mice revealed strongly decreased total and high-affinity NP-IgG1 antibodies at day 14 and 30 of the immune response (*Fig. 35C*). While NP-IgG1 titers increased in control/CAR mice with progressing time post immunization, they remained relatively stable in N2IC/hCD2 animals. This finding is not surprising, considering that there is an impairment of GC formation in N2IC/hCD2 mice and thus there is no source of origin for the production of high-affinity IgG1-secreting ASCs.

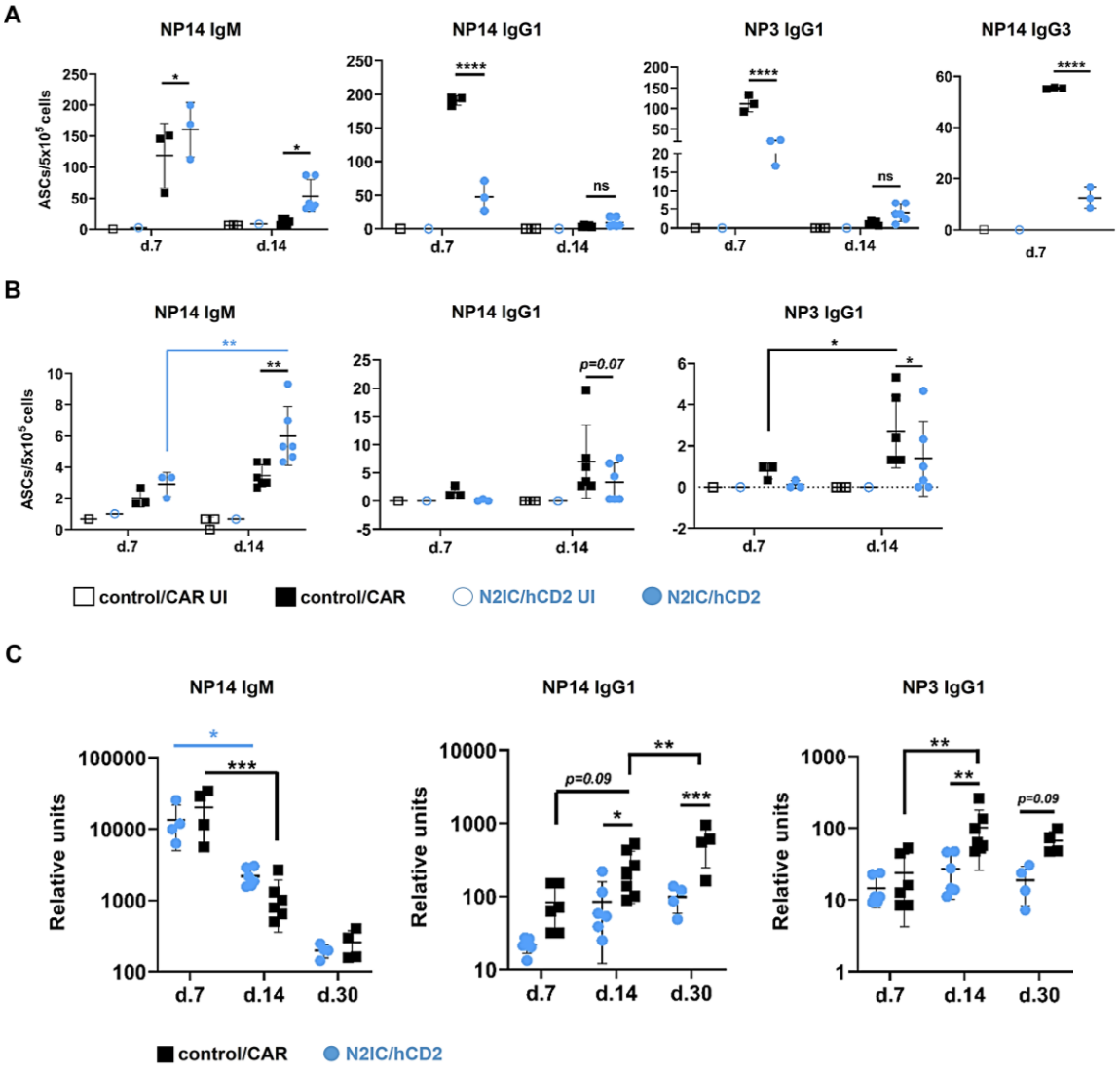

Fig. 35: **Isotype characterization of NP-specific ASCs in spleen and BM, and NP-specific antibody titers in serum of N2IC/hCD2 mice.** Plates were coated with NP14- or NP3-BSA to detect total (high + low affinity) and high affinity-binding ASCs. Numbers of NP-specific antibody-secreting cells (ASCs) from the indicated isotypes were determined in the **(A)** spleen and **(B)** bone marrow of N2IC/hCD2 and control animals via ELISpot at day 7 and 14 p.i. Sidak's 2-way-ANOVA. n=1 UI mouse and n=3 immunized mice per genotype at day 7, n≥1 UI mouse and n≥5 immunized mice per genotype at day 14. **(C)** NP-specific IgM and IgG1 antibody titers were measured by ELISA in serum of N2IC/hCD2 and control/CAR mice at day 7 and 14 p.i. 2-way-ANOVA with Tukey's (NP14-IgM) or Sidak's (NP14-IgG1, NP3-IgG1) multiple comparisons test. n≥4 mice. Similar figure in (Babushku et al., 2022).

Taken together, the findings presented in this section suggest that induction of Notch2IC introduces enhanced PC differentiation in the portion of cells which are Irf4^{high}, but it terminates their PC development at the stage of plasmablasts, most of which are splenic, highly-proliferating, unswitched, IgM-producing cells.

5.4.9 Induction of N2IC triggers enhanced differentiation into MZB cells with a full MZB cell surface phenotype

During B-cell development, the activation of Notch2 signaling by the Dll-1 ligand in the splenic vasculature directs B cells towards MZB cell differentiation and away from the pool of naïve FoB cells, from which GCs are formed during TD immune responses (Pillai and Cariappa, 2009; Valls et al., 2017). Furthermore, induction of a constitutive Notch2IC signal drives the differentiation of FoB cells into MZB cells under homeostatic conditions (Lechner et al., 2021). Considering this prior knowledge, as well as the collective data from the Cγ1-Cre mouse models with deregulated Notch2 signaling, a two-part hypothesis was formed:

(I) B cells which downregulate Notch2 signaling develop to GC B cells.

(II) B cells which receive a strong, above-threshold Notch2 signal upon immunization develop to plasmablasts and MZB cells.

It was already revealed that induction of Notch2IC upon immunization led to the generation of plasmablasts from the Irf4^{high} cells. However, this was a smaller fraction among the N2IC-expressing B cells, suggesting that not all N2IC/hCD2^{+} cells differentiated to plasmablasts. In both control/CAR and N2IC/hCD2 mice, a bigger fraction of reporter^{+} B cells had an Irf4^{mid}B220^{+} phenotype, common for activated B cells and GC B cells (*Fig. 36A*). In control animals, these cells had high Bcl6 levels that facilitated their predominant GC phenotype. But, in N2IC/hCD2 animals the Irf4^{mid}B220^{+} subpopulation was generally higher in the Irf4 expression and was also clearly Bcl6^{-} (*Fig. 36B*). For this reason, I examined whether the Irf4^{mid}B220^{+} N2IC-expressing cells, which did not produce plasmablasts or GC B cells, differentiated into MZB cells instead. If this is the case, then it could explain why N2IC/hCD2^{+} cells were navigated away from the GC and were localized towards the middle of the B cell follicle (see *Fig. 24*). The intracellular staining of N2IC/hCD2^{+}Irf4^{mid}B220^{+} cells at day 7 revealed a marker shift of CD23 and CD21 in these cells: CD21 was upregulated, whereas CD23 was downregulated (*Fig. 36C*), indicating a possible phenotype shift from typical FoB cells (CD23^{+}CD21^{low}) to MZB cells (CD21^{high}CD23^{low}). To exclude the possibility that the observed increase in the MZB gate

was caused by a targeted CD21 upregulation induced by N2IC early in the immune response (day 7), the CD23/CD21 phenotype of N2IC/hCD2^{+} cells was examined over a broader time period after antigen injection.

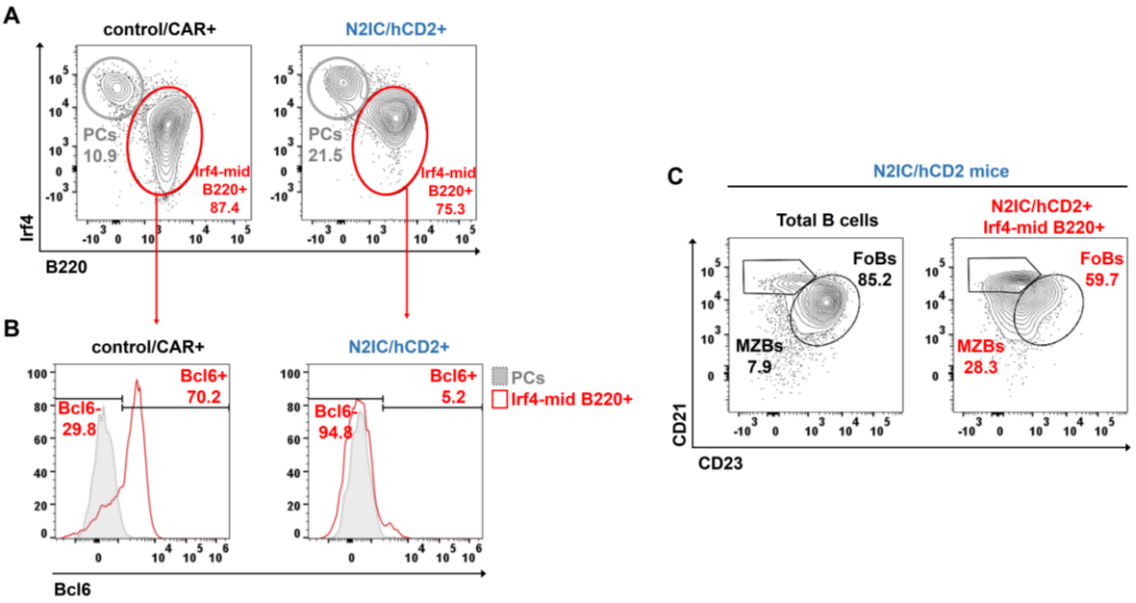

Fig. 36: **A fraction of N2IC/hCD2^{+}Irf4^{mid}Bcl6^{-} B cells shift their CD21/CD23 expression towards the MZB cell phenotype.** FACS analyses are representative for day 7 p.i. Cells were stained intracellularly after fixation and permeabilization, and were pre-gated on living reporter^{+} lymphocytes. **(A)** Reporter^{+} cells were separated into two Irf4/B220 subpopulations: PB and PCs (Irf4^{high}B220^{-}) and Irf4^{mid}B220^{+} B cells. **(B)** The histograms depict overlays of Bcl6 expression in the gated Irf4/B220 cell populations from (A). Gates and percentages refer to the red histogram for the Irf4^{mid}B220^{+} cells. **(C)** Gating example for MZB (CD21^{high}CD23^{low}) and FoB (CD23^{high}CD21^{low}) cells in N2IC/hCD2 mice. The left plot is pre-gated on total B220^{+} cells, the right plot is pre-gated on N2IC/hCD2^{+}Irf4^{mid}B220^{+} cells from (A). n≥4 mice per genotype. Similar figure in (Babushku et al., 2022).

It was discovered that N2IC-expressing cells gradually shifted their phenotype from FoB cells (CD23^{+}CD21^{low}) to MZB cells (CD21^{high}CD23^{low}) in a time frame of 4 weeks post immunization (*Fig. 37A*). The amounts of N2IC/hCD2^{+} MZB cells progressively increased with ongoing time, constituting app. 40% of all N2IC-expressing cells at day 30 (*Fig. 37B*). In addition, the kinetics of the newly-generated MZB cells was strongly comparable with the overall kinetics of the reporter^{+} B cells in N2IC/hCD2 mice. This implied that the induction of N2IC upon immunization is an irreversible event and once it happens, it introduces a permanent conversion of reporter^{+} B cells into MZB cells, which then continue to persist in a terminal MZB cell state even after the NP-CGG antigen is cleared in the spleen (day 30). Of note, the percentage of N2IC/hCD2^{+} cells in the total MZB population was rather high (20-40%) and followed an increasing trend over time, but the frequencies of total MZB cells in N2IC/hCD2 animals remained relatively stable

(*Fig. 37C*). This finding may suggest a replacement of wildtype MZB cells by the newly-generated N2IC/hCD2^{+} MZB cells.

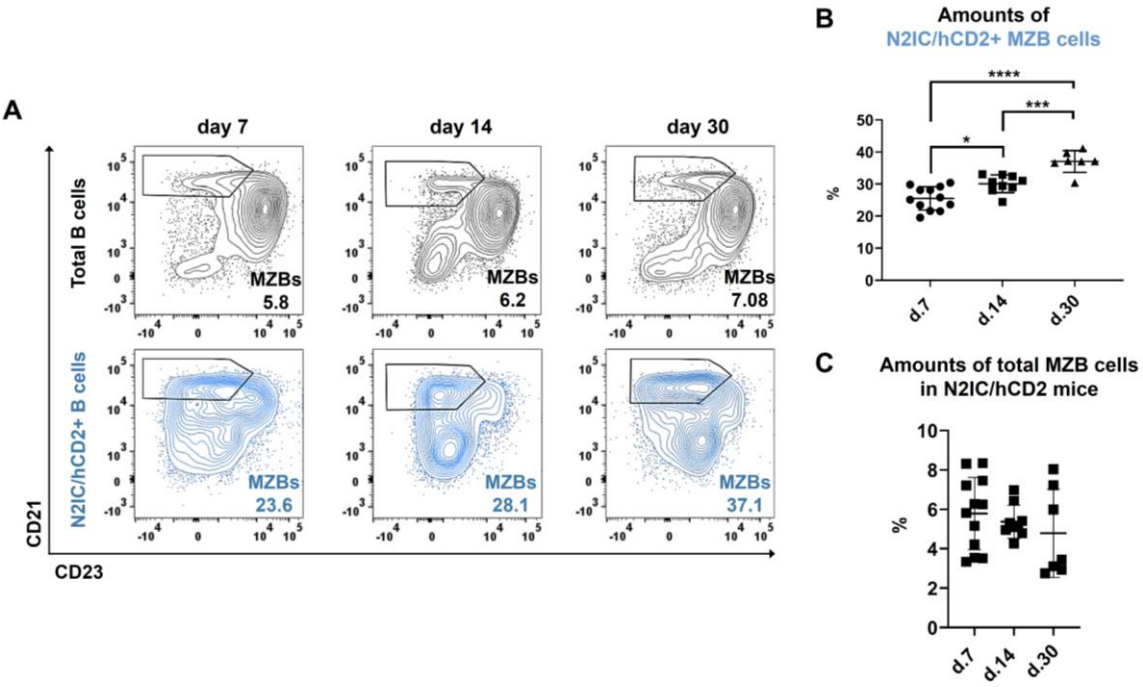

Fig. 37: **N2IC-expressing B cells produce increasing amounts of MZB cells over time. (A)** Representative CD23/CD21 staining for each time point after immunization, to separate and quantify CD21^{high}CD23^{low} MZB cells in N2IC/hCD2 mice. Top row (grey): MZB cells in total B220^{+} B cells. Bottom row (blue): MZB cells among N2IC/hCD2^{+} B cells. **(B)** Percentages of N2IC-expressing CD21^{high}CD23^{low} MZB cells for all analyzed mice at the indicated time points. 1-way-ANOVA, Tukey's multiple comparisons test. **(C)** Graphical summary of the frequencies (%) of total MZB cells in N2IC/hCD2 mice at indicated time points. **(B-C)** n=12 at day 7, n=9 at day 14, n=7 at day 30. Similar figure in (Babushku et al., 2022).

To show that the transgenic N2IC/hCD2^{+} MZB cells resemble wildtype MZB cells from uninjected control/CAR animals, additional surface phenotyping was performed to examine the expression of other cell surface markers and properties of MZB cells. N2IC-expressing MZB cells not only upregulated CD21 and downregulated CD23, but also increased their size (FSC) and induced the expression of IgM, CD1d and CD38, compared to wildtype FoB cells and hCD2^{-} B cells (*Fig. 38*). Thereby, they adopted an almost identical surface phenotype as wildtype MZB cells in unimmunized mice (CD23^{low}CD21^{high}IgM^{high}CD1d^{high}CD38^{high}), affirmative of their authenticity as true marginal zone B cells.

Collectively, these data showed that induction of Notch2IC expression upon TD-immunization introduces a strong phenotypic conversion from antigen-responding FoB cells (similar to hCD2^{-} B cells in their phenotype) towards MZB cells (hCD2^{+}), with regards to the analyzed surface markers.

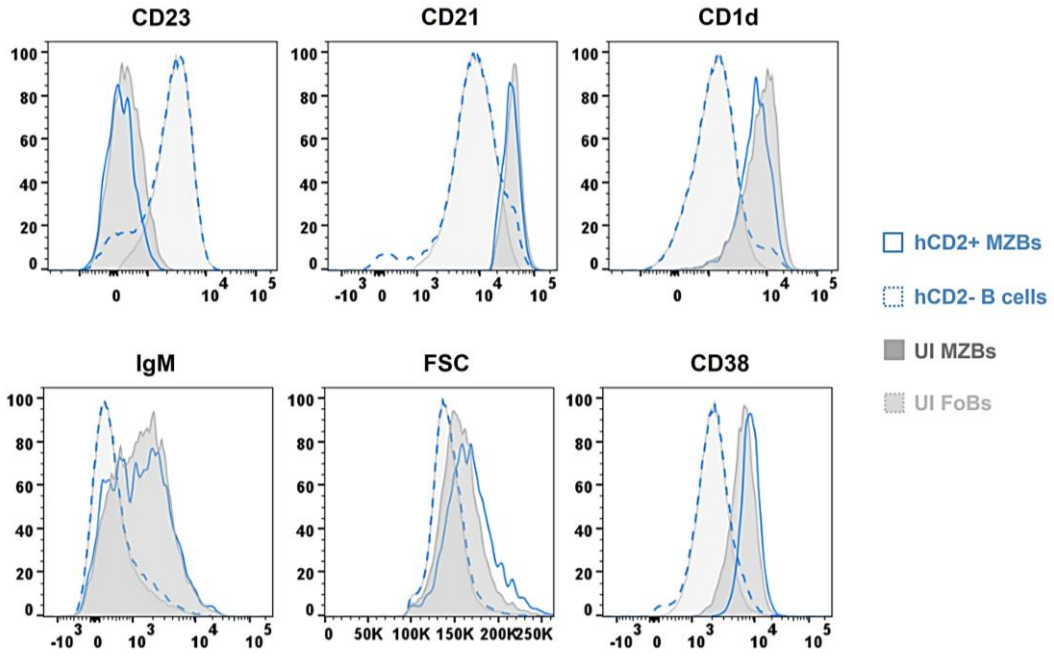

Fig. 38: **The N2IC/hCD2$^+$ MZB cells fully resemble control MZB cells in terms of their cell surface phenotype.** FACS analysis is representative for n=9 mice from day 7 p.i. Histograms show the surface levels of the indicated markers, which are typically conversely expressed in FoB vs. MZB cells. The overlays compare N2IC/hCD2$^+$ MZB cells and non-transgenic hCD2$^-$ B cells with the total MZB and FoB cells from uninjected control/CAR animals (greyscales). Similar figure in (Babushku et al., 2022).

5.4.10 The newly-generated N2IC-expressing MZB cells localize outside of the follicle in the splenic marginal zone (MZ)

MZB cells are residents of a specific splenic microenvironment called the marginal zone (MZ). The MZ surrounds the follicle which contains a T cell and B cell zone, the latter harboring FoB cells. The follicle is demarcated by a ring-like Laminin$^+$ MZ sinus, filled with specialized MOMA1-expressing metallophilic macrophages. To inspect whether the N2IC-induced MZB cell differentiation is accompanied by a migration of the MZB cells from the follicle to their anatomically correct location in the MZ, combined immunohistochemical staining for hCD2 and Laminin was done. In this way, the N2IC-expressing transgenic cells (hCD2$^+$) were visualized and tracked over time for their splenic localization. The histology images showed that already 7 days post immunization, hCD2-expressing B cells appeared at their defined splenic location in the MZ. Interestingly, some hCD2$^+$ cells were still visible in the middle of the B cell follicle, as well as towards the inner edges of the follicle. In the second week of the immune response (day 14), more hCD2$^+$ cells correctly resided in the MZ or were lining the inner edges of the follicle adjacent to the MZ, compared to the earlier time point. By day 30, all hCD2$^+$ MZB cells were located in the ring around the follicle, and almost no hCD2-expressing B cells were visible anywhere inside the follicle (*Fig. 39*). In sum, induction of Notch2IC upon B cell

activation in the primary immune response not only triggered a shift of the surface phenotype towards MZB cells, but also guided these newly-differentiated MZB cells to their resident anatomic location in the spleen.

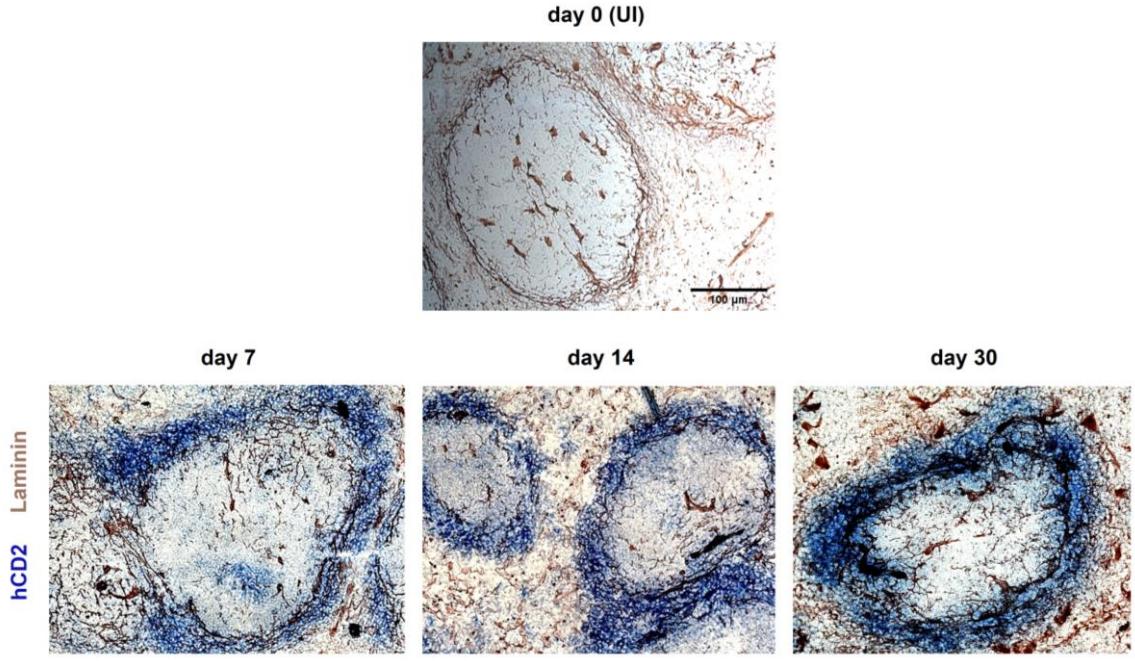

Fig. 39: **The newly-generated N2IC/hCD2^{+} MZB cells correctly localize in the splenic MZ over time.** Immunohistochemical co-staining for hCD2 and Laminin in splenic tissues from NP-CGG-injected and uninjected (UI) N2IC/hCD2 mice at indicated time points. Images are representative for n=3 mice per time point. Sections were stained for reporter^{+} cells (hCD2, blue) and for basal membranes of endothelial cells in the MZ sinus (Laminin, brown). Scale bar represents 100 µm. Similar figure in (Babushku et al., 2022).

5.4.11 Generation of cells with a MZB phenotype is Notch2-dependent in the primary immune response

The results thus far demonstrated that induction of Notch2IC in B cells by a TD antigen drives an enhanced differentiation into MZB cells. However, the constitutive active Notch2IC signal does not mimic the physiological Notch2 signaling scenario in wildtype animals. Therefore, the next step was to examine whether MZB cell differentiation in the course of the immune response also occurs in a more natural setting, i.e. in control/CAR animals with unaltered, normally functioning Notch2 signaling. Considering that a conditional inactivation of Notch2 in all B cells attenuates MZB cell differentiation (Hozumi et al., 2004; Saito et al., 2003), I additionally analyzed antigen-responding reporter^{+} B cells from N2KO//CAR mice and examined their capacity to produce new MZB cells, when Notch2 signaling is inactivated.

FACS analyses confirmed the existence of a population of reporter^{+}CD23^{low}CD21^{high} B cells in the spleen of control/CAR mice (*Fig. 40A*). The first cells with an MZB phenotype

appeared at day 7 and their frequencies gradually increased with ongoing time, ranging between 3% and 6% at day 14 post immunization (*Fig. 40B*). They were also clearly reporter$^+$ and expressed the CAR receptor on the cell surface, suggesting they had been generated during the TD immune response from B cells that responded to the antigen. More importantly, it was evidenced that reporter$^+$CD23^{low}CD21^{high} B cells were strongly diminished in N2KO//CAR mice upon immunization (*Fig. 40A-B*). Although these mice had a similar CD38/CD95 phenotype and comparable frequencies of reporter$^+$ GC and activated B cells like control/CAR animals, their N2KO//CAR$^+$ cells were not fully capable to differentiate into MZB cells at any given time point after antigen injection (*Fig. 40B*). Taken together, these data suggest that the generation of cells with a MZ phenotype upon immunization only happens from antigen-responding B cells that also receive a Notch2-signal upon activation, i.e. N2IC/hCD2$^+$ and control/CAR$^+$ cells. Thus, *de novo* MZB cell differentiation during the primary immune response is Notch2 signal-dependent.

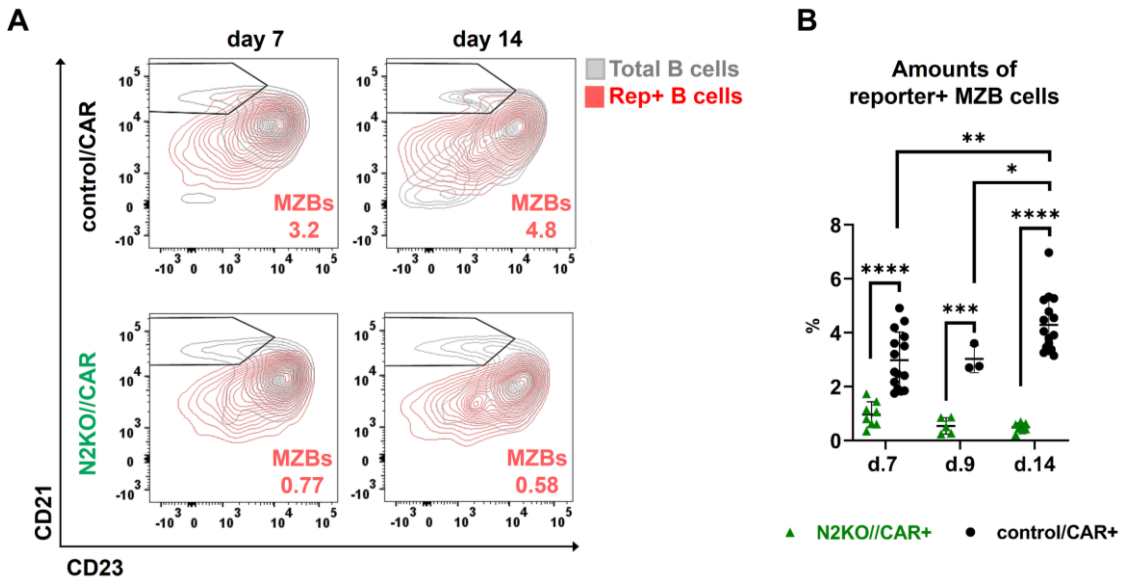

Fig. 40: **Functional Notch2 signaling is crucial for the generation of MZB cells in the primary immune response. (A)** Exemplary FACS analysis for the separation and gating of CD21$^+$CD23^{low} MZB cells at day 7 and 14 p.i.. Splenic cells were pre-gated on living B220$^+$ lymphocytes. The contour plots show overlays between the CD23/CD21 expression in reporter$^+$ B cells (red) and the total B220$^+$ B cells (grey) in control/CAR and N2KO//CAR animals. Gates and percentages refer to the red contour plot of reporter$^+$ B cells. **(B)** Summary of the frequencies (%) of reporter$^+$ MZB cells (gated as in A) at days 7, 9 and 14 p.i. in mice of the indicated genotypes. 2-way-ANOVA multiple comparisons tests. n≥8 at day 7, n≥3 at day 9, n≥7 at day 14. Similar figure in (Babushku et al., 2022).

5.5 A closer look at the immunization-induced MZB cell differentiation in control mice

5.5.1 Notch2 surface expression is induced on CAR$^+$ activated B cells upon TD immunization

The results presented thus far implied that only FoB cells that receive an above-threshold Notch2 signal upon B cell activation will eventually develop into MZB cells. Taking into account the haploinsufficiency of Notch2 in the regulation of MZB cell development, it was postulated that high Notch2 levels on the cell surface are a prerequisite for the differentiation into MZB cells. The previously presented findings from the in vitro stimulation assays of purified B cells (see chapter 5.2 and *Fig. 14*) already revealed that the Notch2 surface expression was strongly upregulated on differentially activated B cells in wildtype-like animals. Therefore, I examined next whether Notch2 receptor expression is also induced in-vivo, following immunization of control/CAR mice with NP-CGG. Looking at the reporter$^+$ B cells which responded to the antigen, Notch2 surface levels were compared between GC (CD38^{low}CD95^{high}), CD38$^+$CD95$^+$ and CD38$^+$ B cells.

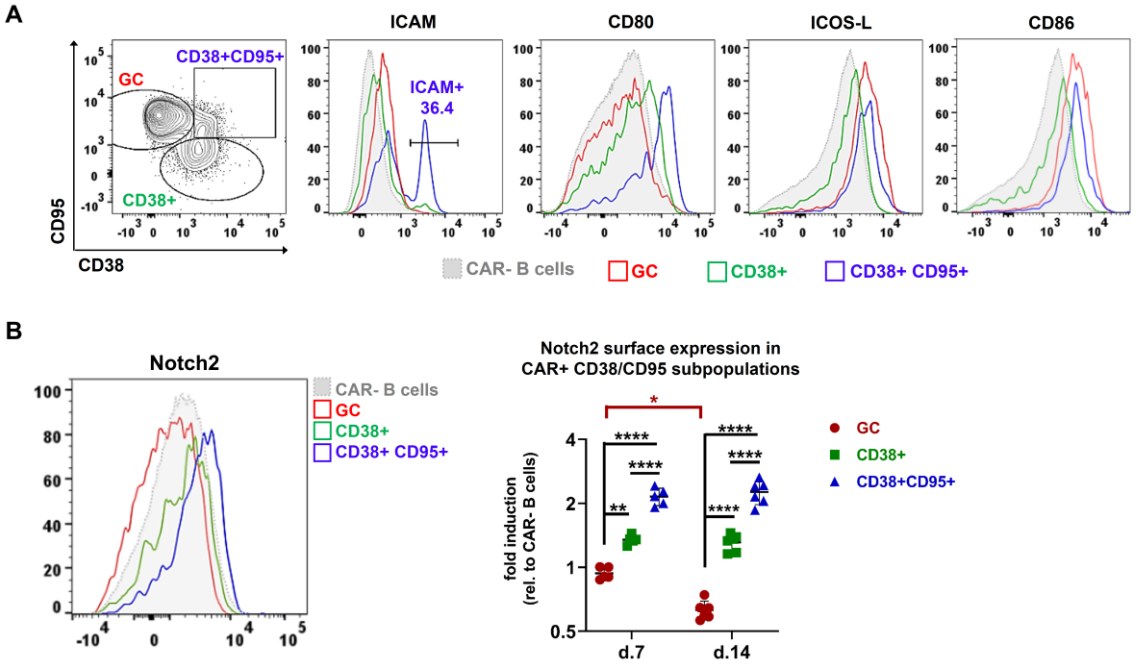

Fig. 41: **Expression of common B cell activation markers and the Notch2 surface receptor on control/CAR$^+$ CD38/CD95 subpopulations upon immunization.** FACS analyses are representative for day 14 after NP-CGG immunization of control/CAR mice. **(A)** Splenic cells were pre-gated on alive CAR$^+$B220$^+$ lymphocytes and subdivided into 3 populations according to the CD38 and CD95 distribution: GC (CD95$^+$CD38$^-$), CD38$^+$CD95$^+$ and CD38$^+$ cells. The histograms show overlays of the expression of the indicated activation markers in each of the 3 subpopulations, compared to their levels in CAR$^-$ B cells. **(B)** Histogram overlay of the Notch2 surface expression in the indicated cell populations at day 14 p.i. (gated as in (A)). The graph shows the fold induction of Notch2 expression (MFI) in the CAR$^+$ CD38/CD95 subpopulations

relative to its expression in CAR$^-$ B cells (calculated as ratio for each mouse individually). Sidak's 2-way-ANOVA of paired values. n=5 at day 7, n=6 at day 14. Similar figure in (Babushku et al., 2022).

Data revealed that CD38$^+$CD95$^+$ B cells strongly upregulated, but GC B cells progressively downregulated the Notch2 surface expression over a 2-week time span, compared to control CD38$^+$ B cells (*Fig. 41B*). Moreover, the reporter$^+$CD38$^+$CD95$^+$ cells also expressed higher levels of the common activation markers ICAM, ICOS-L, CD80 and CD86 in comparison to the GC and CD38$^+$ B cells, suggesting that these are activated B cells (*Fig. 41A*). These findings demonstrated that Notch2 receptor expression is upregulated on activated B cells upon TD immunization. These activated B cells with a high Notch2 expression on the cell surface may be the precursors for MZB cells, if they encounter a Dll-1 ligand-expressing cell. In contrast, cells that do not receive a Notch2 signal in the course of this activation process will eventually start to downregulate the Notch2 receptor surface expression (*Fig. 41B*), most likely at around 2 to 3 days of antigen encounter (48 h - 72 h, *Fig. 15B*), allowing them to turn down Notch2 signaling altogether and thus enabling their entry into the GC reaction.

5.5.2 CAR$^+$ MZB cells are generated until day 30 of the immune response and exhibit high IgM and CD1d expression

The appearance of reporter$^+$ cells with a CD21^{high}CD23$^-$ phenotype in the first 2 weeks of the immune response prompted us to closely investigate the kinetics of these newly-generated MZB cells over a broader time span upon immunization. It seemed interesting to examine whether these cells are continuously generated and persist over 4 weeks of antigen injection in the spleen, and whether they express a full plethora of typical MZB cell surface markers, just like the N2IC-expressing MZB cells in the N2IC/hCD2 mouse model. For this purpose, control/CAR animals were additionally analyzed after 4, 7, 9, 14, 17, 22, 26 and 30 days of NP-CGG immunization.

First, the efficiency of the deletion of the lox-P-flanked regions post injection was validated by the amounts of CAR-expressing B cells in the spleen. Both the percentages, as well as the total cell numbers of CAR$^+$ B cells reflected similar kinetics (*Fig. 42*). The first CAR$^+$ B cells appeared at day 4 post injection and continuously increased with the progression of the immune response up until day 14, when the peak of the GC reaction was reached. In the second two weeks upon immunization, between day 17 and 30, the amounts of these cells gradually decreased in the spleen (*Fig. 42*).

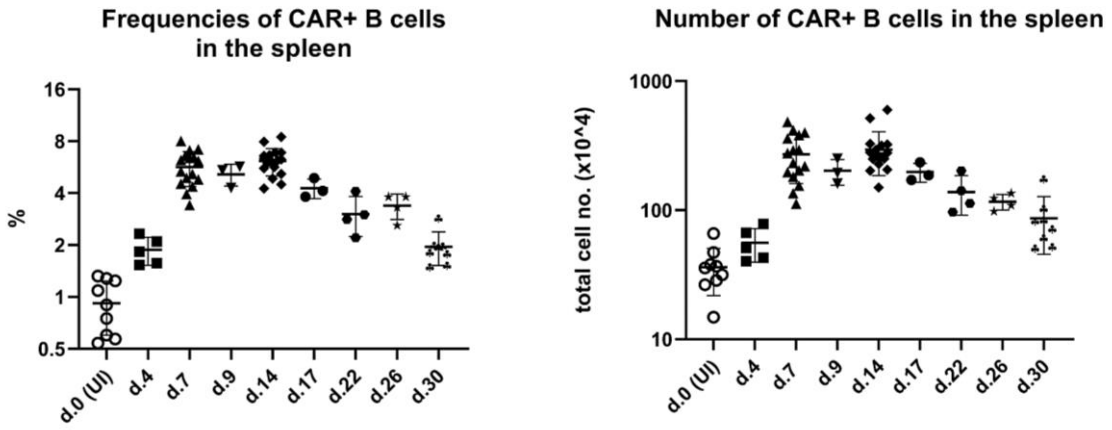

Fig. 42: **Deletion efficiency of the lox-P regions in the spleen over time.** Graphical summary of the amounts of CAR$^+$ B cells in the spleen of uninjected (d.0) and NP-CGG-injected mice. Cells were pre-gated on living B220$^+$ lymphocytes. The percentages of reporter$^+$ B cells acquired in FACS were directly plotted in the left graph. The graph on the right shows total cell numbers (x10^4) of CAR$^+$ B cells, which were calculated using the FlowJo-gated percentages for CAR$^+$ B cells within the living DAPI$^-$B220$^+$ cells and the total numbers of splenocytes counted for each mouse. n=13 (d.0, UI), n=15 (d.7 and d.14), n=3 (d.9, d.17 and d.22), n=5 (d.4 and d.26), n=8 (d.30).

Subsequent staining for CD21$^+$CD23^{low} cells confirmed the existence of CAR$^+$ MZB cells in the spleen beyond the first two weeks of the immune response (*Fig. 43A-B*). The percentages of the newly-generated MZB cells followed a seemingly increasing trend with ongoing time after immunization, ranging between 6-13% of all reporter-expressing cells at days 26 and 30 p.i. (*Fig. 43B*). This progression was indicative of a moderate, more physiological progression of MZB development compared to the one in N2IC/hCD2 mice. Furthermore, it was revealed that the CAR$^+$ MZB cells also expressed high levels of MZB cell surface markers IgM and CD1d. Interestingly, a portion of the cells were still CD1d^{low} at day 7 and 14, however, by day 30, all CAR$^+$ MZB cells were uniformly CD1d^{high} (*Fig. 43A, red arrows*). The percentages of CD1d^{low}CAR$^+$ MZB cells progressively decreased over analyzed time (*Fig. 43C*), suggesting that CAR$^+$ MZBs gradually acquired their full MZB cell surface phenotype in the course of the TD immune response.

Calculations of the absolute number of CAR$^+$ cells within the total MZB population (*Fig. 44*) revealed that most CAR$^+$ MZBs seemed to be generated in the first 14 days during the peak of the immune response, and their numbers remained rather stable between day 17 and 30 after immunization (*Fig. 44*). Rather than an unrestricted exponential growth over time as suggested by their percentages, the CAR$^+$ MZB cell numbers followed a restricted logarithmic curve and reached a plateau after 2 weeks of the immune response.

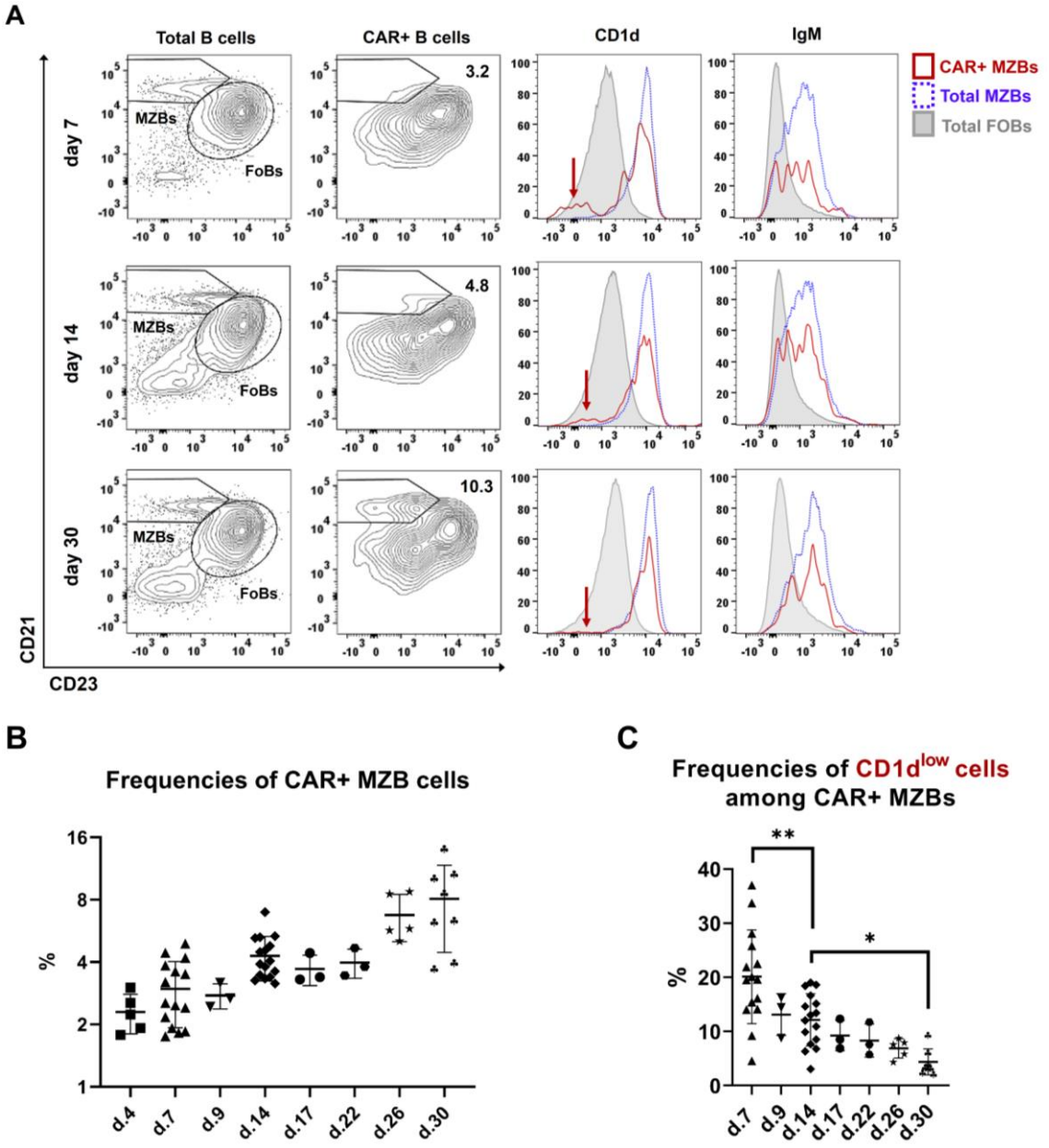

Fig. 43: **CAR⁺ MZB cells are generated up to day 30 and express high levels of CD1d and IgM. (A)** Representative FACS analyses of splenic B cells at days 7, 14 and 30 after immunization. Cells were pre-gated on living B220⁺ lymphocytes. Contour plots depict the gating of MZB ($CD23^{low}CD21^{high}$) and FoB cells ($CD23^{+}CD21^{low}$) among the total B cell population ($B220^{+}$), and of MZB cells among the reporter⁺ B cells (CAR^{+}). Histograms show overlays of the CD1d and IgM expression in CAR^{+} MZB cells (red), compared to total MZB (blue, dotted) and total FoB cells (grey, tinted) from the same mouse. Red arrows point to the CAR^{+} MZB cells without any CD1d expression. **(B)** Summary graph of the frequencies (%) of gated CAR^{+} MZB cells at indicated time points post injection. **(C)** Summary graph depicting the percentages of $CD1d^{low}$ cells (marked by red arrows in (A)) among the CAR^{+} MZB cells (gated as in (A)) at all indicated time points p.i. At day 4, the CD1d marker was unfortunately not included in the FACS analyses, therefore the respective values for this time point are missing in the graph. **(B-C)** n=15 (d.7 and d.14), n=3 (d.9, d.17 and d.22), n=5 (d.4 and d.26), n=8 (d.30), one symbol=one mouse in the graphs. Similar figure in (Babushku et al., 2022).

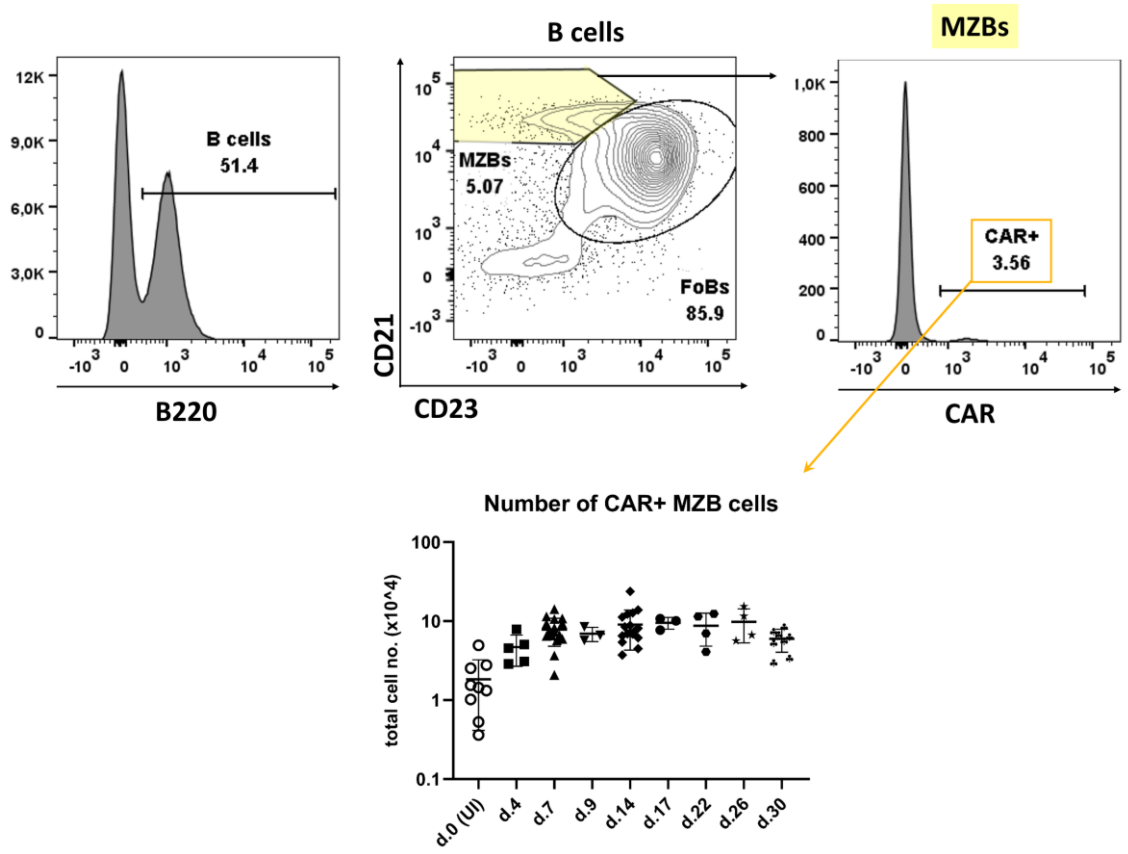

Fig. 44: **The numbers of reporter⁺ B cells within the total MZB population mildly increase with time post immunization.** Representative FlowJo gating strategy from day 7 p.i., to show the identification of CAR⁺ B cells among the total B220⁺CD21^{high}CD23^{low} MZB cells. Splenic cells were pre-gated on living lymphocytes. The graph below shows the amounts of CAR⁺ B cells in the spleen of uninjected (d.0) and NP-CGG-injected mice at the indicated time points as total cell numbers (x10^4). Calculations were done using the sequentially gated percentages for CAR⁺ B cells within the DAPI⁻B220⁺CD21^{high}CD23^{low} cells and the total counted splenic cell number for each mouse. n=13 (d.0, UI), n=15 (d.7 and d.14), n=3 (d.9, d.17 and d.22), n=5 (d.4 and d.26), n=8 (d.30).

Interestingly, there was a slight decline of CAR⁺ MZB cells setting in between days 26 and 30 p.i. (*Fig. 44*). One possible explanation could be a re-differentiation of at least some CAR⁺ MZB cells back to FoB cells at later time points, or a further differentiation into a new second wave of PCs upon antigen re-encounter. On the other hand, the observed drop may also be attributed to the half-life of the newly-generated CAR⁺ MZB cells.

Overall, this progression (*Fig. 44*) suggested that splenic CAR⁺ MZB cells are generated in the early weeks of the immune response, and there seems to be little to no new MZB cell differentiation at later time points. Instead, the already-produced MZB cells only further persist as sessile residents of the spleen. Of note, CAR⁺ cells also differentiated into GC, memory and plasma cells in the first 2 to 3 weeks after immunization. However,

most of these cell types become cleared from the spleen between day 21 and 30 due to migration in the circulation and to their homing organs (BM, peritoneum) or cell death. Thus, the CAR-expressing MZB cells are likely the only cell population which can be found and detected in the spleen at later time points beyond day 21. This may explain why seemingly the percentages of CAR$^+$ MZBs exponentially increase over time, while the frequencies of all CAR-expressing B cells start to decrease after day 14. For this reason, the absolute cell numbers of CAR$^+$ B cells in the total MZB cell population of mice better reflect the true kinetics of MZB differentiation from antigen-responding cells in the course of the primary TD immune response.

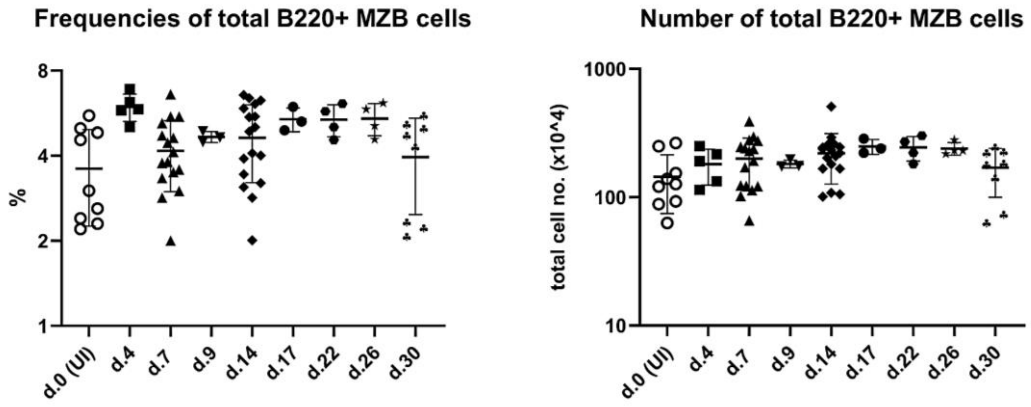

Fig. 45: **The amounts of total naïve MZB cells in mice remain unchanged over time after NP-CGG immunization.** Graphs depicting the amounts of total B220$^+$CD21^{high}CD23^{low} MZB cells in uninjected (d.0) and NP-CGG-injected mice at the indicated time points. The percentages of MZB cells were directly plotted in the graph on the left. The right graph shows the total cell numbers (x10^4) of MZB cells, calculated using the percentages of CD21^{high}CD23^{low} cells within the DAPI$^-$ B220$^+$ cells and the total cell numbers of counted splenocytes for each mouse. n=13 (d.0, UI), n=15 (d.7 and d.14), n=3 (d.9, d.17 and d.22), n=5 (d.4 and d.26), n=8 (d.30).

Lastly, the analyses disclosed that the total amounts of MZB cells in control/CAR animals remained relatively stable during the overall observation period (*Fig. 45*). Considering that the amounts of newly-generated CAR$^+$ MZBs slightly increased up until day 14 (*Fig. 44*), these findings may imply a replacement of at least some pre-existing wildtype MZB cells by the newly-generated CAR-expressing MZB cells in the early stages of the immune response (day 4 – day 14). In this way, the natural purpose of immunization-induced *de novo* MZB cell differentiation may be to replenish the murine pool of existing MZB cells, which in turn can be easily deprived by early extra-follicular antibody production once there is a breach of the immune system.

5.5.3 Evidence of CAR$^+$ MZB cells with a CD38$^-$CD95^{high} phenotype: at least some MZBs may be GC-derived

The previously presented findings revealed that CAR$^+$ MZB cells were mostly generated in the first two weeks post immunization. At later time points, there seemed to be no new MZB differentiation from reporter$^+$ B cells, but only a maintenance or persistence of the already existing CAR$^+$ MZB cells in the spleen. Furthermore, it was shown that the CAR$^+$ GC B cells continuously increased between day 4 and 14 post immunization, which is in accord with the progression of the mature GC in mice. Thus, most CAR$^+$ MZB cells were generated in parallel with the ongoing maturation of the GC reaction. Therefore, an important question remains, whether the newly-produced CAR$^+$ MZB cells are derived directly from activated pre-GC cells, or if they show any signs of prior GC experience and have been generated from early GC B cells. In this regard, the reporter$^+$CD21^{high}CD23^{low} population was analyzed for the existence of cells with a GC phenotype.

The FACS data showed that most CAR$^+$ MZB cells had a CD38^{high}CD95$^{mid/low}$ activated and non-GC phenotype. However, a few of these cells were CD38$^-$CD95^{high} and had a typical GC B cell phenotype (*Fig. 46*). The frequencies of CAR$^+$ MZBs with a GC phenotype were the highest at day 7 post immunization (app. 10-15%), but proceeded to gradually drop in the next weeks by day 30 (app. 1-3%) (*Fig. 46, Fig. 47*). Thus, at around 4 weeks after immunization, almost all CAR$^+$ MZB cells had the typical resting MZB cell phenotype and were CD21^{high}CD23^{low}CD38^{high}CD95$^{low/neg}$. The decreasing trend of CAR$^+$ MZB cells with a GC phenotype (*Fig. 47*) correlated with the directly opposing, increasing trend of GC B cells in the same time frame, implying that at least some reporter$^+$ MZB cells may be derived from the early stages of the GC reaction (day 7-14). With ongoing time (day 17-30), most likely as they start to settle in the splenic MZ, the CAR$^+$ MZB cells may upregulate CD38 and moderately downregulate CD95 expression, fitting with the pre-activated phenotype of MZB cells. In this way, they may adopt a typical terminal marginal zone cell phenotype similar to wildtype MZBs at steady-state conditions.

Taken together, these findings suggest that most CAR$^+$ MZB cells generated during the primary immune response may be derived from activated CD38$^+$CD95$^+$ pre-GC cells, but a small fraction of them may also originate from the early GC. As time progresses and most reporter$^+$ B cells differentiate into GC B cells or PCs, these few CAR$^+$ MZBs lose their GC phenotype and become indistinguishable from the ones derived from activated B cells in the pool of total CAR$^+$ MZB cells. Alternatively, it may also be possible that all CAR$^+$ MZB cells generated during the primary TD immune response originate from the GC reaction, however, they can quickly modify i.e. lose their GC B cell surface markers, right after adopting the common CD23^{low}CD21^{high}CD1d$^+$IgM$^+$ MZB cell phenotype.

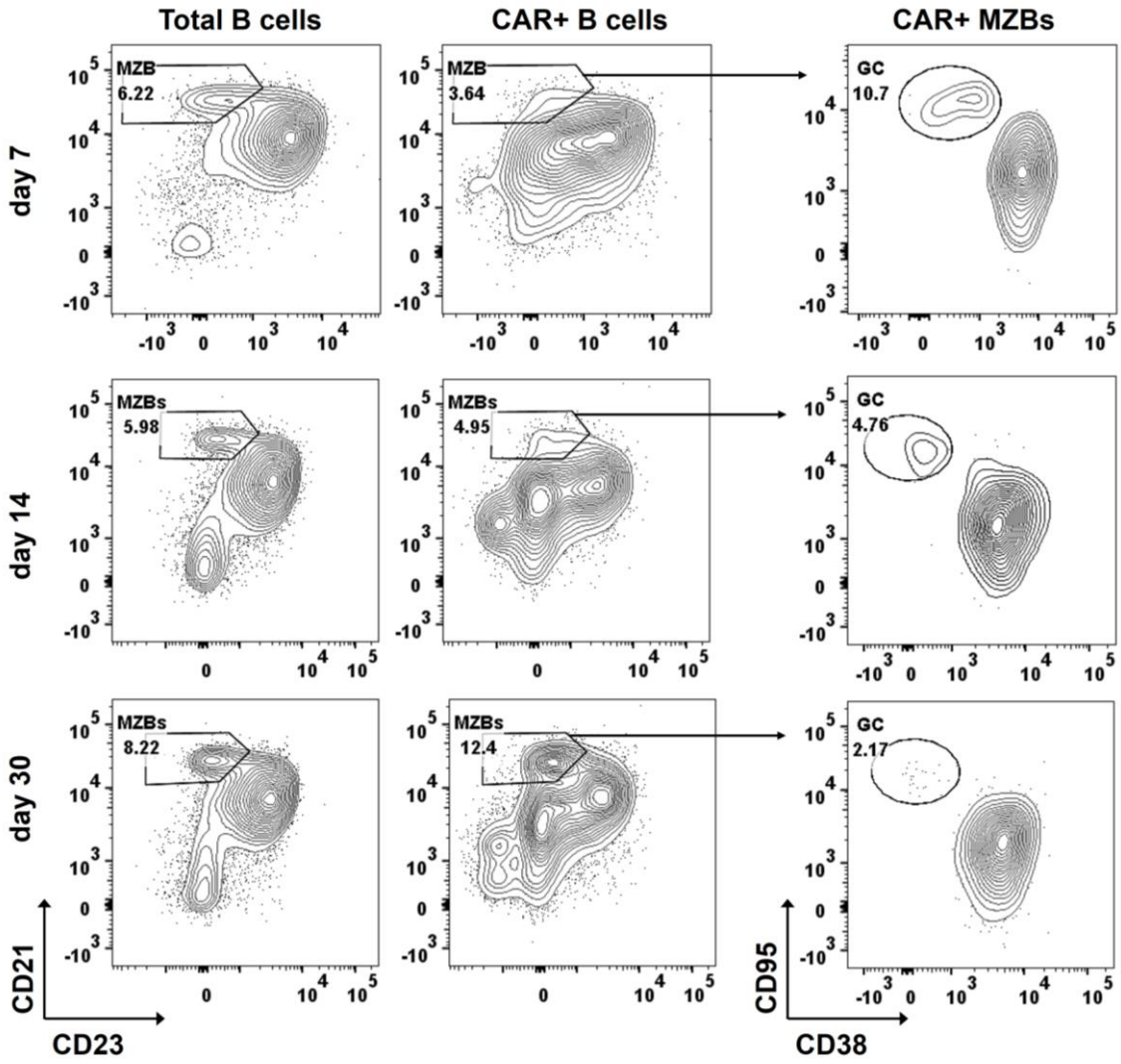

Fig. 46: **Some CAR⁺ MZB cells have a GC B cell phenotype. (A)** Representative FACS analyses from days 7, 14 and 30 after immunization. Splenic cells were pre-gated on living B220⁺ lymphocytes. Contour plots depict the gating of MZB cells ($CD23^{low}CD21^{high}$) among the total B cell population ($B220^{+}$, first column), and among the reporter⁺ B cells (CAR^{+}, second column). The contour plots in the column on the far right show the CD38/CD95 staining to identify GC B cells ($CD38^{low}CD95^{high}$) among the previously gated CAR^{+} MZB cells.

Nonetheless, it is still largely elusive from these FACS analyses whether the newly-generated MZB cells, seemingly derived from the GC, have mutated BCRs, true prior GC experience or any memory cell potential. It is possible that these are simple unmutated MZB cells, which entered the GC only for a short time (explaining their acquired GC phenotype), but were then quickly pushed out by day 7 before the mature GC is formed. This may happen due to the increased Notch2 signaling in cells destined to become MZBs, which normally has to be strongly counter-regulated to allow for the entrance and persistence of cells in the GC.

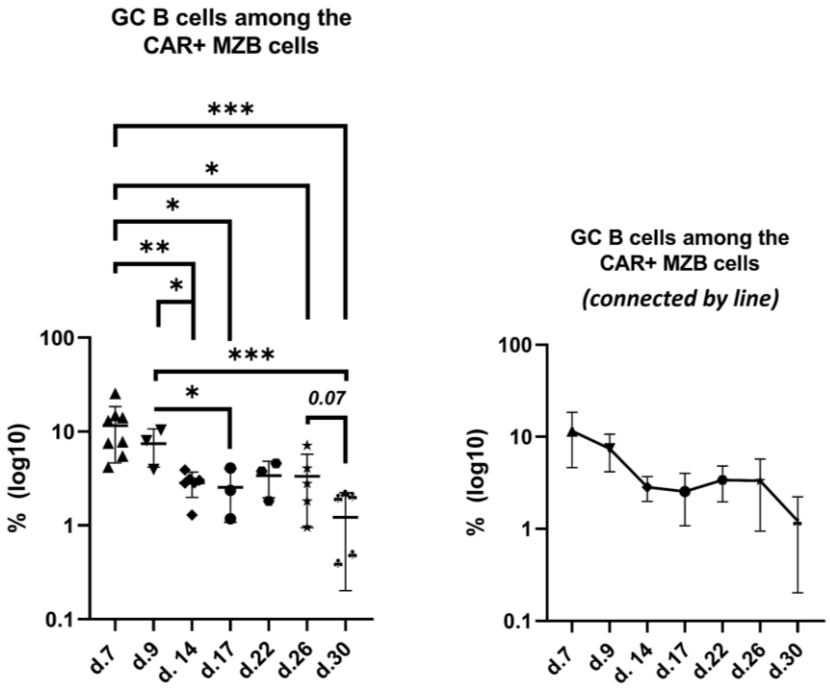

Fig. 47: **The percentages of CAR$^+$ MZB cells with a GC phenotype gradually decrease over time after immunization.** Graphs depicting the amounts of CAR$^+$ MZB cells (CD21^{high}CD23^{low}) with a GC phenotype (CD95^{high}CD38^{low}) in NP-CGG-injected mice at indicated time points. The percentages of these cells were directly plotted in the graph on the left as scattered values per time point (one symbol=one mouse). The right graph shows the same frequencies, but visualized as a mean+SD of all analyzed mice for each time point. The values between time points are linked with a line, to better depict the decreasing trend over time. n=8 (d.7), n=3 (d.9, d.17 and d.22), n=5 (d.26), n=6 (d.14 and d.30).

5.6 Graphical abstract of the main findings from this study

The data presented in this dissertation enabled us to unravel a novel and dynamic role of Notch2 signaling in cell fate decisions during the primary immune response to a TD antigen in mice (*Fig. 48*).

We could show that Notch2 surface expression is strongly induced upon B cell activation, mediated by BCR and CD40R engagement after T-/B- cell contact in vivo. The above-threshold Notch2 receptor levels on activated B cells increase their chances for Notch-ligand binding on the surrounding Dll-1-expressing follicular fibroblasts or T cells in the B cell follicle. If the Dll-1-ligand-Notch2 interaction is weaker and persists only transiently upon antigen encounter, a portion of the activated B cells will downregulate Notch2 surface expression again, likely through regulatory mechanisms of Notch signaling activity that occur at the level of the Notch receptor. This will allow the cells to down modulate Notch2-IC signaling activity altogether and introduce the GC gene expression program by induction of Bcl6, ultimately leading to GC B cell differentiation and entry into the GC reaction.

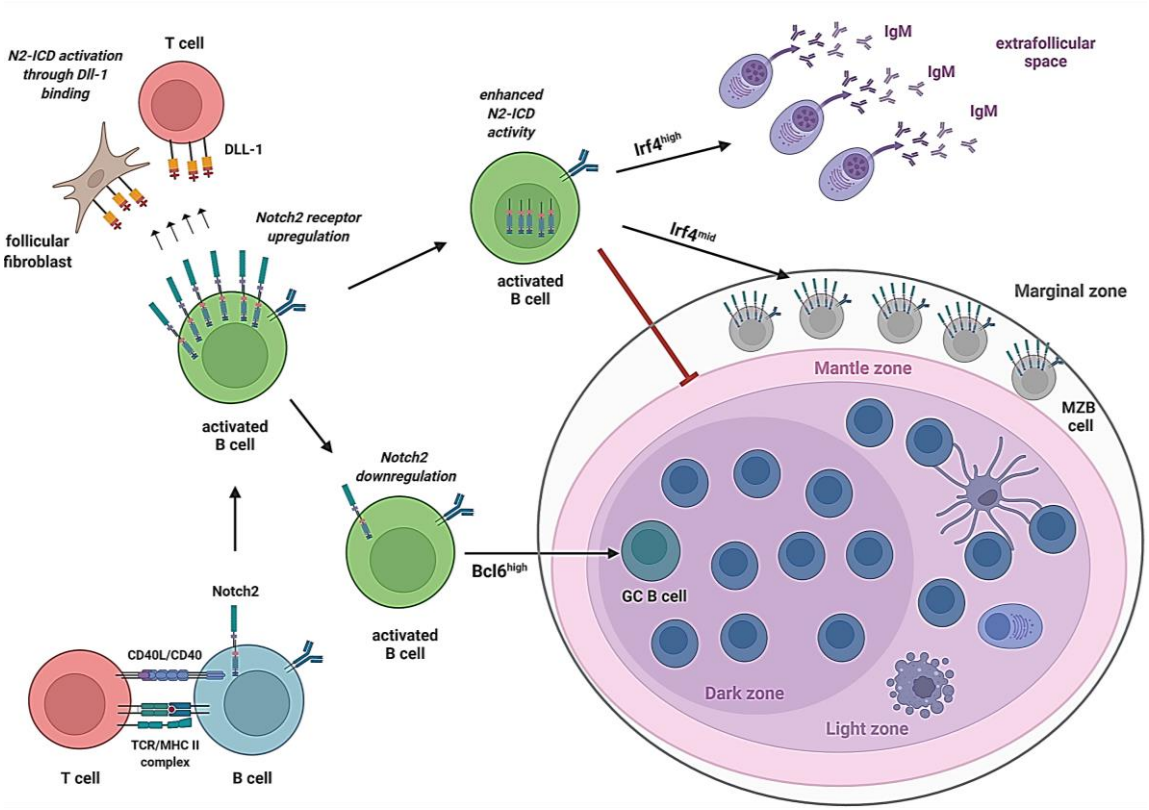

Fig. 48: **Illustrative summary of the main findings presented in this work.** The scheme gathers all data, which led us to form a conclusion about the distinct dynamic regulation of Notch2 signaling during TD immune responses. Notch2 signaling has a pivotal regulatory role in the binary decision of antigen-activated B cells between two opposed cell fates: GC B cell differentiation on one hand, MZB cell and PC differentiation on the other hand. (Own original illustration created using BioRender, biorender.com).

However, if a successful Dll-1-Notch2 interaction is established between activated B cells and their ligand-providing counterparts, which is stronger and persists long enough beyond the first 3-4 days of antigen encounter, then these cells will exhibit enhanced Notch2 intracellular signaling, resulting with suppression of GC initiation factor Bcl6 and induction of PC differentiation factor Irf4. The silencing of Bcl6 will further enhance Irf4 expression through a negative regulatory loop, so that cells receiving an above-threshold Notch2 signal also exhibit above-transient expression of Irf4. This will drive the $Irf4^{high}$ cells to differentiate into extrafollicular IgM^{+} PB/PCs. However, a bigger fraction of them will exhibit sustained intermediate Irf4 levels, which are not high enough to convert them all into PB/PCs. Thus, the $Irf4^{mid}$ cell population will give rise to new MZB cells with a full surface phenotype and a correct splenic localization in the MZ.

6 Discussion

The Dll-1-ligand, expressed on splenic follicular fibroblasts (Fasnacht et al., 2014), provides the necessary signal for Notch2 pathway activation, which then drives MZB cell differentiation, often in concert with other signaling pathways. Thus, the possibility exists that peripheral B cell subsets are continuously exposed to Dll-1-ligands in the splenic follicle, and upon close cell-to-cell contact with follicular fibroblasts, they can be recipients of a Notch2-signal at times. Our study aimed to examine this more closely, and further postulated that the strength and/or duration of the receiving Notch2 signal will determine whether a precursor cell (T2 or FoB cell) will ultimately develop into a MZB cell. Additionally, we hypothesized that FoB cell activation via BCR and CD40 engagement synergizes with Notch2 and positively regulates its subsequent signaling activity. Considering that such a TD activation mechanism induces the mobility of FoB cells throughout the follicle towards the T-cell zone, it may place them into a close enough proximity with Dll-1-expressing fibroblasts along the way, thus facilitating enhanced Notch2 signaling in at least a portion of these activated FoB cells. In this sense, the Notch2 signaling pathway and B cell activation may both be necessary to drive FoB cells towards MZB cell differentiation during TD immune responses, instead of driving them towards alternative cell fates, such as GC B cell differentiation.

The results from this work finally proved that antigen-activated FoB cells can make a binary cell fate decision between GC or MZB cell and PC differentiation, and this bifurcation is dependent on the receiving Notch2-signal: downregulation of Notch2 signaling in FoB cells facilitates their entry into the GC, whereas FoB cells that get a strong Notch2 signal upon immunization give rise to extrafollicular plasmablasts and to new MZB cells (Babushku et al., 2022). The generation of MZB cells happens as a systematic response to TD-immunization and may be a natural mechanism of replenishment of the pre-existing MZB cell pool in mice, once there is a breach in the immune system by foreign invaders.

6.1 Notch signaling in bone marrow B lymphocytes and peripheral B cell subsets

To unravel which B lymphocytes receive a Notch signal during early B cell development and peripheral B cell maturation, CBF:H2B-Venus mice were analyzed under steady state conditions. These are specialized Notch-reporter mice, which express the nuclear fluorescent protein Venus upon active Notch signaling (Nowotschin et al., 2013). Both immature developing B lymphocytes, as well as the transitional and mature B cell subsets in the spleen were Venus-positive, indicating they all get a Notch signal at times.

Thus, it seems that Notch-ligand-expressing cell types are not restricted to the splenic microenvironment, but can be encountered by all B lymphocytes in the bone marrow and the periphery. Indeed, over 95% of $CD19^+$ cells in the lymph nodes also exhibited high Venus expression, indicative of ongoing Notch signaling activity in B cells at other SLO sites as well. Moreover, Venus expression progressively increased during sequential stages of early and late B cell development and culminated in the splenic MZB cells. This suggested that Notch signaling is purposely enhanced during B lymphocyte development and is the prerequisite for the final establishment of the mature MZB cell lineage. Interestingly, there was a portion of cells in the MZB pool which had downregulated or completely lost the Venus expression. We suspect that once settled in the splenic MZ compartment, MZB cells do not receive a *de novo* Notch signal and thus lose the Venus expression over time, likely because of the restricted availability of Notch-ligand-expressing fibroblasts outside the B cell follicle. In this sense, loss of their usually high and sustained Notch signal may introduce a downregulation of the Sphingosine-1-phosphate-receptors S1PR1 and S1PR3 and may thus facilitate the migration of MZB cells back inside the follicles (Cinamon et al., 2008; Lechner et al., 2021). In line with our view are previous data showing that impediment of Notch2 signaling in MZB cells induces them to leave the MZ and shuttle back into the B cell follicle to be indistinguishable from the FoB cell population (Simonetti et al., 2013), suggesting a significant dynamic plasticity between FoB and MZB cells dependent on Notch signaling. An alternative explanation would be that the Venus-low MZB cells with a down modulated Notch signal were on the trajectory towards mature PC development at the time of analysis. Indeed, murine MZB cells can produce antibody-secreting PCs not only after infection, but also under resting, homeostatic conditions. It was shown that in addition to interacting with epitopes expressed by foreign pathogens, MZB cells can also bind to antigenic determinants from bacteria in the intestinal tract, which occasionally breach the mucosal barrier and recirculate to the spleen (Cerutti et al., 2013). Thus, the murine intestinal microbiota can modulate and enhance the function of resting MZB cells. In this sense, we may speculate that some MZB cells lost their Notch signal upon mouse-intrinsic pathogen encounter and further underwent the stages of PC differentiation.

6.2 Notch signaling in splenic and peritoneal B1 cell subsets

B1 cells are the less abundant mature B cell subset in the spleen, as their main niche is the murine peritoneum (Baumgarth, 2017, 2016; Hayakawa et al., 1986). In general, research studies examining Notch receptor expression or the potential influence of Notch1 and Notch2 signaling in B1 cells inhabiting the spleen are rather scarce, likely because B2 cells are the dominant splenic B cell subset. Unlike mature $CD23^+$ B2 cells, we found

that most splenic B1 cells were Venus-low or –negative, indicating that B1 cells are not in constant spatiotemporal proximity to Notch-ligand-providing cells and are therefore devoid of a Notch signal. The lower Venus expression in B1 compared to B2 cells implied a dispensable role of Notch signaling in the survival and maintenance of splenic B1 cells, as opposed to its crucial role in mature FoB and MZB cells. In contrast to the spleen, we discovered that most B1a and B1b cells in the peritoneal cavity were uniformly Venus-positive, suggesting they strongly rely on Notch signaling in this microenvironment. Previous studies showed that Notch2, but not Notch1 mRNA, is highly-expressed in B1 cells of the peritoneal cavity (Saito et al., 2003). Mice expressing only one functional *Notch2* allele (Notch2$^{+/-}$) have been reported to show a reduction in peritoneal B1 cells (Witt et al., 2003b). In contrast, mice with floxed Notch2 alleles crossed to CD19-Cre mice (complete B-cell-specific ablation of Notch2), as well as mice with loss-of-function of the RBPJ co-activator of Notch signaling exhibited fully normal B1 cell numbers in the peritoneum (Saito et al., 2003; Tanigaki et al., 2002). The reason for this difference in the B1 phenotype between these strains remains still largely unknown (Garis and Garrett-Sinha, 2021). Thus, the observed Venus expression in peritoneal B1 cells may be only transient and necessary to support their survival and maintenance at given times. Taken together, we can conclude that Notch signaling seems crucial for the B1 cell subset in the peritoneum, but is expendable in most B1 cells which localize in the spleen.

6.3 Notch signaling in B cell populations, arising during an active TD immune response

To examine the dynamics of Notch signaling during an ongoing TD immune response, we analyzed TD-antigen injected CBF:H2B-Venus mice for their Venus expression, as well as transgenic mice with conditional deletion (N2KO//CAR) or constitutive activation (N2IC/hCD2) of Notch2 in GC B cells (Cγ1-Cre strains). In the GC-B-cell-specific strains, expression of the CAR or hCD2 reporter on the cell surface was irreversible and stable upon immunization, allowing us to track the antigen-responding Notch2-transgene/reporter expressing cells among the B cell population over a 4 week-time period. The percentages of reporter^{+} B cells showed overall similar kinetics: continuous increase in the first two weeks, peak at day 14, followed by a strong drop at day 30. The peak at day 14 is in accordance with the progression of the TD immune response, accompanied by cell proliferation and expansion upon B cell activation. The decrease by day 30 can be discussed as a combination of several factors: (1) B cells do not come in contact with the antigen anymore, which is already cleared from the spleen, so there is no new deletion of the lox-P-flanked regions in additional cells; (2) most reporter^{+} cells had terminally differentiated into a certain B cell type (e.g. PCs, memory B cells) and are no longer

located in the spleen, but homed to other organs (bone marrow, blood, peritoneum); (3) their half-life restricts the detectable amounts, suggesting there is a certain fraction of reporter$^+$ cells that underwent cell death or were cleared off in the absence of antigen.

6.4 Notch2 signaling supports B cell activation and is incompatible with GC B cell differentiation

Our immunization data with different mouse models revealed that Notch2 signaling is dispensable for GC formation and needs to be strongly downregulated to allow for the differentiation of GC B cells. Accordingly, induction of Notch2IC in B cells fully impaired the normal GC reaction by suppression of the GC initiation factor Bcl6 (data from N2IC/hCD2 mice). Our findings are in line with previous studies showing that a strong Notch2 signal interferes with GC formation in mice and that Notch2 expression is inversely correlated with Bcl6 in GC B cells from human tonsils (Hampel et al., 2011; Valls et al., 2017).

Collective results from the N2KO//CAR and CBF:H2B-Venus animals led to the conclusion that Notch2 signaling not only has to be counter-regulated to allow for GC B cell differentiation, but its complete abolishment is even beneficial for the Bcl6-induced GC formation. Given that Venus expression was progressively diminished in GC B cells of the spleen, lymph nodes and Peyer's Patches during the course of the TD immune response, we suspect that loss of Notch signaling physiologically happens in GC B cells. Our findings revealed that down modulation of the Notch2 signal seems to happen very quickly in GC B cells. However, this rapid loss of Notch2 signaling may not be possible solely by eliminating the presence of Dll-1 ligands. Additionally, a degradation of Notch2IC signaling may be required, possibly through targeted degradation of the active Notch-ICD, as a mechanism of regulation of the Notch signaling pathway activity. The family of E3 ligases contains some good candidates for mediating the Notch2 counter-regulation in GC B cells. Two prominent examples are the Cbl/Cbl-b and Fbw7 ligases, both of which are more highly expressed in GC B cells, compared to naïve B cells (publicly available data from Immgen Gene Skyline, (Heng and Painter, 2008)). Furthermore, both ligases have been described to target the Notch1- and Notch2-ICD for rapid proteasomal degradation, thus controlling their intracellular levels (Jehn et al., 2002; Wu et al., 2001). A recent study supporting our view revealed that deleting Cbl and Cbl-b in GC B cells led to an early exit of high-affinity B cells from the GC reaction and an impaired clonal expansion, implying that Cbl/Cbl-b expression has to be sustained for the proper

GC progression (Li et al., 2018). In this sense, we believe that a controlled down modulation of Notch signaling upon antigen-activation may be necessary to prevent pre-mature GC exit or early PC production in the wildtype situation.

Previous studies revealed that Notch2 signaling not only blocks the GC formation (Hampel et al., 2011; Valls et al., 2017), but also strongly synergizes with BCR and CD40 signaling in in vitro-stimulated FoB cells, to enhance and sustain prolonged B cell activation (Thomas et al., 2007). This is in line with our revelations that (1) Notch2 receptor-expression was strongly induced on in vitro-activated B cells upon CD40, IgM and LPS stimulation and the elevated expression was sustained for at least 3 days post stimulation; (2) B cells from Notch2/hCD2 mice were trapped in an activated $CD38^{high}CD95^{mid-}Bcl6^{-}$ non-GC phenotype due to a strong induction of CD38, correlating well with their impaired GC B cell differentiation potential. In addition, we found that Notch2 receptor levels were strongly upregulated on antigen-responding activated B cells following TD immunization, but were progressively downregulated on fully-differentiated GC B cells over the course of the immune response. Thus, when Dll1-ligand is limited or absent for most GC B cells, the Notch2 surface levels may be negatively regulated via continuous receptor endocytosis, followed by trafficking to late endosomes and subsequent degradation. This could explain both the diminished Notch2 receptor expression on GC B cells and the lower Notch-IC signaling activity reflected by the loss of Venus expression. Additionally, in our in-vitro assays with anti-CD40 and interleukins (IL4, IL21), which mimicked the TD immunization-induced activation of B cells, we observed a counter-regulation of Notch2 receptor expression on activated B cells after 48 and 72 h post stimulation. The progressive downregulation of Notch2 surface receptor with time was concomitantly accompanied by an increasing adoption of a $CD38^{low}CD95^{high}$ GC-like phenotype, confirming once again that Notch2 receptor expression is downregulated on the cell surface at the transition of activated B cells into GC B cells.

Interestingly, the dominant $CD38^{high}Bcl6^{-}$ non-GC phenotype in B cells of N2IC/hCD2 mice resembled a previously published phenotype of LMP1/CD40 mice, mimicking a constitutive active CD40 signal in all B cells (Hömig-Hölzel et al., 2008). Upon TD-immunization, they also failed to generate GC B cells, but predominantly had an activated B cell phenotype. Furthermore, it was shown that LMP1/CD40 was also able to suppress Bcl6 (Panagopoulos et al., 2004), similar to the N2IC induction in B cells of N2IC/hCD2 mice. In addition, the constitutive CD40 signaling activity led to activation of components from the non-canonical NF-κB pathway (Relb and p52) (Hömig-Hölzel et al., 2008) and LMP1/CD40 FoB cells had increased expression of Notch2 on the cell surface and Notch2-ICD inside the cell (unpublished data from our lab). Considering these findings and the strong similarities of the phenotype in N2IC/hCD2 and LMP1/CD40 mice, we

speculate that Notch2IC-induction may positively regulate downstream non-canonical NF-κB signaling through synergism with CD40 signaling in activated B cells, ultimately causing the suppression of Bcl6 and the inhibition of GC formation.

6.5 Notch2 signaling is crucial in the LZ of the GC and supports production of IgG1$^+$ B cells

Although most GC B cells were devoid of Notch signaling (Venus-low), a small portion of splenic GC B cells with high Venus expression was found to be enriched in the LZ. These cells may receive a Notch signal during the positive selection in the GC, likely upon interaction with ligand-providing T helper cells or FDCs. Our assumption is supported by previous data demonstrating that FDCs in human and murine GCs express high levels of the Notch ligands Dll-1 and Jagged-1, whereas some GC B cells may express Notch1 and Notch2 (Santos et al., 2007; Yoon et al., 2009). The FDCs are located in the LZ, where highly-mutated B cells require close contact with them and with the activated follicular T_{fh} cells during the course of positive selection and GC exit (Rodda et al., 2015; Victora and Nussenzweig, 2012).

During positive selection, IgG1 class-switch recombination is performed at high rates in GC B cells (Sundling et al., 2021). Our data suggest that Notch2 signaling plays a crucial role in facilitating the proper switching to IgG1, as demonstrated by the strongly diminished IgG1$^+$ GC B cell numbers in N2KO//CAR mice, compared to controls. Furthermore, we could show that Venus expression was lost in most IgG1$^+$ B cells, both with a GC and non-GC phenotype. Considering that functional Notch2 was proven beneficial for the switching of B cells into the IgG1 isotype, we believe that the downregulation of Notch signaling in IgG1$^+$ B cells is related to their predominant origin from the GC reaction, rather than to the IgG1 CSR process alone. Nonetheless, some IgG1$^+$ GC B cells and increasing amounts of IgG1$^+$ non-GC B cells still exhibited high Venus expression, which further supports our view that during positive selection in the LZ, some GC B cells that switch to IgG1$^+$ cells rely on Notch signaling activity. In line with our discoveries are in-vitro studies showing that Notch signaling through the Dll1-ligand greatly enhances the production of IgG1$^+$ B cells in BCR- and CD40-stimulated FoB cells (Thomas et al., 2007). Based on these previous findings and our joint data from N2KO//CAR and CBF:H2B-Venus animals, we propose a physiological scenario where Notch2 signaling has to be attenuated to allow for GC formation, likely in most DZ centroblasts which are the founders of the GC. Later on, as B cells undergo IgG-CSR and interact with Dll1-expressing FDCs and T_{fh} cells in the LZ, functional Notch2 signaling is again necessary

to induce the production of IgG1-switched B cells, or alternatively, through cooperation with other pathways, to regulate the survival and proliferation of $IgG1^+$ GC B cells.

6.6 Notch2 signaling initiates enhanced PC differentiation, but terminates the process at the plasmablast stage

Earlier studies suggested that the ability of Bcl6 to interfere with Notch signaling may be needed to prevent premature differentiation into antibody-secreting cells (ASCs) (reviewed in (Garis and Garrett-Sinha, 2021)). On the other hand, expression of the PC differentiation factor Irf4 is necessary for GC initiation, but it is counter-indicated for the further maintenance of the GC (Klein et al., 2006; Ochiai et al., 2013). A moderate, transient expression of Irf4 in B cells induces the expression of Bcl6 and promotes proper GC development (Ochiai et al., 2013). If there is a persistent above-threshold Irf4 expression after the first few days of antigen encounter, which exceeds the transient levels, the sustained Irf4 expression will be sufficient to directly repress Bcl6 and to promote PC differentiation instead (Saito et al., 2007; Sciammas et al., 2006; Shapiro-Shelef and Calame, 2005). Our data revealed that N2IC-expressing cells strongly induced and sustained the Irf4 expression over 2 weeks post immunization, which ultimately resulted in an enhanced production of $Irf4^{high}B220^{low}$ plasmablasts and PCs, and impaired GC formation. Accordingly, the increased frequencies of N2IC-expressing $Irf4^{high}B220^{low}$ cells must have a GC-independent origin and are likely derived from an enhanced extrafollicular response. Thus, it is fitting that most N2IC/$hCD2^+Irf4^{high}B220^{low}$ cells were restricted to the spleen, were abundant with intracellular IgM and secreted predominantly low-affinity IgM^+ antibodies in the circulation. Furthermore, our discovery that N2IC-expressing $Irf4^{high}B220^{low}$ cells had attenuated expression levels of Blimp1 compared to controls, implies that N2IC-expression initiates the PC differentiation process, but blocks terminal PC development at the earlier stage of plasmablasts. This finding comes together with the immunization data from CBF:H2B-Venus mice, where we noticed retained Notch signaling activity in plasmablasts ($CD19^+B220^{mid}$), but strong downregulation in terminally differentiated splenic PCs ($CD19^-B220^-$) and in the long-lived PCs homing in the BM. These data implied that Notch2 signaling needs to be counter-regulated and turned off in the later stages of mature PC production. Interestingly, we found that N2IC-expressing $Irf4^{high}B220^{low}$ cells had strongly upregulated the proliferation marker Ki67, compared to controls, and further sustained its high expression levels over 2 weeks upon TD immunization. Considering that plasmablasts need to stop proliferating in order to differentiate into mature short- and long-lived PCs, it is plausible that N2IC-expressing cells cannot attenuate their ongoing proliferation and are therefore impaired in their terminal PC development.

Throughout the years, most studies based on in vitro experiments were focused on examining Notch1 receptor signaling and implied that it is more important for the positive regulation of PC production, than Notch2 (Kang et al., 2014; Santos et al., 2007; Thomas et al., 2007; Zhu et al., 2017). Thus, these previous findings may explain why the frequencies of splenic PCs were only slightly reduced in N2KO//CAR mice with abolished Notch2, but intact Notch1 signaling. In contrast, antigen-induced Notch2IC expression, which indubitably mimics constitutively active Notch1- and Notch2 signaling in N2IC/hCD2 mice, distinctly enhanced the entrance into the PC differentiation process.

In sum, we conclude from our findings that Notch2 signaling is crucial to initiate the PC differentiation from antigen-activated B cells up until the plasmablast stage. Afterwards, it has to be shut off in the final stages of PC maturation, to allow for short- and long-lived PC production. We propose that this mechanism of controlled mature PC production happens physiologically and that Notch signaling is counter-regulated in wildtype mice in order to establish a longer-lived PC compartment. This may happen in a similar fashion as in GC B cells, through E3 ubiquitin ligase activity, which targets Notch-ICD for proteasomal degradation and thus regulates the activity of the Notch signaling pathway. For instance, Fbw7 is one such ubiquitin ligase, whose mRNA expression is highly upregulated in splenic PCs, but markedly reduced in plasmablasts (publicly available data from Immgen GeneSkyline, (Heng and Painter, 2008)). Studies have shown that Fbw7 regulates Notch signaling by rapid targeting of the active Notch-ICD for degradation through its C-terminal PEST domain (Wu et al., 2001). Furthermore, the functional relationship between Fbw7b and Notch has been established as a double-negative i.e. double-positive feedback loop (Sancho et al., 2013). This means that increasing levels of Notch activity result in reduced expression of Fbw7b through transcriptional suppression, which in turn will lead to a further increase in Notch-ICD levels. Considering these findings, we postulate that increased Fbw7 expression leads to enhanced Notch-ICD degradation and thus to loss of Notch signaling in terminally-matured PCs. However, this is not the case in the proliferating plasmablasts, where Fbw7 is lower and thus Notch signaling is still profoundly active.

6.7 Advantages of the inducible Notch2 transgenic mouse models to study its effects on PC differentiation

Previous studies examining the role of Notch signaling in PC production made use of mouse models with a B-cell-specific deregulation of components from the Notch signaling pathway. However, all of these mouse models exhibited reduced or expanded MZB cell numbers on the account of FoB cells, which is in accordance with the potent role of

Notch2 signaling to drive MZB cell differentiation. On the other hand, the used control animals had no disruption in splenic B cell subsets and displayed intact MZB and FoB compartments. Therefore, such an experimental setting may not be optimal for comparable analysis of the PC response, given that MZB cells have been proposed to respond to TD antigens and contribute to the PC pool by generation of antibody-secreting cells (Song and Cerny, 2003). Indeed, the lack of a study with inducible- deleted or activated Notch2 signaling in mature B cells has been discussed, which would allow to specifically test its function in generation of PCs from already committed MZB and FoB cells (Garis and Garrett-Sinha, 2021; Thomas et al., 2007). Our study addressed this elusive point by using mouse models with inducible Notch2 inactivation or constitutive Notch2IC activation upon TD immunization in activated, GC and post-GC B cells. These mouse models had intact total amounts of FoB and MZB cells prior to and after TD-antigen injection, similar to control animals. By looking at the cells which responded to the antigen, we could specifically follow the PC production capability of only antigen-activated FoB cells with modified Notch2 receptor signaling. In this way, we revealed a dynamic regulation of Notch2 signaling during individual stages of PC development, a novel discovery which was lacking in mice thus far.

6.8 Notch2 signaling triggers *de novo* MZB cell differentiation from TD antigen-activated FoB cells

The discovery of upregulated Notch2 surface expression on control/CAR$^+$ B cells expressing a full plethora of typical activation markers led to the belief that at least a subset of these cells already possessed the necessary pre-requisite – higher Notch2 receptor cell surface levels - to compete for the Dll1-ligand, thus reaching an above-threshold Notch2 intracellular activity and converting into MZB cells. Indeed, lineage tracing of antigen-responding B cells showed that a substantial fraction of these cells differentiated into MZB cells with a full MZB cell surface phenotype (CD21^{high}CD23^{low}IgM^{high}CD1d^{high}CD38^{high}), accompanied by a complete spatial re-localization of the cells from the B cell follicle to the MZ over time. The uniformly high and sustained CD38 expression on reporter-positive MZB cells was further in accord with the well-established, pre-activated cellular state of MZB cells, compared to FoB cells (Zouali and Richard, 2011). The frequencies of reporter$^+$CD1d^{low} MZB cells progressively dropped over time and by day 30 all reporter$^+$ MZB cells were uniformly CD1d^{high}. This revelation was a strong indicator that the newly-generated MZB cells developed from activated CD1d^{low} FoB cells and gradually acquired the expected marker expression levels of MZB cells in the course of the TD immune response. Furthermore, we found that complete absence of Notch2 in reporter-positive cells resulted in an attenuated MZB cell

differentiation upon immunization, whereas control/CAR$^+$ cells with physiological Notch2 signaling produced moderate amounts of MZB cells, compared to N2IC/hCD2-expressing cells. This indicated that the generation of MZB cells upon TD immunization is strongly dependent on Notch2 signaling and the strength and/or persistence of the Notch2 signal in cells directly correlates with the frequencies of newly-generated MZB cells.

Prior research already pointed towards an antigen-dependent production of MZB cells in both rats and mice (Liu et al., 1988; Obukhanych and Nussenzweig, 2006; Pape et al., 2003; White and Meng, 2012; Yang Shih et al., 2002). Moreover, clonally related subsets of FoB and MZB cells were discovered in rats, and mutated IgM$^+$ memory-like B cells were found in their splenic MZ compartment (Hendricks et al., 2019). Nonetheless, whether these newly-produced MZB cells arise from pre-GC or fully-committed GC B cells as their precursors is still a subject of discussion. We found the appearance of reporter$^+$ MZB cells with a GC phenotype in the first week of the immune response. However, by day 30 all reporter$^+$ MZB cells had the typical resting MZB phenotype (CD21^{high}CD23^{low}CD38^{high}CD95^{low}). Thus, we believe that two pathways can lead to the antigen-induced MZB cell generation, either separately or combined together: (1) CAR$^+$ MZB cells originate from activated pre-GC cells, which in our analyses were shown to have upregulated Notch2 receptor expression and thus to possess the biggest pre-requisite for MZB cell differentiation; (2) CAR$^+$ MZB cells arise from a fraction of GC B cells, which may upregulate Notch2 receptor signaling and receive a new Notch signal early after GC initiation or later during positive selection in the LZ. The higher Notch signaling activity interferes with their persistence as GC B cells, leading to exit from the GC reaction. Upon arrival into the splenic MZ, these newly-formed MZB cells lose their CD38$^-$ CD95^{high} phenotype and fully adopt the mature resting MZB cell phenotype with temporal progression of the immune response.

Even though our findings do not clearly propose which pathway of antigen-induced MZB cell differentiation is preferred, the one from activated pre-GC cells or from already committed GC B cells, they imply that both pathways likely contribute together to the CAR$^+$ MZB compartment, and this process is clearly Notch2-signal-dependent. Thus, one has to consider that the CAR$^+$ MZB cells can harbor different antigen affinities and in this way can contribute to the heterogeneity of the total MZB cell compartment in mice. This means that the newly generated MZB cells may contain classical memory B cells with somatic hypermutation of the IgV genes and possibly even class-switched surface Igs, but also unmutated IgM$^+$ cells. To confirm the existence of such heterogeneity, it would be necessary to further examine the levels of somatic hypermutation in the BCR repertoire of the CAR$^+$ MZB cells produced after TD immunization at a single-cell level.

Closer examination of the kinetics of CAR$^+$ MZB cells revealed that these cells were mostly produced in the first 2 weeks of the immune response, whereas their numbers remained relatively stable at later time points. These findings may imply that there is no new MZB cell differentiation from reporter$^+$ B cells in the second 2 weeks post immunization, but rather a maintenance or persistence of the existing CAR$^+$ MZB cells as sessile residents of the spleen. Interestingly, we observed a slight drop in the CAR-expressing MZB cell population, starting to settle in somewhere between days 26 and 30 post immunization. We speculate that some CAR$^+$ MZB cells may differentiate into PCs upon antigen re-encounter in the spleen, which could explain their slight loss from the MZB compartment in this time frame. In support of our assumption are previous data which showed that ongoing *c-Myc* expression and mTOR/Notch2 signaling can be highly-activated in MZB cells and can thus induce rapid division-independent PC differentiation of MZB cells (Gaudette et al., 2021; Limon and Fruman, 2012). Considering that the total numbers of MZB cells remained relatively stable in the overall analyzed time frame, but the newly-generated CAR$^+$ MZB cells followed an increasing trend up until day 14 post TD immunization, we assume there may be a replacement of some pre-existing MZB cells by newly-produced antigen-experienced MZB cells in the early stages of the immune response. Thus, the possibility exists that the natural purpose of immunization-triggered de novo MZB cell production is to replenish the pool of already committed MZB cells in mice, after it has been partially deprived by antigen-induced early extra-follicular PC production in cases of an immune system breach.

To this end, our collective data hint towards a bigger resemblance between the human and murine MZB cell compartments than previously believed, despite the significantly different splenic architecture between the two species. In humans, most of the IgM$^+$ B cells in the MZ were shown to be IgV gene-mutated and have an enhanced immune response potential (Dunn-Walters et al., 1995; Garraud et al., 2012; Weller et al., 2005). They also expressed markers similar to a well-established IgM$^+$IgD$^+$CD27$^+$ memory B cell subset in the peripheral blood (Seifert and Küppers, 2016; Tangye et al., 1998). Therefore, many of these studies imply that the human MZ compartment is heterogeneous and its composition changes throughout life, mostly comprising IgM$^+$ memory cells in adults, which completed the GC reaction and entered the marginal zone as quiescent cells (Dunn-Walters et al., 1995). Interestingly, a specific smaller subset of MZB cells has been described in young children under the age of two years (Descatoire et al., 2014), whose MZ compartment predominantly consisted of non-clonal cells with low mutation frequencies. With increasing age, this cell subset was demonstrated to further develop into memory B cells (IgM$^+$CD27$^+$IgD$^+$) in the MZ, via a pathway that involved ligation of Notch2 by Dll1-ligand (Descatoire et al., 2014; Kibler et al., 2021). Additionally, in

older children and adults, the pool of MZB cells was hypermutated and displayed clonal relationships, hinting towards the idea that naïve MZB cells become gradually replaced by antigen-experienced cells during the lifespan of humans (Kibler et al., 2021). Considering our similar findings in young mice, which in terms of their lifespan resemble children at the age of two, we propose that the murine MZB cell compartment is comparable to that of young children. In a similar manner as in humans, the MZB cell pool in mice may also change with age and upon antigen challenge. In this regard, it is of great importance for the future to examine whether the clonal relationships and the numbers of hypermutated MZB cells change during progressive aging of mice. An intriguing outcome would be to see if the ratio of naïve to antigen-experienced MZB cells becomes shifted in favor of the antigen-experienced MZB cell pool through repeated rounds of TD-immunization.

List of references

Agenès, F., Freitas, A.A., 1999. Transfer of Small Resting B Cells into Immunodeficient Hosts Results in the Selection of a Self-renewing Activated B Cell Population. J. Exp. Med. 189, 319–330. https://doi.org/10.1084/jem.189.2.319

Alberi, L., Hoey, S.E., Brai, E., Scotti, A.L., Marathe, S., 2013. Notch signaling in the brain: in good and bad times. Ageing Res. Rev. 12, 801–814. https://doi.org/10.1016/j.arr.2013.03.004

Alinikula, J., Lassila, O., 2011. Gene Interaction Network Regulates Plasma Cell Differentiation. Scand. J. Immunol. 73, 512–519. https://doi.org/10.1111/j.1365-3083.2011.02556.x

Alinikula, J., Nera, K.-P., Junttila, S., Lassila, O., 2011. Alternate pathways for Bcl6-mediated regulation of B cell to plasma cell differentiation. Eur. J. Immunol. 41, 2404–2413. https://doi.org/10.1002/eji.201141553

Allman, D., Calamito, M., 2009. Instructing B Cell Fates on the Fringe. Immunity 30, 175–177. https://doi.org/10.1016/j.immuni.2009.01.003

Allman, D., Lindsley, R.C., DeMuth, W., Rudd, K., Shinton, S.A., Hardy, R.R., 2001. Resolution of Three Nonproliferative Immature Splenic B Cell Subsets Reveals Multiple Selection Points During Peripheral B Cell Maturation. J. Immunol. 167, 6834–6840. https://doi.org/10.4049/jimmunol.167.12.6834

Allman, D., Pillai, S., 2008. Peripheral B cell subsets. Curr. Opin. Immunol. 20, 149–157. https://doi.org/10.1016/j.coi.2008.03.014

Allman, D., Srivastava, B., Lindsley, R.C., 2004. Alternative routes to maturity: branch points and pathways for generating follicular and marginal zone B cells. Immunol. Rev. 197, 147–160. https://doi.org/10.1111/j.0105-2896.2004.0108.x

Alugupalli, K.R., Leong, J.M., Woodland, R.T., Muramatsu, M., Honjo, T., Gerstein, R.M., 2004. B1b lymphocytes confer T cell-independent long-lasting immunity. Immunity 21, 379–390. https://doi.org/10.1016/j.immuni.2004.06.019

Arámburo-Galvez, J., Sotelo-Cruz, N., Flores-Mendoza, L., Gracia-Valenzuela, M., Chiquete-Elizalde, F., Espinoza-Alderete, J., Trejo-Martínez, H., Canizalez-Román, V., Ontiveros, N., Cabrera-Chávez, F., 2018. Assessment of the Sensitizing Potential of Proteins in BALB/c Mice: Comparison of Three Protocols of Intraperitoneal Sensitization. Nutrients 10, 903. https://doi.org/10.3390/nu10070903

Arnon, T.I., Horton, R.M., Grigorova, I.L., Cyster, J.G., 2013. Visualization of splenic marginal zone B-cell shuttling and follicular B-cell egress. Nature 493, 684–688. https://doi.org/10.1038/nature11738

Babushku, T., Rane, S., Lechner, M., Zimber-Strobl, U., Strobl, L.J., 2022. Notch2 signaling guides B cells away from germinal centers towards marginal zone B cell and plasma cell differentiation. bioRxiv 2022.06.13.495961. https://doi.org/10.1101/2022.06.13.495961

Bajénoff, M., Glaichenhaus, N., Germain, R.N., 2008. Fibroblastic Reticular Cells Guide T Lymphocyte Entry into and Migration within the Splenic T Cell Zone. J. Immunol. 181, 3947. https://doi.org/10.4049/jimmunol.181.6.3947

Basso, K., Klein, U., Niu, H., Stolovitzky, G.A., Tu, Y., Califano, A., Cattoretti, G., Dalla-Favera, R., 2004. Tracking CD40 signaling during germinal center development. Blood 104, 4088–4096. https://doi.org/10.1182/blood-2003-12-4291

Batten, M., Groom, J., Cachero, T.G., Qian, F., Schneider, P., Tschopp, J., Browning, J.L., Mackay, F., 2000. Baff Mediates Survival of Peripheral Immature B Lymphocytes. J. Exp. Med. 192, 1453–1466. https://doi.org/10.1084/jem.192.10.1453

Baumgarth, N., 2017. A Hard(y) Look at B-1 Cell Development and Function. J. Immunol. 199, 3387–3394. https://doi.org/10.4049/jimmunol.1700943

Baumgarth, N., 2016. B-1 Cell Heterogeneity and the Regulation of Natural and Antigen-Induced IgM Production. Front. Immunol. 7. https://doi.org/10.3389/fimmu.2016.00324

Bekeredjian-Ding, I., Jego, G., 2009. Toll-like receptors--sentries in the B-cell response. Immunology 128, 311–323. https://doi.org/10.1111/j.1365-2567.2009.03173.x

Benedito, R., Roca, C., Sörensen, I., Adams, S., Gossler, A., Fruttiger, M., Adams, R.H., 2009. The notch ligands Dll4 and Jagged1 have opposing effects on angiogenesis. Cell 137, 1124–1135. https://doi.org/10.1016/j.cell.2009.03.025

Besseyrias, V., Fiorini, E., Strobl, L.J., Zimber-Strobl, U., Dumortier, A., Koch, U., Arcangeli, M.-L., Ezine, S., MacDonald, H.R., Radtke, F., 2007. Hierarchy of Notch–Delta interactions promoting T cell lineage commitment and maturation. J. Exp. Med. 204, 331–343. https://doi.org/10.1084/jem.20061442

Bhattacharya, M., 2019. Understanding B Lymphocyte Development: A Long Way to Go, in: Salih Istifli, E., Basri İla, H. (Eds.), Lymphocytes. IntechOpen. https://doi.org/10.5772/intechopen.79663

Blaumueller, C.M., Qi, H., Zagouras, P., Artavanis-Tsakonas, S., 1997. Intracellular cleavage of Notch leads to a heterodimeric receptor on the plasma membrane. Cell 90, 281–291. https://doi.org/10.1016/s0092-8674(00)80336-0

Boller, S., Grosschedl, R., 2014. The regulatory network of B-cell differentiation: a focused view of early B-cell factor 1 function. Immunol. Rev. 261, 102–115. https://doi.org/10.1111/imr.12206

Bonilla, F.A., Oettgen, H.C., 2010. Adaptive immunity. J. Allergy Clin. Immunol. 125, S33–S40. https://doi.org/10.1016/j.jaci.2009.09.017

Borggrefe, T., Oswald, F., 2009. The Notch signaling pathway: Transcriptional regulation at Notch target genes. Cell. Mol. Life Sci. 66, 1631–1646. https://doi.org/10.1007/s00018-009-8668-7

Bossy, D., Milili, M., Zucman, J., Thomas, G., Fougereau, M., Schiff, C., 1991. Organization and expression of the lambda-like genes that contribute to the mu-psi light chain complex in human pre-B cells. Int. Immunol. 3, 1081–1090. https://doi.org/10.1093/intimm/3.11.1081

Bray, S.J., 2006. Notch signalling: a simple pathway becomes complex. Nat. Rev. Mol. Cell Biol. 7, 678–689. https://doi.org/10.1038/nrm2009

Brou, C., 2009. Intracellular trafficking of Notch receptors and ligands. Exp. Cell Res. 315, 1549–1555. https://doi.org/10.1016/j.yexcr.2008.09.010

Busslinger, M., 2004. Transcriptional Control of Early B Cell Development. Annu. Rev. Immunol. 22, 55–79. https://doi.org/10.1146/annurev.immunol.22.012703.104807

Calabro, S., Liu, D., Gallman, A., Nascimento, M.S.L., Yu, Z., Zhang, T.-T., Chen, P., Zhang, B., Xu, L., Gowthaman, U., Krishnaswamy, J.K., Haberman, A.M., Williams, A., Eisenbarth, S.C., 2016. Differential Intrasplenic Migration of Dendritic Cell Subsets Tailors Adaptive Immunity. Cell Rep. 16, 2472–2485. https://doi.org/10.1016/j.celrep.2016.07.076

Calado, D.P., Sasaki, Y., Godinho, S.A., Pellerin, A., Köchert, K., Sleckman, B.P., de Alborán, I.M., Janz, M., Rodig, S., Rajewsky, K., 2012. The cell-cycle regulator c-Myc is essential for the formation and maintenance of germinal centers. Nat. Immunol. 13, 1092–1100. https://doi.org/10.1038/ni.2418

Cancro, M.P., 2009. Signalling crosstalk in B cells: managing worth and need. Nat. Rev. Immunol. 9, 657–661. https://doi.org/10.1038/nri2621

Cariappa, A., Boboila, C., Moran, S.T., Liu, H., Shi, H.N., Pillai, S., 2007. The Recirculating B Cell Pool Contains Two Functionally Distinct, Long-Lived, Posttransitional, Follicular B Cell Populations. J. Immunol. 179, 2270–2281. https://doi.org/10.4049/jimmunol.179.4.2270

Cariappa, A., Liou, H.C., Horwitz, B.H., Pillai, S., 2000. Nuclear factor kappa B is required for the development of marginal zone B lymphocytes. J. Exp. Med. 192, 1175–1182. https://doi.org/10.1084/jem.192.8.1175

Cariappa, A., Tang, M., Parng, C., Nebelitskiy, E., Carroll, M., Georgopoulos, K., Pillai, S., 2001. The follicular versus marginal zone B lymphocyte cell fate decision is regulated by Aiolos, Btk, and CD21. Immunity 14, 603–615. https://doi.org/10.1016/s1074-7613(01)00135-2

Carrasco, Y.R., Batista, F.D., 2007. B cells acquire particulate antigen in a macrophage-rich area at the boundary between the follicle and the subcapsular sinus of the lymph node. Immunity 27, 160–171. https://doi.org/10.1016/j.immuni.2007.06.007

Casola, S., Cattoretti, G., Uyttersprot, N., Koralov, S.B., Seagal, J., Hao, Z., Waisman, A., Egert, A., Ghitza, D., Rajewsky, K., 2006. Tracking germinal center B cells expressing germ-line immunoglobulin gamma1 transcripts by conditional gene targeting. Proc. Natl. Acad. Sci. U. S. A. 103, 7396–7401. https://doi.org/10.1073/pnas.0602353103

Cerutti, A., Cols, M., Puga, I., 2013. Marginal zone B cells: virtues of innate-like antibody-producing lymphocytes. Nat. Rev. Immunol. 13, 118–132. https://doi.org/10.1038/nri3383

Chastagner, P., Israël, A., Brou, C., 2008. AIP4/Itch regulates Notch receptor degradation in the absence of ligand. PloS One 3, e2735. https://doi.org/10.1371/journal.pone.0002735

Chen, J., Moloney, D.J., Stanley, P., 2001. Fringe modulation of Jagged1-induced Notch signaling requires the action of beta 4galactosyltransferase-1. Proc. Natl. Acad. Sci. U. S. A. 98, 13716–13721. https://doi.org/10.1073/pnas.241398098

Chillakuri, C.R., Sheppard, D., Lea, S.M., Handford, P.A., 2012. Notch receptor–ligand binding and activation: Insights from molecular studies. Semin. Cell Dev. Biol. 23, 421–428. https://doi.org/10.1016/j.semcdb.2012.01.009

Chung, J.B., Sater, R.A., Fields, M.L., Erikson, J., Monroe, J.G., 2002. CD23 defines two distinct subsets of immature B cells which differ in their responses to T cell help signals. Int. Immunol. 14, 157–166. https://doi.org/10.1093/intimm/14.2.157

Chung, J.B., Silverman, M., Monroe, J.G., 2003. Transitional B cells: step by step towards immune competence. Trends Immunol. 24, 343–349. https://doi.org/10.1016/s1471-4906(03)00119-4

Ci, W., Polo, J.M., Cerchietti, L., Shaknovich, R., Wang, L., Yang, S.N., Ye, K., Farinha, P., Horsman, D.E., Gascoyne, R.D., Elemento, O., Melnick, A., 2009. The BCL6 transcriptional program features repression of multiple oncogenes in primary B cells and is deregulated in DLBCL. Blood 113, 5536–5548. https://doi.org/10.1182/blood-2008-12-193037

Cinamon, G., Matloubian, M., Lesneski, M.J., Xu, Y., Low, C., Lu, T., Proia, R.L., Cyster, J.G., 2004. Sphingosine 1-phosphate receptor 1 promotes B cell localization in the splenic marginal zone. Nat. Immunol. 5, 713–720. https://doi.org/10.1038/ni1083

Cinamon, G., Zachariah, M.A., Lam, O.M., Foss, F.W., Cyster, J.G., 2008. Follicular shuttling of marginal zone B cells facilitates antigen transport. Nat. Immunol. 9, 54–62. https://doi.org/10.1038/ni1542

Clark, M.R., Mandal, M., Ochiai, K., Singh, H., 2014. Orchestrating B cell lymphopoiesis through interplay of IL-7 receptor and pre-B cell receptor signalling. Nat. Rev. Immunol. 14, 69–80. https://doi.org/10.1038/nri3570

Cooper, M.D., Alder, M.N., 2006. The Evolution of Adaptive Immune Systems. Cell 124, 815–822. https://doi.org/10.1016/j.cell.2006.02.001

Cyster, J.G., 2010. B cell follicles and antigen encounters of the third kind. Nat. Immunol. 11, 989–996. https://doi.org/10.1038/ni.1946

Cyster, J.G., 2005. Chemokines, sphingosine-1-phosphate, and cell migration in secondary lymphoid organs. Annu. Rev. Immunol. 23, 127–159. https://doi.org/10.1146/annurev.immunol.23.021704.115628

Cyster, J.G., 2000. B cells on the front line. Nat. Immunol. 1, 9–10. https://doi.org/10.1038/76859

Cyster, J.G., Schwab, S.R., 2012. Sphingosine-1-phosphate and lymphocyte egress from lymphoid organs. Annu. Rev. Immunol. 30, 69–94. https://doi.org/10.1146/annurev-immunol-020711-075011

Dammers, P.M., de Boer, N.K., Deenen, G.J., Nieuwenhuis, P., Kroese, F.G., 1999. The origin of marginal zone B cells in the rat. Eur. J. Immunol. 29, 1522–1531. https://doi.org/10.1002/(SICI)1521-4141(199905)29:05<1522::AID-IMMU1522>3.0.CO;2-0

Davies, L.C., Jenkins, S.J., Allen, J.E., Taylor, P.R., 2013. Tissue-resident macrophages. Nat. Immunol. 14, 986–995. https://doi.org/10.1038/ni.2705

Deimling, J., Thompson, K., Tseu, I., Wang, J., Keijzer, R., Tanswell, A.K., Post, M., 2007. Mesenchymal maintenance of distal epithelial cell phenotype during late fetal lung development. Am. J. Physiol. Lung Cell. Mol. Physiol. 292, L725-741. https://doi.org/10.1152/ajplung.00221.2006

Delogu, A., Schebesta, A., Sun, Q., Aschenbrenner, K., Perlot, T., Busslinger, M., 2006. Gene repression by Pax5 in B cells is essential for blood cell homeostasis and is reversed in plasma cells. Immunity 24, 269–281. https://doi.org/10.1016/j.immuni.2006.01.012

Demitrack, E.S., Gifford, G.B., Keeley, T.M., Horita, N., Todisco, A., Turgeon, D.K., Siebel, C.W., Samuelson, L.C., 2017. NOTCH1 and NOTCH2 regulate epithelial cell proliferation in mouse and human gastric corpus. Am. J. Physiol.-Gastrointest. Liver Physiol. 312, G133–G144. https://doi.org/10.1152/ajpgi.00325.2016

Dent, A.L., Shaffer, A.L., Yu, X., Allman, D., Staudt, L.M., 1997. Control of Inflammation, Cytokine Expression, and Germinal Center Formation by BCL-6. Science 276, 589–592. https://doi.org/10.1126/science.276.5312.589

Descatoire, M., Weller, S., Irtan, S., Sarnacki, S., Feuillard, J., Storck, S., Guiochon-Mantel, A., Bouligand, J., Morali, A., Cohen, J., Jacquemin, E., Iascone, M., Bole-Feysot, C., Cagnard, N., Weill, J.-C., Reynaud, C.-A., 2014. Identification of a human splenic marginal zone B cell precursor with NOTCH2-dependent differentiation properties. J. Exp. Med. 211, 987–1000. https://doi.org/10.1084/jem.20132203

Doherty, D.G., Melo, A.M., Moreno-Olivera, A., Solomos, A.C., 2018. Activation and Regulation of B Cell Responses by Invariant Natural Killer T Cells. Front. Immunol. 9. https://doi.org/10.3389/fimmu.2018.01360

Dominguez-Sola, D., Victora, G.D., Ying, C.Y., Phan, R.T., Saito, M., Nussenzweig, M.C., Dalla-Favera, R., 2012. The proto-oncogene MYC is required for selection in the germinal center and cyclic reentry. Nat. Immunol. 13, 1083–1091. https://doi.org/10.1038/ni.2428

Duchez, S., Rodrigues, M., Bertrand, F., Valitutti, S., 2011. Reciprocal Polarization of T and B Cells at the Immunological Synapse. J. Immunol. 187, 4571–4580. https://doi.org/10.4049/jimmunol.1100600

Dunn-Walters, D.K., Isaacson, P.G., Spencer, J., 1995. Analysis of mutations in immunoglobulin heavy chain variable region genes of microdissected marginal zone (MGZ) B cells suggests that the MGZ of human spleen is a reservoir of memory B cells. J. Exp. Med. 182, 559–566. https://doi.org/10.1084/jem.182.2.559

Dustin, M.L., 2014. The immunological synapse. Cancer Immunol. Res. 2, 1023–1033. https://doi.org/10.1158/2326-6066.CIR-14-0161

Dutta, D., Sharma, V., Mutsuddi, M., Mukherjee, A., 2022. Regulation of Notch signaling by E3 ubiquitin ligases. FEBS J. 289, 937–954. https://doi.org/10.1111/febs.15792

Edry, E., Melamed, D., 2004. Receptor Editing in Positive and Negative Selection of B Lymphopoiesis. J. Immunol. 173, 4265–4271. https://doi.org/10.4049/jimmunol.173.7.4265

Ellisen, L.W., Bird, J., West, D.C., Soreng, A.L., Reynolds, T.C., Smith, S.D., Sklar, J., 1991. TAN-1, the human homolog of the Drosophila notch gene, is broken by chromosomal translocations in T lymphoblastic neoplasms. Cell 66, 649–661. https://doi.org/10.1016/0092-8674(91)90111-b

Fairfax, K.A., Corcoran, L.M., Pridans, C., Huntington, N.D., Kallies, A., Nutt, S.L., Tarlinton, D.M., 2007. Different Kinetics of Blimp-1 Induction in B Cell Subsets Revealed by Reporter Gene. J. Immunol. 178, 4104. https://doi.org/10.4049/jimmunol.178.7.4104

Fairfax, K.A., Kallies, A., Nutt, S.L., Tarlinton, D.M., 2008. Plasma cell development: from B-cell subsets to long-term survival niches. Semin. Immunol. 20, 49–58. https://doi.org/10.1016/j.smim.2007.12.002

Fasnacht, N., Huang, H.-Y., Koch, U., Favre, S., Auderset, F., Chai, Q., Onder, L., Kallert, S., Pinschewer, D.D., MacDonald, H.R., Tacchini-Cottier, F., Ludewig, B., Luther, S.A., Radtke, F., 2014. Specific fibroblastic niches in secondary lymphoid organs orchestrate distinct Notch-regulated immune responses. J. Exp. Med. 211, 2265–2279. https://doi.org/10.1084/jem.20132528

Ferguson, A.R., Corley, R.B., 2005. Accumulation of marginal zone B cells and accelerated loss of follicular dendritic cells in NF-κB p50-deficient mice. BMC Immunol. 6, 8. https://doi.org/10.1186/1471-2172-6-8

Finn, J., Sottoriva, K., Pajcini, K.V., Kitajewski, J.K., Chen, C., Zhang, W., Malik, A.B., Liu, Y., 2019. Dlk1-Mediated Temporal Regulation of Notch Signaling Is Required for Differentiation of Alveolar Type II to Type I Cells during Repair. Cell Rep. 26, 2942-2954.e5. https://doi.org/10.1016/j.celrep.2019.02.046

Förster, R., Davalos-Misslitz, A.C., Rot, A., 2008. CCR7 and its ligands: balancing immunity and tolerance. Nat. Rev. Immunol. 8, 362–371. https://doi.org/10.1038/nri2297

Förster, R., Schubel, A., Breitfeld, D., Kremmer, E., Renner-Müller, I., Wolf, E., Lipp, M., 1999. CCR7 coordinates the primary immune response by establishing functional microenvironments in secondary lymphoid organs. Cell 99, 23–33. https://doi.org/10.1016/s0092-8674(00)80059-8

Fortini, C., Cesselli, D., Beltrami, A.P., Bergamin, N., Caragnano, A., Moretti, L., Cecaro, F., Aquila, G., Rizzo, P., Riberti, C., Tavazzi, L., Fucili, A., Beltrami, C.A., Ferrari, R., 2014. Alteration of Notch signaling and functionality of adipose tissue derived mesenchymal stem cells in heart failure. Int. J. Cardiol. 174, 119–126. https://doi.org/10.1016/j.ijcard.2014.03.173

Fouillade, C., Monet-Leprêtre, M., Baron-Menguy, C., Joutel, A., 2012. Notch signalling in smooth muscle cells during development and disease. Cardiovasc. Res. 95 2, 138–46.

Garg, V., Muth, A.N., Ransom, J.F., Schluterman, M.K., Barnes, R., King, I.N., Grossfeld, P.D., Srivastava, D., 2005. Mutations in NOTCH1 cause aortic valve disease. Nature 437, 270–274. https://doi.org/10.1038/nature03940

Garis, M., Garrett-Sinha, L.A., 2021. Notch Signaling in B Cell Immune Responses. Front. Immunol. 11, 609324. https://doi.org/10.3389/fimmu.2020.609324

Garraud, O., Borhis, G., Badr, G., Degrelle, S., Pozzetto, B., Cognasse, F., Richard, Y., 2012. Revisiting the B-cell compartment in mouse and humans: more than one B-cell subset exists in the marginal zone and beyond. BMC Immunol. 13, 63. https://doi.org/10.1186/1471-2172-13-63

Gaudette, B.T., Roman, C.J., Ochoa, T.A., Gómez Atria, D., Jones, D.D., Siebel, C.W., Maillard, I., Allman, D., 2021. Resting innate-like B cells leverage sustained Notch2/mTORC1 signaling to achieve rapid and mitosis-independent plasma cell differentiation. J. Clin. Invest. 131, e151975. https://doi.org/10.1172/JCI151975

Gibb, D.R., El Shikh, M., Kang, D.-J., Rowe, W.J., El Sayed, R., Cichy, J., Yagita, H., Tew, J.G., Dempsey, P.J., Crawford, H.C., Conrad, D.H., 2010. ADAM10 is essential for Notch2-dependent marginal zone B cell development and CD23 cleavage in vivo. J. Exp. Med. 207, 623–635. https://doi.org/10.1084/jem.20091990

Gómez Atria, D., Gaudette, B.T., Londregan, J., Kelly, S., Perkey, E., Allman, A., Srivastava, B., Koch, U., Radtke, F., Ludewig, B., Siebel, C.W., Ryan, R.J., Robertson, T.F., Burkhardt, J.K., Pear, W.S., Allman, D., Maillard, I., 2022. Stromal Notch ligands foster lymphopenia-driven functional plasticity and homeostatic proliferation of naïve B cells. J. Clin. Invest. e158885. https://doi.org/10.1172/JCI158885

Gonda, H., Sugai, M., Nambu, Y., Katakai, T., Agata, Y., Mori, K.J., Yokota, Y., Shimizu, A., 2003. The Balance Between Pax5 and Id2 Activities Is the Key to AID Gene Expression. J. Exp. Med. 198, 1427–1437. https://doi.org/10.1084/jem.20030802

Gordon, W.R., Arnett, K.L., Blacklow, S.C., 2008. The molecular logic of Notch signaling--a structural and biochemical perspective. J. Cell Sci. 121, 3109–3119. https://doi.org/10.1242/jcs.035683

Gray, D., Siepmann, K., van Essen, D., Poudrier, J., Wykes, M., Jainandunsing, S., Bergthorsdottir, S., Dullforce, P., 1996. B-T lymphocyte interactions in the generation and survival of memory cells. Immunol. Rev. 150, 45–61. https://doi.org/10.1111/j.1600-065x.1996.tb00695.x

Gross, J.A., Dillon, S.R., Mudri, S., Johnston, J., Littau, A., Roque, R., Rixon, M., Schou, O., Foley, K.P., Haugen, H., McMillen, S., Waggie, K., Schreckhise, R.W., Shoemaker, K., Vu, T., Moore, M., Grossman, A., Clegg, C.H., 2001. TACI-Ig neutralizes molecules critical for B cell development and autoimmune disease. impaired B cell maturation in mice lacking BLyS. Immunity 15, 289–302. https://doi.org/10.1016/s1074-7613(01)00183-2

Haas, K.M., Poe, J.C., Steeber, D.A., Tedder, T.F., 2005. B-1a and B-1b cells exhibit distinct developmental requirements and have unique functional roles in innate and adaptive immunity to S. pneumoniae. Immunity 23, 7–18. https://doi.org/10.1016/j.immuni.2005.04.011

Haines, N., Irvine, K.D., 2003. Glycosylation regulates Notch signalling. Nat. Rev. Mol. Cell Biol. 4, 786–797. https://doi.org/10.1038/nrm1228

Hammad, H., Vanderkerken, M., Pouliot, P., Deswarte, K., Toussaint, W., Vergote, K., Vandersarren, L., Janssens, S., Ramou, I., Savvides, S.N., Haigh, J.J., Hendriks, R., Kopf, M., Craessaerts, K., de Strooper, B., Kearney, J.F., Conrad, D.H., Lambrecht, B.N., 2017. Transitional B cells commit to marginal zone B cell fate by Taok3-mediated surface expression of ADAM10. Nat. Immunol. 18, 313–320. https://doi.org/10.1038/ni.3657

Hampel, F., Ehrenberg, S., Hojer, C., Draeseke, A., Marschall-Schröter, G., Kühn, R., Mack, B., Gires, O., Vahl, C.J., Schmidt-Supprian, M., Strobl, L.J., Zimber-Strobl, U., 2011. CD19-independent instruction of murine marginal zone B-cell development by constitutive Notch2 signaling. Blood 118, 6321–6331. https://doi.org/10.1182/blood-2010-12-325944

Hardy, R.R., Hayakawa, K., 2001. B Cell Development Pathways. Annu. Rev. Immunol. 19, 595–621. https://doi.org/10.1146/annurev.immunol.19.1.595

Hardy, R.R., Hayakawa, K., Parks, D.R., Herzenberg, L.A., 1983. Demonstration of B-cell maturation in X-linked immunodeficient mice by simultaneous three-colour immunofluorescence. Nature 306, 270–272. https://doi.org/10.1038/306270a0

Hargreaves, D.C., Hyman, P.L., Lu, T.T., Ngo, V.N., Bidgol, A., Suzuki, G., Zou, Y.R., Littman, D.R., Cyster, J.G., 2001. A coordinated change in chemokine responsiveness guides plasma cell movements. J. Exp. Med. 194, 45–56. https://doi.org/10.1084/jem.194.1.45

Hayakawa, K., Hardy, R.R., Herzenberg, L.A., 1986. Peritoneal Ly-1 B cells: Genetic control, autoantibody production, increased lambda light chain expression. Eur. J. Immunol. 16, 450–456. https://doi.org/10.1002/eji.1830160423

Haynes, N.M., Allen, C.D.C., Lesley, R., Ansel, K.M., Killeen, N., Cyster, J.G., 2007. Role of CXCR5 and CCR7 in follicular Th cell positioning and appearance of a programmed cell death gene-1high germinal center-associated subpopulation. J. Immunol. Baltim. Md 1950 179, 5099–5108. https://doi.org/10.4049/jimmunol.179.8.5099

Heesters, B.A., Myers, R.C., Carroll, M.C., 2014. Follicular dendritic cells: dynamic antigen libraries. Nat. Rev. Immunol. 14, 495–504. https://doi.org/10.1038/nri3689

Heger, K., Kober, M., Rieß, D., Drees, C., de Vries, I., Bertossi, A., Roers, A., Sixt, M., Schmidt-Supprian, M., 2015. A novel Cre recombinase reporter mouse strain facilitates selective and efficient infection of primary immune cells with adenoviral vectors. Eur. J. Immunol. 45, 1614–1620. https://doi.org/10.1002/eji.201545457

Hendricks, J., Visser, A., Dammers, P.M., Burgerhof, J.G.M., Bos, N.A., Kroese, F.G.M., 2019. The formation of mutated IgM memory B cells in rat splenic marginal zones is an antigen dependent process. PLOS ONE 14, 1–23. https://doi.org/10.1371/journal.pone.0220933

Heng, T.S.P., Painter, M.W., 2008. The Immunological Genome Project: networks of gene expression in immune cells. Nat. Immunol. 9, 1091–1094. https://doi.org/10.1038/ni1008-1091

Herzog, S., Reth, M., Jumaa, H., 2009. Regulation of B-cell proliferation and differentiation by pre-B-cell receptor signalling. Nat. Rev. Immunol. 9, 195–205. https://doi.org/10.1038/nri2491

Hicks, C., Johnston, S.H., diSibio, G., Collazo, A., Vogt, T.F., Weinmaster, G., 2000. Fringe differentially modulates Jagged1 and Delta1 signalling through Notch1 and Notch2. Nat. Cell Biol. 2, 515–520. https://doi.org/10.1038/35019553

Hikida, M., Johmura, S., Hashimoto, A., Takezaki, M., Kurosaki, T., 2003. Coupling between B cell receptor and phospholipase C-gamma2 is essential for mature B cell development. J. Exp. Med. 198, 581–589. https://doi.org/10.1084/jem.20030280

Hoffman, W., Lakkis, F.G., Chalasani, G., 2016. B Cells, Antibodies, and More. Clin. J. Am. Soc. Nephrol. 11, 137–154. https://doi.org/10.2215/CJN.09430915

Hömig-Hölzel, C., Hojer, C., Rastelli, J., Casola, S., Strobl, L.J., Müller, W., Quintanilla-Martinez, L., Gewies, A., Ruland, J., Rajewsky, K., Zimber-Strobl, U., 2008. Constitutive CD40 signaling in B cells selectively activates the noncanonical NF-κB pathway and promotes lymphomagenesis. J. Exp. Med. 205, 1317–1329. https://doi.org/10.1084/jem.20080238

Honjo, T., Kinoshita, K., Muramatsu, M., 2002. Molecular mechanism of class switch recombination: linkage with somatic hypermutation. Annu. Rev. Immunol. 20, 165–196. https://doi.org/10.1146/annurev.immunol.20.090501.112049

Horcher, M., Souabni, A., Busslinger, M., 2001. Pax5/BSAP Maintains the Identity of B Cells in Late B Lymphopoiesis. Immunity 14, 779–790. https://doi.org/10.1016/S1074-7613(01)00153-4

Hozumi, K., Negishi, N., Suzuki, D., Abe, N., Sotomaru, Y., Tamaoki, N., Mailhos, C., Ish-Horowicz, D., Habu, S., Owen, M.J., 2004. Delta-like 1 is necessary for the generation of marginal zone B cells but not T cells in vivo. Nat. Immunol. 5, 638–644. https://doi.org/10.1038/ni1075

Hsu, M.-C., Toellner, K.-M., Vinuesa, C.G., MacLennan, I.C.M., 2006. B cell clones that sustain long-term plasmablast growth in T-independent extrafollicular antibody responses. Proc. Natl. Acad. Sci. 103, 5905–5910. https://doi.org/10.1073/pnas.0601502103

Jehn, B.M., Dittert, I., Beyer, S., von der Mark, K., Bielke, W., 2002. c-Cbl Binding and Ubiquitin-dependent Lysosomal Degradation of Membrane-associated Notch1. J. Biol. Chem. 277, 8033–8040. https://doi.org/10.1074/jbc.M108552200

Jones, K., Savulescu, A.F., Brombacher, F., Hadebe, S., 2020. Immunoglobulin M in Health and Diseases: How Far Have We Come and What Next? Front. Immunol. 11, 595535. https://doi.org/10.3389/fimmu.2020.595535

Jundt, F., Anagnostopoulos, I., Förster, R., Mathas, S., Stein, H., Dörken, B., 2002. Activated Notch1 signaling promotes tumor cell proliferation and survival in Hodgkin and anaplastic large cell lymphoma. Blood 99, 3398–3403. https://doi.org/10.1182/blood.v99.9.3398

Kallies, A., Hasbold, J., Fairfax, K., Pridans, C., Emslie, D., McKenzie, B.S., Lew, A.M., Corcoran, L.M., Hodgkin, P.D., Tarlinton, D.M., Nutt, S.L., 2007. Initiation of plasma-cell differentiation is independent of the transcription factor Blimp-1. Immunity 26, 555–566. https://doi.org/10.1016/j.immuni.2007.04.007

Kanayama, N., Cascalho, M., Ohmori, H., 2005. Analysis of Marginal Zone B Cell Development in the Mouse with Limited B Cell Diversity: Role of the Antigen Receptor Signals in the Recruitment of B Cells to the Marginal Zone. J. Immunol. 174, 1438–1445. https://doi.org/10.4049/jimmunol.174.3.1438

Kang, J.-A., Kim, W.-S., Park, S.-G., 2014. Notch1 is an important mediator for enhancing of B-cell activation and antibody secretion by Notch ligand. Immunology 143, 550–559. https://doi.org/10.1111/imm.12333

Kearney, J.F., Won, W.-J., Benedict, C., Moratz, C., Zimmer, P., Oliver, A., Martin, F., Shu, F., 1997. B Cell Development in Mice. Int. Rev. Immunol. 15, 207–241. https://doi.org/10.3109/08830189709068177

Kenneth M. Murphy, C.W., 2016. Janeway's Immunobiology, 9th, illustrated ed. Garland Science, Taylor & Francis Group, LLC, 2016.

Kibler, A., Budeus, B., Homp, E., Bronischewski, K., Berg, V., Sellmann, L., Murke, F., Heinold, A., Heinemann, F.M., Lindemann, M., Bekeredjian-Ding, I., Horn, P.A., Kirschning, C.J., Küppers, R., Seifert, M., 2021. Systematic memory B cell archiving and random display shape the human splenic marginal zone throughout life. J. Exp. Med. 218, e20201952. https://doi.org/10.1084/jem.20201952

Kidd, S., Kelley, M.R., Young, M.W., 1986. Sequence of the notch locus of Drosophila melanogaster: relationship of the encoded protein to mammalian clotting and growth factors. Mol. Cell. Biol. 6, 3094–3108. https://doi.org/10.1128/mcb.6.9.3094-3108.1986

Kiel, M.J., Velusamy, T., Betz, B.L., Zhao, L., Weigelin, H.G., Chiang, M.Y., Huebner-Chan, D.R., Bailey, N.G., Yang, D.T., Bhagat, G., Miranda, R.N., Bahler, D.W., Medeiros, L.J., Lim, M.S., Elenitoba-Johnson, K.S.J., 2012. Whole-genome sequencing identifies recurrent somatic NOTCH2 mutations in splenic marginal zone lymphoma. J. Exp. Med. 209, 1553—1565. https://doi.org/10.1084/jem.20120910

Klein, U., Casola, S., Cattoretti, G., Shen, Q., Lia, M., Mo, T., Ludwig, T., Rajewsky, K., Dalla-Favera, R., 2006. Transcription factor IRF4 controls plasma cell differentiation and class-switch recombination. Nat. Immunol. 7, 773–782. https://doi.org/10.1038/ni1357

Klein, U., Dalla-Favera, R., 2008. Germinal centres: role in B-cell physiology and malignancy. Nat. Rev. Immunol. 8, 22–33. https://doi.org/10.1038/nri2217

Koch, U., Lehal, R., Radtke, F., 2013. Stem cells living with a Notch. Dev. Camb. Engl. 140, 689–704. https://doi.org/10.1242/dev.080614

Koch, U., Radtke, F., 2007. Notch and cancer: a double-edged sword. Cell. Mol. Life Sci. CMLS 64, 2746–2762. https://doi.org/10.1007/s00018-007-7164-1

Kopan, R., Ilagan, M.X.G., 2009. The canonical Notch signaling pathway: unfolding the activation mechanism. Cell 137, 216–233. https://doi.org/10.1016/j.cell.2009.03.045

Kovall, R.A., Gebelein, B., Sprinzak, D., Kopan, R., 2017. The Canonical Notch Signaling Pathway: Structural and Biochemical Insights into Shape, Sugar, and Force. Dev. Cell 41, 228–241. https://doi.org/10.1016/j.devcel.2017.04.001

Kraus, M., Alimzhanov, M.B., Rajewsky, N., Rajewsky, K., 2004. Survival of resting mature B lymphocytes depends on BCR signaling via the Igalpha/beta heterodimer. Cell 117, 787–800. https://doi.org/10.1016/j.cell.2004.05.014

Kreslavsky, T., Wong, J.B., Fischer, M., Skok, J.A., Busslinger, M., 2018. Control of B-1a cell development by instructive BCR signaling. Curr. Opin. Immunol. 51, 24–31. https://doi.org/10.1016/j.coi.2018.01.001

Kuroda, K., Han, H., Tani, S., Tanigaki, K., Tun, T., Furukawa, T., Taniguchi, Y., Kurooka, H., Hamada, Y., Toyokuni, S., Honjo, T., 2003. Regulation of marginal zone B cell development by MINT, a suppressor of Notch/RBP-J signaling pathway. Immunity 18, 301–312. https://doi.org/10.1016/s1074-7613(03)00029-3

Lake, R.J., Grimm, L.M., Veraksa, A., Banos, A., Artavanis-Tsakonas, S., 2009. In vivo analysis of the Notch receptor S1 cleavage. PloS One 4, e6728. https://doi.org/10.1371/journal.pone.0006728

Lalor, P.A., Nossal, G.J.V., Sanderson, R.D., McHeyzer-Williams, M.G., 1992. Functional and molecular characterization of single, (4-hydroxy-3-nitrophenyl)acetyl (NP)-specific, IgG1+ B cells from antibody-secreting and memory B cell pathways in the C57BL/6 immune response to NP. Eur. J. Immunol. 22, 3001–3011. https://doi.org/10.1002/eji.1830221136

Lam, K.-P., Kühn, R., Rajewsky, K., 1997. In Vivo Ablation of Surface Immunoglobulin on Mature B Cells by Inducible Gene Targeting Results in Rapid Cell Death. Cell 90, 1073–1083. https://doi.org/10.1016/S0092-8674(00)80373-6

Lanzavecchia, A., 1990. Receptor-mediated antigen uptake and its effect on antigen presentation to class II-restricted T lymphocytes. Annu. Rev. Immunol. 8, 773–793. https://doi.org/10.1146/annurev.iy.08.040190.004013

Larson, E.D., Maizels, N., 2004. Transcription-coupled mutagenesis by the DNA deaminase AID. Genome Biol. 5, 211. https://doi.org/10.1186/gb-2004-5-3-211

LeBien, T.W., Tedder, T.F., 2008. B lymphocytes: how they develop and function. Blood 112, 1570–1580. https://doi.org/10.1182/blood-2008-02-078071

Lechner, M., Engleitner, T., Babushku, T., Schmidt-Supprian, M., Rad, R., Strobl, L.J., Zimber-Strobl, U., 2021. Notch2-mediated plasticity between marginal zone and follicular B cells. Nat. Commun. 12, 1111. https://doi.org/10.1038/s41467-021-21359-1

Lee, S., Kumano, K., Nakazaki, K., Sanada, M., Matsumoto, A., Yamamoto, G., Nannya, Y., Suzuki, R., Ota, S., Ota, Y., Izutsu, K., Sakata-Yanagimoto, M., Hangaishi, A., Yagita, H., Fukayama, M., Seto, M., Kurokawa, M., Ogawa, S., Chiba, S., 2009. Gain-of-function mutations and copy number increases of Notch2 in diffuse large B-cell lymphoma. Cancer Sci. 100, 920–926. https://doi.org/10.1111/j.1349-7006.2009.01130.x

Lewis, S.M., Williams, A., Eisenbarth, S.C., 2019. Structure and function of the immune system in the spleen. Sci. Immunol. 4, eaau6085. https://doi.org/10.1126/sciimmunol.aau6085

Li, J., Gordon, J., Chen, E.L.Y., Xiao, S., Wu, L., Zúñiga-Pflücker, J.C., Manley, N.R., 2020. NOTCH1 signaling establishes the medullary thymic epithelial cell progenitor pool during mouse fetal development. Development 147, dev178988. https://doi.org/10.1242/dev.178988

Li, X., Gadzinsky, A., Gong, L., Tong, H., Calderon, V., Li, Y., Kitamura, D., Klein, U., Langdon, W.Y., Hou, F., Zou, Y.-R., Gu, H., 2018. Cbl Ubiquitin Ligases Control B Cell Exit from the Germinal-Center Reaction. Immunity 48, 530-541.e6. https://doi.org/10.1016/j.immuni.2018.03.006

Liao, W., Hua, Z., Liu, C., Lin, L., Chen, R., Hou, B., 2017. Characterization of T-Dependent and T-Independent B Cell Responses to a Virus-like Particle. J. Immunol. Baltim. Md 1950 198, 3846–3856. https://doi.org/10.4049/jimmunol.1601852

Limon, J.J., Fruman, D.A., 2012. Akt and mTOR in B Cell Activation and Differentiation. Front. Immunol. 3. https://doi.org/10.3389/fimmu.2012.00228

Lin, K.-I., Angelin-Duclos, C., Kuo, T.C., Calame, K., 2002. Blimp-1-dependent repression of Pax-5 is required for differentiation of B cells to immunoglobulin M-secreting plasma cells. Mol. Cell. Biol. 22, 4771–4780. https://doi.org/10.1128/MCB.22.13.4771-4780.2002

Lin, Y., Wong, K., Calame, K., 1997. Repression of c-myc transcription by Blimp-1, an inducer of terminal B cell differentiation. Science 276, 596–599. https://doi.org/10.1126/science.276.5312.596

Linderson, Y., Eberhard, D., Malin, S., Johansson, A., Busslinger, M., Pettersson, S., 2004. Corecruitment of the Grg4 repressor by PU.1 is critical for Pax5-mediated repression of B-cell-specific genes. EMBO Rep. 5, 291–296. https://doi.org/10.1038/sj.embor.7400089

Liu, Y.J., de Bouteiller, O., Fugier-Vivier, I., 1997. Mechanisms of selection and differentiation in germinal centers. Curr. Opin. Immunol. 9, 256–262. https://doi.org/10.1016/s0952-7915(97)80145-8

Liu, Y.-J., Oldfield, S., Maclennan, I.C.M., 1988. Memory B cells in T cell-dependent antibody responses colonize the splenic marginal zones. Eur. J. Immunol. 18, 355–362. https://doi.org/10.1002/eji.1830180306

Liu, Z., Brunskill, E., Varnum-Finney, B., Zhang, C., Zhang, A., Jay, P.Y., Bernstein, I., Morimoto, M., Kopan, R., 2015. The intracellular domains of Notch1 and Notch2 are functionally equivalent during development and carcinogenesis. Dev. Camb. Engl. 142, 2452–2463. https://doi.org/10.1242/dev.125492

Lo, C.G., Lu, T.T., Cyster, J.G., 2003. Integrin-dependence of lymphocyte entry into the splenic white pulp. J. Exp. Med. 197, 353–361. https://doi.org/10.1084/jem.20021569

Loder, B.F., Mutschler, B., Ray, R.J., Paige, C.J., Sideras, P., Torres, R., Lamers, M.C., Carsetti, R., 1999. B Cell Development in the Spleen Takes Place in Discrete Steps and Is Determined by the Quality of B Cell Receptor–Derived Signals. J. Exp. Med. 190, 75–90. https://doi.org/10.1084/jem.190.1.75

Logeat, F., Bessia, C., Brou, C., LeBail, O., Jarriault, S., Seidah, N.G., Israël, A., 1998. The Notch1 receptor is cleaved constitutively by a furin-like convertase. Proc. Natl. Acad. Sci. U. S. A. 95, 8108–8112. https://doi.org/10.1073/pnas.95.14.8108

Lopes-Carvalho, T., Kearney, J.F., 2004. Development and selection of marginal zone B cells. Immunol. Rev. 197, 192–205. https://doi.org/10.1111/j.0105-2896.2004.0112.x

MacLennan, I.C.M., Gulbranson-Judge, A., Toellner, K.-M., Casamayor-Palleja, M., Sze, D.M.-Y., Chan, E.Y.-T., Luther, S.A., Orbea, H.A., 1997. The changing preference of T and B cells for partners as T-dependent antibody responses develop. Immunol. Rev. 156, 53–66. https://doi.org/10.1111/j.1600-065X.1997.tb00958.x

MacLennan, I.C.M., Toellner, K.-M., Cunningham, A.F., Serre, K., Sze, D.M.-Y., Zúñiga, E., Cook, M.C., Vinuesa, C.G., 2003. Extrafollicular antibody responses: MacLennan et al · Extrafollicular antibody responses. Immunol. Rev. 194, 8–18. https://doi.org/10.1034/j.1600-065X.2003.00058.x

Maillard, I., Fang, T., Pear, W.S., 2005. REGULATION OF LYMPHOID DEVELOPMENT, DIFFERENTIATION, AND FUNCTION BY THE NOTCH PATHWAY. Annu. Rev. Immunol. 23, 945–974. https://doi.org/10.1146/annurev.immunol.23.021704.115747

Maity, P.C., Datta, M., Nicolò, A., Jumaa, H., 2018. Isotype Specific Assembly of B Cell Antigen Receptors and Synergism With Chemokine Receptor CXCR4. Front. Immunol. 9. https://doi.org/10.3389/fimmu.2018.02988

Mårtensson, I.-L., Keenan, R.A., Licence, S., 2007. The pre-B-cell receptor. Curr. Opin. Immunol. 19, 137–142. https://doi.org/10.1016/j.coi.2007.02.006

Martin, F., Kearney, J.F., 2002. Marginal-zone B cells. Nat. Rev. Immunol. 2, 323–335. https://doi.org/10.1038/nri799

Martin, F., Kearney, J.F., 2000. Positive Selection from Newly Formed to Marginal Zone B Cells Depends on the Rate of Clonal Production, CD19, and btk. Immunity 12, 39–49. https://doi.org/10.1016/S1074-7613(00)80157-0

Martin, F., Oliver, A.M., Kearney, J.F., 2001. Marginal Zone and B1 B Cells Unite in the Early Response against T-Independent Blood-Borne Particulate Antigens. Immunity 14, 617–629. https://doi.org/10.1016/S1074-7613(01)00129-7

Martins, G., Calame, K., 2008. Regulation and functions of Blimp-1 in T and B lymphocytes. Annu. Rev. Immunol. 26, 133–169. https://doi.org/10.1146/annurev.immunol.26.021607.090241

McDaniell, R., Warthen, D.M., Sanchez-Lara, P.A., Pai, A., Krantz, I.D., Piccoli, D.A., Spinner, N.B., 2006. NOTCH2 mutations cause Alagille syndrome, a heterogeneous disorder of the notch signaling pathway. Am. J. Hum. Genet. 79, 169–173. https://doi.org/10.1086/505332

McGill, M.A., Dho, S.E., Weinmaster, G., McGlade, C.J., 2009. Numb regulates post-endocytic trafficking and degradation of Notch1. J. Biol. Chem. 284, 26427–26438. https://doi.org/10.1074/jbc.M109.014845

Mebius, R.E., Kraal, G., 2005. Structure and function of the spleen. Nat. Rev. Immunol. 5, 606–616. https://doi.org/10.1038/nri1669

Medvedovic, J., Ebert, A., Tagoh, H., Busslinger, M., 2011. Chapter 5 - Pax5: A Master Regulator of B Cell Development and Leukemogenesis, in: Alt, F.W. (Ed.), Advances in Immunology. Academic Press, pp. 179–206. https://doi.org/10.1016/B978-0-12-385991-4.00005-2

Melchers, F., 2015. Checkpoints that control B cell development. J. Clin. Invest. 125, 2203–2210. https://doi.org/10.1172/JCI78083

Mesin, L., Ersching, J., Victora, G.D., 2016. Germinal Center B Cell Dynamics. Immunity 45, 471–482. https://doi.org/10.1016/j.immuni.2016.09.001

Minges Wols, H.A., Johnson, K.M., Ippolito, J.A., Birjandi, S.Z., Su, Y., Le, P.T., Witte, P.L., 2010. Migration of immature and mature B cells in the aged microenvironment. Immunology 129, 278–290. https://doi.org/10.1111/j.1365-2567.2009.03182.x

Minguet, S., Dopfer, E.P., Pollmer, C., Freudenberg, M.A., Galanos, C., Reth, M., Huber, M., Schamel, W.W., 2008. Enhanced B-cell activation mediated by TLR4 and BCR cross-talk. Eur. J. Immunol. 38, 2475–2487. https://doi.org/10.1002/eji.200738094

Mittrücker, H.W., Matsuyama, T., Grossman, A., Kündig, T.M., Potter, J., Shahinian, A., Wakeham, A., Patterson, B., Ohashi, P.S., Mak, T.W., 1997. Requirement for the transcription factor LSIRF/IRF4 for mature B and T lymphocyte function. Science 275, 540–543. https://doi.org/10.1126/science.275.5299.540

Moloney, D.J., Panin, V.M., Johnston, S.H., Chen, J., Shao, L., Wilson, R., Wang, Y., Stanley, P., Irvine, K.D., Haltiwanger, R.S., Vogt, T.F., 2000. Fringe is a glycosyltransferase that modifies Notch. Nature 406, 369–375. https://doi.org/10.1038/35019000

Mond, J.J., Lees, A., Snapper, C.M., 1995. T cell-independent antigens type 2. Annu. Rev. Immunol. 13, 655–692. https://doi.org/10.1146/annurev.iy.13.040195.003255

Moore, P.A., Belvedere, O., Orr, A., Pieri, K., LaFleur, D.W., Feng, P., Soppet, D., Charters, M., Gentz, R., Parmelee, D., Li, Y., Galperina, O., Giri, J., Roschke, V., Nardelli, B., Carrell, J., Sosnovtseva, S., Greenfield, W., Ruben, S.M., Olsen, H.S., Fikes, J., Hilbert, D.M., 1999. BLyS: member of the tumor necrosis factor family and B lymphocyte stimulator. Science 285, 260–263. https://doi.org/10.1126/science.285.5425.260

Morgan, T.H., 1917. The Theory of the Gene. Am. Nat. 51, 513–544. https://doi.org/10.1086/279629

Moriyama, Y., Sekine, C., Koyanagi, A., Koyama, N., Ogata, H., Chiba, S., Hirose, S., Okumura, K., Yagita, H., 2008. Delta-like 1 is essential for the maintenance of marginal zone B cells in normal mice but not in autoimmune mice. Int. Immunol. 20, 763–773. https://doi.org/10.1093/intimm/dxn034

Mumm, J.S., Kopan, R., 2000. Notch Signaling: From the Outside In. Dev. Biol. 228, 151–165. https://doi.org/10.1006/dbio.2000.9960

Mumm, J.S., Schroeter, E.H., Saxena, M.T., Griesemer, A., Tian, X., Pan, D.J., Ray, W.J., Kopan, R., 2000. A ligand-induced extracellular cleavage regulates gamma-secretase-like proteolytic activation of Notch1. Mol. Cell 5, 197–206. https://doi.org/10.1016/s1097-2765(00)80416-5

Muramatsu, M., Kinoshita, K., Fagarasan, S., Yamada, S., Shinkai, Y., Honjo, T., 2000. Class switch recombination and hypermutation require activation-induced cytidine deaminase (AID), a potential RNA editing enzyme. Cell 102, 553–563. https://doi.org/10.1016/s0092-8674(00)00078-7

Muto, A., Ochiai, K., Kimura, Y., Itoh-Nakadai, A., Calame, K.L., Ikebe, D., Tashiro, S., Igarashi, K., 2010. Bach2 represses plasma cell gene regulatory network in B cells to promote antibody class switch. EMBO J. 29, 4048–4061. https://doi.org/10.1038/emboj.2010.257

Nelms, K., Keegan, A.D., Zamorano, J., Ryan, J.J., Paul, W.E., 1999. The IL-4 receptor: signaling mechanisms and biologic functions. Annu. Rev. Immunol. 17, 701–738. https://doi.org/10.1146/annurev.immunol.17.1.701

Nera, K.-P., Kohonen, P., Narvi, E., Peippo, A., Mustonen, L., Terho, P., Koskela, K., Buerstedde, J.-M., Lassila, O., 2006. Loss of Pax5 Promotes Plasma Cell Differentiation. Immunity 24, 283–293. https://doi.org/10.1016/j.immuni.2006.02.003

Nicholson, L.B., 2016. The immune system. Essays Biochem. 60, 275–301. https://doi.org/10.1042/EBC20160017

Noah, T.K., Shroyer, N.F., 2013. Notch in the Intestine: Regulation of Homeostasis and Pathogenesis. Annu. Rev. Physiol. 75, 263–288. https://doi.org/10.1146/annurev-physiol-030212-183741

Northrup, D.L., Allman, D., 2008. Transcriptional regulation of early B cell development. Immunol. Res. 42, 106–117. https://doi.org/10.1007/s12026-008-8043-z

Nowell, C.S., Radtke, F., 2017. Notch as a tumour suppressor. Nat. Rev. Cancer 17, 145–159. https://doi.org/10.1038/nrc.2016.145

Nowotschin, S., Xenopoulos, P., Schrode, N., Hadjantonakis, A.-K., 2013. A bright single-cell resolution live imaging reporter of Notch signaling in the mouse. BMC Dev. Biol. 13, 15. https://doi.org/10.1186/1471-213X-13-15

Nutt, S.L., Eberhard, D., Horcher, M., Rolink, A.G., Busslinger, M., 2001. Pax5 determines the identity of B cells from the beginning to the end of B-lymphopoiesis. Int. Rev. Immunol. 20, 65–82. https://doi.org/10.3109/08830180109056723

Obukhanych, T.V., Nussenzweig, M.C., 2006. T-independent type II immune responses generate memory B cells. J. Exp. Med. 203, 305–310. https://doi.org/10.1084/jem.20052036

Ochiai, K., Maienschein-Cline, M., Simonetti, G., Chen, J., Rosenthal, R., Brink, R., Chong, A.S., Klein, U., Dinner, A.R., Singh, H., Sciammas, R., 2013. Transcriptional Regulation of Germinal Center B and Plasma Cell Fates by Dynamical Control of IRF4. Immunity 38, 918–929. https://doi.org/10.1016/j.immuni.2013.04.009

Oda, T., Elkahloun, A.G., Pike, B.L., Okajima, K., Krantz, I.D., Genin, A., Piccoli, D.A., Meltzer, P.S., Spinner, N.B., Collins, F.S., Chandrasekharappa, S.C., 1997. Mutations in the human Jagged1 gene are responsible for Alagille syndrome. Nat. Genet. 16, 235–242. https://doi.org/10.1038/ng0797-235

Oliver, A.M., Martin, F., Kearney, J.F., 1999. $IgM^{high}CD21^{high}$ Lymphocytes Enriched in the Splenic Marginal Zone Generate Effector Cells More Rapidly Than the Bulk of Follicular B Cells. J. Immunol. 162, 7198.

O'Neil, J., Look, A.T., 2007. Mechanisms of transcription factor deregulation in lymphoid cell transformation. Oncogene 26, 6838–6849. https://doi.org/10.1038/sj.onc.1210766

Oracki, S.A., Walker, J.A., Hibbs, M.L., Corcoran, L.M., Tarlinton, D.M., 2010. Plasma cell development and survival: Plasma cell development and survival. Immunol. Rev. 237, 140–159. https://doi.org/10.1111/j.1600-065X.2010.00940.x

Oyama, T., Harigaya, K., Muradil, A., Hozumi, K., Habu, S., Oguro, H., Iwama, A., Matsuno, K., Sakamoto, R., Sato, M., Yoshida, N., Kitagawa, M., 2007. Mastermind-1 is required for Notch signal-dependent steps in lymphocyte development *in vivo*. Proc. Natl. Acad. Sci. 104, 9764–9769. https://doi.org/10.1073/pnas.0700240104

Panagopoulos, D., Victoratos, P., Alexiou, M., Kollias, G., Mosialos, G., 2004. Comparative Analysis of Signal Transduction by CD40 and the Epstein-Barr Virus Oncoprotein LMP1 In Vivo. J. Virol. 78, 13253–13261. https://doi.org/10.1128/JVI.78.23.13253-13261.2004

Pape, K.A., Kouskoff, V., Nemazee, D., Tang, H.L., Cyster, J.G., Tze, L.E., Hippen, K.L., Behrens, T.W., Jenkins, M.K., 2003. Visualization of the genesis and fate of isotype-switched B cells during a primary immune response. J. Exp. Med. 197, 1677–1687. https://doi.org/10.1084/jem.20012065

Paus, D., Phan, T.G., Chan, T.D., Gardam, S., Basten, A., Brink, R., 2006. Antigen recognition strength regulates the choice between extrafollicular plasma cell and germinal center B cell differentiation. J. Exp. Med. 203, 1081–1091. https://doi.org/10.1084/jem.20060087

Paust, S., Senman, B., Von Andrian, U.H., 2010. Adaptive immune responses mediated by natural killer cells: Adaptive immune responses mediated by natural killers. Immunol. Rev. 235, 286–296. https://doi.org/10.1111/j.0105-2896.2010.00906.x

Peng, S.L., 2005. Signaling in B cells via Toll-like receptors. Curr. Opin. Immunol. 17, 230–236. https://doi.org/10.1016/j.coi.2005.03.003

Peng, X., Kasran, A., Warmerdam, P.A., de Boer, M., Ceuppens, J.L., 1996. Accessory signaling by CD40 for T cell activation: induction of Th1 and Th2 cytokines and synergy with interleukin-12 for interferon-gamma production. Eur. J. Immunol. 26, 1621–1627. https://doi.org/10.1002/eji.1830260732

Perrimon, N., Pitsouli, C., Shilo, B.-Z., 2012. Signaling mechanisms controlling cell fate and embryonic patterning. Cold Spring Harb. Perspect. Biol. 4, a005975. https://doi.org/10.1101/cshperspect.a005975

Pillai, S., Cariappa, A., 2009. The follicular versus marginal zone B lymphocyte cell fate decision. Nat. Rev. Immunol. 9, 767–777. https://doi.org/10.1038/nri2656

Pillai, S., Cariappa, A., Moran, S.T., 2005. MARGINAL ZONE B CELLS. Annu. Rev. Immunol. 23, 161–196. https://doi.org/10.1146/annurev.immunol.23.021704.115728

Pracht, K., Meinzinger, J., Daum, P., Schulz, S.R., Reimer, D., Hauke, M., Roth, E., Mielenz, D., Berek, C., Côrte-Real, J., Jäck, H.-M., Schuh, W., 2017. A new staining protocol for detection of murine antibody-secreting plasma cell subsets by flow cytometry. Eur. J. Immunol. 47, 1389–1392. https://doi.org/10.1002/eji.201747019

Qiu, L., Joazeiro, C., Fang, N., Wang, H.Y., Elly, C., Altman, Y., Fang, D., Hunter, T., Liu, Y.C., 2000. Recognition and ubiquitination of Notch by Itch, a hect-type E3 ubiquitin ligase. J. Biol. Chem. 275, 35734–35737. https://doi.org/10.1074/jbc.M007300200

Radtke, F., Fasnacht, N., Macdonald, H.R., 2010. Notch signaling in the immune system. Immunity 32, 14–27. https://doi.org/10.1016/j.immuni.2010.01.004

Radtke, F., MacDonald, H.R., Tacchini-Cottier, F., 2013. Regulation of innate and adaptive immunity by Notch. Nat. Rev. Immunol. 13, 427–437. https://doi.org/10.1038/nri3445

Radtke, F., Wilson, A., Mancini, S.J.C., MacDonald, H.R., 2004. Notch regulation of lymphocyte development and function. Nat. Immunol. 5, 247–253. https://doi.org/10.1038/ni1045

Radtke, F., Wilson, A., Stark, G., Bauer, M., van Meerwijk, J., MacDonald, H.R., Aguet, M., 1999. Deficient T Cell Fate Specification in Mice with an Induced Inactivation of Notch1. Immunity 10, 547–558. https://doi.org/10.1016/S1074-7613(00)80054-0

Ramírez, J., Lukin, K., Hagman, J., 2010. From hematopoietic progenitors to B cells: mechanisms of lineage restriction and commitment. Curr. Opin. Immunol. 22, 177–184. https://doi.org/10.1016/j.coi.2010.02.003

Rawlings, D.J., Schwartz, M.A., Jackson, S.W., Meyer-Bahlburg, A., 2012. Integration of B cell responses through Toll-like receptors and antigen receptors. Nat. Rev. Immunol. 12, 282–294. https://doi.org/10.1038/nri3190

Reif, K., Ekland, E.H., Ohl, L., Nakano, H., Lipp, M., Förster, R., Cyster, J.G., 2002. Balanced responsiveness to chemoattractants from adjacent zones determines B-cell position. Nature 416, 94–99. https://doi.org/10.1038/416094a

Reljic, R., Wagner, S.D., Peakman, L.J., Fearon, D.T., 2000. Suppression of signal transducer and activator of transcription 3-dependent B lymphocyte terminal differentiation by BCL-6. J. Exp. Med. 192, 1841–1848. https://doi.org/10.1084/jem.192.12.1841

Revilla-I-Domingo, R., Bilic, I., Vilagos, B., Tagoh, H., Ebert, A., Tamir, I.M., Smeenk, L., Trupke, J., Sommer, A., Jaritz, M., Busslinger, M., 2012. The B-cell identity factor Pax5 regulates distinct transcriptional programmes in early and late B lymphopoiesis. EMBO J. 31, 3130–3146. https://doi.org/10.1038/emboj.2012.155

Revy, P., Muto, T., Levy, Y., Geissmann, F., Plebani, A., Sanal, O., Catalan, N., Forveille, M., Dufourcq-Labelouse, R., Gennery, A., Tezcan, I., Ersoy, F., Kayserili, H., Ugazio, A.G., Brousse, N., Muramatsu, M., Notarangelo, L.D., Kinoshita, K., Honjo, T., Fischer, A., Durandy, A., 2000. Activation-induced cytidine deaminase (AID) deficiency causes the autosomal recessive form of the Hyper-IgM syndrome (HIGM2). Cell 102, 565–575. https://doi.org/10.1016/s0092-8674(00)00079-9

Rinkenberger, J.L., Wallin, J.J., Johnson, K.W., Koshland, M.E., 1996. An interleukin-2 signal relieves BSAP (Pax5)-mediated repression of the immunoglobulin J chain gene. Immunity 5, 377–386. https://doi.org/10.1016/s1074-7613(00)80263-0

Robinson, M.J., Ding, Z., Pitt, C., Brodie, E.J., Quast, I., Tarlinton, D.M., Zotos, D., 2020. The Amount of BCL6 in B Cells Shortly after Antigen Engagement Determines Their Representation in Subsequent Germinal Centers. Cell Rep. 30, 1530-1541.e4. https://doi.org/10.1016/j.celrep.2020.01.009

Roco, J.A., Mesin, L., Binder, S.C., Nefzger, C., Gonzalez-Figueroa, P., Canete, P.F., Ellyard, J., Shen, Q., Robert, P.A., Cappello, J., Vohra, H., Zhang, Y., Nowosad, C.R., Schiepers, A., Corcoran, L.M., Toellner, K.-M., Polo, J.M., Meyer-Hermann, M., Victora, G.D.,

Vinuesa, C.G., 2019. Class-Switch Recombination Occurs Infrequently in Germinal Centers. Immunity 51, 337-350.e7. https://doi.org/10.1016/j.immuni.2019.07.001

Rodda, L.B., Bannard, O., Ludewig, B., Nagasawa, T., Cyster, J.G., 2015. Phenotypic and Morphological Properties of Germinal Center Dark Zone *Cxcl12* -Expressing Reticular Cells. J. Immunol. 195, 4781–4791. https://doi.org/10.4049/jimmunol.1501191

Roo, J.J.D. de, Staal, F.J.T., 2020. Cell Signaling Pathway Reporters in Adult Hematopoietic Stem Cells. Cells 9. https://doi.org/10.3390/cells9102264

Roque, M.C., Smith, P.A., Blasquez, V.C., 1996. A developmentally modulated chromatin structure at the mouse immunoglobulin kappa 3' enhancer. Mol. Cell. Biol. 16, 3138–3155. https://doi.org/10.1128/MCB.16.6.3138

Rosati, E., Sabatini, R., Rampino, G., Tabilio, A., Di Ianni, M., Fettucciari, K., Bartoli, A., Coaccioli, S., Screpanti, I., Marconi, P., 2009. Constitutively activated Notch signaling is involved in survival and apoptosis resistance of B-CLL cells. Blood 113, 856–865. https://doi.org/10.1182/blood-2008-02-139725

Rossi, D., Trifonov, V., Fangazio, M., Bruscaggin, A., Rasi, S., Spina, V., Monti, S., Vaisitti, T., Arruga, F., Famà, R., Ciardullo, C., Greco, M., Cresta, S., Piranda, D., Holmes, A., Fabbri, G., Messina, M., Rinaldi, A., Wang, J., Agostinelli, C., Piccaluga, P.P., Lucioni, M., Tabbò, F., Serra, R., Franceschetti, S., Deambrogi, C., Daniele, G., Gattei, V., Marasca, R., Facchetti, F., Arcaini, L., Inghirami, G., Bertoni, F., Pileri, S.A., Deaglio, S., Foà, R., Dalla-Favera, R., Pasqualucci, L., Rabadan, R., Gaidano, G., 2012. The coding genome of splenic marginal zone lymphoma: activation of NOTCH2 and other pathways regulating marginal zone development. J. Exp. Med. 209, 1537–1551. https://doi.org/10.1084/jem.20120904

Roth, K., Oehme, L., Zehentmeier, S., Zhang, Y., Niesner, R., Hauser, A.E., 2014. Tracking plasma cell differentiation and survival. Cytometry A 85, 15–24. https://doi.org/10.1002/cyto.a.22355

Saito, M., Gao, J., Basso, K., Kitagawa, Y., Smith, P.M., Bhagat, G., Pernis, A., Pasqualucci, L., Dalla-Favera, R., 2007. A Signaling Pathway Mediating Downregulation of BCL6 in Germinal Center B Cells Is Blocked by BCL6 Gene Alterations in B Cell Lymphoma. Cancer Cell 12, 280–292. https://doi.org/10.1016/j.ccr.2007.08.011

Saito, T., Chiba, S., Ichikawa, M., Kunisato, A., Asai, T., Shimizu, K., Yamaguchi, T., Yamamoto, G., Seo, S., Kumano, K., Nakagami-Yamaguchi, E., Hamada, Y., Aizawa, S., Hirai, H., 2003. Notch2 Is Preferentially Expressed in Mature B Cells and Indispensable for Marginal Zone B Lineage Development. Immunity 18, 675–685. https://doi.org/10.1016/S1074-7613(03)00111-0

Salguero-Jiménez, A., Grego-Bessa, J., D'Amato, G., Jiménez-Borreguero, L.J., Pompa, J.L. de la, 2018. Myocardial Notch-Rbpj deletion does not affect heart development or function. bioRxiv 393348. https://doi.org/10.1101/393348

Samardzic, T., Gerlach, J., Muller, K., Marinkovic, D., Hess, J., Nitschke, L., Wirth, T., 2002. CD22 regulates early B cell development in BOB.1/OBF.1-deficient mice. Eur. J. Immunol. 32, 2481–2489. https://doi.org/10.1002/1521-4141(200209)32:9<2481::AID-IMMU2481>3.0.CO;2-C

Sancho, R., Blake, S.M., Tendeng, C., Clurman, B.E., Lewis, J., Behrens, A., 2013. Fbw7 Repression by Hes5 Creates a Feedback Loop That Modulates Notch-Mediated Intestinal and Neural Stem Cell Fate Decisions. PLoS Biol. 11, e1001586. https://doi.org/10.1371/journal.pbio.1001586

Santos, M.A., Sarmento, L.M., Rebelo, M., Doce, A.A., Maillard, I., Dumortier, A., Neves, H., Radtke, F., Pear, W.S., Parreira, L., Demengeot, J., 2007. Notch1 engagement by Delta-like-1 promotes differentiation of B lymphocytes to antibody-secreting cells. Proc. Natl. Acad. Sci. 104, 15454–15459. https://doi.org/10.1073/pnas.0702891104

Sasaki, Y., Casola, S., Kutok, J.L., Rajewsky, K., Schmidt-Supprian, M., 2004. TNF Family Member B Cell-Activating Factor (BAFF) Receptor-Dependent and -Independent Roles for BAFF in B Cell Physiology. J. Immunol. 173, 2245. https://doi.org/10.4049/jimmunol.173.4.2245

Sasaki, Y., Derudder, E., Hobeika, E., Pelanda, R., Reth, M., Rajewsky, K., Schmidt-Supprian, M., 2006. Canonical NF-kappaB activity, dispensable for B cell development, replaces BAFF-receptor signals and promotes B cell proliferation upon activation. Immunity 24, 729–739. https://doi.org/10.1016/j.immuni.2006.04.005

Sato, S., Steeber, D.A., Tedder, T.F., 1995. The CD19 signal transduction molecule is a response regulator of B-lymphocyte differentiation. Proc. Natl. Acad. Sci. U. S. A. 92, 11558–11562. https://doi.org/10.1073/pnas.92.25.11558

Scharer, C.D., Patterson, D.G., Mi, T., Price, M.J., Hicks, S.L., Boss, J.M., 2020. Antibody-secreting cell destiny emerges during the initial stages of B-cell activation. Nat. Commun. 11, 3989. https://doi.org/10.1038/s41467-020-17798-x

Schebesta, A., McManus, S., Salvagiotto, G., Delogu, A., Busslinger, G.A., Busslinger, M., 2007. Transcription factor Pax5 activates the chromatin of key genes involved in B cell signaling, adhesion, migration, and immune function. Immunity 27, 49–63. https://doi.org/10.1016/j.immuni.2007.05.019

Scheffler, L., Feicht, S., Babushku, T., Kuhn, L.B., Ehrenberg, S., Frankenberger, S., Lehmann, F.M., Hobeika, E., Jungnickel, B., Baccarini, M., Bornkamm, G.W., Strobl, L.J., Zimber-Strobl, U., 2021. ERK phosphorylation is RAF independent in naïve and activated B cells but RAF dependent in plasma cell differentiation. Sci. Signal. 14, eabc1648. https://doi.org/10.1126/scisignal.abc1648

Schiemann, B., Gommerman, J.L., Vora, K., Cachero, T.G., Shulga-Morskaya, S., Dobles, M., Frew, E., Scott, M.L., 2001. An essential role for BAFF in the normal development of B cells through a BCMA-independent pathway. Science 293, 2111–2114. https://doi.org/10.1126/science.1061964

Schroeter, E.H., Kisslinger, J.A., Kopan, R., 1998. Notch-1 signalling requires ligand-induced proteolytic release of intracellular domain. Nature 393, 382–386. https://doi.org/10.1038/30756

Schweisguth, F., 2004. Regulation of Notch Signaling Activity. Curr. Biol. 14, R129–R138. https://doi.org/10.1016/j.cub.2004.01.023

Sciammas, R., Davis, M.M., 2004. Modular nature of Blimp-1 in the regulation of gene expression during B cell maturation. J. Immunol. Baltim. Md 1950 172, 5427–5440. https://doi.org/10.4049/jimmunol.172.9.5427

Sciammas, R., Shaffer, A.L., Schatz, J.H., Zhao, H., Staudt, L.M., Singh, H., 2006. Graded Expression of Interferon Regulatory Factor-4 Coordinates Isotype Switching with Plasma Cell Differentiation. Immunity 25, 225–236. https://doi.org/10.1016/j.immuni.2006.07.009

Seifert, M., Küppers, R., 2016. Human memory B cells. Leukemia 30, 2283–2292. https://doi.org/10.1038/leu.2016.226

Shaffer, A.L., Lin, K.I., Kuo, T.C., Yu, X., Hurt, E.M., Rosenwald, A., Giltnane, J.M., Yang, L., Zhao, H., Calame, K., Staudt, L.M., 2002. Blimp-1 orchestrates plasma cell differentiation by extinguishing the mature B cell gene expression program. Immunity 17, 51–62. https://doi.org/10.1016/s1074-7613(02)00335-7

Shaffer, A.L., Yu, X., He, Y., Boldrick, J., Chan, E.P., Staudt, L.M., 2000. BCL-6 Represses Genes that Function in Lymphocyte Differentiation, Inflammation, and Cell Cycle Control. Immunity 13, 199–212. https://doi.org/10.1016/S1074-7613(00)00020-0

Shahaf, G., Zisman-Rozen, S., Benhamou, D., Melamed, D., Mehr, R., 2016. B Cell Development in the Bone Marrow Is Regulated by Homeostatic Feedback Exerted by Mature B Cells. Front. Immunol. 7. https://doi.org/10.3389/fimmu.2016.00077

Shapiro-Shelef, M., Calame, K., 2005. Regulation of plasma-cell development. Nat. Rev. Immunol. 5, 230–242. https://doi.org/10.1038/nri1572

Shapiro-Shelef, M., Lin, K.-I., McHeyzer-Williams, L.J., Liao, J., McHeyzer-Williams, M.G., Calame, K., 2003. Blimp-1 is required for the formation of immunoglobulin secreting plasma cells and pre-plasma memory B cells. Immunity 19, 607–620. https://doi.org/10.1016/s1074-7613(03)00267-x

Shawber, C.J., Brown-Grant, D.-A., Wu, T., Kitajewski, J.K., Douglas, N.C., 2019. Dominant-negative inhibition of canonical Notch signaling in trophoblast cells does not disrupt placenta formation. Biol. Open 8. https://doi.org/10.1242/bio.037721

Shlomchik, M.J., Weisel, F., 2012. Germinal center selection and the development of memory B and plasma cells. Immunol. Rev. 247, 52–63. https://doi.org/10.1111/j.1600-065X.2012.01124.x

Simonetti, G., Carette, A., Silva, K., Wang, H., De Silva, N.S., Heise, N., Siebel, C.W., Shlomchik, M.J., Klein, U., 2013. IRF4 controls the positioning of mature B cells in the lymphoid microenvironments by regulating NOTCH2 expression and activity. J. Exp. Med. 210, 2887–2902. https://doi.org/10.1084/jem.20131026

Singh, M., Birshtein, B.K., 1993. NF-HB (BSAP) is a repressor of the murine immunoglobulin heavy-chain 3' alpha enhancer at early stages of B-cell differentiation. Mol. Cell. Biol. 13, 3611–3622. https://doi.org/10.1128/mcb.13.6.3611-3622.1993

Smith, K.G., Hewitson, T.D., Nossal, G.J., Tarlinton, D.M., 1996. The phenotype and fate of the antibody-forming cells of the splenic foci. Eur. J. Immunol. 26, 444–448. https://doi.org/10.1002/eji.1830260226

Song, H., Cerny, J., 2003. Functional Heterogeneity of Marginal Zone B Cells Revealed by Their Ability to Generate Both Early Antibody-forming Cells and Germinal Centers with Hypermutation and Memory in Response to a T-dependent Antigen. J. Exp. Med. 198, 1923–1935. https://doi.org/10.1084/jem.20031498

Sperling, S., Fiedler, P., Lechner, M., Pollithy, A., Ehrenberg, S., Schiefer, A.-I., Kenner, L., Feuchtinger, A., Kühn, R., Swinerd, G., Schmidt-Supprian, M., Strobl, L.J., Zimber-Strobl, U., 2019. Chronic CD30 signaling in B cells results in lymphomagenesis by driving the expansion of plasmablasts and B1 cells. Blood 133, 2597–2609. https://doi.org/10.1182/blood.2018880138

Srivastava, B., Lindsley, R.C., Nikbakht, N., Allman, D., 2005a. Models for peripheral B cell development and homeostasis. Semin. Immunol. 17, 175–182. https://doi.org/10.1016/j.smim.2005.02.008

Srivastava, B., Quinn, W.J., Hazard, K., Erikson, J., Allman, D., 2005b. Characterization of marginal zone B cell precursors. J. Exp. Med. 202, 1225–1234. https://doi.org/10.1084/jem.20051038

Stebegg, M., Kumar, S.D., Silva-Cayetano, A., Fonseca, V.R., Linterman, M.A., Graca, L., 2018. Regulation of the Germinal Center Response. Front. Immunol. 9, 2469. https://doi.org/10.3389/fimmu.2018.02469

Stein, K.E., 1992. Thymus-independent and thymus-dependent responses to polysaccharide antigens. J. Infect. Dis. 165 Suppl 1, S49-52. https://doi.org/10.1093/infdis/165-supplement_1-s49

Suan, D., Kräutler, N.J., Maag, J.L.V., Butt, D., Bourne, K., Hermes, J.R., Avery, D.T., Young, C., Statham, A., Elliott, M., Dinger, M.E., Basten, A., Tangye, S.G., Brink, R., 2017. CCR6 Defines Memory B Cell Precursors in Mouse and Human Germinal Centers, Revealing Light-Zone Location and Predominant Low Antigen Affinity. Immunity 47, 1142-1153.e4. https://doi.org/10.1016/j.immuni.2017.11.022

Sundling, C., Lau, A.W.Y., Bourne, K., Young, C., Laurianto, C., Hermes, J.R., Menzies, R.J., Butt, D., Kräutler, N.J., Zahra, D., Suan, D., Brink, R., 2021. Positive selection of IgG+ over IgM+ B cells in the germinal center reaction. Immunity 54, 988-1001.e5. https://doi.org/10.1016/j.immuni.2021.03.013

Takeuchi, H., Haltiwanger, R.S., 2014. Significance of glycosylation in Notch signaling. Biochem. Biophys. Res. Commun. 453, 235–242. https://doi.org/10.1016/j.bbrc.2014.05.115

Takeuchi, H., Haltiwanger, R.S., 2010. Role of glycosylation of Notch in development. Semin. Cell Dev. Biol. 21, 638–645. https://doi.org/10.1016/j.semcdb.2010.03.003

Tan, J.B., Xu, K., Cretegny, K., Visan, I., Yuan, J.S., Egan, S.E., Guidos, C.J., 2009. Lunatic and manic fringe cooperatively enhance marginal zone B cell precursor competition for

delta-like 1 in splenic endothelial niches. Immunity 30, 254–263. https://doi.org/10.1016/j.immuni.2008.12.016

Tangye, S.G., Liu, Y.J., Aversa, G., Phillips, J.H., de Vries, J.E., 1998. Identification of functional human splenic memory B cells by expression of CD148 and CD27. J. Exp. Med. 188, 1691–1703. https://doi.org/10.1084/jem.188.9.1691

Tanigaki, K., Han, H., Yamamoto, N., Tashiro, K., Ikegawa, M., Kuroda, K., Suzuki, A., Nakano, T., Honjo, T., 2002. Notch–RBP-J signaling is involved in cell fate determination of marginal zone B cells. Nat. Immunol. 3, 443–450. https://doi.org/10.1038/ni793

Tanigaki, K., Honjo, T., 2007. Regulation of lymphocyte development by Notch signaling. Nat. Immunol. 8, 451–456. https://doi.org/10.1038/ni1453

Teng, G., Papavasiliou, F.N., 2007. Immunoglobulin Somatic Hypermutation. Annu. Rev. Genet. 41, 107–120. https://doi.org/10.1146/annurev.genet.41.110306.130340

Thomas, M., Calamito, M., Srivastava, B., Maillard, I., Pear, W.S., Allman, D., 2007. Notch activity synergizes with B-cell–receptor and CD40 signaling to enhance B-cell activation. Blood 109, 3342–3350. https://doi.org/10.1182/blood-2006-09-046698

Tonegawa, S., 1993. The Nobel Lectures in Immunology. The Nobel Prize for Physiology or Medicine, 1987. Somatic generation of immune diversity. Scand. J. Immunol. 38, 303–319. https://doi.org/10.1111/j.1365-3083.1993.tb01731.x

Trøen, G., Wlodarska, I., Warsame, A., Hernández Llodrà, S., De Wolf-Peeters, C., Delabie, J., 2008. NOTCH2 mutations in marginal zone lymphoma. Haematologica 93, 1107–1109. https://doi.org/10.3324/haematol.11635

Tunyaplin, C., Shaffer, A.L., Angelin-Duclos, C.D., Yu, X., Staudt, L.M., Calame, K.L., 2004. Direct repression of prdm1 by Bcl-6 inhibits plasmacytic differentiation. J. Immunol. Baltim. Md 1950 173, 1158–1165. https://doi.org/10.4049/jimmunol.173.2.1158

Tze, L.E., Schram, B.R., Lam, K.-P., Hogquist, K.A., Hippen, K.L., Liu, J., Shinton, S.A., Otipoby, K.L., Rodine, P.R., Vegoe, A.L., Kraus, M., Hardy, R.R., Schlissel, M.S., Rajewsky, K., Behrens, T.W., 2005. Basal Immunoglobulin Signaling Actively Maintains Developmental Stage in Immature B Cells. PLOS Biol. 3, null. https://doi.org/10.1371/journal.pbio.0030082

Vale, A.M., Kearney, J.F., Nobrega, A., Schroeder, H.W., 2015. Chapter 7 - Development and Function of B Cell Subsets, in: Alt, F.W., Honjo, T., Radbruch, A., Reth, M. (Eds.), Molecular Biology of B Cells (Second Edition). Academic Press, London, pp. 99–119. https://doi.org/10.1016/B978-0-12-397933-9.00007-2

Valls, E., Lobry, C., Geng, H., Wang, L., Cardenas, M., Rivas, M., Cerchietti, L., Oh, P., Yang, S.N., Oswald, E., Graham, C.W., Jiang, Y., Hatzi, K., Agirre, X., Perkey, E., Li, Z., Tam, W., Bhatt, K., Leonard, J.P., Zweidler-McKay, P.A., Maillard, I., Elemento, O., Ci, W., Aifantis, I., Melnick, A., 2017. BCL6 Antagonizes NOTCH2 to Maintain Survival of Human Follicular Lymphoma Cells. Cancer Discov. 7, 506–521. https://doi.org/10.1158/2159-8290.CD-16-1189

van Kooten, C., Banchereau, J., 2000. CD40-CD40 ligand. J. Leukoc. Biol. 67, 2–17. https://doi.org/10.1002/jlb.67.1.2

van Tetering, G., van Diest, P., Verlaan, I., van der Wall, E., Kopan, R., Vooijs, M., 2009. Metalloprotease ADAM10 is required for Notch1 site 2 cleavage. J. Biol. Chem. 284, 31018–31027. https://doi.org/10.1074/jbc.M109.006775

van Tetering, G., Vooijs, M., 2011. Proteolytic cleavage of Notch: “HIT and RUN”. Curr. Mol. Med. 11, 255–269. https://doi.org/10.2174/156652411795677972

Victora, G.D., 2014. SnapShot: the germinal center reaction. Cell 159, 700-700.e1. https://doi.org/10.1016/j.cell.2014.10.012

Victora, G.D., Nussenzweig, M.C., 2012. Germinal Centers. Annu. Rev. Immunol. 30, 429–457. https://doi.org/10.1146/annurev-immunol-020711-075032

Vinuesa, C.G., Sze, D.M.-Y., Cook, M.C., Toellner, K.-M., Klaus, G.G.B., Ball, J., MacLennan, I.C.M., 2003. Recirculating and germinal center B cells differentiate into cells responsive

to polysaccharide antigens. Eur. J. Immunol. 33, 297–305. https://doi.org/10.1002/immu.200310003

Vos, Q., Lees, A., Wu, Z.Q., Snapper, C.M., Mond, J.J., 2000. B-cell activation by T-cell-independent type 2 antigens as an integral part of the humoral immune response to pathogenic microorganisms. Immunol. Rev. 176, 154–170. https://doi.org/10.1034/j.1600-065x.2000.00607.x

Walker, L., Carlson, A., Tan-Pertel, H.T., Weinmaster, G., Gasson, J., 2001. The notch receptor and its ligands are selectively expressed during hematopoietic development in the mouse. Stem Cells Dayt. Ohio 19, 543–552. https://doi.org/10.1634/stemcells.19-6-543

Weller, S., Reynaud, C.-A., Weill, J.-C., 2005. Splenic marginal zone B cells in humans: Where do they mutate their Ig receptor? Eur. J. Immunol. 35, 2789–2792. https://doi.org/10.1002/eji.200535446

Wen, L., Brill-Dashoff, J., Shinton, S.A., Asano, M., Hardy, R.R., Hayakawa, K., 2005. Evidence of Marginal-Zone B Cell- Positive Selection in Spleen. Immunity 23, 297–308. https://doi.org/10.1016/j.immuni.2005.08.007

Wen, R., Chen, Y., Xue, L., Schuman, J., Yang, S., Morris, S.W., Wang, D., 2003. Phospholipase Cgamma2 provides survival signals via Bcl2 and A1 in different subpopulations of B cells. J. Biol. Chem. 278, 43654–43662. https://doi.org/10.1074/jbc.M307318200

Weniger, M.A., Tiacci, E., Schneider, S., Arnolds, J., Rüschenbaum, S., Duppach, J., Seifert, M., Döring, C., Hansmann, M.-L., Küppers, R., 2018. Human CD30+ B cells represent a unique subset related to Hodgkin lymphoma cells. J. Clin. Invest. 128, 2996–3007. https://doi.org/10.1172/JCI95993

Wharton, K.A., Johansen, K.M., Xu, T., Artavanis-Tsakonas, S., 1985. Nucleotide sequence from the neurogenic locus notch implies a gene product that shares homology with proteins containing EGF-like repeats. Cell 43, 567–581. https://doi.org/10.1016/0092-8674(85)90229-6

White, H.N., Meng, Q.-H., 2012. Recruitment of a distinct but related set of VH sequences into the murine CD21hi/CD23- marginal zone B cell repertoire to that seen in the class-switched antibody response. J. Immunol. Baltim. Md 1950 188, 287–293. https://doi.org/10.4049/jimmunol.1101264

Winkler, T.H., Mårtensson, I.-L., 2018. The Role of the Pre-B Cell Receptor in B Cell Development, Repertoire Selection, and Tolerance. Front. Immunol. 9, 2423. https://doi.org/10.3389/fimmu.2018.02423

Witt, C.M., Hurez, V., Swindle, C.S., Hamada, Y., Klug, C.A., 2003a. Activated Notch2 Potentiates CD8 Lineage Maturation and Promotes the Selective Development of B1 B Cells. Mol. Cell. Biol. 23, 8637–8650. https://doi.org/10.1128/MCB.23.23.8637-8650.2003

Witt, C.M., Won, W.-J., Hurez, V., Klug, C.A., 2003b. Notch2 Haploinsufficiency Results in Diminished B1 B Cells and a Severe Reduction in Marginal Zone B Cells. J. Immunol. 171, 2783–2788. https://doi.org/10.4049/jimmunol.171.6.2783

Wu, G., Lyapina, S., Das, I., Li, J., Gurney, M., Pauley, A., Chui, I., Deshaies, R.J., Kitajewski, J., 2001. SEL-10 Is an Inhibitor of Notch Signaling That Targets Notch for Ubiquitin-Mediated Protein Degradation. Mol. Cell. Biol. 21, 7403–7415. https://doi.org/10.1128/MCB.21.21.7403-7415.2001

Yang, L.-T., Nichols, J.T., Yao, C., Manilay, J.O., Robey, E.A., Weinmaster, G., 2005. Fringe glycosyltransferases differentially modulate Notch1 proteolysis induced by Delta1 and Jagged1. Mol. Biol. Cell 16, 927–942. https://doi.org/10.1091/mbc.e04-07-0614

Yang, Q., Jeremiah Bell, J., Bhandoola, A., 2010. T-cell lineage determination: T-cell fate specification and commitment. Immunol. Rev. 238, 12–22. https://doi.org/10.1111/j.1600-065X.2010.00956.x

Yang Shih, T.-A., Meffre, E., Roederer, M., Nussenzweig, M.C., 2002. Role of BCR affinity in T cell–dependent antibody responses in vivo. Nat. Immunol. 3, 570–575. https://doi.org/10.1038/ni803

Yeramilli, V.A., Knight, K.L., 2011. Somatically Diversified and Proliferating Transitional B Cells: Implications for Peripheral B Cell Homeostasis. J. Immunol. 186, 6437. https://doi.org/10.4049/jimmunol.1003897

Yoon, S.-O., Zhang, X., Berner, P., Blom, B., Choi, Y.S., 2009. Notch Ligands Expressed by Follicular Dendritic Cells Protect Germinal Center B Cells from Apoptosis. J. Immunol. 183, 352–358. https://doi.org/10.4049/jimmunol.0803183

Yu, K., Lieber, M.R., 2019. Current insights into the mechanism of mammalian immunoglobulin class switch recombination. Crit. Rev. Biochem. Mol. Biol. 54, 333–351. https://doi.org/10.1080/10409238.2019.1659227

Zanotti, S., Canalis, E., 2013. Notch signaling in skeletal health and disease. Eur. J. Endocrinol. 168, R95-103. https://doi.org/10.1530/EJE-13-0115

Zaretsky, I., Atrakchi, O., Mazor, R.D., Stoler-Barak, L., Biram, A., Feigelson, S.W., Gitlin, A.D., Engelhardt, B., Shulman, Z., 2017. ICAMs support B cell interactions with T follicular helper cells and promote clonal selection. J. Exp. Med. 214, 3435–3448. https://doi.org/10.1084/jem.20171129

Zhang, Y., Tech, L., George, L.A., Acs, A., Durrett, R.E., Hess, H., Walker, L.S.K., Tarlinton, D.M., Fletcher, A.L., Hauser, A.E., Toellner, K.-M., 2018. Plasma cell output from germinal centers is regulated by signals from Tfh and stromal cells. J. Exp. Med. 215, 1227–1243. https://doi.org/10.1084/jem.20160832

Zhu, G., Wang, X., Xiao, H., Liu, X., Fang, Y., Zhai, B., Xu, R., Han, G., Chen, G., Hou, C., Shen, B., Li, Y., Ma, N., Wu, H., Liu, G., Wang, R., 2017. Both Notch1 and its ligands in B cells promote antibody production. Mol. Immunol. 91, 17–23. https://doi.org/10.1016/j.molimm.2017.08.021

Zouali, M., Richard, Y., 2011. Marginal Zone B-Cells, a Gatekeeper of Innate Immunity. Front. Immunol. 2. https://doi.org/10.3389/fimmu.2011.00063

Danksagung

First and foremost, my biggest Thank You goes to my supervisor PD Dr. Ursula Zimber-Strobl for the support and restless guidance during this 4-year PhD journey. Thank You from the bottom of my heart for providing me with this exciting and intellectually challenging project, for your endless trust in me and my work, for your unconditional bolster in the lab and beyond. The numerous discussions, chats and chances you gave me for collaborations on publications trained me and molded me into the scientist I am today.

A special thanks goes to Lothar Strobl, for his enormous expertise on Notch2, he was always a highly-competent source of ideas and a key driver of this project. His support and guidance were much appreciated when I seemingly would hit a “dead-end” in my research.

Next, I want to sincerely thank my TAC members Prof. Dr. Olivier Gires, Dr. rer. nat. Reinhard Obst and Prof. Dr. Robert Oostendorp for their fruitful input, stimulating discussion and helpful ideas every year towards the next steps of my thesis.

I would like to say thank you to Michael Hagemann and his staff at the animal facility for taking care of my mice, breeding and transporting them to the lab whenever asked. The restless work you did with an admirably good mood made my experimental work possible in the first place.

Thanks to my lab colleagues of AG Strobl for the great cooperation, we made a dream team over the years! A special thanks to Laura Kuhn, Markus, Ursula R., Yana and Kris: you made not only great colleagues, but also good friends! You elevated the work atmosphere with attention to details and little gestures throughout daily life. I will always cherish those moments with you.

Additionally, I want to thank the entire department of AGV for the enjoyable seminars, the lending of materials when there were delivery delays, and for the friendly chats in the kitchen and hallways. A special shout out goes to my closest colleague and friend Nini. Thanks for listening to all the rant outs and for our coffee breaks, without you I may have given up when things got tough.

To my closest personal friends (you know who you are!): Thanks for bearing with me through this journey, for boosting my mood and cheering me on when my spirits were down.

To my loving boyfriend **Mladen**, for as long as I live I cannot thank you enough. You have given me strength and support through tough PhD times, when things didn’t go my way. Without you by my side to take care of my mental and emotional well-being and keep my sanity, I may have given up in times of crises. I know I am difficult when stressed and under pressure, so I appreciate everything you did for me in the last few months of my thesis. It made me realize once again that you are my person, Те сакам и Ти благодарам.

Finally, my biggest **THANK YOU** goes to my lovely Mom and Dad. **Бети & Јорго,** your endless love, support, guidance and patience with me when I was at my best and at my worst helped me get to this point. Without you, I would have never started this journey and definitely wouldn’t have finished it with the amazing success as I have today. I dedicate this dissertation to You both, as a way to show appreciation and thankfulness for everything You have done and keep doing for me. ***На најдобрите родители на овој свет: Ве сакам најмногу и Ви благодарам за секој миг од секој ден...***

Affidavit

LMU LUDWIG-MAXIMILIANS-UNIVERSITÄT MÜNCHEN | Promotionsbüro Medizinische Fakultät | MMRS

Eidesstattliche Erklärung

BABUSHKU, TEA

Name, Vorname

Ich erkläre hiermit an Eides statt, dass ich die vorliegende Dissertation mit dem Titel:

Notch2 signaling in the primary T-cell-dependent immune response in mice

selbständig verfasst, mich außer der angegebenen keiner weiteren Hilfsmittel bedient und alle Erkenntnisse, die aus dem Schrifttum ganz oder annähernd übernommen sind, als solche kenntlich gemacht und nach ihrer Herkunft unter Bezeichnung der Fundstelle einzeln nachgewiesen habe.

Ich erkläre des Weiteren, dass die hier vorgelegte Dissertation nicht in gleicher oder in ähnlicher Form bei einer anderen Stelle zur Erlangung eines akademischen Grades eingereicht wurde.

MÜNCHEN, 03/04/2023 TEA BABUSHKU

Ort, Datum Unterschrift Doktorandin bzw. Doktorand

List of Publications

1.

Lechner, M, Engleitner, T, **Babushku, T**, Schmidt-Supprian, M, Rad, R, Strobl LJ & Zimber-Strobl, U. **"Notch2-mediated plasticity between marginal zone and follicular B cells**", *Nat Commun 12, 1111 (2021). https://doi.org/10.1038/s41467-021-21359-1*

2.

Scheffler, L, Feicht, S, **Babushku, T**, Kuhn, LB, Ehrenberg, S, Frankenberger, S, Lehmann FM, Hobeika, E, Jungnickel B, Baccarini M, Bornkamm GW, Strobl LJ & Zimber-Strobl, U. **"ERK phosphorylation is RAF independent in naïve and activated B cells but RAF dependent in plasma cell differentiation**", *Science Signaling Vol. 14, Issue 682 (2021). https://doi.org/10.1126/scisignal.abc1648*

3.

Kuhn, LB, Valentin, S, Stojanovic, K, Strobl, DC, Grath, S, Robbert, DJ, **Babushku, T,** Wang, Y, Rambold, U, Scheffler, L, Blum, H, Feuchtinger, A, Blutke, A, Weih, F, Kitamura, D, Rad, R, Strobl LJ & Zimber-Strobl, U. "**RelB contributes to the survival, migration and lymphomagenesis of B cells with constitutively active CD40 signaling**", *Front. Immunol. 30 August 2022.*

***4.**

First Authorship paper based on the findings of this dissertation currently publicly available as a pre-print on *BioRxiv – The Preprint Server for Biology*

Babushku, T, Rane, S, Lechner, M, Zimber-Strobl, U, & Strobl LJ. "**Notch2 signaling guides B cells away from germinal centers towards marginal zone B cell and plasma cell differentiation",** *BioRxiv 2022.06.13.495961; https://doi.org/10.1101/2022.06.13.495961*

Currently in Revision at *Nature Communications* (resubmission by 15.05.2023)

***** Most figures are shared between this dissertation and the **4.** Manuscript. All figures were created by **Babushku Tea**